JGRG23

Proceedings of
the 23rd Workshop on General Relativity
and Gravitation in Japan

5—8 November 2013

50th Anniversary Auditorium, Hirosaki University

Aomori, Japan

Volume 3

Oral Presentations: Third Day

Contents

Oral Presentations: Third Day

Thursday 7 November

Morning 1 [Chair: Tetsuya Shiromizu]

9:00 Gustav Holzegel (Imperial College) [Invited]
"Construction of Dynamical Vacuum Black Holes"
[JGRG23(2013)110701]

10:00 Zilong Li (Department of Physics, Fudan University)
"Destroying the event horizon of regular black holes"
[JGRG23(2013)110703]

10:20-10:45 Break

Morning 2 [Chair: Hideki Ishihara]

10:45 Masato Nozawa (KEK)
"Supersymmetric Plebanski-Demianski solution"
[JGRG23(2013)110704]

11:05 Kentaro Tanabe (University of Barcelona)
"Large D gravity"
[JGRG23(2013)110705]

11:25 Atsuki Masuda (Osaka city university)
"Propagation of twisted waves in a Kerr space-time"
[JGRG23(2013)110706]

11:45 Tomohiro Nakama (RESCEU, University of Tokyo)
"Relationship between dark matter properties and primordial black holes as seeds of supermassive black holes"
[JGRG23(2013)110707]

12:05 Ryusuke Nishikawa (Osaka City University)
"Newtonian self-gravitating system in a relativistic void universe model"
[JGRG23(2013)110708]

12:25-14:00 Lunch

Afternoon 1 [Chair: Ken-ichi Oohara]

14:00 Naoki Seto (Kyoto University) [Invited]
"GW data analysis beyond first detection"
[JGRG23(2013)110709]

14:50 Kazunari Eda (RESCEU, The University of Tokyo)
"Parameter Estimation of Gravitational Wave from a Stellar Mass and an Intermediate Mass Black Hole Binary Surrounded by a Dark Matter Mini-spike"
[JGRG23(2013)110710]

15:10 Masato Kaneyama (Niigata University)
"The Hilbert-Huang transform in search for gravitational-wave bursts"
[JGRG23(2013)110711]

15:30-50 Break

Afternoon 2 [Chair: Takeshi Chiba]

15:50 Tomohiro Fujita (Kavli IPMU)
"Possible roles of PBH evaporation in cosmology and detection of its gravitational waves"
[JGRG23(2013)110712]

16:10 Ken'ichi Saikawa (Tokyo Institute of Technology)
"Estimation of gravitational wave spectrum from cosmic domain walls"
[JGRG23(2013)110713]

16:30 Hirotaka Yoshino (KEK)
"Axion Bosenova and Gravitational Waves"
[JGRG23(2013)110714]

16:50 Shunichiro Kinoshita (OCAMI, Osaka City University)
"Dynamical process in Holographic QCD"
[JGRG23(2013)110715]

17:10 Dong-han Yeom (Yukawa Institute for Theoretical Physics)
"No-boundary wave function toward good inflation models"
[JGRG23(2013)110716]

17:30 Taro Kunimitsu (RESCEU, University of Tokyo)
"On the graceful exit from Higgs G-inflation"
[JGRG23(2013)110717]

19:00 Banquet

“Construction of Dynamical Vacuum Black Holes”

by Gustav Holzegel (invited)

[JGRG23(2013)110701]

Existence of Dynamical Vacuum Black Holes
(joint with M. Dafermos and I. Rodnianski)

Gustav Holzegel

Department of Mathematics

Imperial College, London

JGRG Hirosaki, November 7th, 2013

Slide 1

Overview

1. Dynamical Formulation of General Relativity
2. Black Hole Stability Problem
3. Construction of Dynamical Black Holes

Slide 2

The dynamical formulation of General Relativity

Recall that the vacuum Einstein equations

$$R_{\mu\nu} = 0$$

admit a geometric initial value formulation ("**Cauchy problem**"):

$$(\Sigma, h_{\mu\nu}, K_{\mu\nu}) + \text{constraints} \to (\mathcal{M}, g_{\mu\nu}) \text{ satisfying } R_{\mu\nu} = 0.$$

This is the natural setting to construct general solutions and to discuss the notion of stability. What are the properties of the maximum development of a given initial data set?

Slide 3

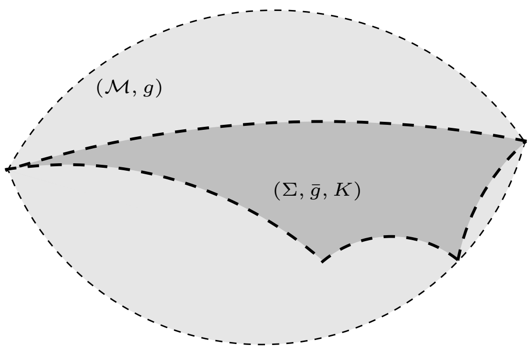

[Choquet-Bruhat, Geroch]

Slide 4

Similarly, there is a '**characteristic initial value problem**" where initial data are being posed on (what will be) null-hypersurfaces of the spacetime.

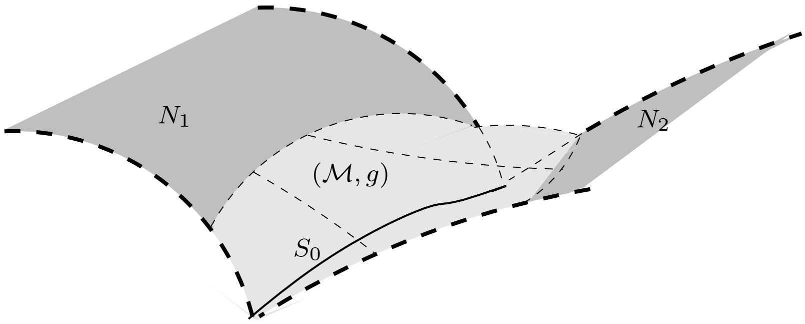

[Rendall, Chrusciel, Luk]

Slide 5

The Black Hole Stability Problem

The Kerr family of solutions $(\mathcal{M}, g_{M,a})$ is believed to play the central role as the final state for vacuum gravitational collapse. The $(\mathcal{M}, g_{M,a})$ satisfy

$$R_{\mu\nu} = 0\,.$$

Do sufficiently small perturbations of Kerr initial data converge

- to a black hole solution?
- another Kerr solution (outside the event horizon)?

This question is still wide open. The only non-linear global stability result of this type (in the asymptotically flat context) is the celebrated "Stability of the Minkowski space" (Christodoulou-Klainerman, Lindblad-Rodnianski).

Slide 6

Common Folklore

- "The Positive Mass Theorem implies stability of Minkowski space" **Positive mass has nothing to do with stability.** Stability of Minkowski space holds even for $R_{\mu\nu} - \frac{1}{2}Rg_{\mu\nu} = -8\pi T_{\mu\nu}$ with $T_{\mu\nu}$ the energy momentum tensor of a scalar field. On the other hand, a PM exists for anti de Sitter space: AdS is a "ground state" and yet (believed to be) classically non-linearly unstable.
- "Extreme black holes are stable" **Stability has nothing to do with being supersymmetric or not.** (see work of Aretakis; Poster 33 by Murata et al)
- "The stability of the Kerr solution is known/ proven." (Only *mode stability* known (Whiting). Not even *linear* stability is known!)

Slide 7

Why the stability problem is hard...

As a PDE, we think of $R_{\mu\nu} = 0$ as $(R = D\Gamma + \Gamma\Gamma)$

$$\Box_g g_{\mu\nu} = (\partial g)^2$$

a coupled system of non-linear wave equations. Even understanding this system around flat space is hard (Stability of Minkowski space is a 500 page book!). The key is to use the **dispersion of linear waves** to control the non-linearities.

In the black hole problem, you have

- final state has fewer symmetries
- final state unknown; not all components of curvature decay
- more complicated geometry (trapping, redshift, superradiance)

Slide 8

The idea is to first understand appropriate *linearized* problems:

- system of gravitational perturbations
- Maxwell
- The wave equation ("poor man's linearization"), $\Box_g \psi = 0$.

There is a huge body of work in the physics literature, including the famous monograph of Chandraskehar.

This is based on mode analysis and doesn't tell you anything about the behavior of general solutions.

Robust tools needed, based on understanding the geometry.

Slide 9

Intense research over the past ten years recently culminated in a complete understanding of $\Box_g \psi = 0$ for g a sub-extremal member of the Kerr family ($|a| < M$) by Dafermos and Rodnianski:

Solutions to the linear wave equation $\Box_g \psi = 0$ for g a fixed sub-extremal Kerr background **decay polynomially in time** *on the black hole exterior, including along the event horizon.*

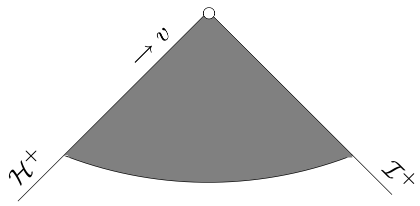

$|\phi| \leq \frac{C}{t}$ for $r > 2M$ and $|\phi| \leq \frac{C}{v}$ for $2M \leq r \leq 3M$

Slide 10

Extremal Case: Instability! Aretakis; Lucietti, Murata, Reall, Tanahashi

This can be generalized to the case of a cosmological constant.

$$\Box_g \psi = 0$$

- de Sitter: **exponential decay** for Kerr-de Sitter (Dafermos-Rodnianski, Melrose, Dyatlov)
- anti de Sitter: **logarithmic decay** for Kerr-anti de Sitter (G.H.-Smulevici)

These results are suggestive for the non-linear problem.

Slide 11

This concludes Part II of the talk.

The non-linear problem is still quite far away. However, there is a simpler question which has not been answered satisfactorily:

Do there exist *any* non-trivial spacetimes converging in time to a member of the Kerr family?

There are examples arising from toy-problems in symmetry classes:

- spherically-symmetric self-gravitating scalar field in 4d [Christodoulou, Dafermos-Rodnianski]; polynom. decay to Schwschild
- vacuum in 5d with bi-axial symmetry; polynomial decay to Schwarzschild [G.H]
- Robinson-Trautman metrics [Chrusciel]; exponential convergence to Schwarzschild

Slide 12

The main result of this talk is the following

Theorem 1. *There exists a large class of smooth vacuum black hole spacetimes which asymptote in time to a Kerr spacetime for any choice of parameters $|a| \leq M$.*

- no symmetry assumptions
- full functional degrees of freedom (for characteristic IVP)
- *exponential* convergence in time to Kerr (non-generic!)
- extremal case included

Slide 13

The construction proceeds by constructing appropriate "finite" problems and then show convergence:

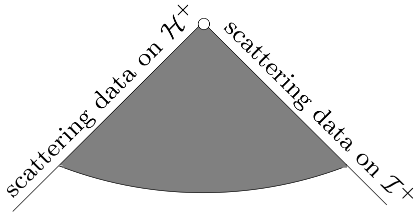

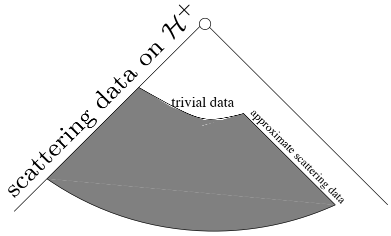

Of course, establishing uniform estimates for the finite backwards problem is key.

Note that one of the main difficulties of the stability problem is absent here: Final state is a-priori presribed!

Slide 14

Remarks

Difference with the stability problem: Now not trying to control arbitrary solutions arising from Cauchy data but constructing *special solutions* from infinity.

The solutions decay to a fixed Kerr solution **exponentially fast**, while generic solutions will decay only polynomially in time.

In this sense, the set of spacetimes constructed in this way is small.

I'll explain to you why the exponential decay is necessary (i.e. why the construction from infinity cannot do better).

Slide 15

On the other hand, the set of spacetimes thus constructed is **large** in the sense that all free functions in the characteristic problem are indeed "free" **except that they have to decay exponentially**.

You can think of the data prescribed as parametrizing how radiation leaves the spacetime.

Again: No symmetry assumptions!

Slide 16

The reason for the exponential decay can be traced back to the blue-shift effect:

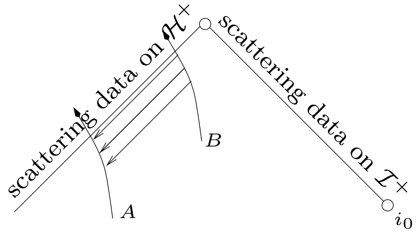

At the level of the analysis, this can already be seen for the linear wave equation $\Box_g \Psi = 0$.

Slide 17

$$T_{\mu\nu} = \partial_\mu \psi \partial_\nu \psi - \frac{1}{2} g_{\mu\nu} (\partial\psi)^2$$
$$\nabla^\mu (T_{\mu\nu} X^\nu) = T_{\mu\nu}{}^{(X)}\pi^{\mu\nu} .$$

Applying this with a vectorfield X everywhere timelike on the exterior [in order to produce non-degenerate energies! $T_{\mu\nu} n^\mu n^\nu \sim |D\psi|^2$], one sees that

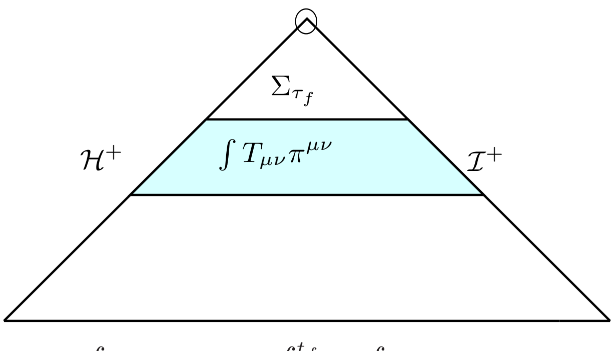

$$\int_{\Sigma_t} |D\psi|^2 \leq C \int_t^{t_f} d\bar{t} \int_{\Sigma_{\bar{t}}} |D\psi|^2 + \text{“}data\text{”}$$

Slide 18

The constant of the bad forcing term is related to the surface gravity of the horizon. From Gronwall's inequality, it is then easy to see that imposing sufficiently strong exponential decay can be propagated.

Remark

Note that we are dealing with *non-degenerate* energies here. For Schwarzschild, one could actually work with the degenerate energies arising from ∂_t and construct an isomorphism between scattering data on $\mathcal{H}^+$ and $\mathcal{I}^+$ and data on Σ_0, cf. Dimock et al.

For Kerr or for a non-linear wave equation on Schwarzschild this breaks down which is why we work with non-degenerate energies from the beginning.

Slide 19

The analogy with the linear wave equation, explains the exponential decay.

- only the "naive" energy estimate is used – in particular, no symmetries/ approximate Killing properties
- the complicated geometry of the black hole exterior (superradiance, trapping) does not enter
- Schwarzschild- and Kerr are "equally difficult"

Slide 20

The full problem

- fix differentiable structure of Schwarzschild/ Kerr, want to equip the manifold with metrics expressed in double null coordinates
- mixed characteristic/ Cauchy problem (data: conformal geometry of the cones [Rendall, Christodoulou])
- in order to estimate solutions need appropriate formulation:

$$\nabla^\alpha W_{\alpha\beta\gamma\delta} = 0 \qquad \text{Bianchi equations}$$

$$\nabla\Gamma + \Gamma\Gamma = W \qquad \text{(null)-structure equations}$$

- Renormalization of these equations: Substract Schwarzschild/ Kerr values from components of Γ and W.

Cf. Newman Penrose. We're doing estimates!

Slide 21

The estimates

For the Bianchi equations, you do (weighted) energy estimates providing in particular decay estimates for L^2-curvature fluxes.

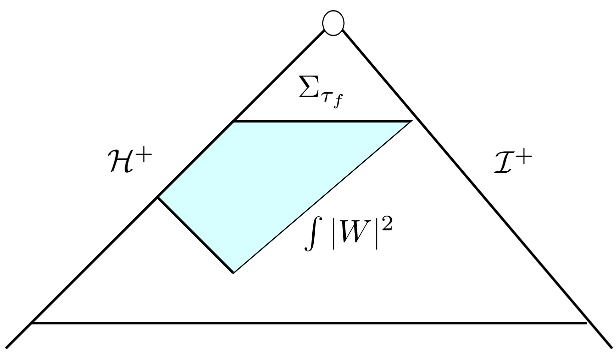

Given the curvature fluxes, you can estimate the Γ's from the transport equations.

Slide 22

Everything is coupled $\rightarrow$ large bootstrap.

Crucial Ingredients

- exponential decay required by blue-shift near the event horizon
- understanding the non-linearities of the Einstein equation near null-infinity (null-condition, hierarchy)

Slide 23

Final comments I

- We constructed a class of smooth dynamical black hole solutions without symmetry depending on the full scattering data. (Previously: symmetry classes & Robinson-Trautman [Chrusciel])
- Some of the estimates, as well as the formalism established, may be useful for the forward problem
- relation with "ultimately Schwarzschildean spacetimes" [G.H]
- Generalization to de Sitter and Anti-de Sitter black holes: Understand boundary initial value-problem cf. [Friedrich, G.H.-Smulevici]
- better results (polynomial decay) in the extremal case?

Slide 24

Final comments II

What about polynomial decay? The theorem is believed to be sharp in the following sense:

Conjecture 1. *Blue shift-conjecture: For* generic*, polynomially decaying scattering data there does* **not** *exist a spacetime* (M, g) *"bounded" by* $\mathcal{H}^+$ *and* $\mathcal{I}^+$ *and smooth up to* $\mathcal{H}^+$*.*

Note the word "generic"! You have to be very lucky to pick data such that you CAN find an infilling solution!

Slide 25

THANK YOU!

Slide 26

Let us turn to the full problem (for Schwarzschild). Particularly important is an appropriate *formulation of the equations*, which involves the issue of *renormalization.* We formulate the vacuum Einstein equations as

$$\nabla^{\alpha} W_{\alpha\beta\gamma\delta} = 0 \qquad \text{Bianchi equations}$$

$$\nabla\Gamma + \Gamma\Gamma = W \qquad \text{(null)-structure equations}$$

null decomposition + renormalization

Slide 27

One fixes the differentiable structure of the Schwarzschild manifold and wants to equip the manifold with metrics of the form

$$g = -4\Omega^2 du dv + \not{g}_{CD}\left(d\theta^C + b^C dv\right)\left(d\theta^D + b^D dv\right)$$

corresponding to a double-null foliation. [In Schwschild $\Omega^2 = 1 - \frac{2M}{r}$, $\not{g} = r^2\,(u,v)\,\gamma$, $b = 0$. We can write the metric arising from the mixed IVP locally in this way (Rendall, Christodoulou). We null-decompose with respect to the foliation and <u>renormalize</u> all quantities (Γ, ψ) with respect to their Schwarzschild values and finally obtain a system of hyperbolic and transport equations for *decaying* quantities:

$$\not{\nabla}_3 \psi = \not{\mathcal{D}}\tilde{\psi} + \Gamma\psi \quad , \quad \not{\nabla}_4 \tilde{\psi} = \not{\mathcal{D}}\psi + \Gamma\psi$$

and

$$\not{\nabla}_3 \Gamma = \Gamma\Gamma + \psi \quad , \quad \not{\nabla}_4 \Gamma = \Gamma\Gamma + \psi$$

Slide 28

The proof proceeds as follows.

1. estimate the curvature on spacelike and null-hypersurfaces (fluxes) via energy estimates from the null-Bianchi equations.
2. estimate the Ricci-coefficients *on the spheres* $S^2(u,v)$ from the transport equations using the curvature fluxes.
3. "Bootstrap" appropriate exponential decay of these norms

Step 1: r-weighted estimates + null-structure in the non-linearities
Step 2: requires another important null structure

Slide 29

The estimates for the Bianchi equations are done separately for each "Bianchi pair" (see "ultimately Schwarzschildean spacetimes" [G.H]).

In fact, we first provide a systematic formulation of the equations.

$$\nabla\!\!\!/_3 \psi_p = \mathcal{D}\!\!\!/\, \psi'_{p'} + E_3[\psi_p] \tag{1}$$

$$\nabla\!\!\!/_4 \psi'_{p'} + \gamma_4(\psi'_{p'})\, tr\chi\, \psi'_{p'} = \mathcal{D}\!\!\!/\, \psi_p + E_4[\psi'_{p'}] \tag{2}$$

with the index p indicating the radial decay at null-infinity.

Structure of equations (i.e. their p-decay) is *preserved* under commutation with the operators $\{\nabla\!\!\!/_3, r\nabla\!\!\!/_4, r\nabla\!\!\!/\}$.

Slide 30

Systematic formulation of the null-structure equations:

$$\nabla\!\!\!/_3 \overset{(3)}{\Gamma}_p = \sum_{p_1+p_2\geq p} (f_{p_1} + \Gamma_{p_1})\,\Gamma_{p_2} + \psi_p$$

$$\nabla\!\!\!/_4 \overset{(4)}{\Gamma}_p = \boxed{\sum_{p_1+p_2=p+1} f_{p_1} \overset{(3)}{\Gamma}_{p_2}} + \sum_{p_1+p_2\geq p+2} (f_{p_1} + \Gamma_{p_1})\,\Gamma_{p_2} + \psi_{p+2}$$

Note the gain of two powers in the 4-direction except for the anomalous boxed term. The key observation is that whenever a boxed term appears, the Γ_p involved satisfies an equation in the 3 direction!

This structure is preserved under commutation with $\{\nabla\!\!\!/_3, r\nabla\!\!\!/_4, r\nabla\!\!\!/\}$!

Slide 31

Think as follows

$$\int_{S^2(u,v)} r^{2p-2}|\Gamma_p|^2\sqrt{g\!\!\!/}d^2\theta \leq data + \int_u^{u_{hoz}} d\bar{u} \int_{S^2} r^{2p-2}|\psi_p|^2\sqrt{g\!\!\!/}d^2\theta$$
$$+ \int_u^{u_{hoz}} d\bar{u} \int_{S^2} r^{2p-2}|\Gamma_p|^2\sqrt{g\!\!\!/}d^2\theta$$

Insert bootstrap assumptions... No loss in r! In the other direction,

$$\int_{S^2(u,v)} r^{2q-2}|\Gamma_p|^2\sqrt{g\!\!\!/}d^2\theta \leq data + \int_v^{v_\infty} d\bar{v} \int_{S^2} r^{2q-2}|\psi_{p+2}|^2\sqrt{g\!\!\!/}d^2\theta$$
$$+ \int_v^{v_\infty} d\bar{v} \int_{S^2} \boxed{\frac{1}{r^2}} r^{2q-2}|\Gamma_p|^2\sqrt{g\!\!\!/}d^2\theta$$

The $\frac{1}{r^2}$ is necessary for integrability near infinity! For the $\frac{1}{r}$-term, $r^{2q-2}|\Gamma_p|^2$ will decay in r to ensure integrability and a smallness factor comes from the fact that the Γ_p involved has already been improved in the 3-direction.

Slide 32

This is, schematically, how the bootstrap assumptions can be improved. It essentially works because the bad linear terms (caused by the blueshift) can be estimated by choosing the exponential rate that is bootstrapped sufficiently large:

$$C \int_{t_1}^{t_2} dt \int_{\Sigma_t} |D\psi|^2 \leq C \frac{1}{A} e^{-At}$$

while all non-linear error-terms can be made small by choosing the t_0 of the bottom slice large. However, recall that understanding the radial decay was crucial!

Slide 33

This gives uniform control for every solution arising from $t_0 < t_f < \infty$. The final step is to obtain convergence. For this one needs to compare (i.e. identify) two spacetimes. The fixed differentiable structure provides a natural setting to do this.

One considers differences of null-structure and Bianchi equations and repeats the estimates. There is a slight simplification if one is willing to use elliptic estimates.

Slide 34

“Destroying the event horizon of regular black holes”

by Zilong Li

[JGRG23(2013)110703]

Destroying the Event Horizon of Regular Black Holes

JGRG23 @ Hirosaki University

Zilong Li

Fudan University

7 Nov. 2013

This talk is mainly based on Z. Li & C. Bambi, PRD 87, 124022 (2013).

Pioneer Works

- One can overspin (overcharge) a near extremal Kerr (Reissner -Nordstrom) black hole by throwing in a test particle, as long as the back reaction effects may be considered negligible.
  —— [V. Hubeny, PRD 59, 064013 (1999); T. Jacobson & T. Sotiriou, PRL 104, 021101 (2010)]

- For all orbits capable of producing naked singularities, the conservative self-force is non-negligible and seems to have the right sign to prevent the particles from being captured, thus saving the cosmic censorship conjecture.
  —— [E. Barausse et al., PRL 105, 261102 (2010); P. Zimmerman et al., arXiv:1211.3889]

Spacetime Metric

The line element in Boyer-Lindquist coordinates can be written as

$$ds^2 = g_{tt}dt^2 + g_{rr}dr^2 + g_{\theta\theta}d\theta^2 + 2g_{t\phi}dtd\phi + g_{\phi\phi}d\phi^2 \,,$$

the non-vanishing spacetime metric coefficients are

$$g_{tt} = -\left(1 - \frac{2mr}{\Sigma}\right) \,, \quad g_{rr} = \frac{\Sigma}{\Delta} \,,$$

$$g_{t\phi} = -\frac{2amr\sin^2\theta}{\Sigma} \,, \quad g_{\theta\theta} = \Sigma \,,$$

$$g_{\phi\phi} = \left(r^2 + a^2 + \frac{2a^2mr\sin^2\theta}{\Sigma}\right)\sin^2\theta \,,$$

$$\text{where} \quad \Sigma = r^2 + a^2\cos^2\theta \,, \quad \Delta = r^2 - 2mr + a^2 \,.$$

Black holes vs. Regular black holes

In the metric coefficients, the mass term m is given by

$$m_{\rm Kerr} = M \qquad \text{Kerr Black Holes (KBHs)},$$

$$m_{\rm KN} = M - \frac{Q^2}{2r} \qquad \text{Kerr-Newman Black Holes (KNBHs)},$$

$$m_{\rm B} = \frac{Mr^3}{(r^2+g^2)^{3/2}} \qquad \text{Bardeen Black Holes (BBHs)},$$

$$m_{\rm H} = \frac{Mr^3}{r^3+g^3} \qquad \text{Hayward Black Holes (HBHs)}.$$

The event horizon of black holes can be obtained by solving $\Delta = 0$.
[C. Bambi & L. Modesto, PLB 721, 329 (2013)]

Test-particle approximation

One can imagine an experiment in which a black hole absorbs a small particle of energy E, angular momentum L, and electric charge $q = 0$.

- Absorption condition:

$$E \geq \frac{-g_{t\phi} L}{g_{\phi\phi}} \, ;$$

- Destroying condition:

$$\Delta(r) = 0 \quad \text{has no solutions} \, .$$

Once these two conditions are satisfied, the test particle can be plunged into the black hole and destroy its event horizon.

Test-particle approximation: KNBHs

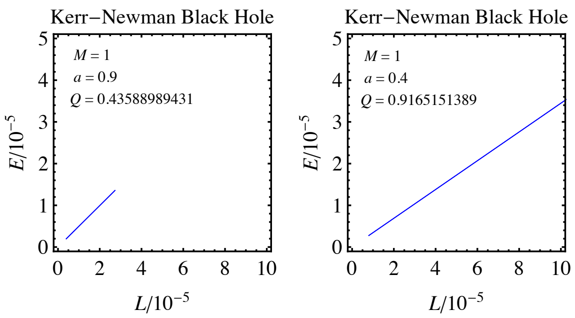

Combination of $(E,\, L)$ that can destroy a near extremal black hole. The allowed energy range of E is of order L^2/M^3, which is comparable to the correction of the self-force. [E. Barausse et. al, PRD 84, 104006 (2011); S. Gao and Y. Zhang, PRD 87, 044028 (2013)] That is, the horizon of the Kerr-Newman black hole survived.

Test-particle approximation: BBHs & HBHs

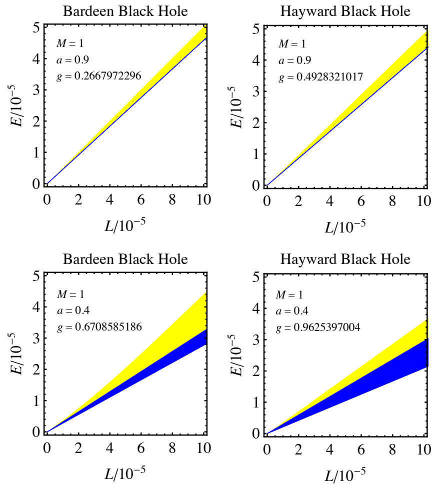

The horizon of the Bardeen/Hayward black hole can be destroyed.

Thin disk accretion process

In the case of a thin disk on the equatorial plane, the neutral gas reaches the innermost stable circular orbit (ISCO) and it then plunges quickly onto the compact object, which changes its mass M and spin J by

$$M \to M + \delta M\,, \quad J \to J + \delta J\,,$$

where

$$\delta M = \epsilon_{\rm ISCO}\delta m\,, \quad \delta J = \lambda_{\rm ISCO}\delta m\,,$$

$\epsilon_{\rm ISCO}$ and $\lambda_{\rm ISCO}$ are, respectively, the specific energy and the specific angular momentum of a test-particle at the ISCO, while δm is its rest-mass.

Thin disk accretion process: KNBHs

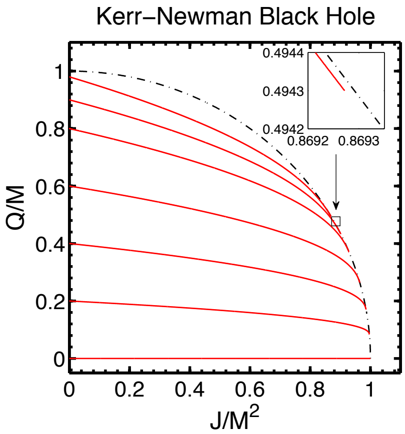

Tracks of the evolution of black holes.

Thin disk accretion process: BBHs & HBHs

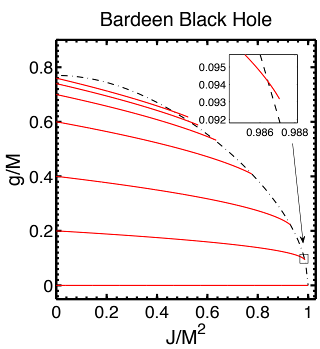

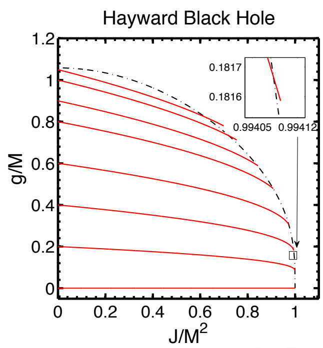

The evolution of the Bardeen/Hayward black hole ends up with horizonless state.

Conclusions

We have presented two different examples strongly suggesting that regular black hole can be destroyed:

Test particle plunging and **thin disk accretion**.

It should be noted that regular black holes have no central singularities. And we can destroy the event horizon because we do not violate the cosmic censorship conjecture. So, our work support this conjecture, but the true reason may be more fundamental and needs further discussion.

Thank You !

“Supersymmetric Plebanski-Demianski solution”

by Masato Nozawa

[JGRG23(2013)110704]

Supersymmetric Plebański-Demiański solution

Masato Nozawa (KEK)

cowork with
Dietmar Klemm (Università di Milano)

based on
D.Klemm and M.N, JHEP 1305 (2013) 123

JGRG23 at Hirosaki Univ.

Introduction

Supersymmetric (BPS) solutions in supergravities

- gravitational backgrounds preserving supersymmetries

  characterized by the existence of Killing spinors ϵ
  obeying 1st-order differential eqs. $\delta\psi_\mu \sim (\nabla_\mu + \cdots)\epsilon = 0\,.$

- attracted much attention in a variety of contexts

  microscopic utilization　　non-perturbative objects

  - theoretical playgrounds for superstrings
    - black hole entropy counting　　Strominger-Vafa 1996
    - AdS/CFT correspondence　　Maldacena 1998

  classical utilization:　　Witten 1981, Nester 1981

  - positive energy theorem a la Witten-Nester
    - stability of ground states

BPS geometry: an example

Einstein-Maxwell theory (bosonic sector of N=2 SUGRA)

$$L = R - F_{\mu\nu}F^{\mu\nu}\,. \qquad \hat{\nabla}_\mu \epsilon = \left(\nabla_\mu + \frac{\mathrm{i}}{4} F_{\nu\rho}\gamma^{\nu\rho}\gamma_\mu\right)\epsilon = 0\,.$$

Gibbons-Hull 1992

Majumbdar-Papapetrou solution

$$\mathrm{d}s^2 = -H^{-2}\mathrm{d}t^2 + H^2 \mathrm{d}\vec{x}^2\,, \quad \Delta H = 0\,, \quad F = \mathrm{d}(H^{-1}) \wedge \mathrm{d}t$$

$\epsilon = H^{-1}\epsilon_0\,,$ ϵ_0 :constant spinor

$\mathrm{i}\gamma^0\epsilon = \epsilon$:half-BPS state ($\mathrm{i}\gamma^0\epsilon = -\epsilon$ is projected out)

- Characteristic properties
  - Mechanical equilibrium $\quad H = 1 + \sum_i^N \frac{Q_i}{|\vec{x} - \vec{x}_i|}$ (N=1 recovers extremal RN)
  - Zero Hawking temperature
  - BPS inequality ($M \geqq Q$) is saturated $\quad M = \sum_i Q_i$
  - Vacuum interpolation

    (analogue of instanton)

$$\left.\begin{array}{l}\text{near horizon: } AdS_2 \times S^2 \\ \text{infinity: Minkowski}\end{array}\right\} \text{Maximal SUSY}$$

BPS solutions

Questions:

- to what extent these properties are universal?

  desirable if we can find *all* BPS solutions

- systematic classification
  - BPS solutions are restrictive $\quad \hat{\nabla}_\mu \epsilon = 0 \qquad \epsilon$: Killing spinor

    Killing spinor eq. is 1st-order & linear

  - various classification schemes

    Newman-Penrose, spinor bilinears, spinorial geometries

    Tod 1983, Gauntlett et al 2002, Gran et al 2004 and many others

  BPS solutions are obtained systematically

  4D, 5D, 6D, 10D (IIA, IIB), 11D supergravities

Our work

- BPS solutions in **gauged** supergravities

  focus on 4D Einstein-Maxwell-Λ(<0) theory

  - important in AdS/CFT correspondence
  - systematic classification is possible   Caldarelli and Klemm 2003

    $\longrightarrow$ the BPS system obeys **nonlinear** set of PDEs

    whole picture of BPS geometries is far from understood

- what we have done

  finding of the most general Petrov D BPS solutions
  (Plabanski-Demianski family)

  explored physical properties

Contents

- Classification of BPS solutions

  bilinear methods

- Supersymmetric Plebanski-Demianski solutions

  BPS conditions

  Wick rotation to Euclidean solutions

- Concluding remarks

4D N=2 gauged supergravity

- Einstein-Maxwell-Λ system

$$S = \frac{1}{16\pi G}\int (R-2\Lambda)\star 1 - 2F\wedge\star F\,, \qquad \Lambda = -3\ell^{-2}\,. \qquad F = \mathrm{d}A\,.$$

- Killing spinor equation

$$\hat{\nabla}_\mu\epsilon \equiv \left(\nabla_\mu + \frac{\mathrm{i}}{4}F_{\nu\rho}\gamma^{\nu\rho}\gamma_\mu + \frac{1}{2\ell}\gamma_\mu - \frac{\mathrm{i}}{\ell}A_\mu\right)\epsilon = 0\,.$$

Kosteleck-Perry 1996

- Killing spinor has a gauge charge

$$A_\mu \to A_\mu + \nabla_\mu\chi\,, \quad \epsilon \to \exp(\mathrm{i}\chi/\ell)\epsilon$$
$$\nabla_\mu \to \nabla_\mu - \mathrm{i}\ell^{-1}A_\mu$$

ℓ^{-1} plays the role of *gauge* coupling

(R-symmetry is made local)

- Λ must be -ve (no deSitter SUGRA)

ℓ^{-1} :gravitino mass

Spinor bilinears

Caldarelli-Klemm '03, M.N '08

Given a Dirac spinor ϵ, one can define spinor bilinears

$$\boxed{E := \bar{\epsilon}\epsilon\,, \quad B := \mathrm{i}\bar{\epsilon}\gamma_5\epsilon\,, \quad V_\mu := \mathrm{i}\bar{\epsilon}\gamma_\mu\epsilon\,, \quad U_\mu := \mathrm{i}\bar{\epsilon}\gamma_5\gamma_\mu\epsilon\,, \quad \Phi_{\mu\nu} := \mathrm{i}\bar{\epsilon}\gamma_{\mu\nu}\epsilon\,,}$$

$$\eta_{ab} = \mathrm{diag}(-1,1,1,1), \quad \bar{\epsilon} \equiv i\epsilon^\dagger\gamma^0$$

A matrix $\epsilon\bar{\epsilon}$ can be expanded in a basis $\Gamma_{(A)} = \{1, \gamma_5, \gamma_\mu, \gamma_5\gamma_\mu, \gamma_{\mu\nu}\}$

$$4\epsilon\bar{\epsilon} = E\mathbf{1} - \mathrm{i}V^\mu\gamma_\mu + \frac{\mathrm{i}}{2}\Phi^{\mu\nu}\gamma_{\mu\nu} + \mathrm{i}U^\mu\gamma_5\gamma_\mu - \mathrm{i}B\gamma_5\,,$$

bilinears satisfy algebraic relations (Fierz identity)

$$V^\mu U_\mu = V^\mu W_\mu = U^\mu W_\mu = 0$$

$\boxed{W_\mu := \epsilon^T C\gamma_\mu\epsilon \ \text{: complex vector}}$

$$-V^\mu V_\mu = U^\mu U_\mu = W^\mu \bar{W}_\mu = E^2 + B^2$$

V is timelike/null

$$EV_\mu = \star\Phi_{\mu\nu}U^\nu\,, \qquad EB = -\tfrac{1}{4}\Phi_{\mu\nu}\star\Phi^{\mu\nu}\,,$$
$$BV_\mu = \Phi_{\mu\nu}U^\nu\,, \qquad E\Phi_{\mu\nu} = -\epsilon_{\mu\nu\rho\sigma}V^\rho U^\sigma + B\star\Phi_{\mu\nu}\,,$$
$$(E^2+B^2)g_{\mu\nu} = -V_\mu V_\nu + U_\mu U_\nu + W_{(\mu}\bar{W}_{\nu)}\,,$$

etc

Differential relations

Suppose ϵ satisfies a KS eq $\hat{\nabla}_\mu \epsilon = \left(\nabla_\mu + \frac{\mathrm{i}}{4} F_{\nu\rho}\gamma^{\nu\rho}\gamma_\mu + \frac{1}{2\ell}\gamma_\mu - \frac{\mathrm{i}}{\ell}A_\mu\right)\epsilon = 0$

e.g, $\nabla_\mu E = \overline{\nabla_\mu \epsilon}\epsilon + \bar{\epsilon}\nabla_\mu \epsilon$

$= \frac{\mathrm{i}}{4} F_{ab}\bar{\epsilon}[\gamma_\mu, \gamma^{ab}]\epsilon = F_{\mu\nu}V^\nu$ E: electric potential

$$\nabla_\mu B = -\frac{1}{\ell}U_\mu - \star F_{\mu\nu}V^\nu ,$$

B: magnetic potential

$$\nabla_\mu V_\nu = \frac{1}{\ell}\Phi_{\mu\nu} - EF_{\mu\nu} + B \star F_{\mu\nu} ,$$
$$\nabla_\mu U_\nu = -\frac{1}{\ell}Bg_{\mu\nu} - 2F_{(\mu}{}^\rho \star \Phi_{\nu)\rho} + \frac{1}{2}g_{\mu\nu}F_{\rho\sigma} \star \Phi^{\rho\sigma} ,$$
$$\nabla_\mu \Phi_{\nu\rho} = \frac{2}{\ell}g_{\mu[\nu}V_{\rho]} - (U_\mu \star F_{\nu\rho} + 2\epsilon_{\nu\rho\sigma[\mu}F_{\tau]}{}^\sigma U^\tau) .$$
$$\nabla_\mu W_\nu = -\frac{\mathrm{i}}{2}\epsilon^T C\gamma_{(\mu}\gamma^{\rho\sigma}\gamma_{\nu)}\epsilon F_{\rho\sigma} + \frac{1}{\ell}\epsilon^T C\gamma_{\mu\nu}\epsilon + \frac{2\,\mathrm{i}}{\ell}A_\mu \epsilon^T C\gamma_\nu \epsilon .$$

Differential relations

Suppose ϵ satisfies a KS eq $\hat{\nabla}_\mu \epsilon = \left(\nabla_\mu + \frac{\mathrm{i}}{4} F_{\nu\rho}\gamma^{\nu\rho}\gamma_\mu + \frac{1}{2\ell}\gamma_\mu - \frac{\mathrm{i}}{\ell}A_\mu\right)\epsilon = 0$

e.g, $\nabla_\mu E = \overline{\nabla_\mu \epsilon}\epsilon + \bar{\epsilon}\nabla_\mu \epsilon$

$= \frac{\mathrm{i}}{4} F_{ab}\bar{\epsilon}[\gamma_\mu, \gamma^{ab}]\epsilon = F_{\mu\nu}V^\nu$ E: electric potential

$$\nabla_\mu B = -\frac{1}{\ell}U_\mu - \star F_{\mu\nu}V^\nu ,$$

B: magnetic potential

$$\nabla_\mu V_\nu = \frac{1}{\ell}\Phi_{\mu\nu} - EF_{\mu\nu} + B \star F_{\mu\nu} , \quad \longrightarrow \quad \nabla_{(\mu}V_{\nu)} = 0 ,$$: Killing vector

$$\nabla_\mu U_\nu = -\frac{1}{\ell}Bg_{\mu\nu} - 2F_{(\mu}{}^\rho \star \Phi_{\nu)\rho} + \frac{1}{2}g_{\mu\nu}F_{\rho\sigma} \star \Phi^{\rho\sigma} ,$$

BPS sols. are stationary

$$\nabla_\mu \Phi_{\nu\rho} = \frac{2}{\ell}g_{\mu[\nu}V_{\rho]} - (U_\mu \star F_{\nu\rho} + 2\epsilon_{\nu\rho\sigma[\mu}F_{\tau]}{}^\sigma U^\tau) .$$
$$\nabla_\mu W_\nu = -\frac{\mathrm{i}}{2}\epsilon^T C\gamma_{(\mu}\gamma^{\rho\sigma}\gamma_{\nu)}\epsilon F_{\rho\sigma} + \frac{1}{\ell}\epsilon^T C\gamma_{\mu\nu}\epsilon + \frac{2\,\mathrm{i}}{\ell}A_\mu \epsilon^T C\gamma_\nu \epsilon .$$

Differential relations

Suppose ϵ satisfies a KS eq $\quad \hat{\nabla}_\mu \epsilon = \left(\nabla_\mu + \frac{\mathrm{i}}{4} F_{\nu\rho}\gamma^{\nu\rho}\gamma_\mu + \frac{1}{2\ell}\gamma_\mu - \frac{\mathrm{i}}{\ell} A_\mu \right) \epsilon = 0$

e.g, $\quad \nabla_\mu E = \overline{\nabla_\mu \epsilon}\epsilon + \bar{\epsilon}\nabla_\mu \epsilon$

$$= \frac{\mathrm{i}}{4} F_{ab}\bar{\epsilon}[\gamma_\mu, \gamma^{ab}]\epsilon = F_{\mu\nu}V^\nu$$

E: electric potential

$$\nabla_\mu B = -\frac{1}{\ell}U_\mu - \star F_{\mu\nu}V^\nu \,,$$

B: magnetic potential

$$\nabla_\mu V_\nu = \frac{1}{\ell}\Phi_{\mu\nu} - EF_{\mu\nu} + B \star F_{\mu\nu} \,, \quad \longrightarrow \quad \nabla_{(\mu}V_{\nu)} = 0 \,,$$

: Killing vector

BPS sols. are stationary

$$\nabla_\mu U_\nu = -\frac{1}{\ell}Bg_{\mu\nu} - 2F_{(\mu}{}^\rho \star \Phi_{\nu)\rho} + \frac{1}{2}g_{\mu\nu}F_{\rho\sigma} \star \Phi^{\rho\sigma} \,,$$

$$\nabla_\mu \Phi_{\nu\rho} = \frac{2}{\ell}g_{\mu[\nu}V_{\rho]} - \left(U_\mu \star F_{\nu\rho} + 2\epsilon_{\nu\rho\sigma[\mu}F_{\tau]}{}^\sigma U^\tau \right) .$$

$$\nabla_\mu W_\nu = -\frac{\mathrm{i}}{2}\epsilon^T C\gamma_{(\mu}\gamma^{\rho\sigma}\gamma_{\nu)}\epsilon F_{\rho\sigma} + \frac{1}{\ell}\epsilon^T C\gamma_{\mu\nu}\epsilon + \frac{2\,\mathrm{i}}{\ell}A_\mu \epsilon^T C\gamma_\nu \epsilon \,.$$

- solutions fall into 2 family
  - timelike class (black holes) $\quad V^\mu V_\mu < 0$
  - null class (plane waves) $\quad V^\mu V_\mu = E = B = 0$

Timelike class in ungauged sugra (Λ=0)

Tod '83, M.N '08

Suppose V is timelike

$$-V^\mu V_\mu = U^\mu U_\mu = W^\mu \bar{W}_\mu = E^2 + B^2$$

$$(E^2 + B^2)g_{\mu\nu} = -V_\mu V_\nu + U_\mu U_\nu + W_{(\mu}\bar{W}_{\nu)} \,, \quad \longrightarrow$$

(V, U, W) constitutes basis

- diff-cond. for (V, U, W) gives

$$\nabla_{(\mu}V_{\nu)} = 0 \,, \quad \nabla_{[\mu}U_{\nu]} = 0 \quad \nabla_{[\mu}W_{\nu]} = 0$$

$$\longrightarrow \quad V = \partial/\partial t \qquad U = \mathrm{d}z \qquad W = \mathrm{d}x + \mathrm{i}\mathrm{d}y \,.$$

$$\boxed{\mathrm{d}s^2 = -f(\mathrm{d}t + \omega)^2 + f^{-1}(\mathrm{d}x^2 + \mathrm{d}y^2 + \mathrm{d}z^2) \,.} \qquad f = E^2 + B^2$$

- diff-cond. for (E, B) gives $\quad F_{\mu\nu} = f^{-1}\left(2V_{[\mu}\nabla_{\nu]}E + \epsilon_{\mu\nu\rho\sigma}V^\rho \nabla^\sigma B\right) \,,$

$$\mathrm{d}(F + \mathrm{i} \star F) = 0 \quad \longrightarrow \quad \Delta \Psi^{-1} = 0 \qquad \Psi \equiv E - \mathrm{i}B$$

- diff-cond. for V gives ω

$$V = -f(\mathrm{d}t + \omega) \quad \longrightarrow \quad \mathrm{d}\omega = 2 \star [V \wedge (E\mathrm{d}B - B\mathrm{d}E)]$$

Timelike class in ungauged sugra (Λ=0)

- General BPS solutions are given by IWP family   Israel-Wilon, Perjes 1971

$$ds^2 = -|\Psi|^2(dt+\omega)^2 + |\Psi|^{-2}d\vec{x}^2\,, \qquad d\omega = 2\mathrm{Im}(\Psi d\bar{\Psi})\,.$$
$$\Delta\Psi^{-1} = 0\,, \qquad i_V(F - i\star F) = d\Psi\,.$$

Killing spinor equation is solved by

$$\epsilon = \left(\sqrt{E - iB} + i\gamma^0\sqrt{E + iB}\right)\frac{1+\gamma_5}{2}\eta\,,$$ η: constant spinor

$$i\gamma^0\epsilon = f^{-1/2}(E + iB\gamma_5)\epsilon\,.$$: preserves at least 1/2-SUSY

$$\Delta\Psi^{-1} = 0\,,$$: system is completely linearized

Timelike class in gauged supergravity (Λ<0)

Canonical form for timelike family   Caldarelli-Klemm '03

$$\nabla_{(\mu}V_{\nu)} = 0\,,\ \nabla_{[\mu}U_{\nu]} = 0\,,\ \nabla_{[\mu}W_{\nu]} \neq 0 \longrightarrow V = \partial_t\,,\ U = dz\,,\ W = e^{\phi}(dx + idy)$$

$$ds^2 = -f(dt+\omega)^2 + f^{-1}[dz^2 + e^{2\phi}(dx^2 + dy^2)]\,, \qquad f = E^2 + B^2$$

BPS system

$$\Delta F + e^{2\phi}[F^3 + 3FF' + F''] = 0\,,$$
$$\Delta\phi + \frac{1}{2}e^{2\phi}[F' + \bar{F}' + F^2 + \bar{F}^2 - F\bar{F}] = 0\,,$$
$$\phi' - \mathrm{Re}(F) = 0\,,$$

$$F = \frac{2i}{\ell(E - iB)}$$

- need to solve a set of nonlinear PDEs
- in the canonical form, AdS takes nonstandard form

$$ds^2 = \frac{dz^2}{1 + z^2/\ell^2} + (1 + z^2/\ell^2)\left[\underline{-\left(dt + \frac{ydx}{2x^2}\right)^2 + \frac{dx^2 + dy^2}{4x^2}}\right].$$

AdS(3) in SL(2,**R**) bi-invariant form

$V^\mu = i\bar{\epsilon}\gamma^\mu\epsilon = (\partial_t)^\mu$ is not hypersurface-orthogonal

Contents

Plebanski-Demianski solution

Goal: BPS conditions for Plebanski-Demianski family   Plebanski-Demianski '76

- the most general Petrov type D metric with non-null Maxwell field
- 7 parameters (mass,ang-momentum, electric charge, magnetic charge, nut, acceleration, cosmological constant)

$$\mathrm{d}s^2 = \frac{1}{(1-pq)^2}\left[-\frac{Q(q)}{p^2+q^2}(\mathrm{d}\tau - p^2\mathrm{d}\sigma)^2 + \frac{p^2+q^2}{Q(q)}\mathrm{d}q^2 + \frac{p^2+q^2}{P(p)}\mathrm{d}p^2 + \frac{P(p)}{p^2+q^2}(\mathrm{d}\tau + q^2\mathrm{d}\sigma)^2\right],$$

$$\begin{aligned} P(p) &= (-\Lambda/6 - \mathsf{P}^2 + \alpha) + 2np - \varepsilon p^2 + 2mp^3 + (-\Lambda/6 - \mathsf{Q}^2 - \alpha)p^4\,, \\ Q(q) &= (-\Lambda/6 + \mathsf{Q}^2 + \alpha) - 2mq + \varepsilon q^2 - 2nq^3 + (-\Lambda/6 + \mathsf{P}^2 - \alpha)q^4\,. \end{aligned}$$

$$A = \frac{(-p\mathsf{P} + q\mathsf{Q})\mathrm{d}\tau - pq(\mathsf{Q}p + \mathsf{P}q)\mathrm{d}\sigma}{p^2+q^2}\,,$$

- contains many interesting subclasses (Kerr-Newman-AdS, Reissner-Nordstrom-AdS, AdS C-metric)

- Boyer-Lindquist analysis for Kerr-Newman-AdS doesn't work

  (KS eq. depends nontrivially on r & θ)   Caldarelli-Klemm 1999

BPS conditions

▸ BPS conditions for Plebanski-Demianski family   Klemm+MN 2013

$$\mathrm{d}s^2 = \frac{1}{(1-pq)^2}\left[-\frac{Q(q)}{p^2+q^2}(\mathrm{d}\tau - p^2\mathrm{d}\sigma)^2 + \frac{p^2+q^2}{Q(q)}\mathrm{d}q^2 + \frac{p^2+q^2}{P(p)}\mathrm{d}p^2 + \frac{P(p)}{p^2+q^2}(\mathrm{d}\tau + q^2\mathrm{d}\sigma)^2\right],$$

$$P(p) = (-\Lambda/6 - \mathsf{P}^2 + \alpha) + 2np - \varepsilon p^2 + 2mp^3 + (-\Lambda/6 - \mathsf{Q}^2 - \alpha)p^4\,,$$
$$Q(q) = (-\Lambda/6 + \mathsf{Q}^2 + \alpha) - 2mq + \varepsilon q^2 - 2nq^3 + (-\Lambda/6 + \mathsf{P}^2 - \alpha)q^4\,.$$

$$A = \frac{(-p\mathsf{P} + q\mathsf{Q})\mathrm{d}\tau - pq(\mathsf{Q}p + \mathsf{P}q)\mathrm{d}\sigma}{p^2+q^2},$$

necessary conditions for SUSYs

$$\hat{\nabla}_\mu \epsilon \equiv \left(\nabla_\mu + \frac{\mathrm{i}}{4}F_{\nu\rho}\gamma^{\nu\rho}\gamma_\mu + \frac{1}{2\ell}\gamma_\mu - \frac{\mathrm{i}}{\ell}A_\mu\right)\epsilon = 0\,. \longrightarrow \det([\hat{\nabla}_\mu, \hat{\nabla}_\nu]) = 0$$

BPS conditions

$$n[m^2+n^2-(\mathsf{P}^2+\mathsf{Q}^2)\varepsilon] + 2m(\mathsf{P}^2+\mathsf{Q}^2)(\mathsf{P}^2-\alpha) + \frac{1}{\ell^2}\left[2n\mathsf{P}\mathsf{Q} + m(\mathsf{P}^2-\mathsf{Q}^2)\right] = 0\,,$$
$$(\mathsf{P}^2+\mathsf{Q}^2)[m^2\mathsf{P}^2 - n^2\mathsf{Q}^2 - (m^2+n^2)\alpha] + \frac{1}{\ell^2}\left[2mn\mathsf{P}\mathsf{Q} + \frac{1}{2}(\mathsf{P}^2-\mathsf{Q}^2)(m^2-n^2)\right] = 0\,.$$

Bilinears & Killing spinors

▸ BPS conditions for Plebanski-Demianski family   Klemm+MN 2013

$$\mathrm{d}s^2 = \frac{1}{(1-pq)^2}\left[-\frac{Q(q)}{p^2+q^2}(\mathrm{d}\tau - p^2\mathrm{d}\sigma)^2 + \frac{p^2+q^2}{Q(q)}\mathrm{d}q^2 + \frac{p^2+q^2}{P(p)}\mathrm{d}p^2 + \frac{P(p)}{p^2+q^2}(\mathrm{d}\tau + q^2\mathrm{d}\sigma)^2\right],$$

sufficient conditions for SUSY

under BPS conditions, we can find canonical form of BPS metric

$$\mathrm{d}s^2 = -f(\mathrm{d}t+\omega)^2 + f^{-1}[\mathrm{d}z^2 + e^{2\phi}(\mathrm{d}x^2+\mathrm{d}y^2)]\,, \qquad f = E^2 + B^2$$

1/4-SUSY $\quad \epsilon = \frac{1}{4}\exp\left(\frac{i}{\ell}\int A_z \mathrm{d}z\right)(\sqrt{E-iB} + i\gamma^0\sqrt{E+iB})(1-i\gamma^{12})(1+\gamma_5)\eta\,.$

$$V = c_+\partial_\tau - c_-\partial_\sigma\,, \quad c_- = m\mathsf{Q} - n\mathsf{P}\,, \quad c_+ = m\mathsf{P} + n\mathsf{Q}\,, \quad e^{2\phi} = \frac{4c_+^2c_-^2P(p)Q(q)}{(1-pq)^4},$$

$$E = \frac{(\mathsf{P}^2+\mathsf{Q}^2)[c_-pq(p\mathsf{Q}+\mathsf{P}q) - c_+(p\mathsf{P}-q\mathsf{Q})] - c_+c_-(p^2+q^2)}{(p^2+q^2)(\mathsf{P}^2+\mathsf{Q}^2)}, \qquad z = \ell\frac{m^2+n^2-(\mathsf{P}^2+\mathsf{Q}^2)(mp+nq)}{1-pq}.$$

$$B = -\frac{c_-^2pq + c_+^2}{(1-pq)(\mathsf{P}^2+\mathsf{Q}^2)} + \frac{c_+[\mathsf{P}(p^3+q) + \mathsf{Q}(p+q^3)] - c_-[\mathsf{P}q^2(p^3+q) - \mathsf{Q}p^2(p+q^3)]}{(1-pq)(p^2+q^2)},$$

BPS conditions are necessary & sufficient for supersymmetry

Limits

- Carter class   Carter 1968

$$\mathrm{d}s^2 = -\frac{Q(q)}{p^2+q^2}(\mathrm{d}\tau - p^2\mathrm{d}\sigma)^2 + \frac{p^2+q^2}{Q(q)}\mathrm{d}q^2 + \frac{p^2+q^2}{P(p)}\mathrm{d}p^2 + \frac{P(p)}{p^2+q^2}(\mathrm{d}\tau + q^2\mathrm{d}\sigma)^2\,,$$

Kerr-Newman-AdS limit   Alonso-Alberca, Meessen & Ortın 2000

$$q = r\,,\ p = a\cos\theta\,,\quad \sigma = -\frac{\phi}{a\Xi}\,,\ \tau = \tilde t - \frac{a\phi}{\Xi}\,, \qquad n = 0\,,\ \ \varepsilon = 1 + \frac{a^2}{\ell^2}\,,\quad \alpha = a^2 + \mathsf{P}^2\,,$$

$$\longrightarrow \quad \mathrm{d}s^2 = -\frac{\Delta}{\Sigma^2}\left(\mathrm{d}\tilde t - \frac{a\sin^2\theta}{\Xi}\mathrm{d}\phi\right)^2 + \frac{\Sigma^2}{\Delta}\mathrm{d}r^2 + \frac{\Sigma^2}{\Delta_\theta}\mathrm{d}\theta^2 + \frac{\Delta_\theta\sin^2\theta}{\Sigma^2}\left(a\mathrm{d}\tilde t - \frac{r^2+a^2}{\Xi}\mathrm{d}\phi\right)^2,$$

$$m^2 = \left(1 - \frac{a}{\ell}\right)\mathsf{Q}^2\,,\quad \mathsf{P} = 0 \quad \longrightarrow \quad \Delta = \left(\frac{r^2}{\ell} - a\right)^2 + \left[\mathsf{Q} - \left(1 + \frac{a}{\ell}\right)r\right]^2$$

no magnetic charge

naked singularity in general

$$\mathsf{Q} = \sqrt{a\ell}(1 - a/\ell)\,. \quad \longrightarrow \quad r_+ = \sqrt{a\ell}$$

SUSY BH must rotate

- C-metric   Kinnersly 1969

describes pair of accelerating black holes

BPS limit in general gives naked singularity

Euclidean solutions

- Wick rotation gives a solution with Euclidean signature

$$\mathrm{d}s^2 = \frac{1}{(1-pq)^2}\left[\frac{Q(q)}{q^2-\omega^2p^2}(\mathrm{d}\tau - \omega p^2\mathrm{d}\sigma)^2 + \frac{q^2-\omega^2p^2}{Q(q)}\mathrm{d}q^2 + \frac{q^2-\omega^2p^2}{P(p)}\mathrm{d}p^2 + \frac{P(p)}{q^2-\omega^2p^2}(-\omega\mathrm{d}\tau + q^2\mathrm{d}\sigma)^2\right],$$

$$P(p) = k + 2\omega^{-1}np - \varepsilon p^2 + 2mp^3 + (\omega^2 k - \mathsf{P}^2 + \mathsf{Q}^2 + \omega^2\Lambda/3)p^4\,,$$
$$Q(q) = (-\omega^2 k + \mathsf{P}^2 - \mathsf{Q}^2) - 2mq + \varepsilon q^2 - 2\omega^{-1}nq^3 - (k + \Lambda/3)q^4\,.$$

$$k = -\Lambda/6 - \mathsf{P}^2 + \alpha.$$

- complex structures

self-dual 2-form $\quad \Omega = e^1\wedge e^2 + e^3\wedge e^4$

$$e^1 = \sqrt{\frac{Q}{q^2-\omega^2p^2}}\frac{(\mathrm{d}\tau - \omega p^2\mathrm{d}\sigma)}{1-pq}\,,\qquad e^2 = \sqrt{\frac{q^2-\omega^2p^2}{Q}}\frac{\mathrm{d}q}{1-pq}\,,$$
$$e^3 = \sqrt{\frac{q^2-\omega^2p^2}{P}}\frac{\mathrm{d}p}{1-pq}\,,\qquad e^4 = \sqrt{\frac{P}{q^2-\omega^2p^2}}\frac{(-\omega\mathrm{d}\tau + q^2\mathrm{d}\sigma)}{1-pq}\,,$$

$\longrightarrow$

$J\cdot J = -1 \quad : J^\mu{}_\nu := g^{\mu\rho}\Omega_{\nu\rho}$. is almost complex

Nijenhuis tensor: $\quad N_{ab}{}^c \equiv 2\left(J_a{}^d\partial_{[d}J_{b]}{}^c - J_b{}^d\partial_{[d}J_{a]}{}^c\right) = 0\,,$

- almost complex structure J is integrable

  N.B. this does not guarantee the global existence of J

- Ω fails to give a Kähler structure ($\mathrm{d}\Omega\neq 0$)

Euclidean solutions

- Wick rotation gives a solution with Euclidean signature

$$\mathrm{d}s^2 = \frac{1}{(1-pq)^2}\left[\frac{Q(q)}{q^2-\omega^2p^2}(\mathrm{d}\tau-\omega p^2\mathrm{d}\sigma)^2+\frac{q^2-\omega^2p^2}{Q(q)}\mathrm{d}q^2+\frac{q^2-\omega^2p^2}{P(p)}\mathrm{d}p^2+\frac{P(p)}{q^2-\omega^2p^2}(-\omega\mathrm{d}\tau+q^2\mathrm{d}\sigma)^2\right],$$

$$P(p) = k+2\omega^{-1}np-\varepsilon p^2+2mp^3+(\omega^2k-\mathsf{P}^2+\mathsf{Q}^2+\omega^2\Lambda/3)p^4\,,$$
$$Q(q) = (-\omega^2k+\mathsf{P}^2-\mathsf{Q}^2)-2mq+\varepsilon q^2-2\omega^{-1}nq^3-(k+\Lambda/3)q^4\,.$$

$$k=-\Lambda/6-\mathsf{P}^2+\alpha.$$

- BPS conditions

$$n[m^2-n^2-(\mathsf{P}^2-\mathsf{Q}^2)\varepsilon]+2\omega m(\mathsf{Q}^2-\mathsf{P}^2)(\Lambda/6+k)+\frac{\Lambda\omega}{3}\left[2n\mathsf{PQ}-m(\mathsf{P}^2+\mathsf{Q}^2)\right]=0\,,$$

$$(\mathsf{P}^2-\mathsf{Q}^2)[m^2\mathsf{P}^2-n^2\mathsf{Q}^2+(m^2-n^2)(\omega^2k+\Lambda\omega^2/6-\mathsf{P}^2)]+\frac{\Lambda\omega^2}{3}\left[-2mn\mathsf{PQ}+\frac{1}{2}(\mathsf{P}^2+\mathsf{Q}^2)(m^2+n^2)\right]=0\,.$$

Euclidean bilinear relations given by Dunajski-Gutowski-Tod are satisfied for non (anti-)self dual solutions

generalizations of [Martelli-Passian and Sparks arXiv:12124618] to U(1)xU(1) symmetry

Contents

- Classification of BPS solutions

  bilinear methods

- Supersymmetric Plebanski-Demianski solutions

  BPS conditions

  Wick rotation to Euclidean solutions

- Concluding remarks

Concluding remarks

- Summary
  - worked out necessary and sufficient conditions for which the general Plebanski-Demianski family of solution admits Killing spinors
  - Euclidean solutions give a locally complex mfd

- Future outlook
  - PD solutions in matter coupled SUGRA (vector-& hyper-multiplets)
  - another wick rotation ($\ell \to iL$) gives *fake supergravity*

    general solutions: fibration over Gauduchon-Tod space

    Meessen and Palomo-Lozano '09

    - bilinear vector is no longer Killing

“Large D gravity”

by Kentaro Tanabe

[JGRG23(2013)110705]

LARGE D GRAVITY

KENTARO TANABE

UNIVERSITAT DE BARCELONA

(UNIVERSITY OF BARCELONA)

with R. Emparan, ….

WHY LARGE D

dimension (***D***) is a parameter of GR

gravity can be simplified at **high D** or **low D**

[Emparan, Suzuki, KT (2013)]

earlier work on large D gravity

- Large D limit of Feynman graph of gravitons
  [Strominger (1981),…]
- Gregory-Laflamme mode, Shockwave collision
  [Asnin, et.al. (2007), Camps, et.al. (2010), Coelho, et.al. (2012)]
- Large D gravity and 2-D gravity
  [Soda (1993), Grumiller, et.al. (2003)]

focus on the practical aspect of large D gravity

BH AT LARGE D

WHY simplified? → <u>BH has two scales at large D</u>

$$ds^2 = -f(r)dt^2 + f(r)^{-1}dr^2 + r^2\, d\Omega_{D-2}$$

$$f(r) = 1 - \left(\frac{r_0}{r}\right)^{D-3}$$

- ☐ coordinate scale $\simeq r_0$

  size of BH from asymptotic infinity **(far from BH)**

- ☐ physical scale $\simeq r_0/\mathrm{D}$

  gradient of potential, temperature of BH **(near BH)**

METHOD

we can use the ***<u>Matched Asymptotic Expansion (MAE)</u>***

$$r_0/D \ll r_0$$

near region | **far region**

- GR ~ gravity in 2-D
- 1/D expansion

- BH~ point particle
- Newtonian approximation

overlap region: $\frac{r_0}{D} \ll r - r_0 \ll r_0$

⇨ <u>MAE can be good approximation at large D</u>

EXAMPLE

Gregory-Laflamme instability

[Asnin, et.al. (2007), Emparan, Suzuki, KT (2013)]

- instability of black brane

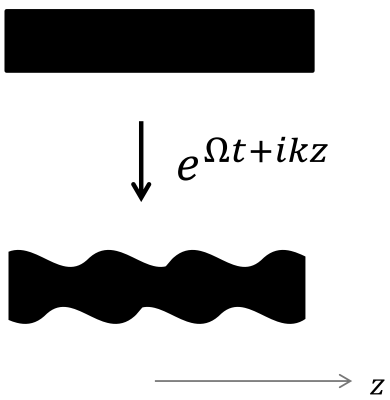

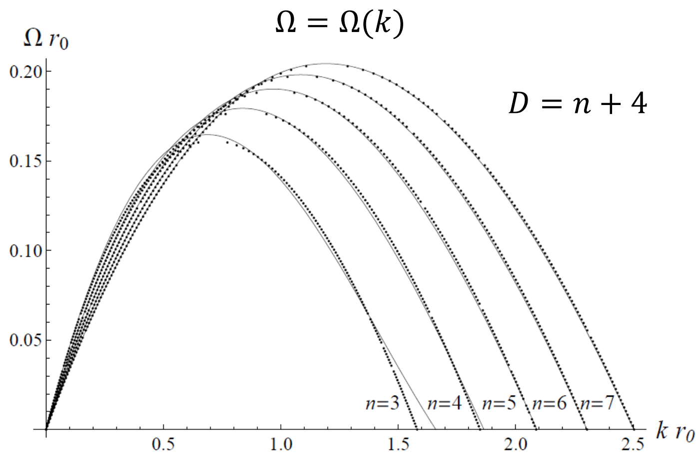

numerical results by P. Figueras

PURPOSE

Large D gravity is useful method to solve the **(any)** gravitational problem

To demonstrate it more,

- apply to QuasiNormal Modes (QNMs)

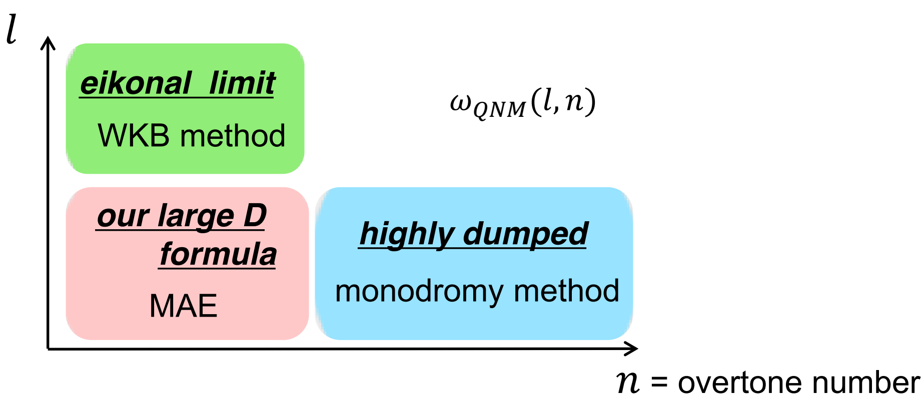

QNM IN LARGE D

BACKGROUND

D-dim Schwarzschild BH

$$ds^2 = -f(r)dt^2 + f\,(r)^{-1}dr^2 + r^2\,d\Omega_{D-2}$$

$$f(r) = 1 - \left(\frac{r_0}{r}\right)^{D-3}$$

tensor

perturbation → vector → Schrodinger type eq

scalar

[Kodama and Ishibashi (2003)]

PERTURBATION EQ.

perturbation equation for the **tensor type**

$$\left(\frac{d^2}{d{r_*}^2} + \omega^2 - V(r)\right)\psi(r) = 0$$

$$dr_* = dr/f(r)$$

potential:

$$V(r) = f(r)\left(\frac{l(l+D-3)}{r^2} + \frac{(D-2)(D-4)}{4r^2}f(r) + \frac{D+2}{2r}f'(r)\right)$$

$$f(r) = 1 - \left(\frac{r_0}{r}\right)^{D-3}$$

WHERE IS QNM?

QNMs

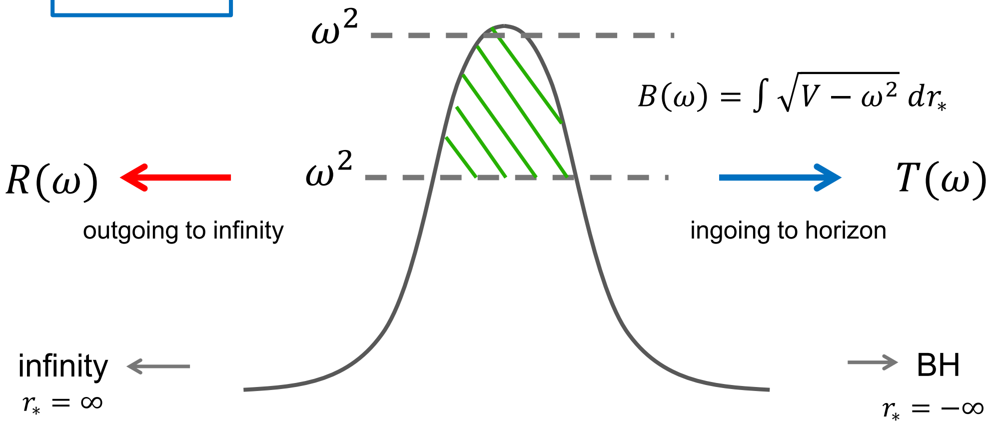

QNM condition: $T(\omega) \simeq R(\omega)$ [Schutz and Will (1985)]

$$T(\omega) \simeq e^{-B(\omega)} R(\omega)$$

TOP OF POTENTIAL

Thus QNMs exists around

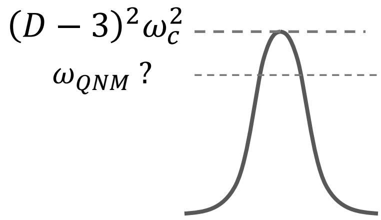

$$\omega_{QNM} \simeq (D-3)\,\omega_c$$

where

$$\boxed{\omega_c r_0 = \frac{2\hat{l}+1}{2} + O(D^{-1})} \quad \text{(critical frequency)}$$

$$\hat{l} = \frac{l}{D-3}$$

$$V(r) = f(r)\left(\frac{l(l+D-3)}{r^2} + \frac{(D-2)(D-4)}{4r^2}f(r) + \frac{D+2}{2r}f'(r)\right)$$

POTENTIAL SHAPE

Near the top of the potential

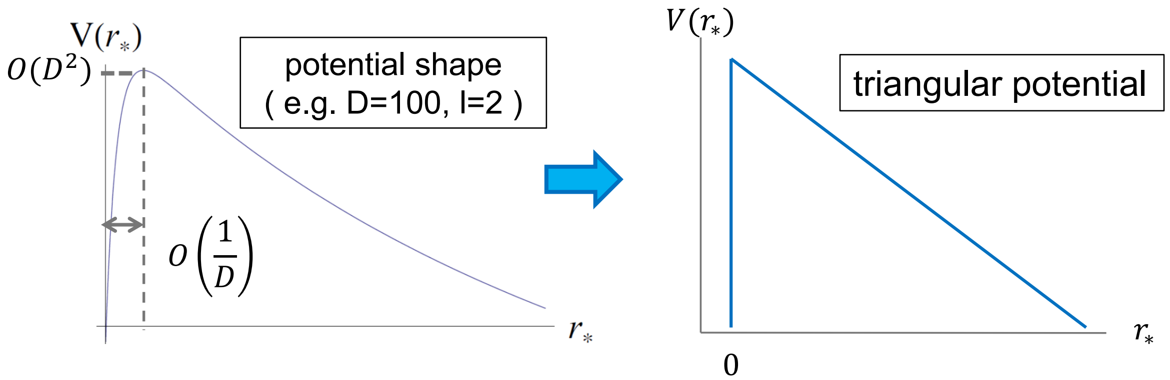

$$V(r) = f(r)\left(\frac{l(l+D-3)}{r^2} + \frac{(D-2)(D-4)}{4r^2}f(r) + \frac{D+2}{2r}f'(r)\right)$$

TRIANGULAR POTENTIAL

we approximate V(r) by triangular potential

QNM will exist around

$$\omega_{QNM} = (D-3)\omega_c(\,1\; + \underbrace{\delta\omega}_{\text{correction}}\,)$$

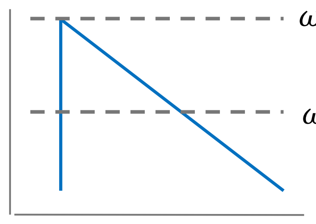

$$\left(\frac{d^2}{d{r_*}^2} + \omega^2 \; - V(r)\right)\psi\,(r) = 0$$

$$\Downarrow$$

$$\left(\frac{d^2}{d{r_*}^2} + (D-3)^2\omega_c\,(\,\delta\omega - r_*\,)\right)\psi\,(r) = 0$$

AIRY FUNCTION

$$\left(\frac{d^2}{d{r_*}^2} + (D-3)^2\omega_c^2(\,\delta\omega - r_*\,)\right)\psi\,(r) = 0$$

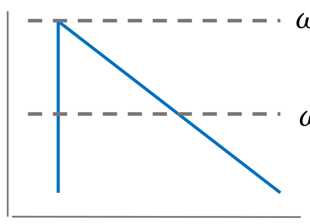

solution is written by **Airy function**

$$\psi(r) = \mathrm{Ai}\,(\,x\,) \quad \text{with} \quad x = (-(D-3)^2\omega_c^2)^{1/3}(\delta\omega - r_*)$$

boundary condition (QNM = bound state)

$$\psi(r)\Big|_{r_*=0} = 0$$

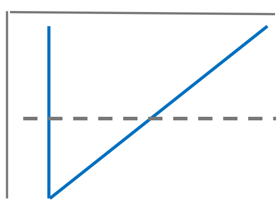

(c.f. tunneling in infinite potential well)

QNM CONDITION

Airy function

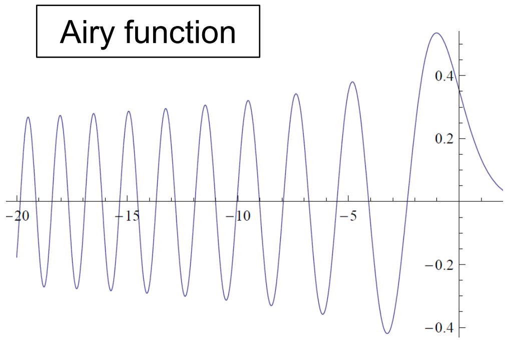

$$\mathrm{Ai}\,(\,x_0\,) = 0$$

with $x_0 = \left(-(D-3)^2\omega_c^2\right)^{1/3}\delta\omega$

QNMs are given by the zeros of the Airy function

$$\omega_{QNM} = (D-3)\omega_C + \left(-(D-3)\omega_C\right)^{1/3}\, \boldsymbol{a_k}$$

$\omega_c r_0 = \dfrac{2\hat{l}\,+1}{2}$

zeros of the Airy function

$a_1 = -2.338..,\, a_2 = -4.088,..\, a_3 = -5.521$ ...

PROPERTIES

- MAE gives same result
  - triangular potential approximation (my naïve argument) is correct
- Imaginary part of QNMs is always negative

$$Im(\omega_{QNM}) = \frac{\sqrt{3}}{2}\,\omega_c\, a_k < 0$$

  - there is **no unstable mode** (stability of Schwarzschild BH)
- there are an infinite number of QNMs labeled by $\boldsymbol{a_k}$
  - k can be regarded as an **overtone number**
- same results for other type perturbation (scalar, vector)
  - isospectrality of QNMs is restored at large D ?

SUMMARY

By using large D gravity, we obtained the **analytic formula** for QNMs of Schwarzschild BH

$$\omega_{QNM} = (D-3)\omega_C + (-(D-3)\omega_C)^{1/3}\, \boldsymbol{a_k}$$

for all type perturbations

Numerical results **agree** with our analytic formula

numerical : $\mathrm{Im}\left(\omega_{QNM}\right) = 1.334\ \mathrm{D}^{1/3}$ (by V. Cardoso)

our formula : $\mathrm{Im}\left(\omega_{QNM}\right) = 1.227\ \mathrm{D}^{1/3}$

for $l=0$ scalar perturbation (lowest), up to $D=25$

now we are updating numerical data up to $D \sim 100$ (with O. Dias, …)

FUTURE WORK

Large D gravity is <u>useful</u> and <u>interesting</u>

- ☐ application
  - gravitational collapse (Choptuik phenomena)
  - QNMs for other black holes (AdS-BH, rotating BH)
  - shockwave collision, apparent horizon formation
  - BS - caged BH transition
  - application to AdS/CFT (e.g. holographic superconductor)
  - relation with the large D technique in condensed matter physics
  - …
- ☐ conceptual
  - why gravity is so simplified at large D

[Emparan, Grumiller, KT (2013)]

“Propagation of twisted waves in a Kerr space-time”

by Atsuki Masuda

[JGRG23(2013)110706]

Propagation of twisted wave in Kerr space-time

Atsuki Masuda
Osaka City University

collaborator: Hideki Ishihara(Osaka City University)
Shunichiro Kinoshita (Osaka City University)

CONTENTS

- property of twisted wave
- propagation of twisted wave in a curved spacetime
- result

What is twisted waves?

$$\psi \propto e^{i(kz+m\phi-\omega t)}$$

m:integer Φ:angular component of cylindical

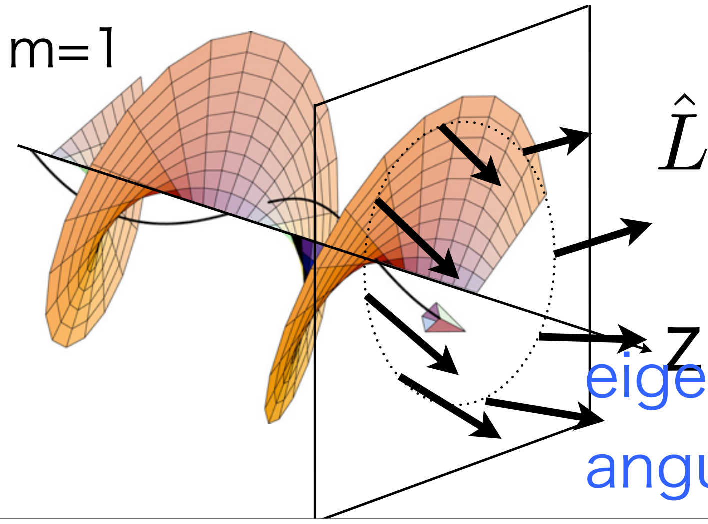

$$\hat{L}_z\psi = -i\frac{\partial}{\partial\phi}\psi$$

$$= m\psi$$

eigenstates of orbital angular momentum!

Twisted wave

Transverse plane

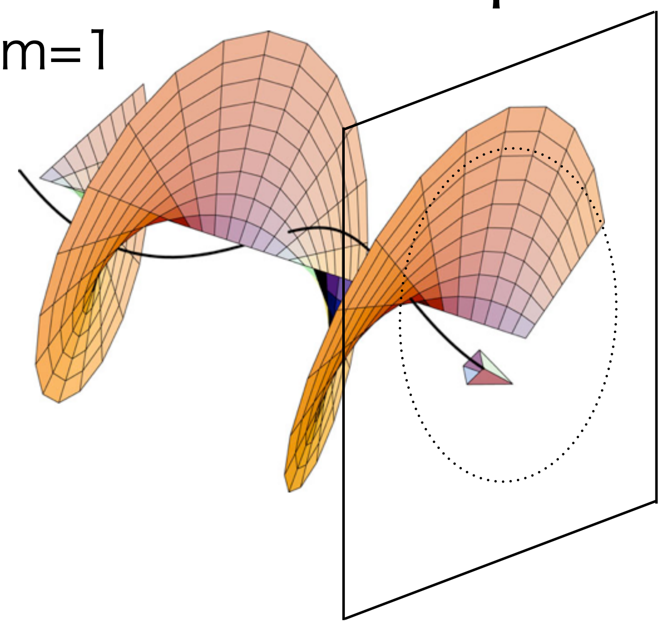

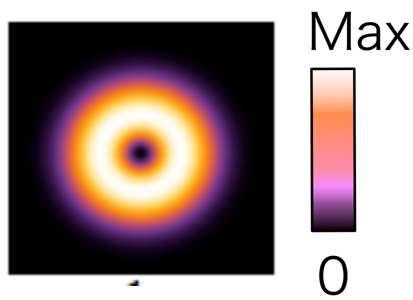

amplitude

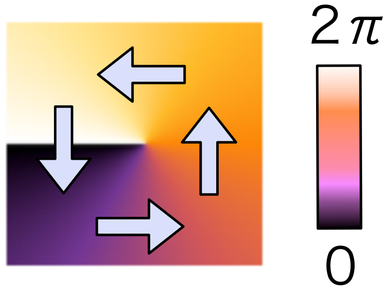

phase

About Twisted wave

- **wave vectors are twisted.**

$$\psi \propto e^{im\phi}$$

- Twisted wave propagates with orbital angular momentum
- **Twisted wave have vortex structure**

Twisted wave is investigated for presence in laboratories

Allen et. al , Phvs. Rev. A, 45, 8185 (1992)
H. He et al ,Phys. Lett. 75, 826-829(1995)

Recently, some application of twisted wave to astrophysics have been considered

F. Tamburini et al
Astronomy and Astrophysics, 488, Issue 3, pp.1159-1165(2008)

wave front

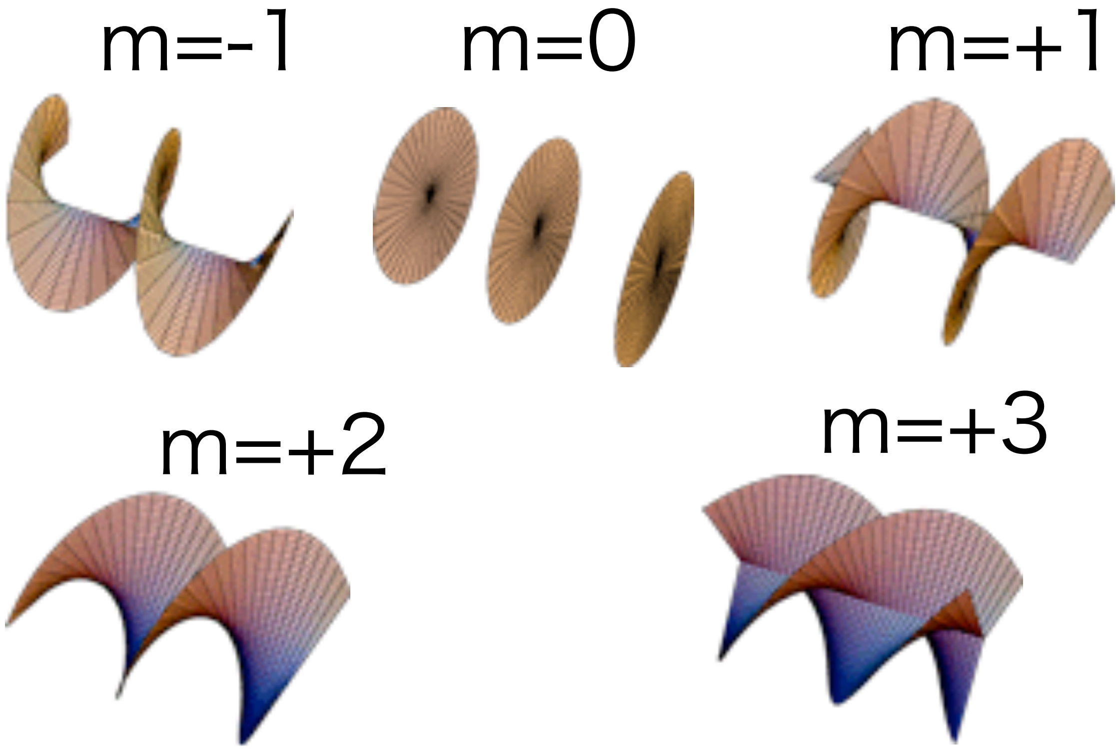

Propagation of twisted waves in a Gravitational field

Propagation of hight frequency waves

Eikonal approximation

＝short-wavelength approximation

$$g^{\mu\nu}\nabla_\mu \nabla_\nu \psi = 0 \qquad \psi \equiv A e^{i\frac{S}{\epsilon}}$$

$$g^{\mu\nu}\nabla_\mu \nabla_\nu (A e^{i\frac{S}{\epsilon}}) \sim \frac{1}{\epsilon^2} g^{\mu\nu}(\nabla_\mu S)(\nabla_\nu S) A e^{i\frac{S}{\epsilon}} = 0$$

$$g^{\mu\nu}(\nabla_\mu S)(\nabla_\nu S) = 0$$

Hamilton Jacobi equation of massless particle

$$\xrightarrow{\nabla_\mu}$$

$$k^\nu \nabla_\nu k^\mu = 0$$

$$k^\mu k_\mu = 0$$

$k_\mu \equiv \nabla_\mu S$

wave vector

Propagation of wave

High frequency wave

Eikonal approximation

Geodesic equation

Twisted wave

Eikonal approximation

?

Perturbative approach

Orbit of Bessel beam in flat spacetime

ψ_B :Bessel beam solution

(exact solution with wave equation in flat spacetime)

$$\psi_B = J_m(q\rho)e^{iS} \quad S = -\omega t + kz + m\phi$$

Jm:Bessel function q,k,ω:constant

$$u_\mu = \nabla_\mu S$$
$$= (-\omega, 0, m, k)$$
$$\bar{u}_\mu = \frac{1}{\int dS}\int u_\mu dS$$

satisfying geodesic equation

$$= (-\omega, 0, 0, k)$$

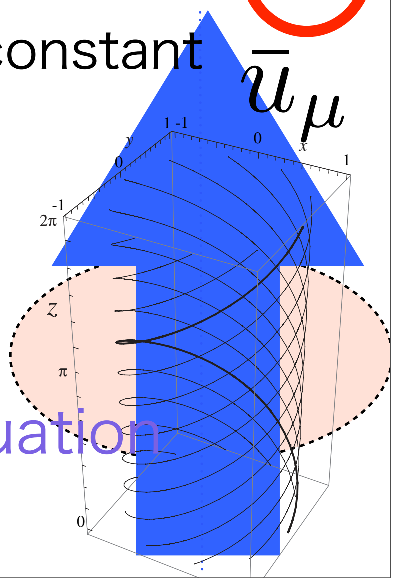

wave vector of Bessel beam in flat spacetime

$$u_\mu = \bar{u}_\mu + v_\mu$$

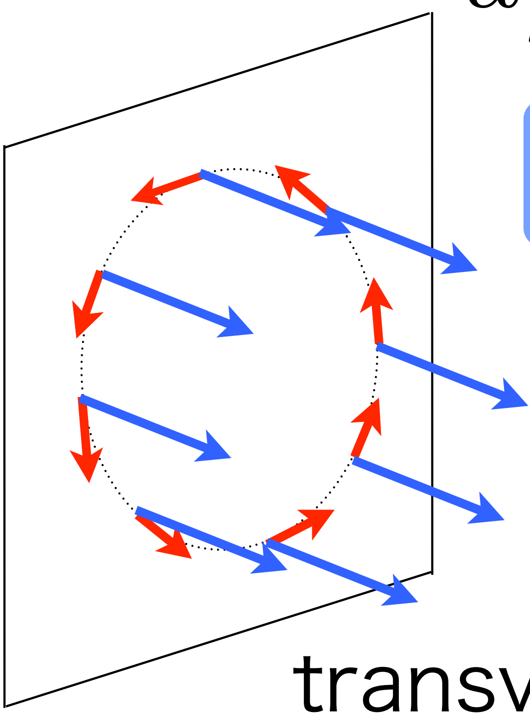

$\bar{u}_\mu$

$$\bar{u}^\mu \partial_\mu \bar{u}_\nu = 0$$

v_μ

transverse plane

Bessel beam in a curved spacetime

$$g_{\mu\nu} = \eta_{\mu\nu} \boxed{+h_{\mu\nu}}$$

perturbation term

$$\psi = J_m(q\rho)e^{iS \boxed{+i\delta S}}$$

correction term

$$\sim \psi_B + \boxed{i\delta S\psi_B}$$

Orbit $\delta u_\mu \equiv \partial_\mu \delta S$

$$\bar{u}_\mu \boxed{+\delta\bar{u}} = \frac{1}{\int dS}\int u_\mu dS \boxed{+\frac{1}{\int dS}\int \delta u_\mu dS}$$

Perturbation equation

$$\frac{1}{\sqrt{-g}}\partial_\mu(\sqrt{-g}g^{\mu\nu}\partial_\nu)\psi = 0$$

Ansatz

$$\boxed{g = \eta + h \qquad \psi = \psi_B + \psi'}$$

$$\eta^{\mu\nu}\bar{u}_\mu\bar{u}_\nu + q^2$$
$$+ \eta^{\mu\nu}\bar{u}_\mu\delta u_\nu - \frac{1}{2}h^{\mu\nu}\bar{u}_\mu\bar{u}_\nu + h^{\mu\nu}\bar{u}_\mu v_\nu = 0$$

factorization

$$(\eta^{\mu\nu} - h^{\mu\nu})(u + \delta u_\mu)(\bar{u}_\nu + \delta u_\nu) = -q^2 + h^{\mu\nu}\bar{u}_\mu v_\nu$$

Perturbation equation

$$(\eta^{\mu\nu} - h^{\mu\nu})(u + \delta u_\mu)(\bar{u}_\nu + \delta u_\nu) = h^{\mu\nu}\bar{u}_\mu v_\nu$$

↓ Differentiation ∇_μ

$$(u^\mu + \delta u^\mu) \nabla_\mu (\bar{u}_\nu + \delta u_\nu) = \nabla_\lambda (h^{\mu\nu}\bar{u}_\mu v_\nu)$$

Perturbation equation

$$(u^\mu + \delta u^\mu) \nabla_\mu (\bar{u}_\nu + \delta u_\nu) = \nabla_\lambda (h^{\mu\nu}\bar{u}_\mu v_\nu)$$

↓ averaging around axis of beam

motion equation of the beam

$$k^\mu \nabla_\mu k_\lambda = \boxed{\frac{1}{\Delta S}\int \nabla_\lambda (h^{\mu\nu}\bar{u}_\mu v_\nu) dS}$$

$$k_\mu = \bar{u}_\mu + \delta\bar{u}_\mu$$

interaction term of Kerr metric and twisted wave

How does twisted wave propagate around Kerr B.H?

$$k^{\mu}\nabla_{\mu}k_{\lambda}=\frac{1}{\Delta S}\int\nabla_{\lambda}(h^{\mu\nu}\bar{u}_{\mu}v_{\nu})dS$$

Orbit of twisted wave on the equatorial plane of a Kerr Black hole

perturbative metric

$$\eta_{\mu\nu} + \epsilon h_{\mu\nu} = \begin{bmatrix} -1 & 0 & 0 & 0 \\ 0 & 1 & 0 & 0 \\ 0 & 0 & 1 & 0 \\ 0 & 0 & 0 & 1 \end{bmatrix}$$

$$+\epsilon \begin{bmatrix} -\frac{2M}{r} & -\frac{2Ma}{r^3}y & \frac{2Ma}{r^3}x & 0 \\ -\frac{2Ma}{r^3}y & -\frac{2M}{r} & & 0 \\ \frac{2Ma}{r^3}x & 0 & -\frac{2M}{r} & 0 \\ 0 & 0 & 0 & -\frac{2M}{r} \end{bmatrix}$$

M:mass of black hole

a : spin parameter

propagation in the direction of parallel to the axis of black hole

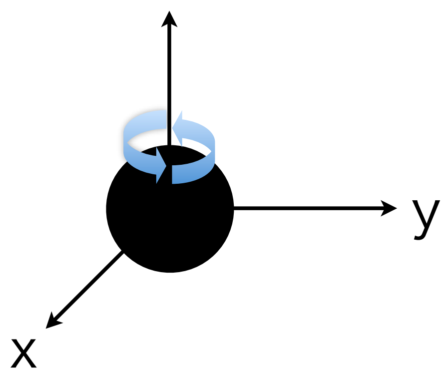

m>0

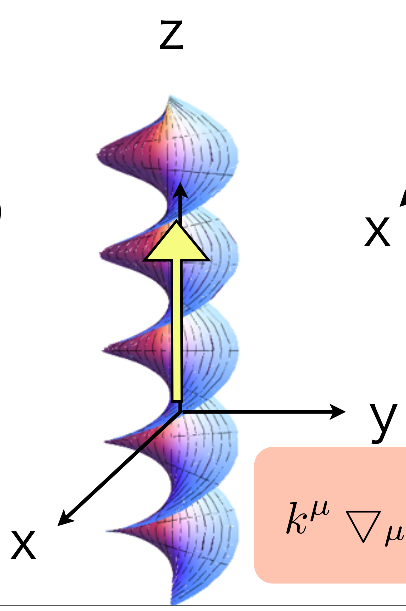

$$k^{\mu} \nabla_{\mu} k_{\lambda} = \frac{1}{\Delta S} \int \nabla_{\lambda} (h^{\mu\nu} \bar{u}_{\mu} v_{\nu}) dS$$

propagation in the direction of parallel to the axis of black hole

$$k^\mu \nabla_\mu k_\lambda = \frac{1}{\Delta S}\int \nabla_\lambda h^{\mu\nu}\bar{u}_\mu v_\nu dS$$

$$= -\frac{2m\omega a M}{\Delta S}\int \partial_\lambda \left(\frac{1}{\rho^3}\frac{\partial \phi'}{\partial \phi}\right) dxdy$$

$$\lambda = x$$

$$= -\frac{2m\omega a M}{\Delta S}\int dy \left[\left(\frac{1}{\rho^3}\frac{\partial \phi'}{\partial \phi}\right)_B - \left(\frac{1}{\rho^3}\frac{\partial \phi'}{\partial \phi}\right)_A\right]$$

$$\sim -\frac{8m\omega a M}{L^4} \quad < 0$$

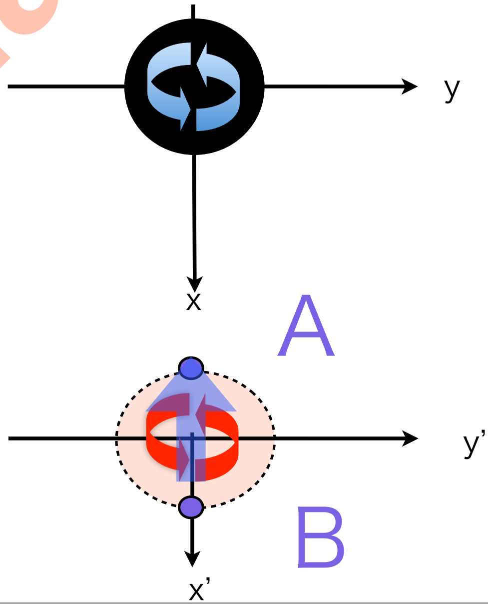

propagation in the direction of parallel to the axis of black hole

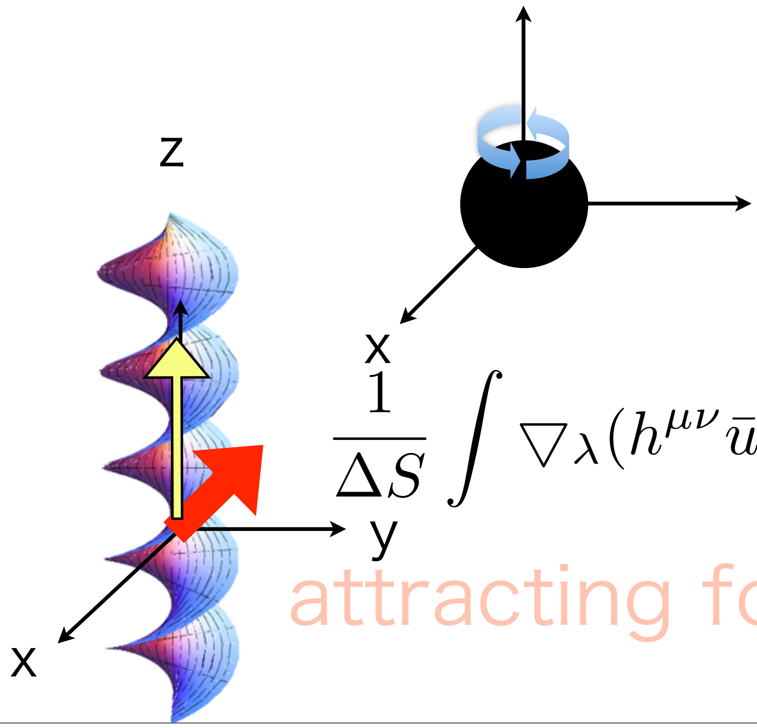

$$\frac{1}{\Delta S}\int \nabla_\lambda (h^{\mu\nu}\bar{u}_\mu v_\nu) dS$$

attracting force !

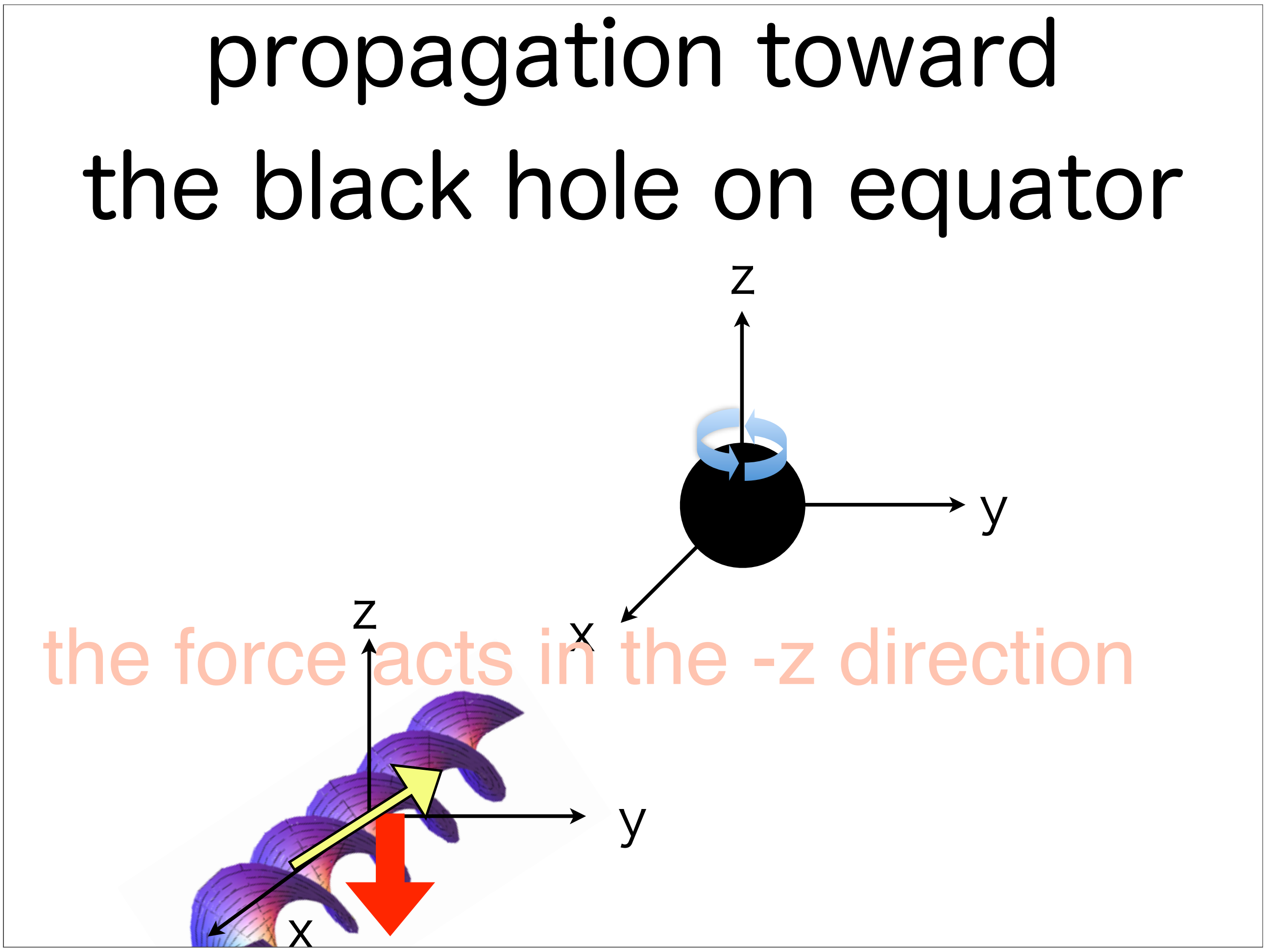
propagation toward
the black hole on equator
z
y
x
the force acts in the -z direction
z
y
x

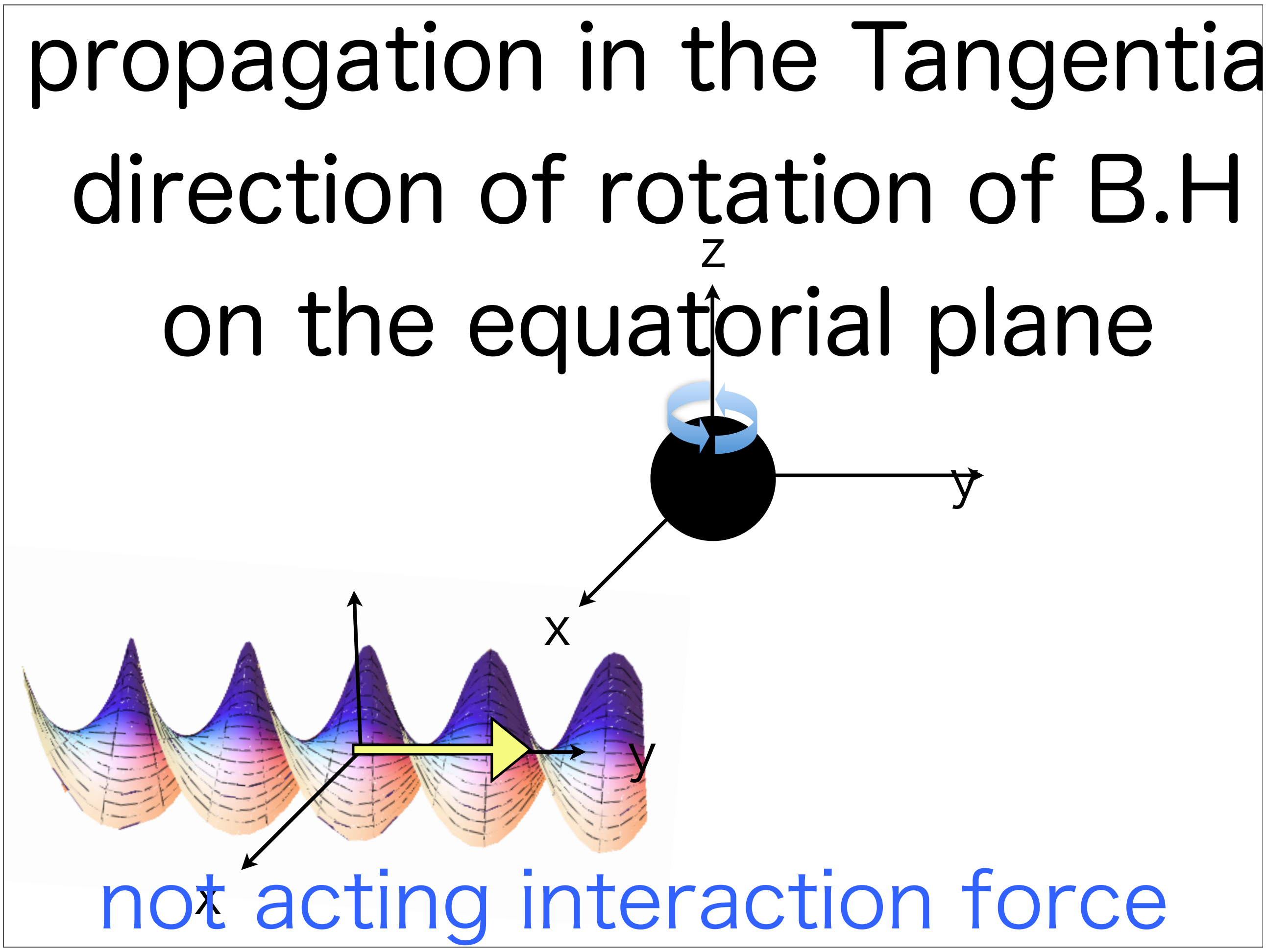
propagation in the Tangentia
direction of rotation of B.H
on the equatorial plane
z
y
x
y
x
not acting interaction force

SUMMARY

- We obtained the equation for orbit of Bessel beam in a Kerr spacetime.

$$k^\mu \nabla_\mu k_\lambda = \frac{1}{\Delta S} \int \partial_\lambda (h^{\mu\nu} \bar{u}_\mu v_\nu) dS$$

- Force term promote to $h_{t\phi} \times m$ term.

Future Work

- By using twisted wave determination of spin parameter

“Relationship between dark matter properties and primordial black holes as seeds of supermassive black holes”

by Tomohiro Nakama

[JGRG23(2013)110707]

Relationship between dark matter properties and primordial black holes as seeds of supermassive black holes

Tomohiro Nakama
RESCEU, The University of Tokyo
JSPS Research Fellow
@Hirosaki 7th Nov.2013

Collaborators:
Kazunori Kohri (KEK)
Teruaki Suyama (RESCEU)

Kohri, Nakama, Suyama, in prep.

What are PBHs and UCMHs?

- $\delta \sim 10^{-5}$ on scales probed by CMB or LSS.
- Perturbation amplitude may be larger on smaller scales.

  →If $\delta \sim 1$, radiation collapses to form primordial black holes(PBHs) during R.D.
  (Zel'dovich&Novikov 1967, Hawking 1971, Carr&Hawking 1974)

  →If $\delta \sim 10^{-3}$, dark matter collapses to form ultracompact minihalos(UCMHs) when $z < z_{eq}$.
  (Ricotti&Gould 2009)

- UCMHs may emit γ-rays due to annihilation of DM.
  (Bringmann, Scott, Akrami, 2012)

What are PBHs and UCMHs?

- $\delta \sim 10^{-5}$ on scales probed by CMB or LSS.
- Perturbation amplitude may be larger on smaller scales.

→If $\delta \sim 1$, radiation collapses to form primordial black holes(PBHs) during R.D.

Formation of UCMHs is a lot easier!

(Zel'dovich&Novikov 1967, Hawking 1971, Carr&Hawking 1974)

→If $\delta \sim 10^{-3}$, dark matter collapses to form ultracompact minihalos(UCMHs) when $z < z_{eq}$.

(Ricotti&Gould 2009)

- UCMHs may emit γ-rays due to annihilation of DM.

(Bringmann, Scott, Akrami, 2012)

Motivation

- Super massive black holes (SMBHs) $\sim 10^9 M_\odot$ have been observed at z=6∼7.

(Mortlock et. al.2011)

- The origin is not known.
- PBHs may explain SMBHs, since $M_{\rm PBH}$ can take various values.

$$M_{\rm PBH} \sim \frac{4\pi}{3}(H(z_{\rm PBH}))^{-3}\rho(z_{\rm PBH}) \sim 10^9 M_\odot \left(\frac{z_{\rm PBH}}{10^8}\right)^{-2}$$

redshift when PBHs formed

Test this scenario using UCMHs!

Key ideas

- Assuming **PBHs (δ∼1)** explain SMBHs, **numerous UCMHs (δ∼10^{-3})** should exist.

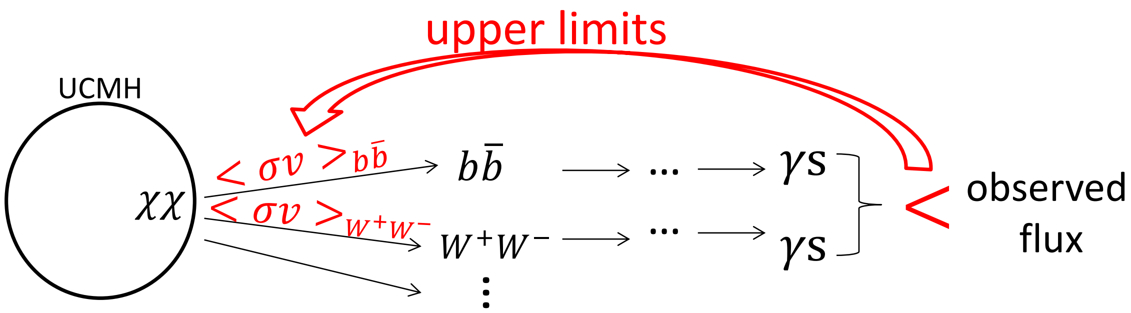

- The scenario of PBHs explaining SMBHs is INCOMPATIBLE with DM models in which the cross sections exceed these upper limits.

Why numerous UCMHs?

$$\beta \equiv \frac{\rho_{\rm PBH}}{\rho_{\rm tot}} = \int_{\bar{\delta}_c}^{\infty} \frac{1}{\sqrt{2\pi}\sigma_{\bar{\delta}}} \exp\left(-\frac{\bar{\delta}^2}{2\sigma_{\bar{\delta}}^2}\right) d\bar{\delta}$$

$\bar{\delta}_c$: 0.5 (Polnarev&Musco, 2007)

$$\| \qquad \frac{\Omega_{\rm PBH}\ \cancel{z_{\rm PBH}^3}}{\Omega_{\rm rad}\ z_{\rm PBH}^{\cancel{4}}}$$

Why numerous UCMHs?

$$\beta \equiv \frac{\rho_{\rm PBH}}{\rho_{\rm tot}} = \int_{\bar\delta_c}^{\infty} \frac{1}{\sqrt{2\pi}\sigma_{\bar\delta}} \exp\left(-\frac{\bar\delta^2}{2\sigma_{\bar\delta}^2}\right) d\bar\delta$$

$\bar\delta_c$: 0.5 (Polnarev&Musco, 2007)

$$\frac{\Omega_{\rm PBH}\ \cancel{z_{\rm PBH}^{3}}}{\Omega_{\rm rad}\ z_{\rm PBH}^{\cancel{4}}} \sim 10^{-18}\left(\frac{M_{\rm PBH}}{10^9 M_\odot}\right)^{3/2}$$

$$M_{\rm PBH} \sim 10^9 M_\odot \left(\frac{z_{\rm PBH}}{10^8}\right)^{-2}$$

Assuming there is a PBH($\sim 10^9 M_\odot$) inside the current Hubble radius,

$$\frac{M_{\rm PBH}}{\frac{4\pi}{3} H_0^{-3}\rho_c} \simeq 2\times 10^{-14}\left(\frac{M_{\rm PBH}}{10^9 M_\odot}\right)$$

Why numerous UCMHs?

$$\beta \equiv \frac{\rho_{\rm PBH}}{\rho_{\rm tot}} = \int_{\bar\delta_c}^{\infty} \frac{1}{\sqrt{2\pi}\sigma_{\bar\delta}} \exp\left(-\frac{\bar\delta^2}{2\sigma_{\bar\delta}^2}\right) d\bar\delta$$

$\bar\delta_c$: 0.5 (Polnarev&Musco, 2007)

$\longrightarrow$ **$\sigma_{\bar\delta}=0.06$**

$$\frac{\Omega_{\rm PBH}\ \cancel{z_{\rm PBH}^{3}}}{\Omega_{\rm rad}\ z_{\rm PBH}^{\cancel{4}}} \sim 10^{-18}\left(\frac{M_{\rm PBH}}{10^9 M_\odot}\right)^{3/2}$$

$$M_{\rm PBH} \sim 10^9 M_\odot \left(\frac{z_{\rm PBH}}{10^8}\right)^{-2}$$

Assuming there is a PBH($\sim 10^9 M_\odot$) inside the current Hubble radius,

$$\frac{M_{\rm PBH}}{\frac{4\pi}{3} H_0^{-3}\rho_c} \simeq 2\times 10^{-14}\left(\frac{M_{\rm PBH}}{10^9 M_\odot}\right)$$

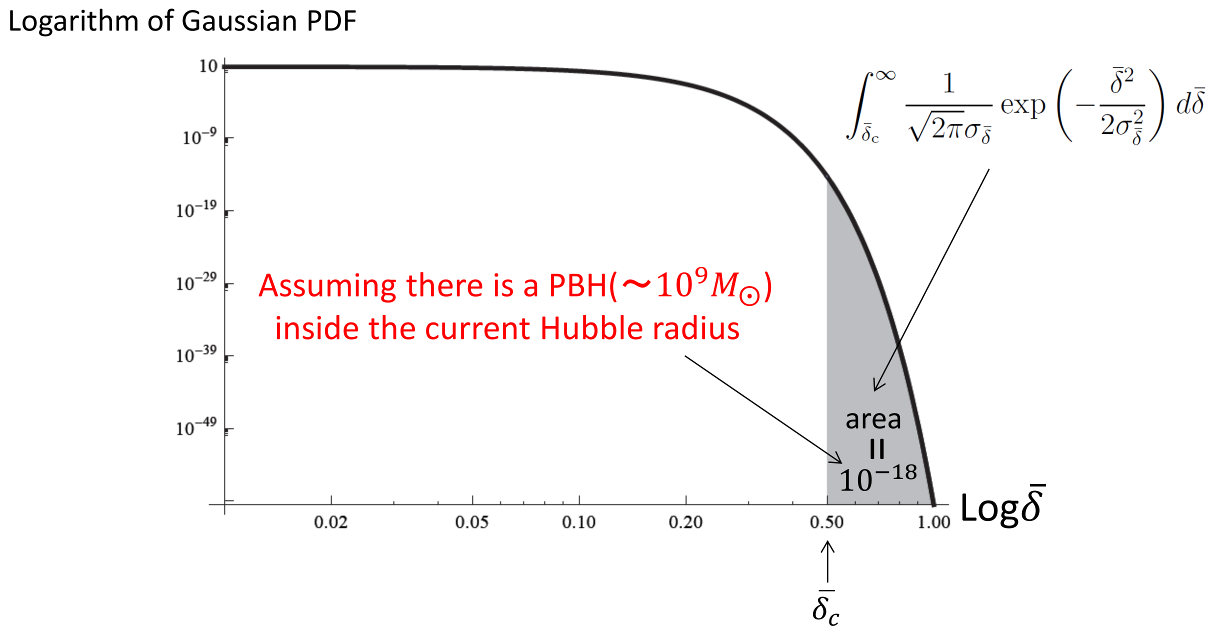
Logarithm of Gaussian PDF
10
10^{-9}
10^{-19}
10^{-29}
10^{-39}
10^{-49}
0.02
0.05
0.10
0.20
0.50
1.00
$\text{Log}\bar{\delta}$
$\bar{\delta}_c$
$\int_{\bar{\delta}_c}^{\infty} \frac{1}{\sqrt{2\pi}\sigma_{\bar{\delta}}} \exp\left(-\frac{\bar{\delta}^2}{2\sigma_{\bar{\delta}}^2}\right) d\bar{\delta}$
Assuming there is a PBH($\sim 10^9 M_\odot$)
inside the current Hubble radius
area
=
10^{-18}

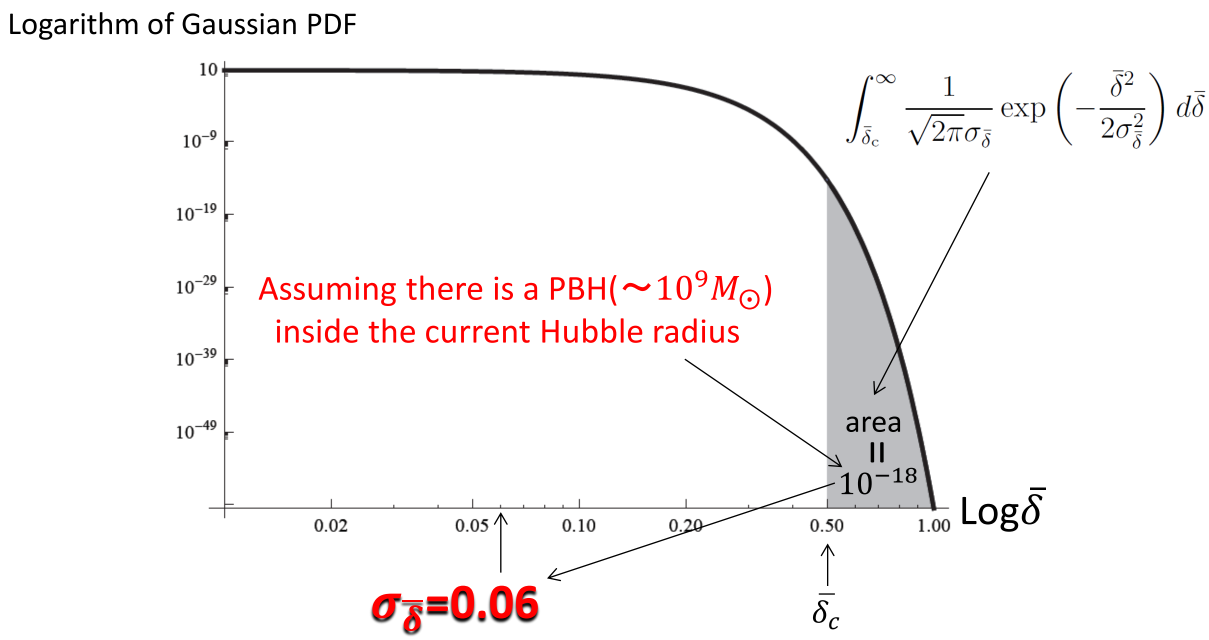
Logarithm of Gaussian PDF
10
10^{-9}
10^{-19}
10^{-29}
10^{-39}
10^{-49}
0.02
0.05
0.10
0.20
0.50
1.00
$\text{Log}\bar{\delta}$
$\bar{\delta}_c$
$\int_{\bar{\delta}_c}^{\infty} \frac{1}{\sqrt{2\pi}\sigma_{\bar{\delta}}} \exp\left(-\frac{\bar{\delta}^2}{2\sigma_{\bar{\delta}}^2}\right) d\bar{\delta}$
Assuming there is a PBH($\sim 10^9 M_\odot$)
inside the current Hubble radius
area
=
10^{-18}
$\sigma_{\bar{\delta}}$=0.06

Logarithm of Gaussian PDF

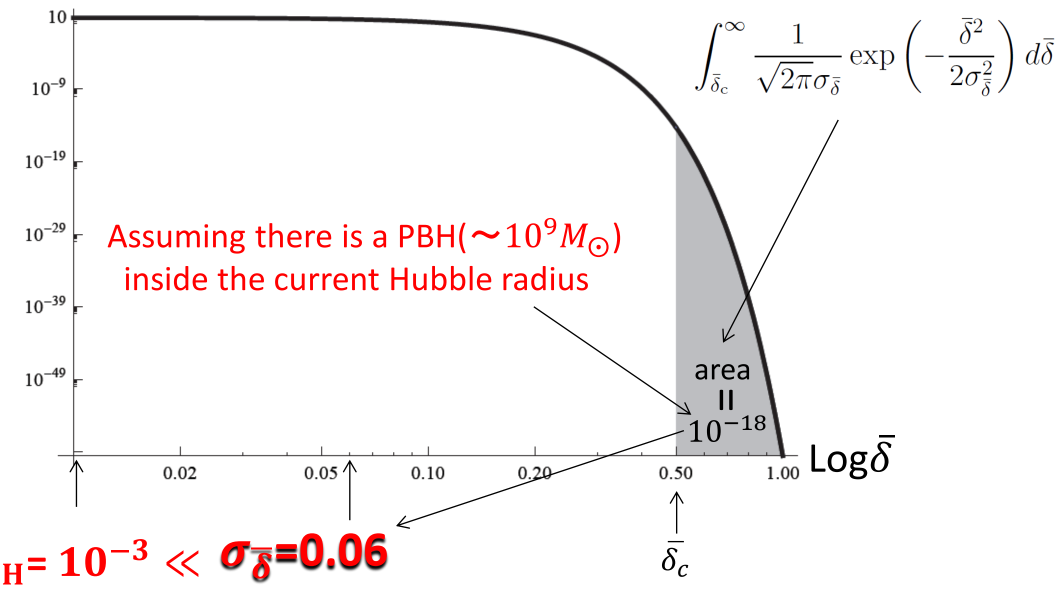

$\bar{\delta}_{c,\mathrm{UCMH}} = 10^{-3} \ll \sigma_{\bar{\delta}} = 0.06$

Perturbations leading to UCMH formation are common.

⇩

Decent fraction of DM particles are contained in UCMHs!

Method of calculation

Bringmann, Scott, Akrami, 2012

Kohri, Nakama, Suyama, in prep.

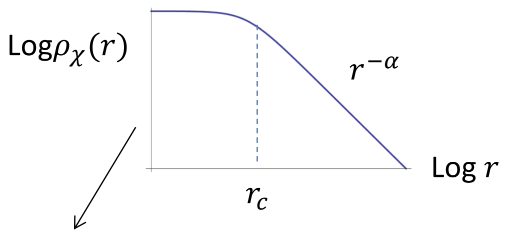

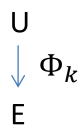

earth↔UCMH

k-th mode

$$\boxed{4\pi d^2 \Phi_k = \int_{\mathrm{UCMH}} d^3x N_k \frac{\rho_\chi^2 \langle \sigma v \rangle_k}{2m_\chi^2}}$$

flux from a UCMH

# of photons per one annihilation

1 TeV

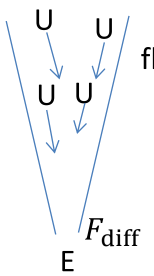

flux from several UCMHs

radius of Milky Way

$$\boxed{E^2 \frac{dF_{\mathrm{diff}}}{dE d\Omega} = \frac{1}{2M_{\mathrm{UCMH}}} \int_{d_E}^{d_{\mathrm{MW}}} \rho_{\mathrm{MW}}(d') E^2 \frac{d\Phi(d')}{dE} d'^2 \mathrm{d}d'}$$

center of Milky Way ↔earth

NFW profile

Comparison of γ-rays from UCMHs and observation

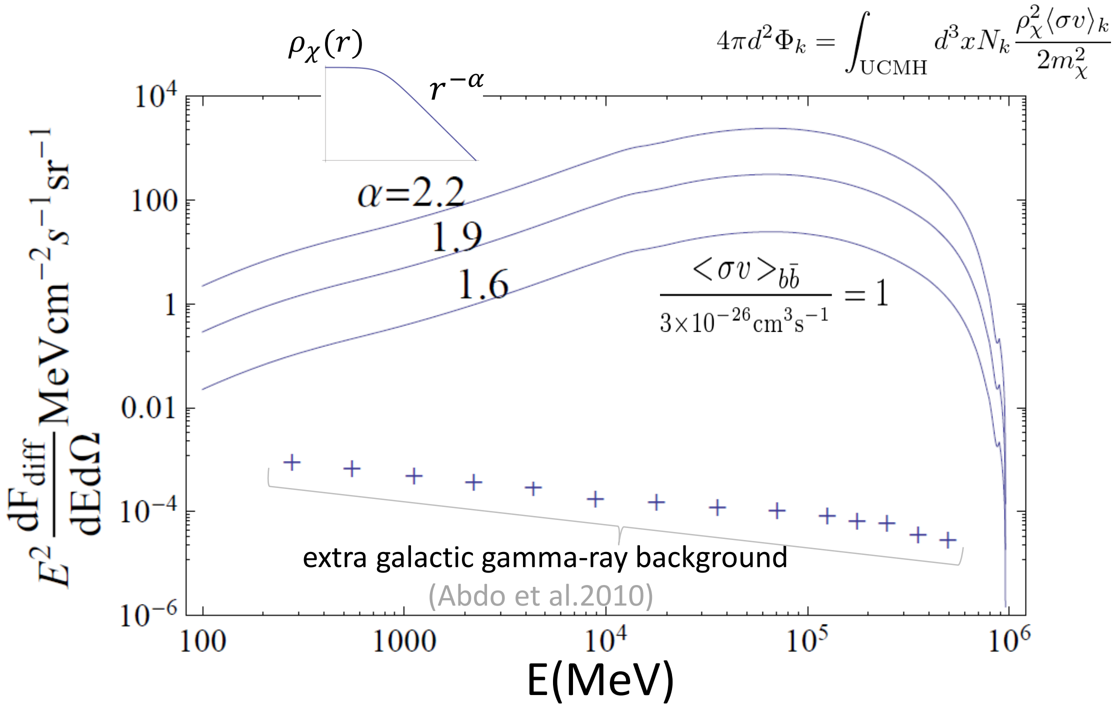

$$\frac{<\sigma v>_{b\bar{b}}}{3\times10^{-26}\mathrm{cm^3s^{-1}}} \lesssim 10^{-5}$$ to be consistent with observation.

Summary

- Assuming **PBHs ($\delta\sim1$)** explains SMBHs, **numerous UCMHs ($\delta\sim10^{-3}$)** should exist.

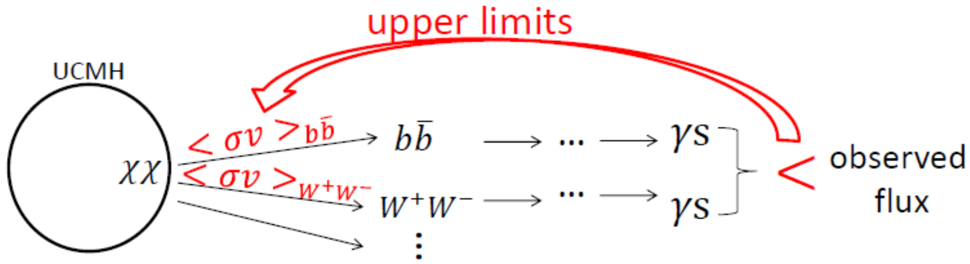

$$\boxed{\frac{<\sigma v>_{b\bar{b},W^+W^-,\tau^+\tau^-}}{3\times10^{-26}\mathrm{cm^3s^{-1}}} \lesssim 10^{-5}}$$

- The scenario of PBHs explaining SMBHs is INCOMPATIBLE with DM models in which the cross sections exceed these upper limits.

Kohri, Nakama, Suyama, in prep.

“Newtonian self-gravitating system

in a relativistic void universe model”

by Ryusuke Nishikawa

[JGRG23(2013)110708]

Newtonian self-gravitating system in a relativistic void universe model

Ryusuke Nishikawa
Osaka City University
with
C.-M. Yoo and K. Nakao
in preparation.

Testing the Copernican Principle

We are not living in the special position in the universe.

- Fundamental working hypothesis in modern cosmology
- Technological developments

A relativistic void universe model

- Non-Copernican cosmological models
  - ✓ Isotropy (CMB) ⇒ isotropic (radial) inhomogeneity

- A relativistic void universe model
  - ✓ Horizon-scale void
  - ✓ distance-redshift relation (SNIa observations)
  - ✓ acoustic peaks (CMB observations)

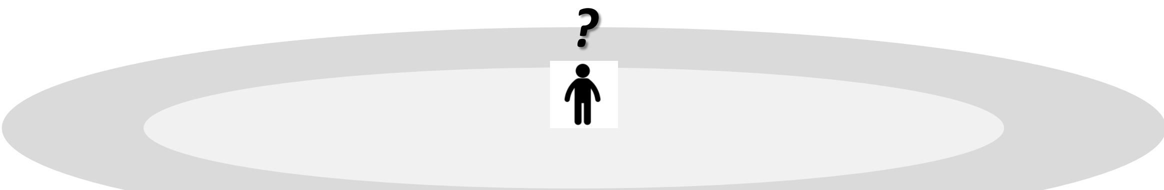

A test of void model by using other observations

Lemaître-Tolman-Bondi(LTB) spacetimes

- void model (dust, spherical) ⇒ LTB spacetimes

- metric & stress energy tensor

$$
\begin{aligned}
ds^2 &= -dt^2 + a_{||}^2(t,r)\frac{dr^2}{1-k(r)r^2} + a_{\perp}^2(t,r)r^2(d\theta^2 + \sin^2\theta d\varphi^2), \\
T^{\mu\nu} &= \rho(t,r)u^\mu u^\nu; \quad u^\mu = (1,0,0,0).
\end{aligned}
$$

  - ✓ **The isometries in LTB are less than those in FLRW**

- Radial-Hubble & Transverse-Hubble

$$H_{||}(t,r) = \frac{\partial_t a_{||}}{a_{||}}, \quad H_{\perp}(t,r) = \frac{\partial_t a_{\perp}}{a_{\perp}}$$

Structure formation in void model

- A test of void universe model
  - ✓ Galaxy distributions
  - ✓ Weak lensing

- The symmetry of LTB spacetimes

⇒ Perturbation equations in LTB cannot be reduced to a decoupled set of ordinary differential equations.

We apply weak gravitational field approximation for void model.

Weak field approximation for void model

- void model
  - ✓ relativistic, non-linear

- The gravitational field is weak at small scales
  - ✓ $|x^i| \ll \mathcal{R} \sim L^{\rm void}$

- The Fermi-normal coordinate expansion is applicable
  - ✓ Weak field approximation

Fermi-normal coordinate

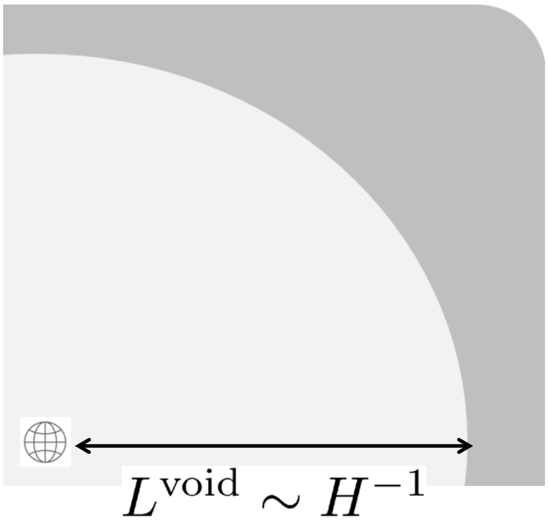

Fermi-normal coordinate

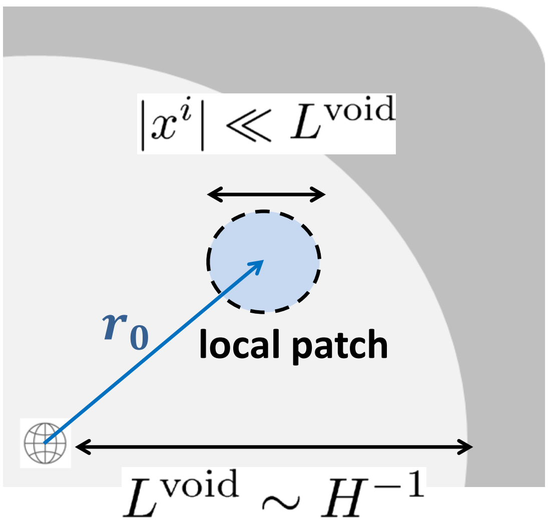

Fermi-normal coordinate

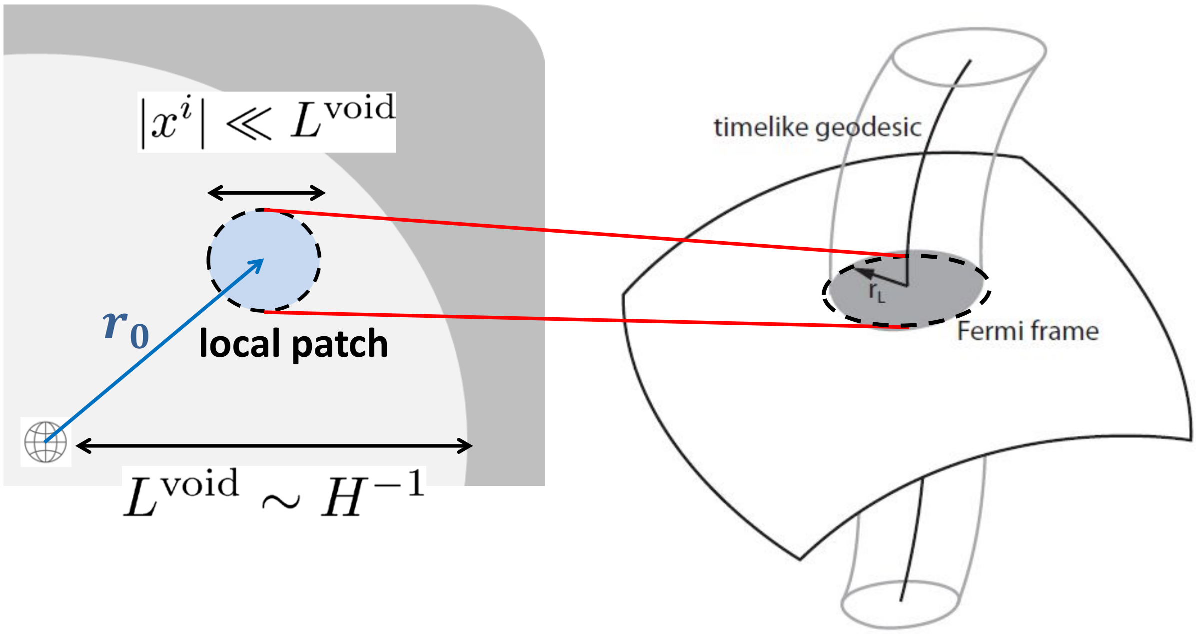

The metric in Fermi coordinate

- The former coordinate

$$ds^2 = -dt^2 + a_{||}^2(t,r)\frac{dr^2}{1-k(r)r^2} + a_\perp^2(t,r)r^2(d\theta^2 + \sin^2\theta d\varphi^2)$$

- Fermi normal coordinate

$$ds^2 = -\left(1 + R^{\rm F}_{0i0j}(t_{\rm F})x^i_{\rm F}x^j_{\rm F}\right)dt_{\rm F}^2 + \left(\delta_{ij} - \frac{1}{3}R^{\rm F}_{ikjl}(t_{\rm F})x^k_{\rm F}x^l_{\rm F}\right)dx^i_{\rm F}dx^j_{\rm F} + \mathcal{O}(x^i_{\rm F})^3.$$

✓ $x_F^i = 0\ (r = r_0)$
✓ Corrections start from $\frac{|x^i_{\rm F}|^2}{\mathcal{R}^2}$

The density and 3-velocity in Fermi coordinate

- Synchronous comoving coordinate

$$T^{\mu\nu} = \rho(t,r)u^\mu u^\nu; \quad u^\mu = (1,0,0,0).$$

- Fermi coordinate

$$\begin{aligned}
\rho(t_{\mathrm{F}}, x^i_{\mathrm{F}}) &= \rho(t,r)|_{r_0} + \partial_r \rho(t,r)|_{r_0}\, e^r_{(1)} x^1_{\mathrm{F}} + \mathcal{O}(x^i_{\mathrm{F}})^2 \\
v^1(t_{\mathrm{F}}, x^i_{\mathrm{F}}) &= H_{||}(t,r)\big|_{r_0} x^1_{\mathrm{F}} + \mathcal{O}(x^i_{\mathrm{F}})^2 \\
v^{2,3}(t_{\mathrm{F}}, x^i_{\mathrm{F}}) &= H_{\perp}(t,r)|_{r_0} x^{2,3}_{\mathrm{F}} + \mathcal{O}(x^i_{\mathrm{F}})^2
\end{aligned}$$

huge void model (LTB spacetime)
$\simeq$ homogeneous density and anisotropic expansion

Newtonian self-gravitating system in void model

- **a huge void + local perturbations**

$$\begin{aligned}
g_{\mu\nu} &= \eta_{\mu\nu} + h^{(\mathrm{B})}_{\mu\nu} + h^{(\mathrm{N})}_{\mu\nu} \\
\rho &= \rho_{(\mathrm{B})}(t_{\mathrm{F}}) + \rho_{(\mathrm{N})}(t_{\mathrm{F}}, x^i_{\mathrm{F}}) \\
v^i &= v^i_{(\mathrm{B})}(t_{\mathrm{F}}, x^i_{\mathrm{F}}) + v^i_{(\mathrm{N})}(t_{\mathrm{F}}, x^i_{\mathrm{F}})
\end{aligned}$$

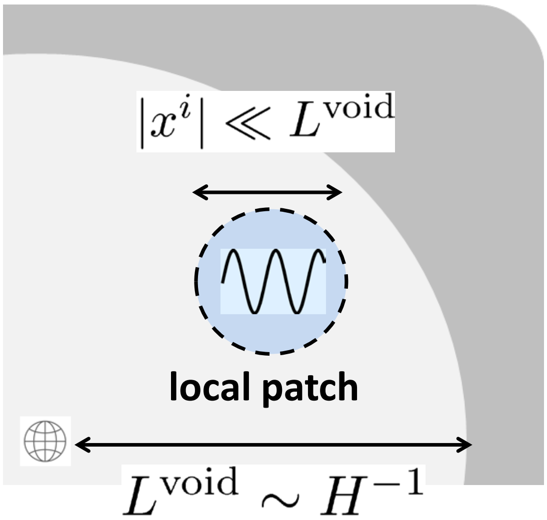

Newtonian system in void model

- slow motion & weak gravitational field

$$|v^i_{(\mathrm{N})}| \ll c, \quad \frac{\partial}{\partial t} \ll \frac{\partial}{\partial x^j}. \qquad |h^{(\mathrm{N})}_{\mu\nu}| \ll 1,$$

- short wave-length scale

$$\ell_{(\mathrm{N})} \ll L^{(\mathrm{void})}.$$

$$\epsilon = \mathcal{O}\left(\frac{v_\mathrm{N}}{c}\right)$$
$$\kappa = \mathcal{O}\left(\frac{\ell_\mathrm{N}}{L^{\mathrm{void}}}\right)$$

- Fixing the gauge

$$\partial^\mu \bar{h}^{(\mathrm{N})}_{\mu\nu} = 0; \quad \bar{h}^{(\mathrm{N})}_{\mu\nu} := h^{(\mathrm{N})}_{\mu\nu} - \frac{1}{2}\eta_{\mu\nu}(\eta^{\alpha\beta}h^{(\mathrm{N})}_{\alpha\beta}).$$

- Field equations

$$G_{\mu\nu} = 8\pi T_{\mu\nu} \text{ and } \nabla_\mu T^{\mu\nu} = 0$$

Derived equations

$$\begin{aligned}
\left(\frac{\partial}{\partial t_\mathrm{F}} + v^j_{(\mathrm{B})}\frac{\partial}{\partial x^j_\mathrm{F}}\right)\delta_{(\mathrm{N})} + \frac{\partial}{\partial x^j_\mathrm{F}}\left[(1+\delta_{(\mathrm{N})})v^j_{(\mathrm{N})}\right] &= 0, \\
\left(\frac{\partial}{\partial t_\mathrm{F}} + v^j_{(\mathrm{B})}\frac{\partial}{\partial x^j_\mathrm{F}}\right)v^i_{(\mathrm{N})} + \underline{H_{ij}(t_\mathrm{F})}v^j_{(\mathrm{N})} + v^j_{(\mathrm{N})}\frac{\partial}{\partial x^j_\mathrm{F}}v^i_{(\mathrm{N})} &= -\frac{\partial}{\partial x^i_\mathrm{F}}\phi_{(\mathrm{N})}, \\
\nabla^2_\mathrm{F}\phi_{(\mathrm{N})} &= 4\pi G\underline{\rho_{(\mathrm{B})}(t_\mathrm{F})}\delta_{(\mathrm{N})}.
\end{aligned}$$

$$\text{where} \quad H_{ij}(t_\mathrm{F}) = \begin{pmatrix} H_{||}(t,r)|_{r_0} & 0 & 0 \\ 0 & H_\perp(t,r)|_{r_0} & 0 \\ 0 & 0 & H_\perp(t,r)|_{r_0} \end{pmatrix}$$

$$\rho_{(B)}(t_\mathrm{F}) = \rho(t,r)|_{r_0}$$

$$\delta_{(\mathrm{N})} = \frac{\rho_{(\mathrm{N})}}{\rho_{(\mathrm{B})}} \qquad \phi_{(\mathrm{N})} = -\frac{1}{2}h^{(\mathrm{N})}_{00}$$

- Numerical N-body simulation **in void universe model**

Linear density perturbations

- Fourier transform: $\delta(t, x^i) = \int d^3k e^{i\mathbf{k}\cdot\mathbf{x}} \tilde{\delta}(t, k^i)$

- Linearized equations

$$\begin{aligned}
\frac{d}{dt}\tilde{\delta}_N &= -\tilde{\theta}_N, \\
\frac{d}{dt}\tilde{\theta}_N &= -\frac{2}{3}\theta_B\tilde{\theta}_N - 3\sigma_{B11}\tilde{\sigma}_{N11} - 4\pi G\rho_B\tilde{\delta}_N, \\
\frac{d}{dt}\tilde{\sigma}_{N11} &= -\frac{2}{3}\sigma_{B11}\tilde{\theta}_N - \frac{2}{3}\theta_B\tilde{\sigma}_{N11} - \sigma_{B11}\tilde{\sigma}_{N11} - 4\pi G\rho_B\left(\mu^2 - \frac{1}{3}\right)\tilde{\delta}_N.
\end{aligned}$$

where $\partial_j v_i^{\mathrm{N}} = \frac{1}{3}\theta^{\mathrm{N}}\delta_{ij} + \sigma^{\mathrm{N}}_{\langle ij\rangle} + \omega^{\mathrm{N}}_{[ij]}$ $\qquad \mu := \frac{k^1}{|\mathbf{k}|}$

⇒ Linearized equations are reduced to a decoupled set of ordinary differential equations.

Linear density perturbations

- Linearized equations

$$\begin{aligned}
\frac{d}{dt}\tilde{\delta}_N &= -\tilde{\theta}_N, \\
\frac{d}{dt}\tilde{\theta}_N &= -\frac{2}{3}\theta_B\tilde{\theta}_N - \underline{3\sigma_{B11}\tilde{\sigma}_{N11}} - 4\pi G\rho_B\tilde{\delta}_N, \\
\frac{d}{dt}\tilde{\sigma}_{N11} &= -\frac{2}{3}\sigma_{B11}\tilde{\theta}_N - \frac{2}{3}\theta_B\tilde{\sigma}_{N11} - \sigma_{B11}\tilde{\sigma}_{N11} - 4\pi G\rho_B\underline{\left(\mu^2 - \frac{1}{3}\right)}\tilde{\delta}_N.
\end{aligned}$$

$$\mu := \frac{k^1}{|\mathbf{k}|}$$

⇒ Growth factor of the density perturbation

$$\tilde{\delta}(t, \mathbf{k}; r_0) = \underline{D^+(t, \mu; r_0)}\delta^{(\mathrm{i})}(\mathbf{k})$$

a huge void model

- Density contrast & Hubble functions

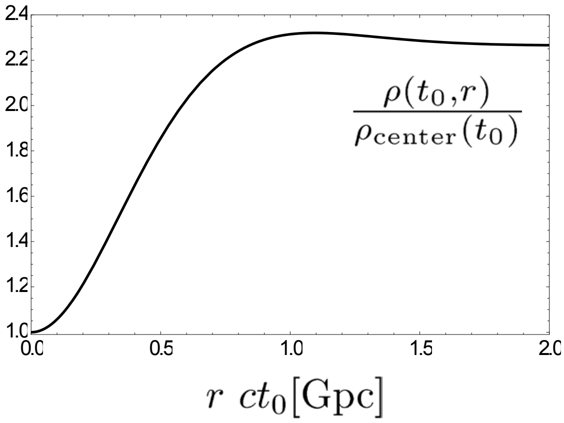

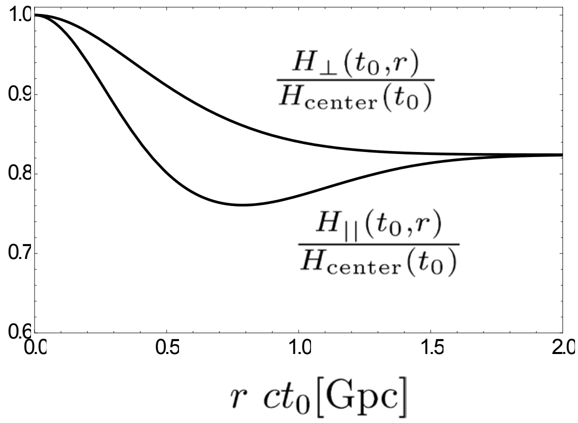

$\Omega_M^{\rm in} = 0.3, \quad \Omega_M^{\rm out} = 1.0$

Growth factors $D^+(t,\mu,r_0)$ at $r_0 = 0.6\ ct_0$[Gpc]

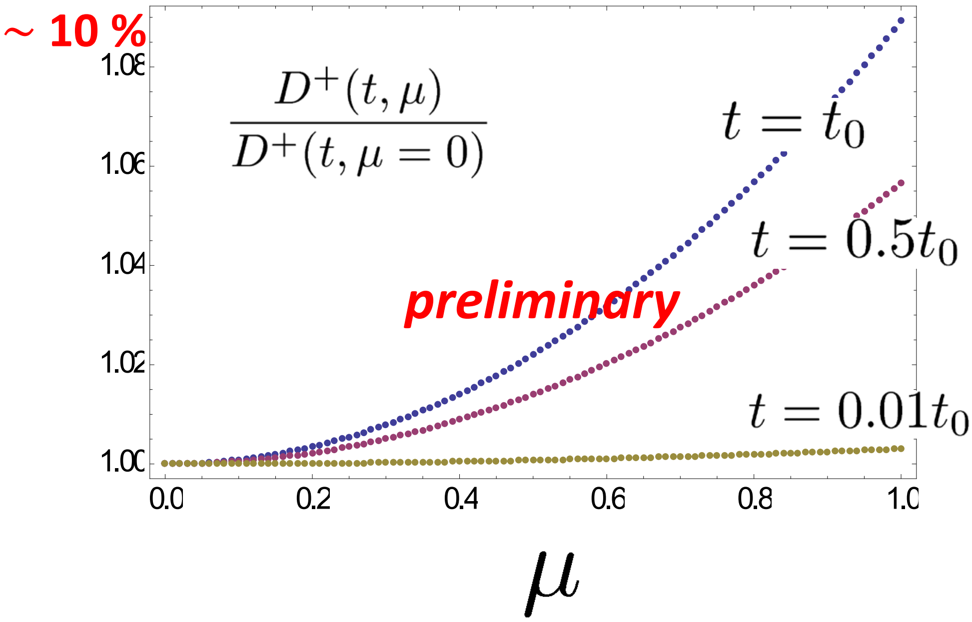

- Anisotropy of growth factor is about 10 %

$D_{||}^+ > D_\perp^+$

Growth factors $D^+(t, \mu, r_0)$ at $r_0 = 0, 0.4, 0.8, 1.2\ ct_0$[Gpc]

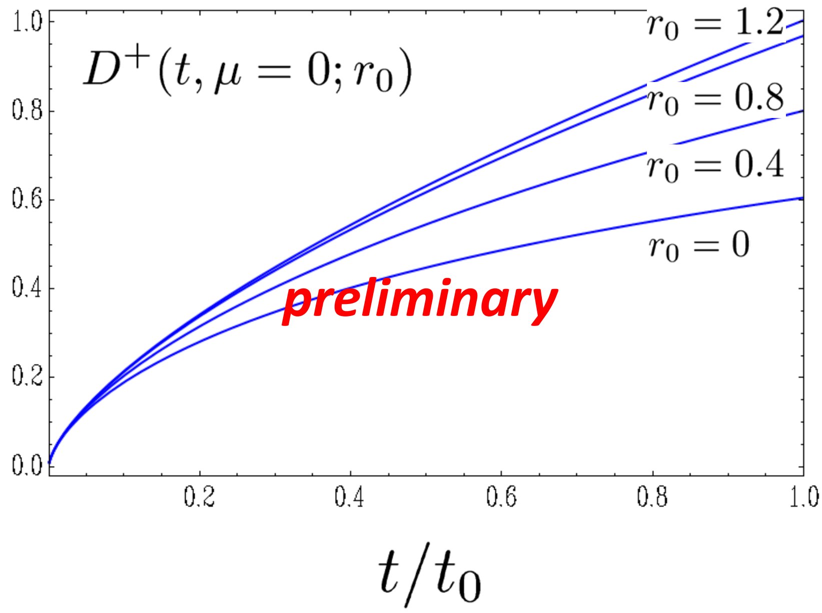

- The speed of growth is an increasing function of the radial distance from the center of the void.

Summary

- By using weak field approximation for void model,
  - ✓ Newtonian equations in void universe model
  - ✓ Linearized Newtonian equations are reduced to ordinary differential equations.

- Growth factors of the linear density perturbations
  - ✓ μ-dependence, r_0-dependence

Future work

- Comparing with observational results on the Redshift Space Distortions.
  - ✓ $P_\ell(\mu)$ with $\ell = 0,2,4, 6, \cdots$

FLRW models

Thank you for your attention.

Linearized solutions

- Rotation

$$\frac{d}{dt}\omega_{(\mathrm{N})ij} \quad = \quad -\frac{2}{3}\theta_{(\mathrm{B})}\omega_{(\mathrm{N})ij} + \sigma_{(\mathrm{B})ki}\omega_{(\mathrm{N})jk} - \sigma_{(\mathrm{B})kj}\omega_{(\mathrm{N})ik}$$

$$\Rightarrow \omega_{(\mathrm{N})12} \propto \omega_{(\mathrm{N})13} \propto \frac{1}{a_{||}^{\mathrm{loc}} a_{\perp}^{\mathrm{loc}}}, \quad \omega_{(\mathrm{N})23} \propto \frac{1}{\left(a_{\perp}^{\mathrm{loc}}\right)^2}.$$

Rotation decays as time grows.

Structure formation in void model

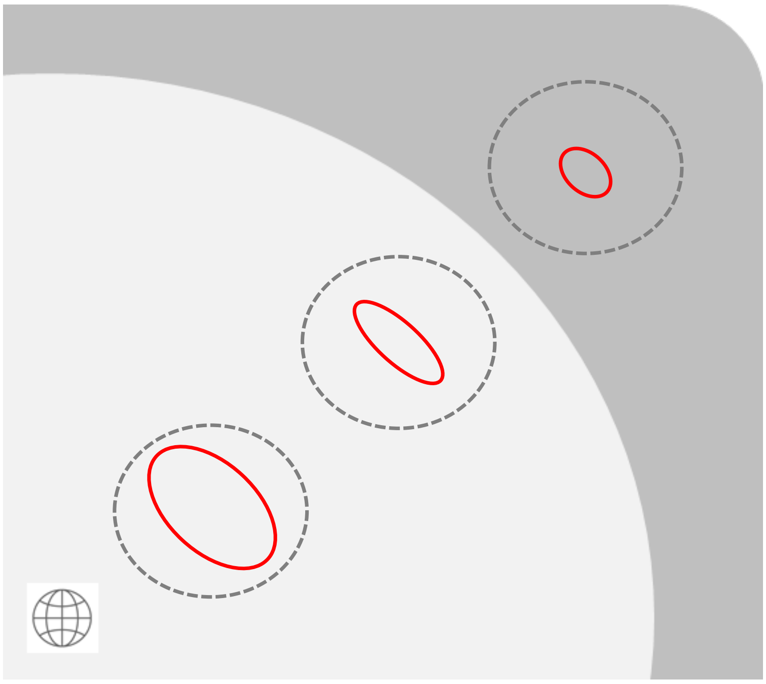

Small parameters

- If we focus on the solar system, the orbital speed of the earth is about v ~ 30km/s and we have ϵ ~ 10−4. The order of the κ is estimated as κ = 1AU/3Gpc ~ 0.2 * 10−14, where we assumed the curvature radius is 3Gpc. Thus the solar system is the case of ϵ > κ. If we see clusters of galaxies whose velocity dispersion is about 1000km/s and spatial scale is about 10Mpc, we have ϵ ~ κ ~ 0.3 * 10−2. If we consider the scale of the BAO, the velocity dispersion is about 600km/s and the spatial scale is about 100Mpc. Thus we have ϵ ~ 0.2 * 10−2 < κ ~ 0.3 * 10−1. In this section, we derive the field equations that can be applied for all cases, as long as ϵ < 1 and κ < 1 are satisfied.

“GW data analysis beyond first detection”

by Naoki Seto (invited)

[JGRG23(2013)110709]

GW data analysis beyond first detection

Naoki Seto (Kyoto U)
JGRG 2013
Hirosaki University
helped by K. Kyutoku

"Ambitious" GW data analysis

This field is evolving very rapidly in various directions

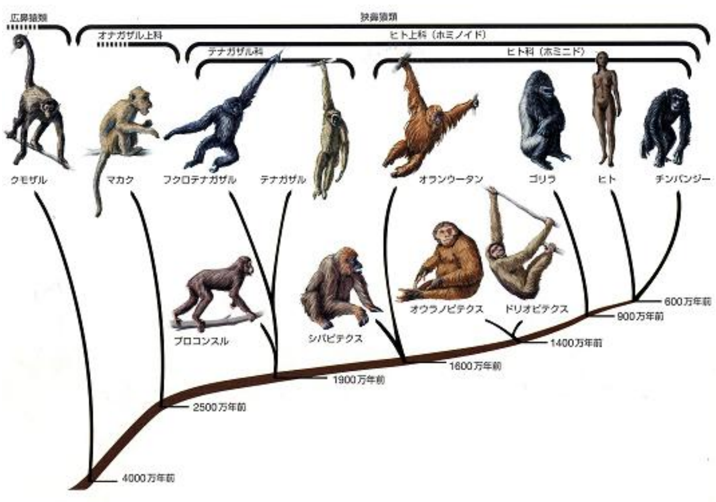

concentrate on three topics

Outline

- GW detectors in near future
  - projects, timelines, sensitivities
- 1. Multi-messenger GW astronomy
  - low latency analysis for compact binary coalescence
- 2. Effects measureable only with high SNR
  - determination of redshift of a binary by its tidal effects
- 3. Limitation of GW data analysis due to available computational power
  - already a fundamental problem for searching unknown pulsar
- Summary

GW detectors network in 2020

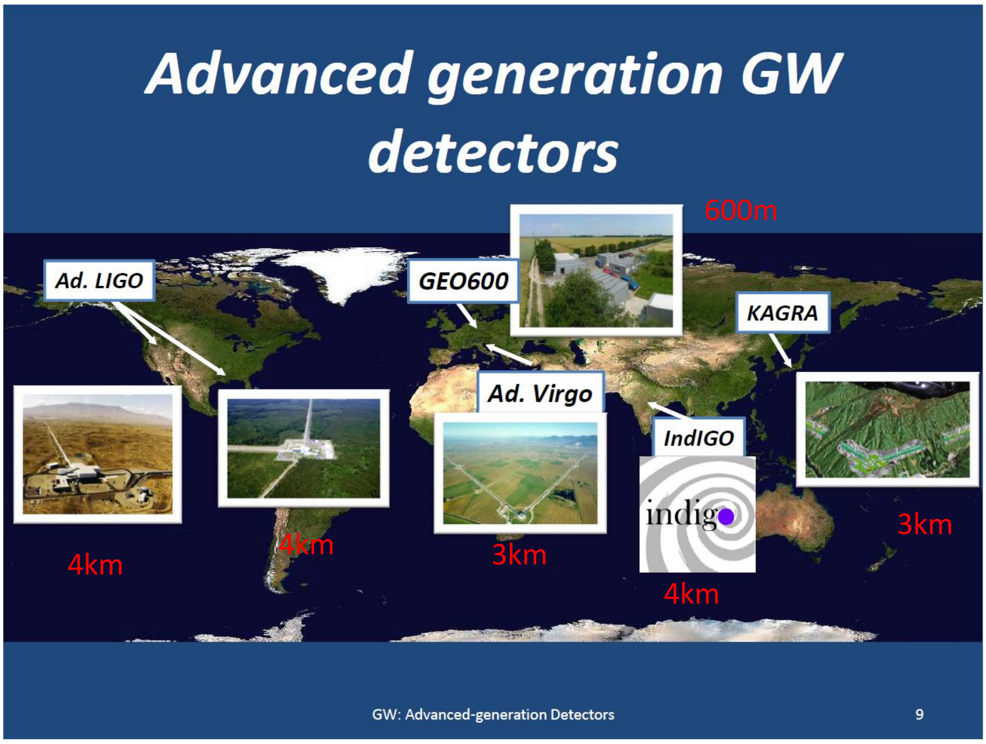

Next 3 slides from Kajita-san's talk

schedule to 2020

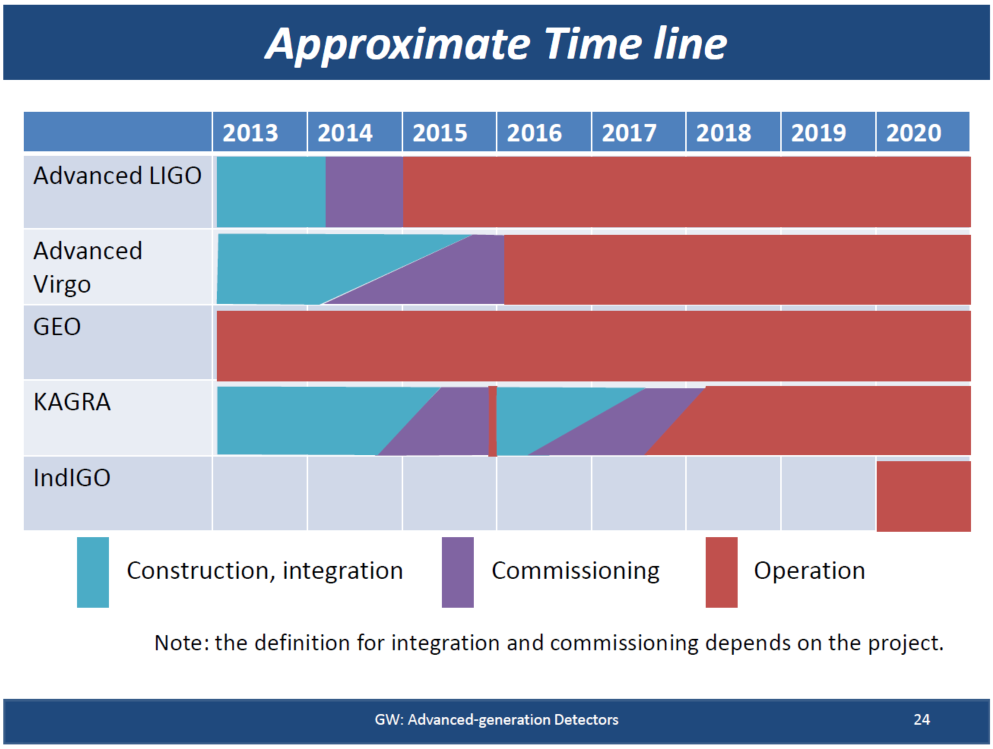

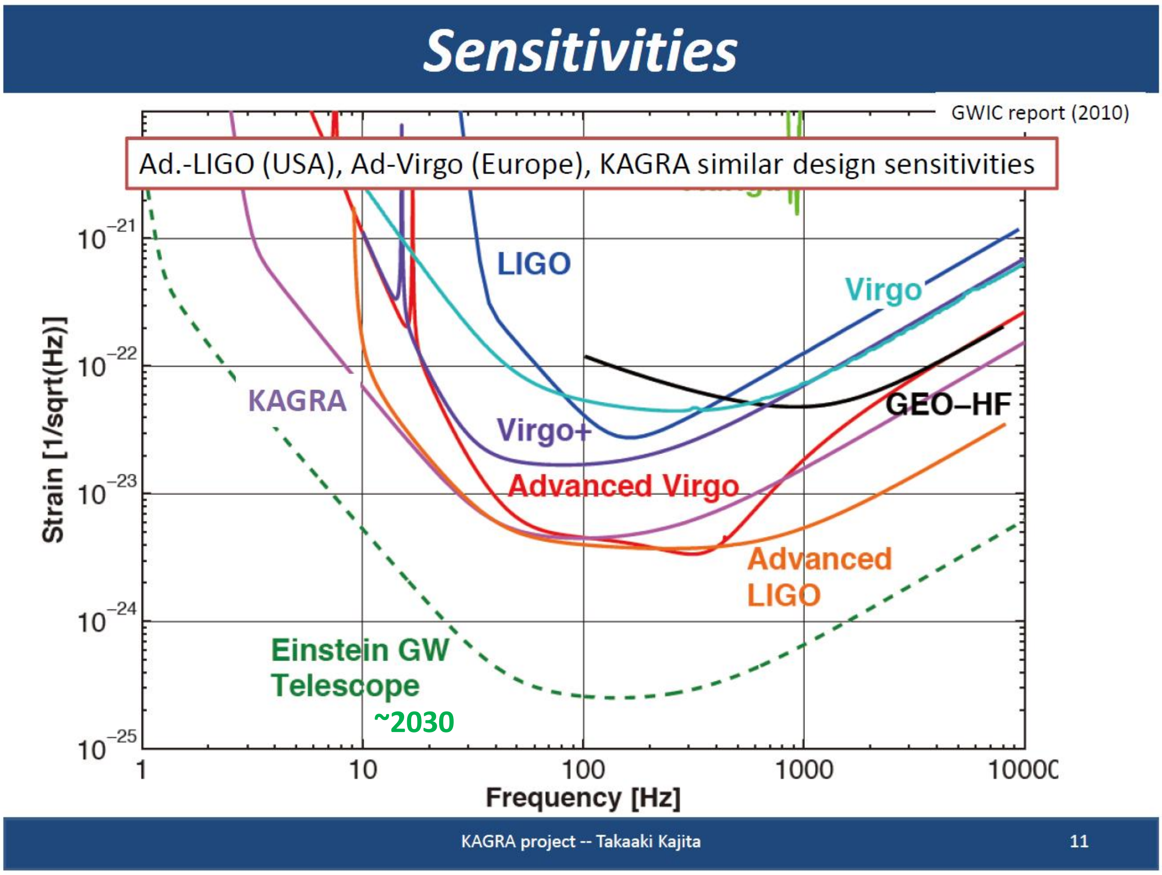

Outline

- GW detectors in near future
  - projects, timelines, sensitivities
- 1. Multi-messenger GW astronomy
  - low latency analysis for compact binary coalescence
- 2. Effects measureable only with high SNR
  - determination of redshift of a binary by its tidal effects
- 3. Limitation of GW data analysis due to available computational power
  - already a fundamental problem for searching unknown pulsar
- Summary

Multi-messenger GW astronomy

simultaneous detections of GW and EMW+ signals

- Supernova
  - complicated burst waveform
- NS-NS, NS-BH (compact binary coalescence)
  - regular chirp waveform at inspiral phase
  - plausible progenitors of Short GRBs (Hotokezaka)
    - prompt EMW signals of ~O(1)sec duration around merger
    - rapid GW detection/localization are crucial
  - generate alert as soon as possible

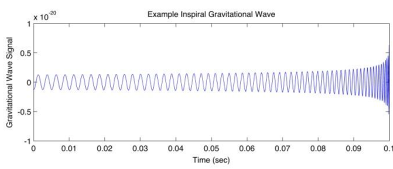

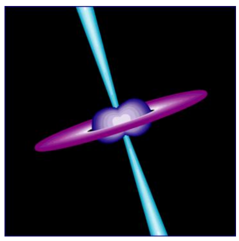

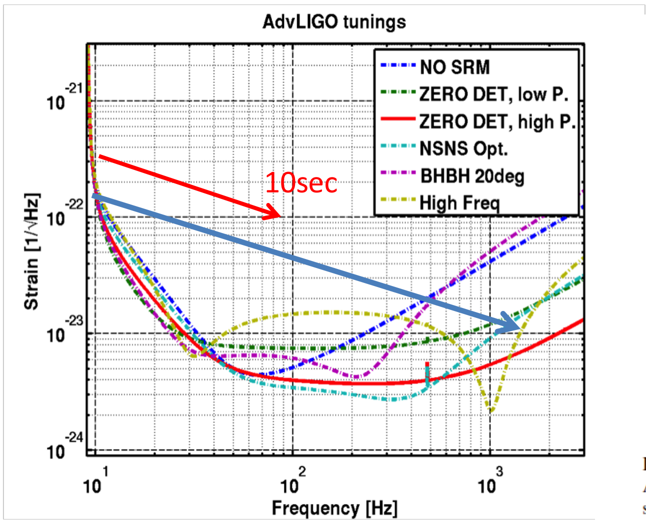

Signal to noise ratio (SNR) accumulates as a function of time

expected NS-NS number detectable (SNR≧8) with Adv-LIGO as a function of time before merger

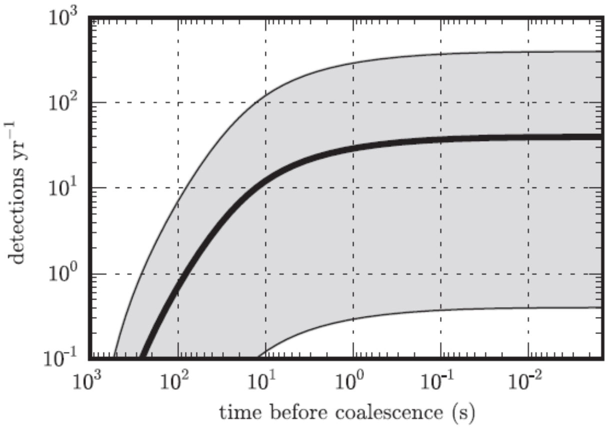

Figure 1. Expected number of NS–NS sources that could be detectable by Advanced LIGO a given number of seconds before coalescence. The heavy solid line corresponds to the most probable yearly rate estimate from Abadie et al. (2010a). The shaded region represents the 5%–95% confidence interval arising from substantial uncertainty in predicted event rates.

total detection rate:40/yr
10sec before : 10yr^{-1}
25sec before : 5yr^{-1}

Cannon et al. 2012

localization

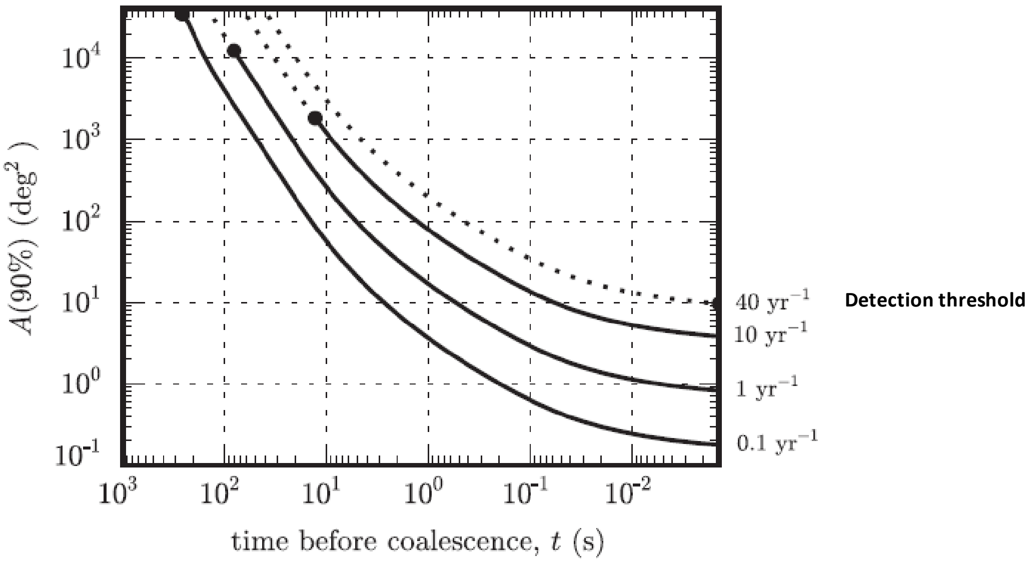

Figure 2. Area of the 90% confidence region as a function of time before coalescence for sources with anticipated detectability rates of 40, 10, 1, and 0.1 yr^{-1}. The heavy dot indicates the time at which the accumulated S/N exceeds a single-detector threshold of 8.

In reality, we need time for alert generation

so far, much longer than 1sec

- Compact binary coalescence
  - data have been analyzed mainly in frequency domain
    - CPU cost, FFT
    - segment length (e.g. O(10^2)sec)
      - Source of time delay
  - LIGO-S6
    - trigger generation (2-5min Cannon et al.2012)
    - total latency for alert ~30min (human validation etc)

We have to reduce the delay time.

- significant effort has been paid for low latency analysis
  - LIGO,… KAGRA (Tagoshi group)
- Cannon et al. 2012
  - using time domain
  - singular value decomposition for template vector
    - templates on nearby grids must be highly correlated
    - save CPU cost
  - down sampling rate @ low frequency
- for trigger generation
  - latency <0.5sec would be possible
  - (LIGO S6; 2-5min)

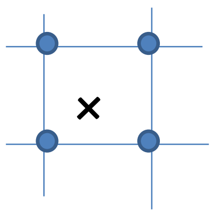

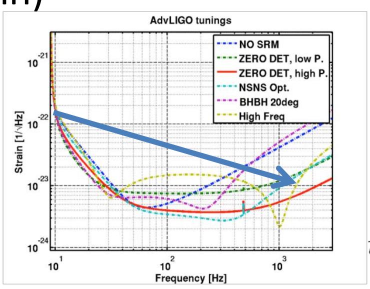

$t \propto f^{-8/3}$

Outline

- GW detectors in near future
  - projects, timelines, sensitivities
- 1. Multi-messenger GW astronomy
  - low latency analysis for compact binary coalescence
- 2. Effects measureable only with high SNR
  - determination of redshift of a binary by its tidal effects
- 3. Limitation of GW data analysis due to available computational power
  - already a fundamental problem for searching unknown pulsar
- Summary

Effects measureable with high SNR

- GW from NS-NS at late inspiral and merger
  - probe EoS of NSs (Hotokezaka)
    - **tidal effects**, hypermassive NS formation, …
- point mass approximation(or BH): simple scaling
  - tidal effect (finite size); destroy the simple scaling
  - important for cosmology (Messenger & Read 12)

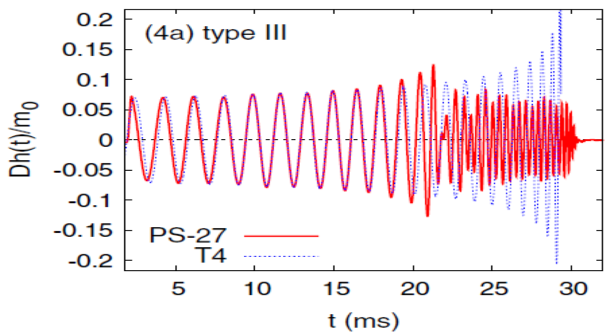

Hotokezaka et al. 2012

Arguments by Schutz (1986)

luminosity distance from GW of chirping binary

chirping GW waveform for a point mass binary (in Fourier space)

$$h(f) = A(f)e^{i\Phi(f)}$$

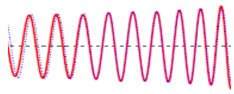

$$A(f) \propto \frac{X(angles) M_{cz}^{5/6} f^{-7/6}}{d_L} \qquad \Phi(f) = const + 2\pi f t_c + \frac{3}{4}(8\pi M_{cz} f)^{-5/3} \times [1 + \ldots]$$

$$M_{cz} \equiv (m_1 m_2)^{3/5}(m_1+m_2)^{-1/5}(1+z)$$

redshifted chirp mass

determined from frequency evolution

d_L :luminosity distance

additionally using the amplitude A

But we cannot separate (1+z) and mass information using phase evolution, reflecting the scaling of the system.
Redshift should be determined by EMW observation (e.g. host galaxy) for dark energy study and so on.
In most case, counterpart search might be difficult ,due to beaming/bad localization

Messenger & Read (2012)

- GW phase has correction terms due to tidal effects. We can solve the degeneracy between redshift and mass

$$\Phi(f) = const + 2\pi f t_c + \frac{3}{4}(8\pi M_{cz} f)^{-5/3} \times [1 + \ldots] + tidal\ terms$$

- redshift can be determined only from GWs
  - Need to estimated tidal Love number (deformation)
    - Calibrate using nearby NS-NS

estimation error of redshift with ET

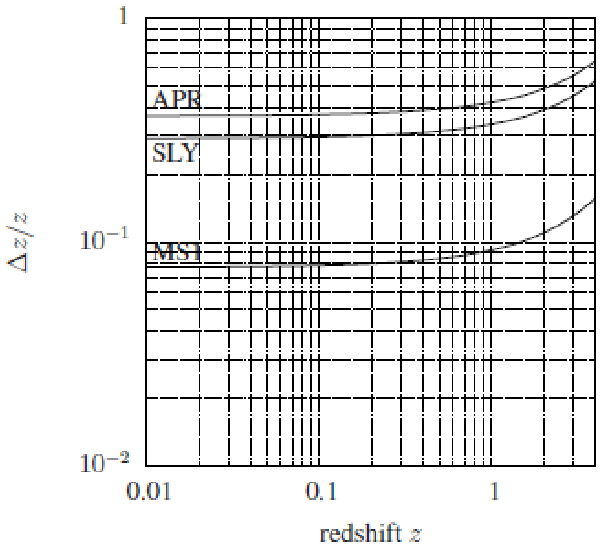

different EoSs

FIG. 1. The fractional uncertainties in the redshift as a function of redshift obtained from the Fisher matrix analysis for BNS systems using 3 representative EOSs, APR [40], SLY [41] and MS1 [42]. In all cases the component NSs have rest masses of $1.4M_\odot$ and waveforms have a cut-off frequency equal to the ISCO frequency (as defined in the BNS rest-frame). We have used a cosmological parameter set $H_0 = 70.5$ kms^{-1}Mpc^{-1}, $\Omega_m = 0.2736$, $\Omega_k = 0, w_0 = -1$ to compute the luminosity distance for given redshifts and have assumed detector noise corresponding to the ET-D [16, 39] design (a frequency domain analytic fit to the noise floor can be found in [43]).

Messenger & Read 2012

PN terms becomes imporatnt
Favata 13, Yagi & Yunes 13
Need >3.5PN

Outline

- GW detectors in near future
  - projects, timelines, sensitivities
- 1. Multi-messenger GW astronomy
  - low latency analysis for compact binary coalescence
- 2. Effects measureable only with high SNR
  - determination of redshift of a binary by its tidal effects
- 3. Limitation of GW data analysis due to available computational power
  - already a fundamental problem for searching unknown pulsars
- Summary

GW from unknown pulsars

- Emitted GWs: relatively simple caused by non-axisymmetric mass distribution (<O(10^{-7}))
  - need long term (>1yr) integration to increase SNR
- no information on frequency and spin-down
  - f, df/dt, d^2f/dt^2, ..
- direction: unknown
  - Observed GW: modulated due to rotation and revolution of the Earth

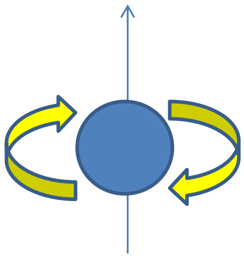

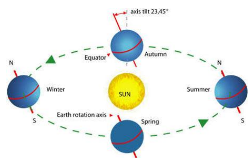

fitting parameters

- intrinsic parameters: related to phase (difficult)
  - f, df/dt, d^2f/dt^2, ..
  - source direction
- extrinsic parameters: related to amplitude (easy)
  - inclination
  - overall amplitude (deformation/distance)
  - …

number of templates for full coherent integration

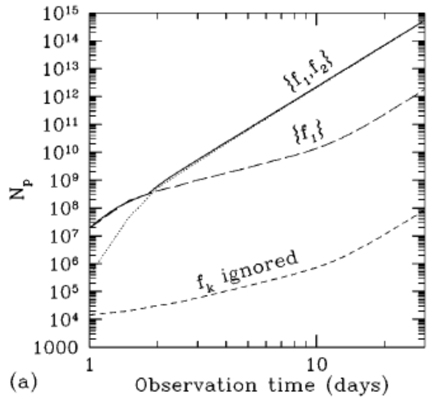

(Brady et al. 98)

f<1000Hz,
spin-down age> 40yr
mismatch 0.3

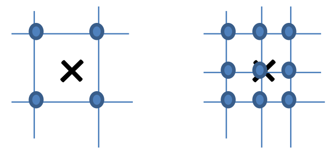

number of templates: increases rapidly with observation time

for example $\Delta \dot{f} T_{obs} \sim T_{obs}^{-1}$ $\Delta \dot{f} \propto T_{obs}^{-2}$

•Due to limitation of computational resources, we cannot make a long-term coherent integration (e.g. >1yr)
•use non-coherent (suboptimal) methods for signal detection

what we need to do

Brady & Creighton 1998
Cutler, Gholami & Krishnan 2005

- find the method
  to get the maximum **sensitivity**
  for given **computing power**
- find the method
  to get the minimum **computing power**
  for given target **sensitivity**

multi-stage stack and slide (Cutler et al. 05)

economically select candidate parameters with increasing data length

- first stage
  - take subset of data of length T_1
  - divide T_1 into segments of ΔT_1
  - coherent integration within ΔT_1
    - on coarse grid points in parameter space
  - Do stack and slide (next slide)

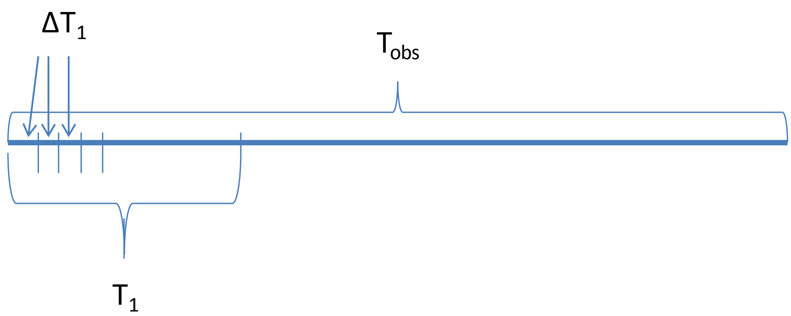

Stack and slide

Cutler, Gholami & Krishnan 2005

- frequency evolution is given by intrinsic parameters (slide)
- simply add powers (stack) along the path for given intrinsic parameters
- select candidates of intrinsic parameters
- 2nd stage: read more data (T_2) and repeat
- finally full coherent integration around the final candidates

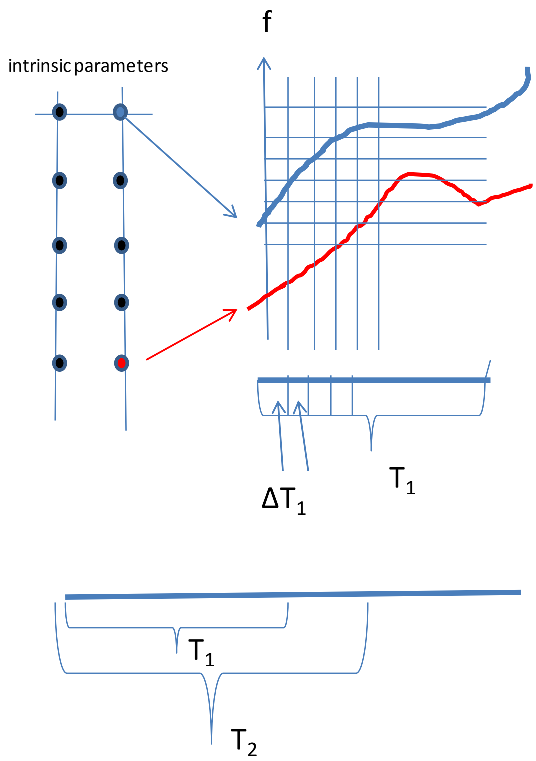

a lot of parameters

Cutler, Gholami & Krishnan 2005

- fix
  - false dismissal rate at each stage (final ~0.1)
  - detection threshold amplitude (corresponding to SN=39.7 for 1yr full coherent integration)
- search the optimal (minimize cpu cost) set of
  - number of stages: n
  - each length: T_i (i=1,n)
  - number of segments in each stage: $T_i/\Delta T_i$
  - maximum mismatch in each stage: μ_i
- used simulating annealing to find minimum

Results

1yr, f<1000Hz, Spin-down age >40 yr

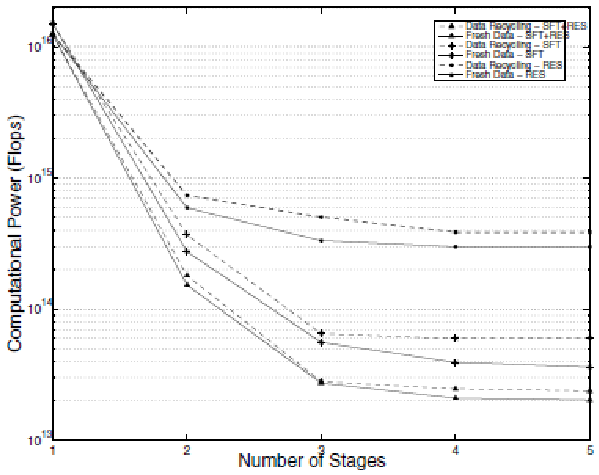

FIG. 2. Computational power versus number of semicoherent stages for different methods of calculating the $\mathcal{F}$-statistic. RES indicates the stroboscopic resampling method (strategy (ii)) and SFT is the SFT method (strategy (i)). SFT + RES corresponds the mixture of these two methods (strategy (iii)). For each strategy, solid lines indicate the result for the fresh-data mode, while the dashed lines are for the data-recycling mode.

Technical details

Cost saturates at n>3

n=3 is fine

Cutler et al. 2005

Optimal parameters for n=3 search

1yr, f<1000Hz, Spin-down age >40 yr

TABLE I. The optimal search parameters in data-recycling mode. $f_{\max} = 1000$ Hz, $\tau_{\min} = 40$ yr, $T_{\max} = 1$ yr, $h_{\rm th}^2/S_n = 2.5 \times 10^{-5}$ sec^{-1}, and η is defined according to Eq. (38).

SNR$_{th}$=39.7

Stage	$\Delta T^{(i)}$ (days)	$\mu^{(i)}$	$N^{(i)}$	$T_{\rm used}^{(i)}$ (days)	$\sqrt{\eta}$
1	2.58	0.7805	10	25.79	9.08
2	3.51	0.1139	12	42.13	13.23
3	45.66	0.8196	8	365.25	33.86

mismatch

3 2 1

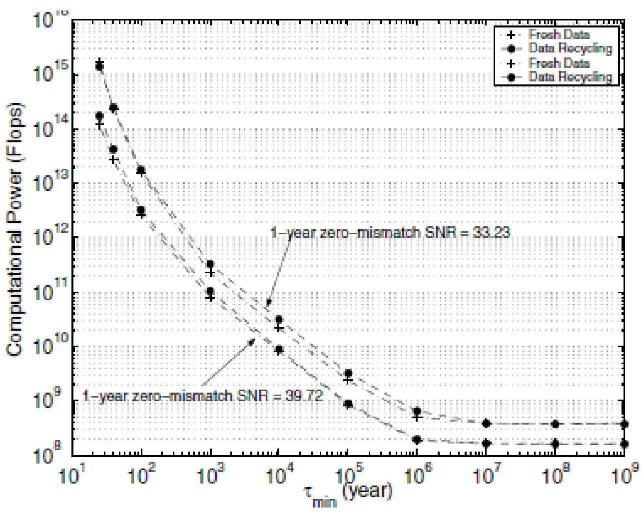

FIG. 6. The minimum computational power P required for analyzing 1 year's worth of data as a function of the pulsar's spin-down age $\tau_{\min}$. We consider a three-stage search in both the data-recycling and fresh-data mode, for two different signal strengths. The data-recycling mode results are shown with dashed lines, while the fresh-data results are in dotted lines. In parts of the curves, the results for the two modes are so close together that it is hard to distinguish them.

false dismissal rate of ~0.1

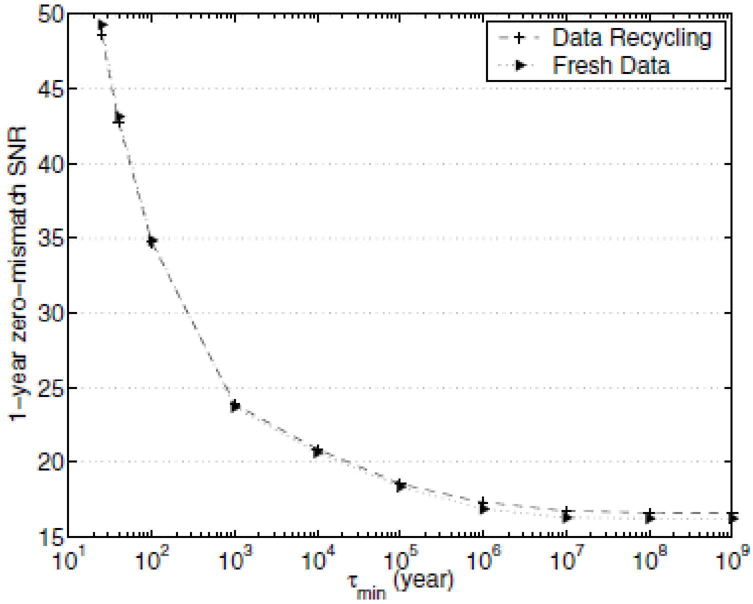

FIG. 7. The 1-year SNR (with zero mismatch) as a function of $\tau_{\rm min}$, for fixed computational power $P = 10^{13}$ Flops. The dashed line indicates the result for data-recycling mode and the dotted line for fresh-data. Since these two results are very close to each other, it may be difficult to distinguish them.

summary for unknown pulsar search

- too many templates to make a full coherent search
- must develop suboptimal methods
- maximize sensitivity for given computing power

We will have similar problems for detecting GW sources with many cycles.

Summary

- sensitivity to GWs
  - continuously improved in the next 15yrs
- GW data analysis
  - evolving rapidly in various directions
- examples
  - low latency data analysis
  - effects measureable with high SNRs
  - how to cope with computational limitations
- and other interesting issues

“Parameter Estimation of Gravitational Wave

from a Stellar Mass and an Intermediate Mass Black Hole Binary

Surrounded by a Dark Matter Mini-spike”

by Kazunari Eda

[JGRG23(2013)110710]

Parameter Estimation of Gravitational Wave from a Stellar Mass and an Intermediate Mass Black Hole Binary Surrounded by a Dark Matter Mini-spike

Kazunari Eda

University of Tokyo, RESCEU

(RESearch Center for the Early Universe)

Collaborators :

Y. Itoh, S. Kuroyanagi, J. Silk

JGRG23

7 Nov. 2013 @ Hirosaki University

Ref. Phys. Rev. Lett. 110, 221101 (2013)

0

Motivation

- Dark Matter (DM)
  - Many reliable evidence for the existence
  - The nature remains unknown
- Searching for DM
  - Producing new particles by high energy collisions
  - Detecting gamma-rays from DM annihilation
  - ……
- We show gravitational waves (GWs) can be a tool to search for Dark Matter.

1

Overview

- Consider a binary system formed of a stellar mass particle and an intermediate-mass black hole (IMBH) surrounded by dark matter (DM) halo.
- Consider the inspiral GW from the binary
- How accurately is DM distribution determined by GW observations ?

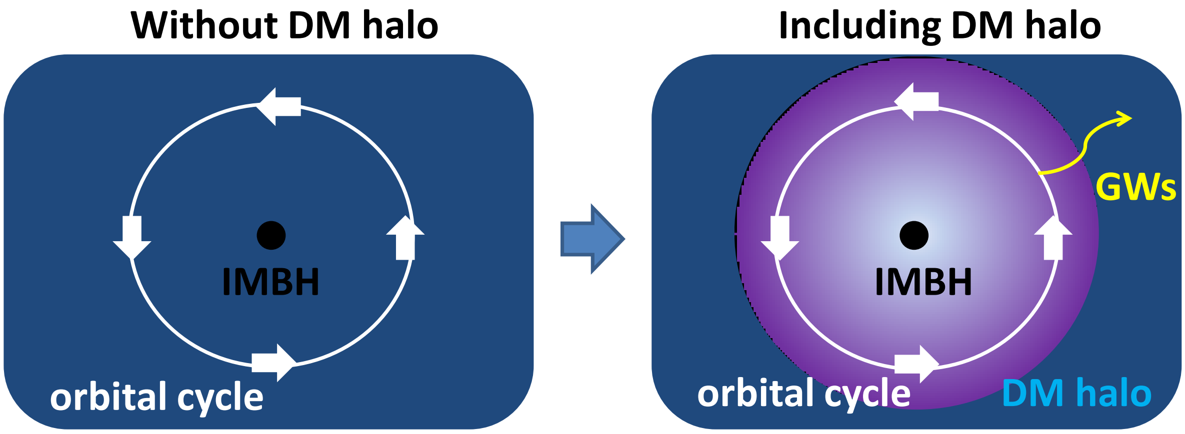

What is the dark matter mini-spike?

- We focus on the DM distribution near the IMBH.
- Intermediate-mass Black Holes (IMBHs)
  - stellar BH < IMBH < SMBH (10^2 $M_\odot$ < M_{IMBH} < 10^6 $M_\odot$)
- Adiabatic growth of IMBH creates a high density DM region
  - This region is called a **DM mini-spike** **Gondolo&Silk (1999) Zhao&Silk (2005)**
  - DM annihilation may be enhanced
  - If this is the case, the DM profile can be investigated by detecting gamma-rays from the DM mini-spike.
- We show GWs can probe the DM profile even if the DM particles don't annihilate.

Profile of DM mini-spike

- Adiabatic growth of IMBH creates high DM region.

This region is called DM mini-spike

- DM density profile
  - ρi(r): initial profile before forming the BH
  - ρf(r): final profile after forming the BH

2.25≦α≦2.5

$$\rho_i\left(r\right) \propto r^{-\gamma} \quad \left(0 \leq \gamma \leq 2\right)$$

$$\rho_f\left(r\right) \propto r^{-\alpha} \left(\alpha = \frac{9-2\gamma}{4-\gamma}\right)$$

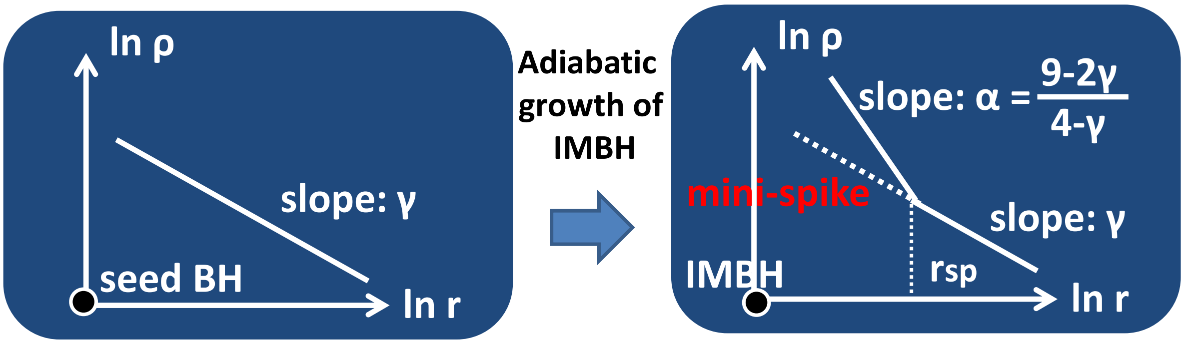

Initial profile ρi(r) **final profile ρf(r)**

Profile of DM mini-spike

- DM mini-spike profile

$$\rho\left(r\right) = \rho_{\rm sp}\left(\frac{r_{\rm sp}}{r}\right)^{\alpha} \quad \left(r_{\rm ISCO} \leq r \leq r_{\rm sp}\right)$$

$$r_{\rm sp} = 0.33 \ {\rm pc}$$

$$\rho_{\rm sp} = 379 \ M_{\odot}/{\rm pc}^3$$

- If initial DM profile is well-approximated by Navarro-Frenk-White (NFW) profile.

$$\rho_{\rm NFW}\left(r\right) = \frac{\rho_s}{\left(r/r_s\right)\left(1+r/r_s\right)^2} \longrightarrow \begin{array}{l} \gamma_{\rm NFW} = 1 \\ \alpha_{\rm NFW} = 7/3 \end{array}$$

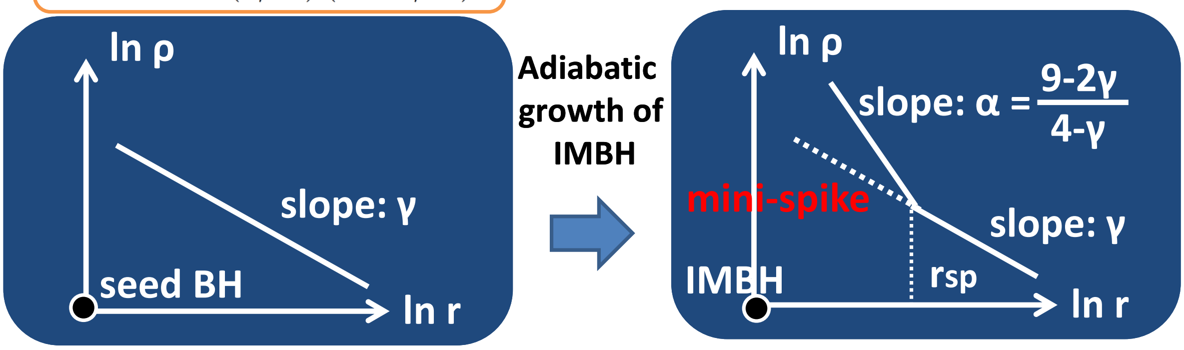

Initial profile ρi(r) **final profile ρf(r)**

Profile of DM mini-spike

This is only for adiabatic BH growth. The value of alpha strongly depends on the BH formation history.

$r_{\rm sp} = 0.33$ pc

$\rho_{\rm sp} = 379\ M_\odot/{\rm pc}^3$

…ated by Navarro-Frenk-White (NFW) profile.

$$\rho_{\rm NFW}(r) = \frac{\rho_s}{(r/r_s)(1+r/r_s)^2} \longrightarrow \gamma_{\rm NFW} = 1, \quad \alpha_{\rm NFW} = 7/3$$

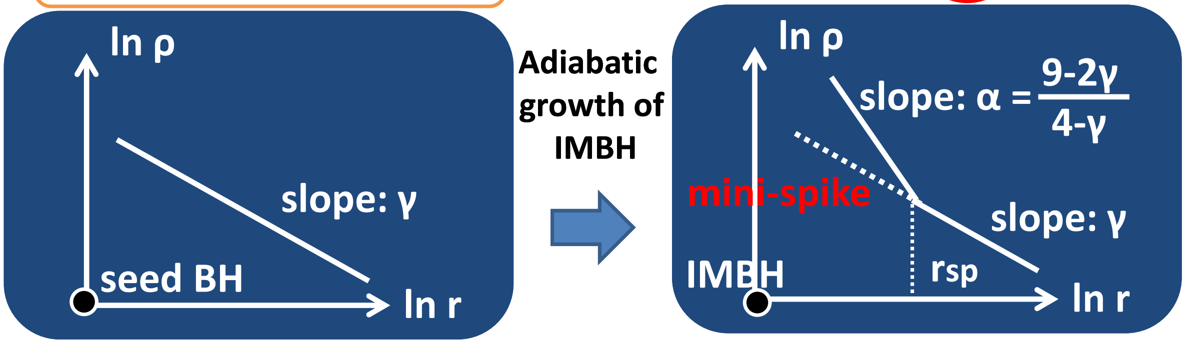

Initial profile ρi(r)

final profile ρf(r)

6

Situation

- Consider a binary system formed of a stellar mass particle and an intermediate-mass BH surrounded by dark matter (DM) halo.
- $M_{\rm DM\ halo} \sim 10^6\ M_\odot$

  $M_{\rm IMBH} \sim 10^3 M_\odot$

  $M_{\rm star} \sim 1\ M_\odot$
- Assumptions
  - Circular orbit
  - Constant DM density

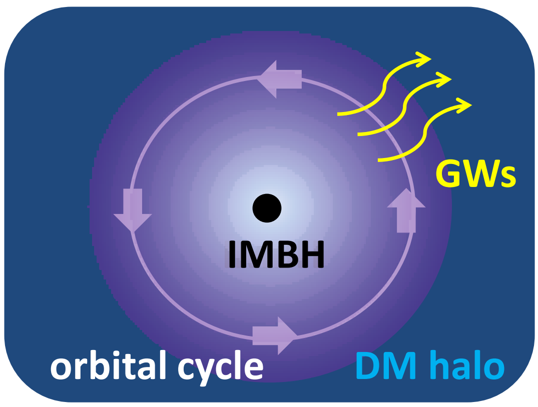

Zhao&Silk (2005)

7

Effect of DM halo on the particle

1. Gravitational potential of the central IMBH
2. Gravitational potential of the DM halo
3. GW back-reaction force
4. Dynamical friction

   from a dense DM halo

DM mini-spike

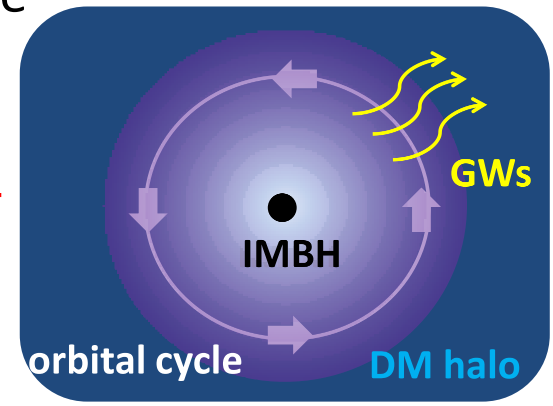

Equation of motion (EOM)

$$\frac{d\mathbf{r}^2}{dt^2} = -\nabla\phi_{\rm IMBH} - \nabla\phi_{\rm DM} + \boxed{\mathbf{f}_{\rm GW} + \mathbf{f}_{\rm DF}}$$

can be treated as a perturbation

8

GW Waveform

- GW waveform for the Newtonian quasi-circular orbit

quadrupole formula

$$h^{jk}_{\rm TT} = \frac{2G}{c^4 R}\ddot{I}^{jk}_{\rm TT}$$

$$I^{jk} \equiv \int d^3x\ \rho x^j x^k$$

GW waveform

$$h_+(t) = \frac{1}{r}\frac{4G\mu\omega_s(t)^2 R(t)^2}{c^4}\frac{1+\cos^2\iota}{2}\cos[\Phi(t)],$$

$$h_\times(t) = \frac{1}{r}\frac{4G\mu\omega_s(t)^2 R(t)^2}{c^4}\cos\iota\sin[\Phi(t)],$$

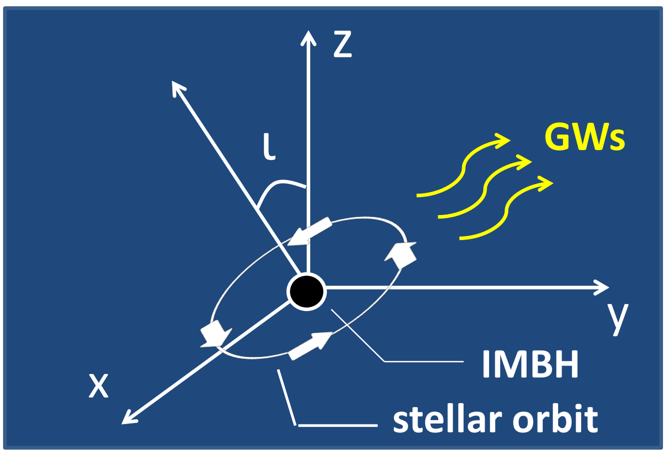

- orbital radius R
- orbital frequency ω_s
- GW phase $\Phi(t)$
- stellar mass μ
- Inclination ι
- distance to the source r

9

GW Waveform in Fourier space

- GW Waveform in Fourier space

$$\tilde{h}(f) = \mathcal{A} f^{-7/6} e^{i\Psi(f)} L(f)^{-1/2},$$

$$\mathcal{A} = \left(\frac{5}{24}\right)^{1/2} \frac{1}{\pi^{2/3}} \frac{c}{r} \left(\frac{GM_c}{c^3}\right)^{5/6} \frac{1+\cos^2\iota}{2}$$

Mc: charp mass

$$M_c \cong \mu^{5/3} M_{\rm BH}^{2/5}$$

- GW Phase

$$\Psi(f) = 2\pi f \tilde{t}_c - \Phi_c - \frac{\pi}{4} - \tilde{\Phi}(f),$$

$$\tilde{\Phi}(f) = \frac{10}{3}\left(\frac{8\pi G M_c}{c^3}\right)^{-5/3}\left[-f\int_\infty^f df'\, f'^{-11/3} L^{-1}(f') + \int_\infty^f df'\, f'^{-8/3} L^{-1}(f')\right]$$

$$\tilde{\Phi} = \Phi + 2\pi i f t, \qquad \Phi = \int \omega_{\rm GW}(t)$$

$$L(f) = 1 + 4c_\varepsilon \left(G/\pi^2 f^2\right)^{(11-2\alpha)/6}$$

$$\rho(r) = \rho_{\rm sp}\left(\frac{r_{\rm sp}}{r}\right)^\alpha$$

Two DM parameters

α : power-law index of DM profile

cε : the combination of rsp and psp

10

GW observation: eLISA

- Consider eLISA observation
  - eLISA: space-craft detector
  - Best sensitivity at about f=0.01Hz
  - 5 years observation until the coalescence

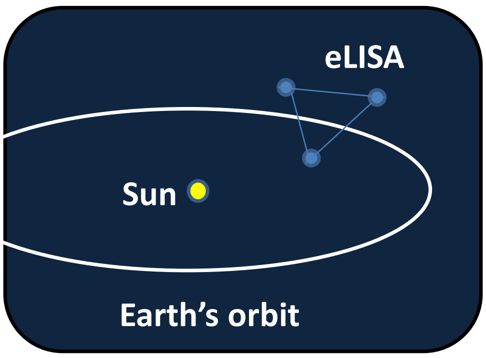

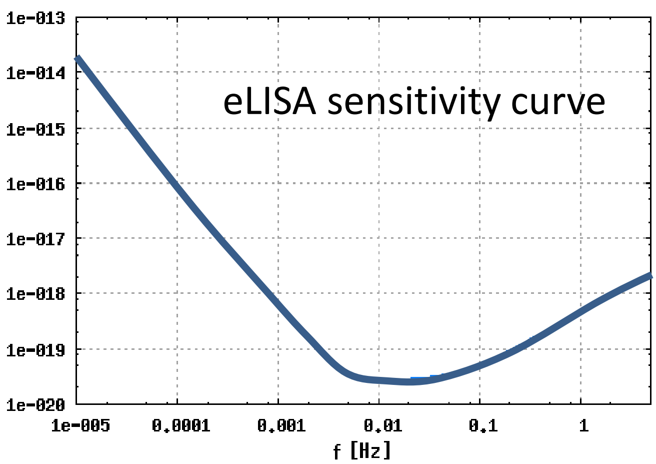

Amaro-Seoan *et al*,(2012) arXiv:1201.3621

11

Parameter Estimation

- Estimation of the measurements accuracies
- GW waveform

$$\tilde{h}(f) = \mathcal{A} f^{-7/6} e^{i\Psi(f)} L(f)^{-1/2},$$

$$\Psi(f) = 2\pi f \tilde{t}_c - \Phi_c - \frac{\pi}{4} - \tilde{\Phi}(f),$$

$$\tilde{\Phi}(f) = \frac{10}{3}\left(\frac{8\pi G \mathcal{M}_c}{c^3}\right)^{-5/3}\left[-f\int_{\infty}^{f} df'\, f'^{-11/3} L^{-1}(f') + \int_{\infty}^{f} df'\, f'^{-8/3} L^{-1}(f')\right]$$

$$L(f) = 1 + 4 c_\varepsilon \left(G/\pi^2 f^2\right)^{(11-2\alpha)/6}$$

- Six waveform parameters θ
  - A: overall amplitude, tc,ϕc : coalescence time and phase
  - Mc : charp mass
  - α, cε : dark matter parameters

$$\rho(r) = \rho_{\mathrm{sp}}\left(\frac{r_{\mathrm{sp}}}{r}\right)^{\alpha}$$

12

α : power-law index of DM profile, cε : the combination of rsp and ρsp

Results: Errors of DM parameters

- Errors of two DM parameters α, cε
  - For larger α, DM parameters are determined more accurately
  - α↑ ⇒ MDM(<r) ↑ ⇒ the effect of the DM on the star ↑
  - For initially NFW profile, α=7/3
  - **DM parameters can be measurable with very good accuracy!**

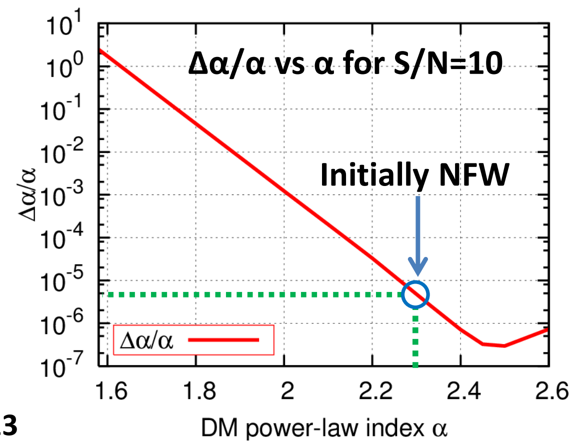

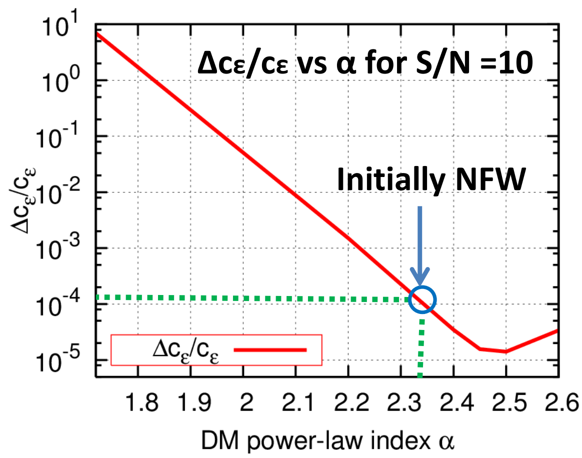

13

Case for the initially NFW profile

- In the case of initially NFW profile, α = 7/3
- Errors of waveform parameters are as follows:

$$\frac{\Delta\mathcal{A}}{\mathcal{A}} = 0.1\left(\frac{10}{S/N}\right),$$

$$\Delta\tilde{t}_c = 1.2\left(\frac{10}{S/N}\right)\ [\mathrm{s}],$$

$$\Delta\Phi_c = 1.4\left(\frac{10}{S/N}\right)\ [\mathrm{rad}],$$

Phase parameters

$$\frac{\Delta\mathcal{M}_c}{\mathcal{M}_c} = 3.3\times10^{-7}\left(\frac{10}{S/N}\right),$$

$$\frac{\Delta\alpha}{\alpha} = 2.6\times10^{-6}\left(\frac{10}{S/N}\right),$$

$$\frac{\Delta c_\varepsilon}{c_\varepsilon} = 1.3\times10^{-4}\left(\frac{10}{S/N}\right).$$

Phase parameters are measurable with very good accuracy.

Why?

For inspiral GWs,

$$\frac{S}{N} \sim \frac{h_0}{f_0 S_n(f_0)} N_{\mathrm{cycle}}^{1/2}$$

$$\Phi \equiv \int \omega_{\mathrm{GW}}\, dt \propto \underline{N_{\mathrm{cycle}}}$$

the number of orbital cycles

GW Phase are strongly related to <u>S/N</u>.

signal-to-noise ratio

Summary

- We consider the binary composed of a stellar mass object and an IMBH surrounded by DM mini-spike.
- We research on how accurately the DM parameters contained in the GW waveform are measurable.

1. DM parameters can be determined very accurately by GW observations.
2. Observation of GWs from IMBHs will be a new tool to probe the DM distribution near the IMBH.
3. This may offer hints on the formation history of BHs.

Thank you !!

“The Hilbert-Huang transform in search for gravitational-wave bursts”

by Masato Kaneyama

[JGRG23(2013)110711]

The Hilbert-Huang Transform in search for gravitational-wave bursts

Masato Kaneyama
Niigata University

in collaboration with
K. Oohara, Y. Hiranuma, T. Wakamatsu (Niigata Univ.)
H. Takahashi (Nagaoka Univ. of Tech.)
and Jordan B. Camp (NASA GSFC)

Introduction

- The Hilbert-Huang transform (HHT) N. E. Huang et al. (1996)
  - a novel, adaptive approach to time series analysis that does not make assumptions about the data form.
    ⇒ non-linear and non-stationary time series data
    - an empirical mode decomposition (EMD)
    - the Hilbert spectrum analysis (HSA)
  - It has been applied to various fields:
    biomedical engineering, financial engineering, image processing, seismic studies, ocean engineering

Waveform reconstruction

- GW bursts from core collapse
  and core bounce of rotating stars

  - non-stationary and short-duration signals

  - The waveform is unknown but strongly reflected in the physical parameters (mass of the progenitor model, precollapse rotation, EoS).

    H. Dimmelmeier et al. (2008)

    C. Rover et al. (2009)

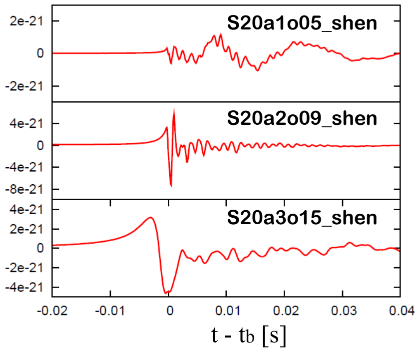

- We investigated the reconstruction of
  GW burst signals with the HHT.

Why the HHT?

- The HHT is not limited by the time-frequency
  uncertainty principle.

  - Traditional time-frequency analysis of GWs:
    the short-time Fourier transform
    the wavelet transform

    the uncertainty principle

$$\sigma_t \, \sigma_f \geq \frac{1}{4\pi}$$

- time-varying amplitudes (or powers)
  and frequencies in the time domain

Hilbert spectrum analysis

- Hilbert transform

$$v(t) = \frac{1}{\pi} P \int_{-\infty}^{\infty} \frac{u(t')}{t - t'} dt'$$

P : the Cauchy principal value

- If $u(t)$ is a real part on the real axis of a holomorphic function $G(t)$

$$G(t) = u(t) + iv(t) = a(t)e^{i\theta(t)} \qquad \theta(t) = \tan^{-1}\left\{\frac{v(t)}{u(t)}\right\}$$

- Instantaneous amplitude (IA)

$$a(t) = \sqrt{u(t)^2 + v(t)^2}$$

- Instantaneous frequency (IF)

$$f(t) = \frac{1}{2\pi}\frac{d\theta(t)}{dt}$$

Hilbert spectrum analysis

- Consider $u(t) = \alpha\cos(2\pi f t) + \beta$

  $v(t) = \alpha\sin(2\pi f t)$

  f, α, β : const.

IA: $a(t) = \sqrt{\alpha^2 + \beta^2 + 2\alpha\beta\cos(2\pi f t)}$

IF: $f(t) = f\left[1 - \frac{\beta^2 + 2\alpha\beta\cos(2\pi f t)}{a(t)^2}\right]$

$\Rightarrow$ β must be equal to zero.

- two conditions to obtain a meaningful IA and IF

(1) difference between number of zero crossings and extreme value is 0 or ± 1

(2) the mean value of the upper and lower envelopes defined by the local maxima and minima = 0

When the data satisfy the above conditions, we call the data intrinsic mode function (IMF).

Empirical mode decomposition

- To obtain the IMFs from the data,
  we perform the empirical mode decomposition.
  - the original data $s(t)$

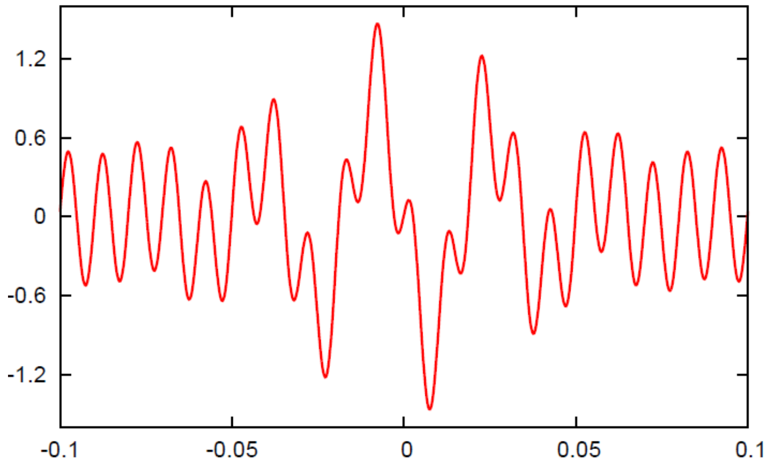

Empirical mode decomposition

- Find the local maxima and minima.

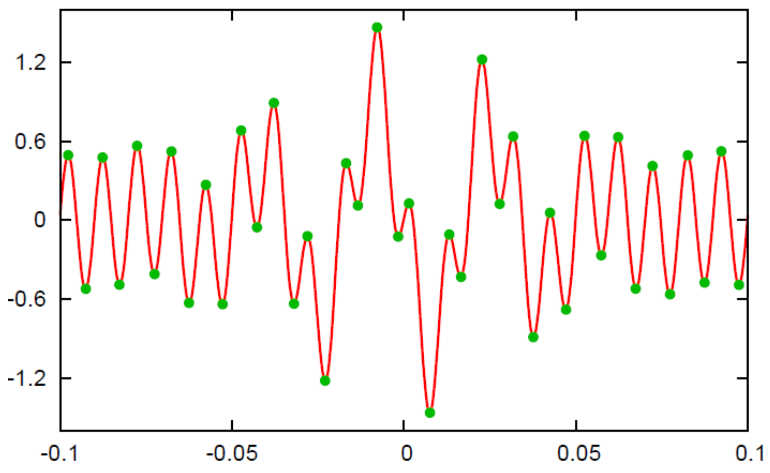

Empirical mode decomposition

- Interpolate the maxima and minima using cubic splines to obtain the upper and lower envelopes, respectively.

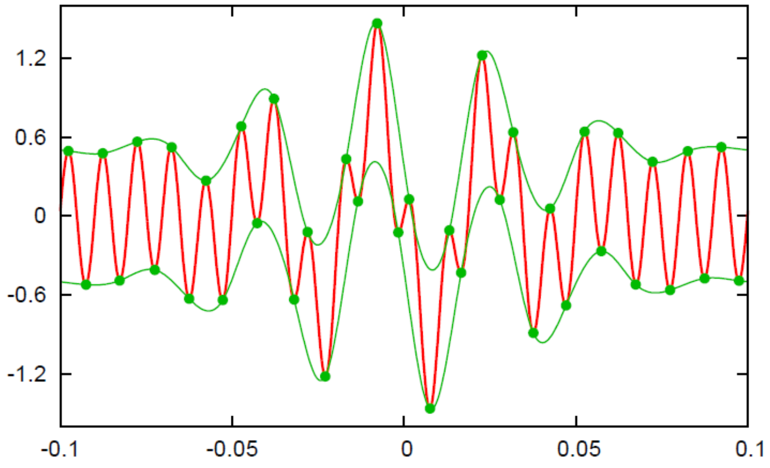

Empirical mode decomposition

- Calculate the local mean of upper and lower envelopes curve $m(t)$.

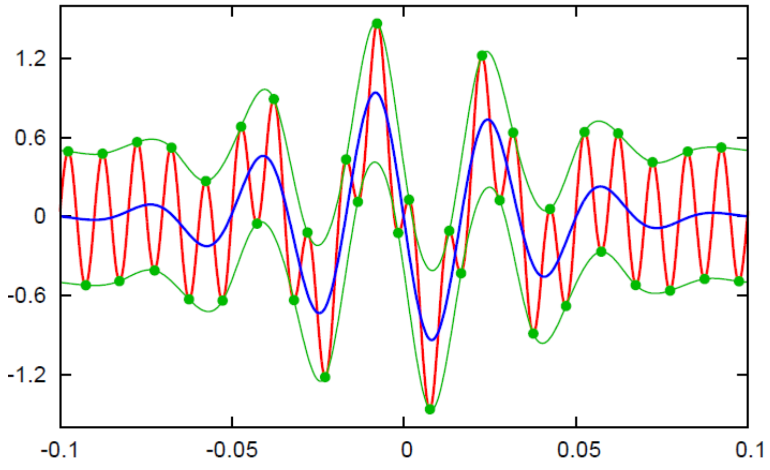

Empirical mode decomposition

- Calculate the local mean of upper and lower envelopes curve $m(t)$.

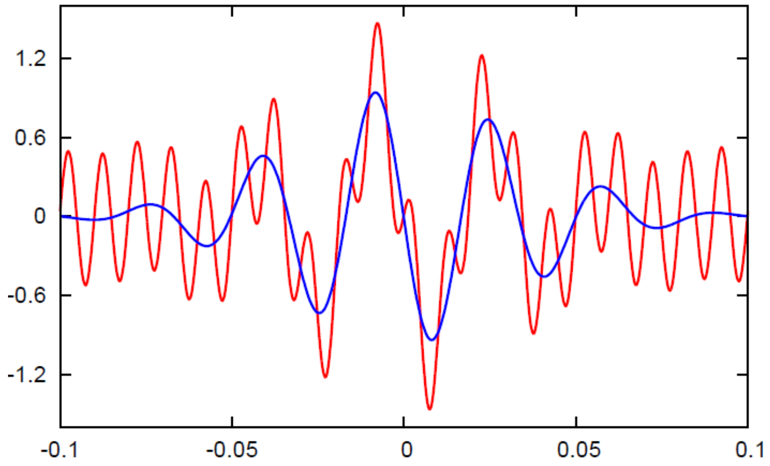

Empirical mode decomposition

- Subtract the mean $m(t)$ from the original data.

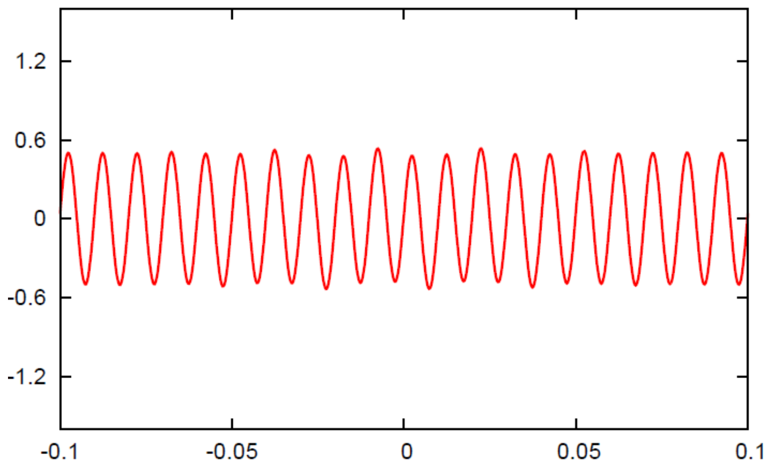

Empirical mode decomposition

- Until a certain stoppage criterion is satisfied, iterate this procedure.

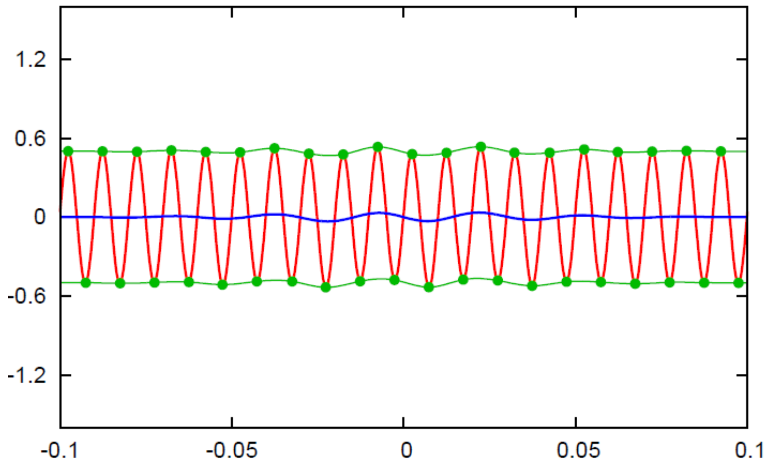

the stoppage criterion

$$\frac{\sum_i |m(t_i)|}{\sum_i |s(t_i)|} < \varepsilon$$

ε : a predetermined value

Empirical mode decomposition

- If the stoppage criterion is satisfied, define the data as **IMF1** $c_1(t)$.

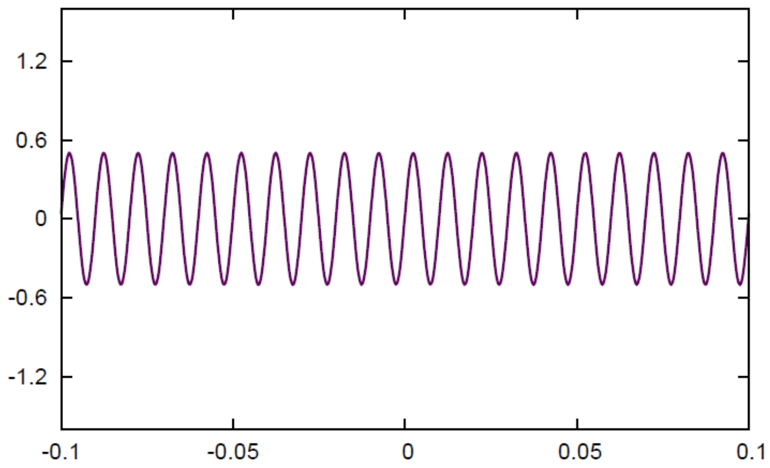

Empirical mode decomposition

- If the stoppage criterion is satisfied, subtract IMF1 from the original data.

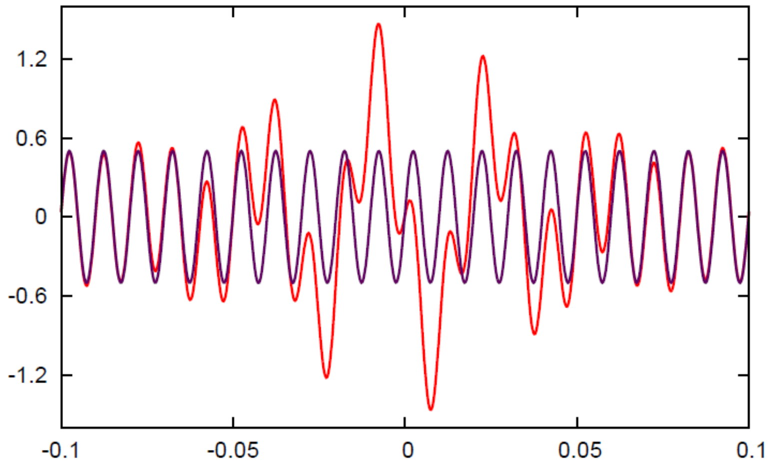

Empirical mode decomposition

- Apply the sifting process on the data to obtain IMF2 $c_2(t)$.

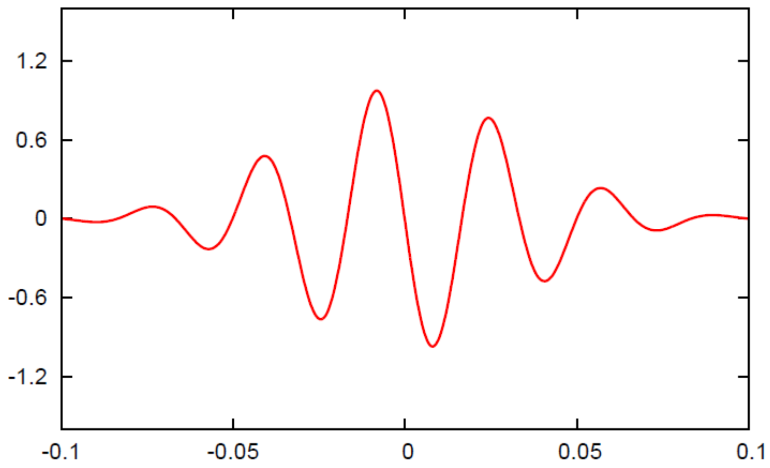

Empirical mode decomposition

- Apply the sifting process on the data to obtain IMF2 $c_2(t)$.

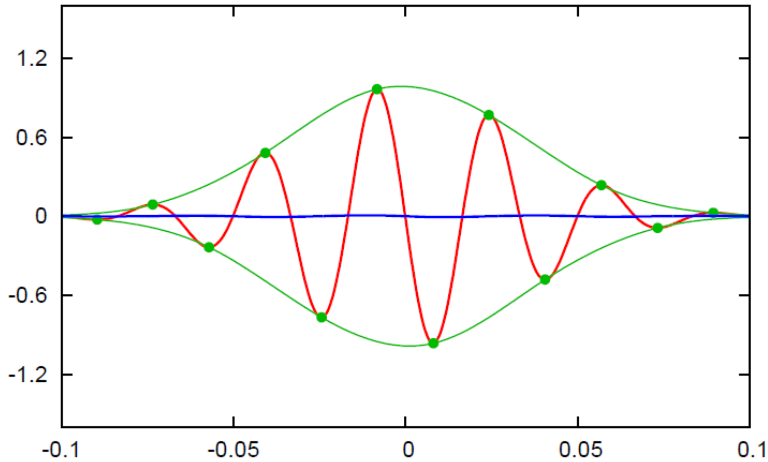

Empirical mode decomposition

- Apply the sifting process on the data to obtain **IMF2** $c_2(t)$.

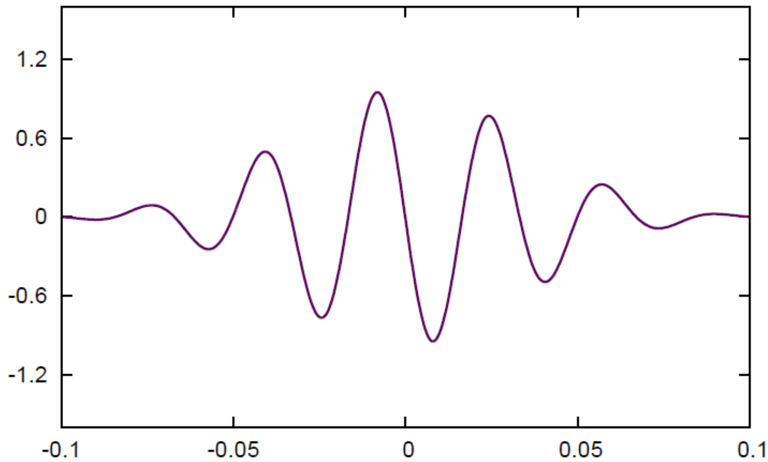

Empirical mode decomposition

- In a similar way, obtain **IMF3** $c_3(t)$ …

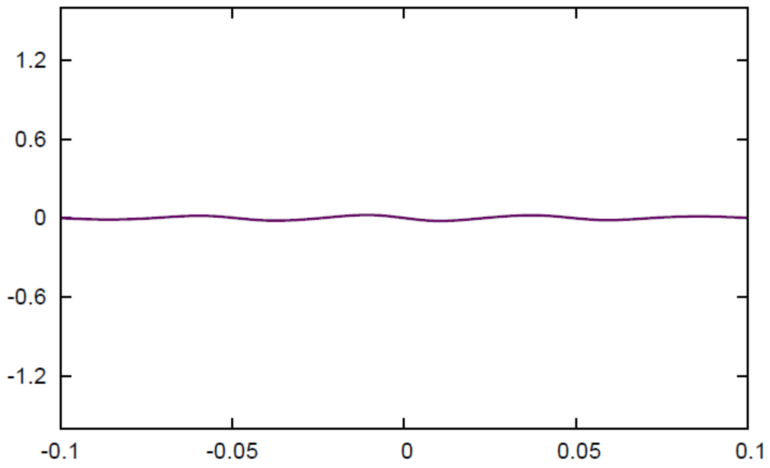

Empirical mode decomposition

- Finally, the original data is decomposed some IMFs $c_1(t), c_2(t)$ … and a residual $r(t)$.

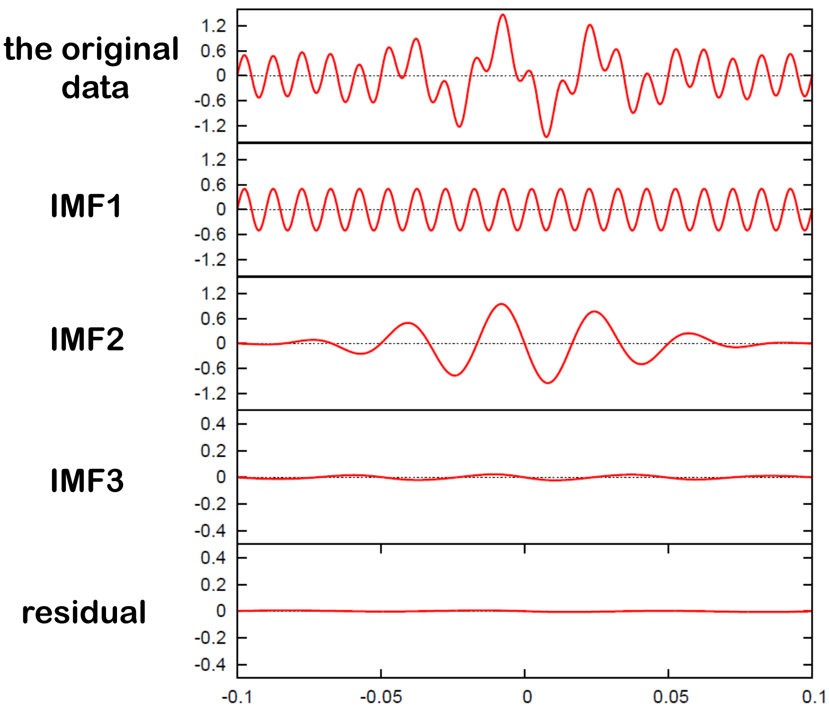

$$s(t) = \sum_i c_i(t) + r(t)$$

Ensemble EMD

- When we use the EMD, mode mixing often occurs.
  - a single IMF consists of signals of widely disparate scale
  - signals of a similar scale reside in different IMF components

- We use a ensemble EMD (EEMD) for minimize the mode mixing.

N. E. Huang et al. (08)

(1) Add white noise to the original data.

(2) Perform EMD on each data with different noise.

(3) For each IMF, take ensemble mean among the data as the final answer.

Setup for simulation

- s(t) = n(t) + h(t)

- Signal h(t): GW bursts from core collapse and core bounce of rotating stars

H. Dimmelmeier et al. (2008)

- Noise n(t): AdvLIGO
  - Angular sensitivity of the detector is simply treated as the angular efficiency factor F = 0.4 .
  - Noise frequency range: 20 Hz – 4096 Hz

  - distance = 10 kpc
  - Sampling frequency = 8192 Hz

Waveform of IMFs

Model: s20a2o13_shen

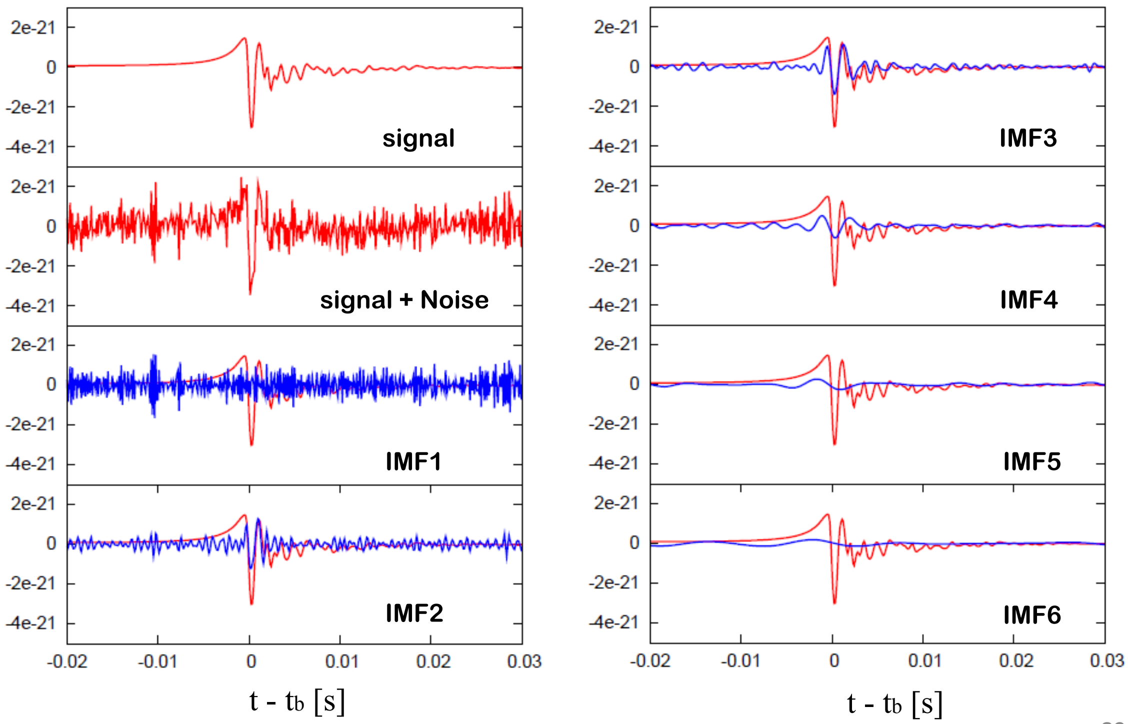

Summation of IMFs

- To obtain a reconstructed GW, we sum IMFs including the signal.

- After the EMD

$$s(t_j) = \sum_{i=1}^{M} c_i(t_j) + r(t_j)$$

$$h(t_j) = \sum_{i=1}^{M} h_i(t_j)$$

$$n(t_j) = \sum_{i=1}^{M} n_i(t_j)$$

IMF i : $c_i(t) = h_i(t) + n_i(t)$

- assume: Noise of IMFs is stationary and Normal distribution.

$$n_i(t_j): X_i \sim N(0, {\sigma_i}^2)$$

- If $c_i(t_j) \geq 4\sigma_i$, this IMFs include the signal and we sum those IMFs to get the reconstructed signal.

Possibility of wave reconstruction

- We performed the EEMD for 100 samples and the reconstructed signal of each samples.

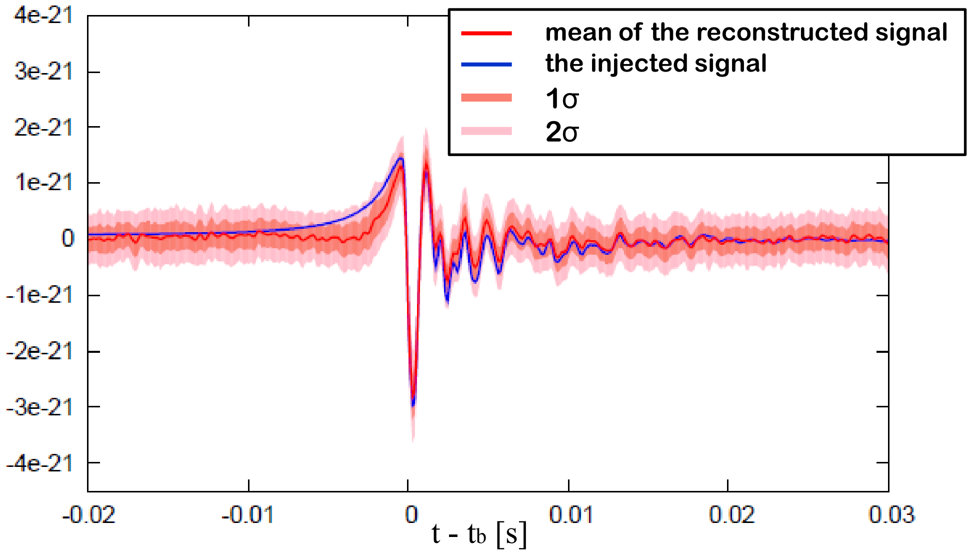

- We get the reconstructed signal, when it is obtained by summing appropriate IMFs.

Statistics of IMFs

- assume: Noise of IMFs is stationary and Normal distribution.

$$n_i(t_j): X_i \sim N(0, {\sigma_i}^2)$$

$$c_i(t_j): Y_{ij} \sim N(\mu_{ij}, {\sigma_i}^2) = \mu_{ij} + N(0, {\sigma_i}^2)$$

$$\mu'_j = \sum_i \mu_{ij}$$

$$\sigma'^2 = \sum_{i,k} \mathrm{cov}(X_i, X_k)$$

$$\sum_i c_i(t_j): W_j \sim N(\mu'_j, \sigma'^2) = \underline{\mu'_j} + N(0, \sigma'^2)$$

- Summation of IMFs is the reconstructed signal including residual noise.

Reconstructed signal

$$\sum_i c_i(t_j):\ W_j \sim N(\mu'_j, \sigma'^2) = \mu'_j + N(0, \sigma'^2)$$

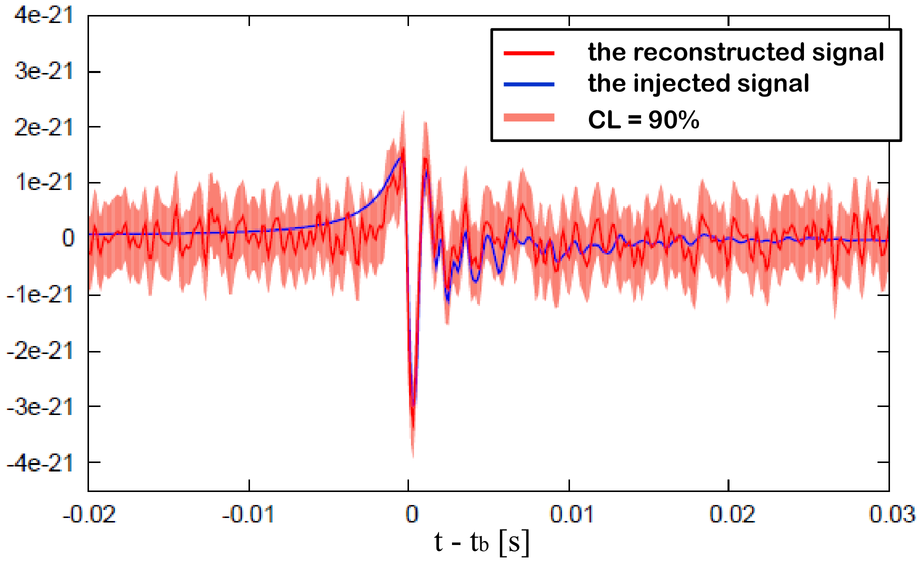

Summary

- The reconstruction of GW bursts is one of the important issue in the GW astronomy.

- We investigated the reconstruction of GW bursts with the HHT.

- The HHT is the adequate technique for reconstruction of waveform.

- We obtained the reconstructed signal with CL = 90%.

“Possible roles of PBH evaporation in cosmology and detection of its gravitational waves”

by Tomohiro Fujita

[JGRG23(2013)110712]


PRESENTATION
Possible roles of
PBH evaporation &
detection of its GW
Based on
T.F., K.Harigaya & M.Kawasaki
[arXiv:1306.6437];
T.F., K. Harigaya, M.Kawasaki
& R. Matuda [in prep].
2013/11/07
JGRG@Hirosaki Univ.
Kavli IPMU/Tokyo Univ.
Tomohiro Fujita

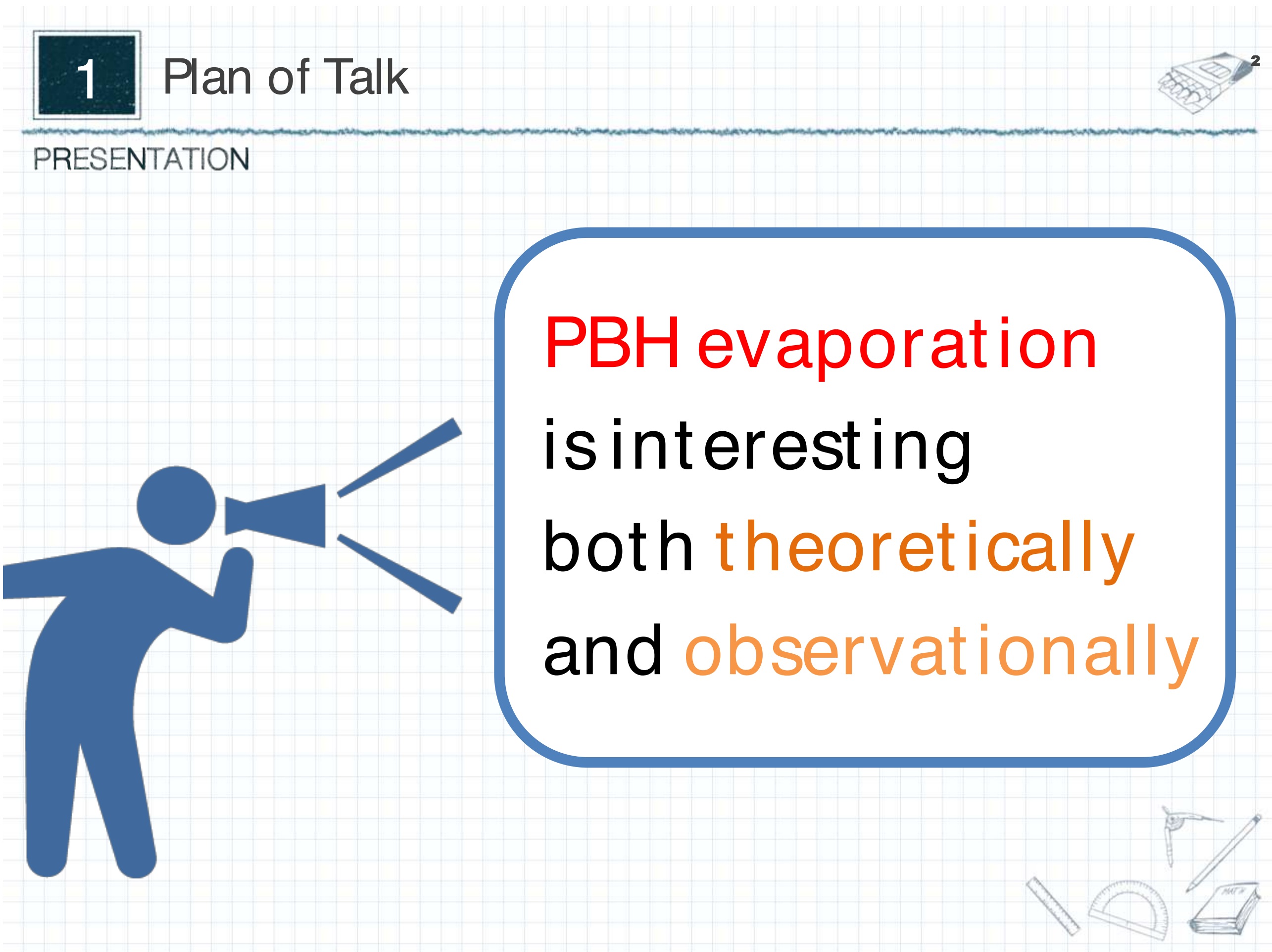
1
Plan of Talk
2
PRESENTATION
PBH evaporation
is interesting
both theoretically
and observationally

1 Introduction

PRESENTATION

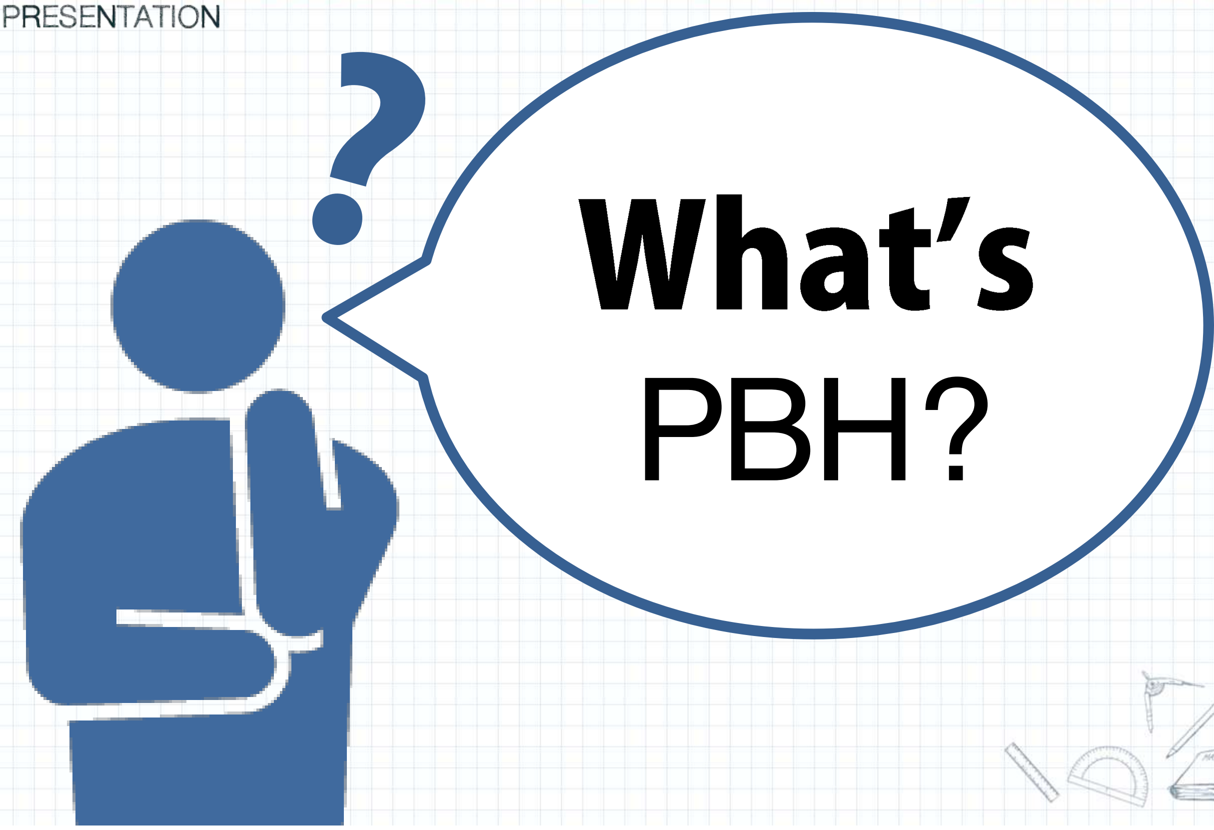

1

THE THEME
OF CHAPTER IS...

Introduction

1 Introduction

PRESENTATION

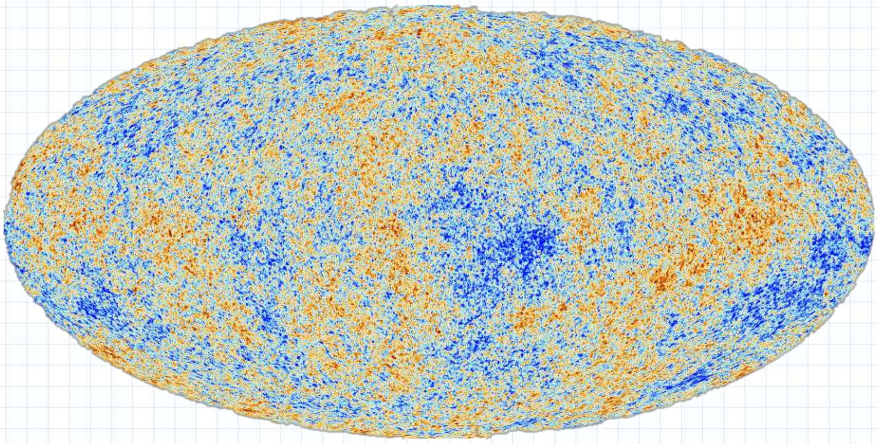

CMB

1 Introduction

PRESENTATION

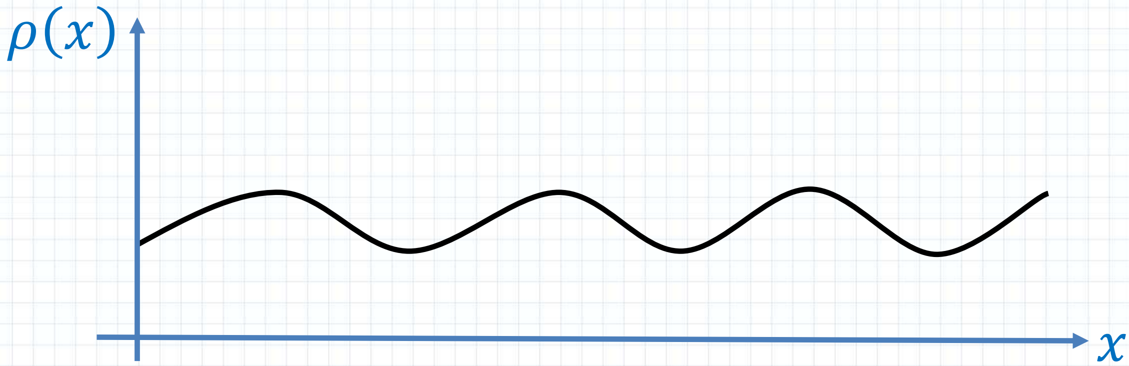

We know large scale pert.

1 Introduction

PRESENTATION

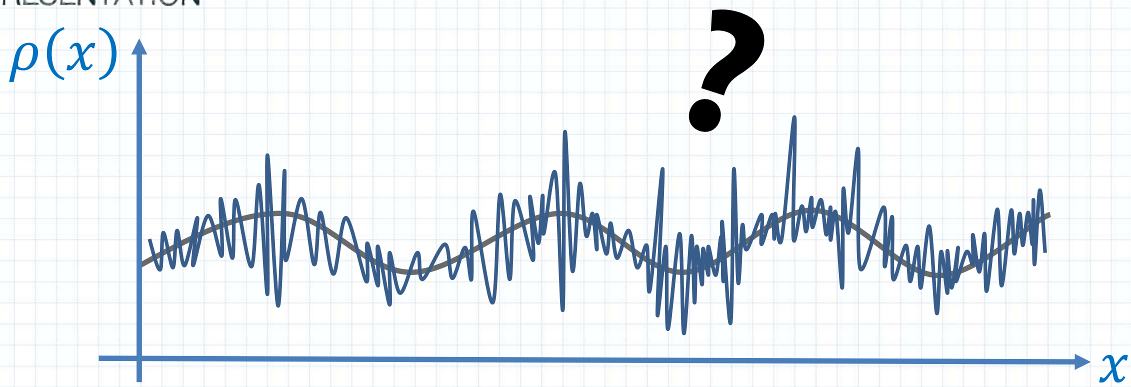

But small scale is unknown

1 Introduction

PRESENTATION

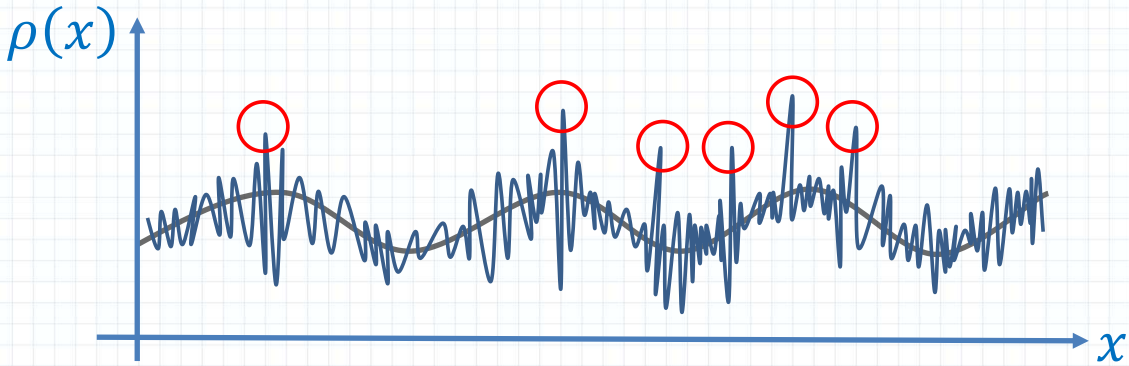

high density regions may exist.

ex) Blue running inflation, Preheating,
Sudden pressure reduction, bubble collision, etc...

1 Introduction

9

PRESENTATION

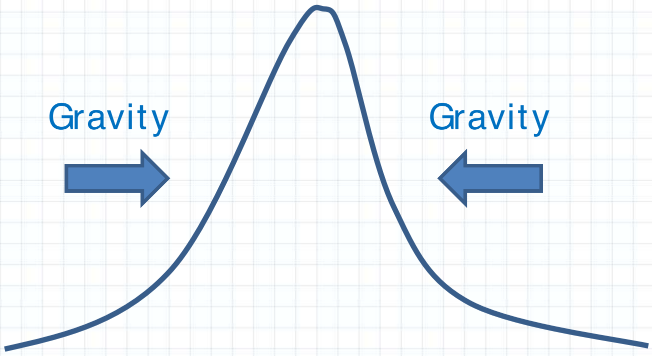

These regions collapse and form black holes.

Zel'dovitch & Novikov(1966), Howking(1971), Carr(1975), Nadezhin et al.(1978), Musco & Miller(2012), Harada, Yoo & Kohri (2013), Nakama et al.(2013)

1 Introduction

10

PRESENTATION

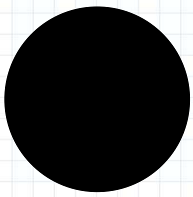

These regions collapse and form black holes.

Zel'dovitch & Novikov(1966), Howking(1971), Carr(1975), Nadezhin et al.(1978), Musco & Miller(2012), Harada, Yoo & Kohri (2013), Nakama et al.(2013)

1 Introduction

PRESENTATION

11

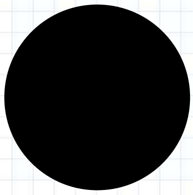

Primordial Black Hole
(PBH)

1 Introduction

PRESENTATION

12

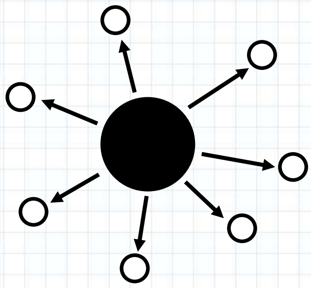

PBHs lose their mass
by Hawking radiation

Howking(1975), Page(1976)

1 Introduction

PRESENTATION

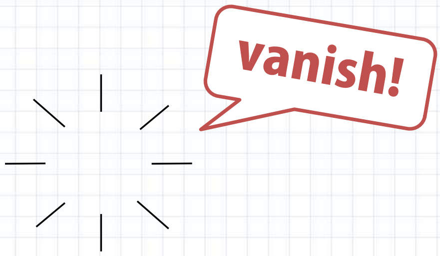

If $m_{BH} < 10^{15}\mathrm{g}$,
they evaporate!

Howking(1975), Page(1976)

1 Introduction

PRESENTATION

Interesting!
But is it relevant
to cosmology?

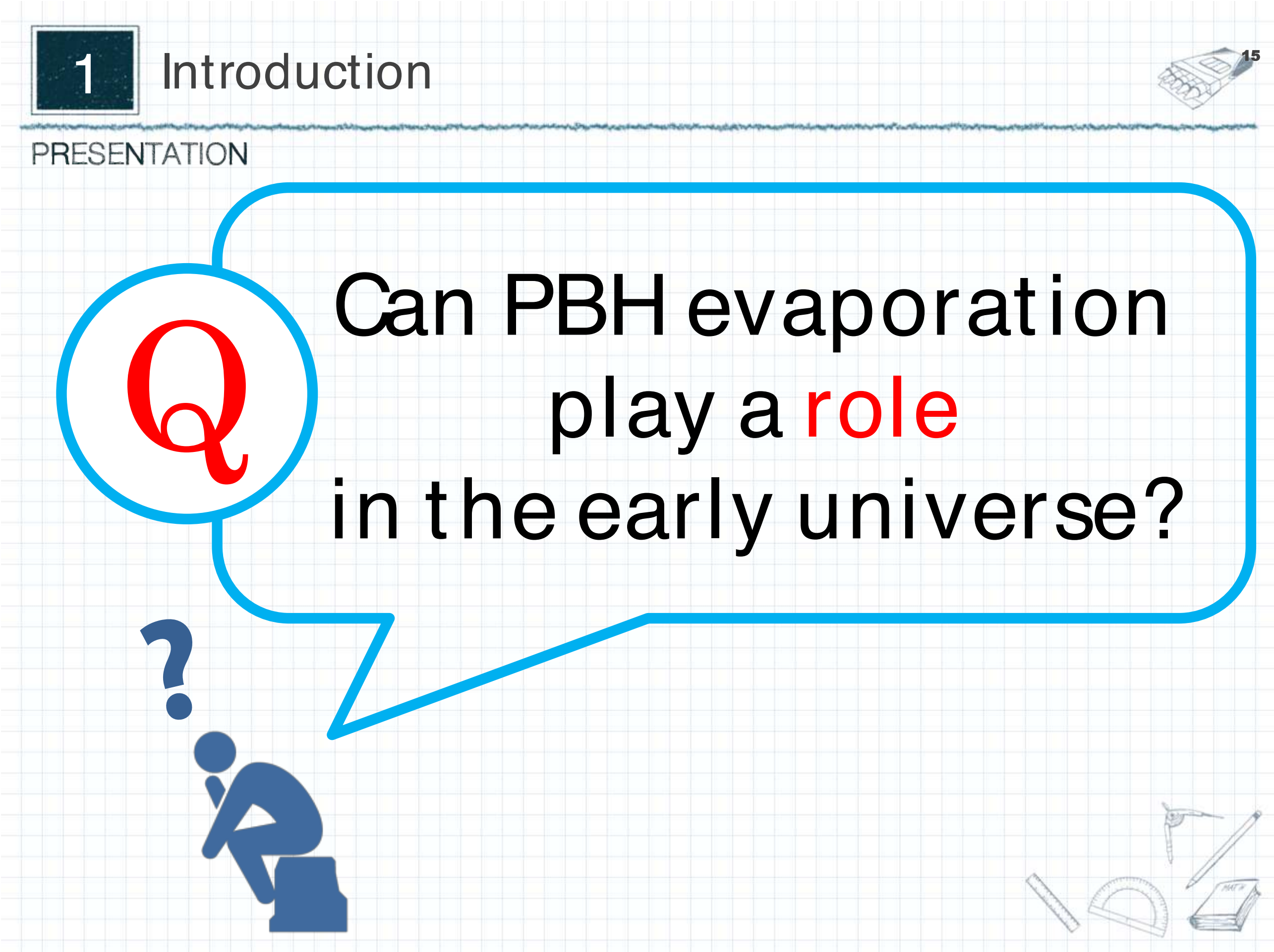
1
Introduction
15
PRESENTATION
Q
Can PBH evaporation
play a role
in the early universe?
?

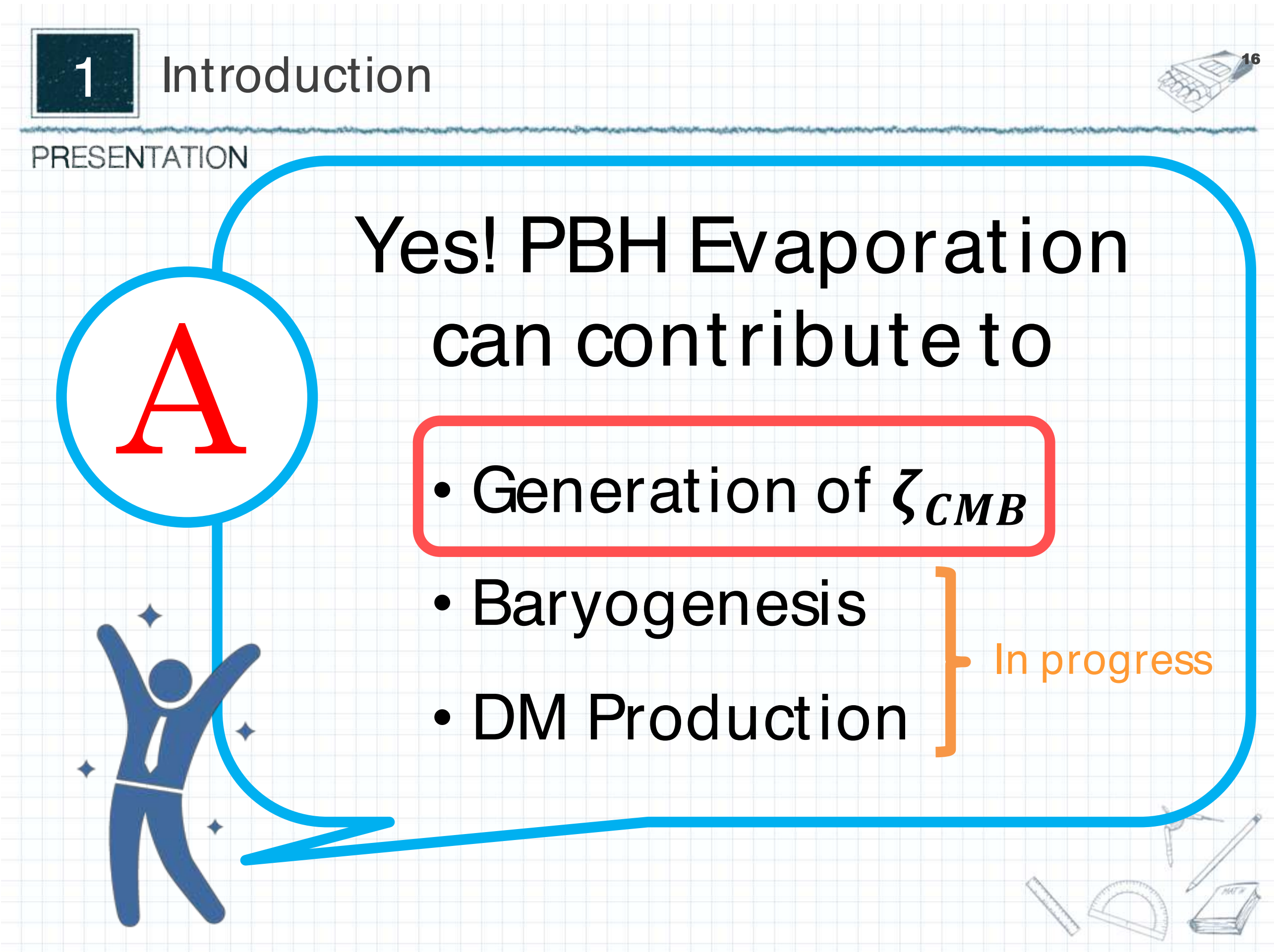
1
Introduction
16
PRESENTATION
A
Yes! PBH Evaporation
can contribute to
• Generation of ζ_{CMB}
• Baryogenesis
• DM Production
In progress

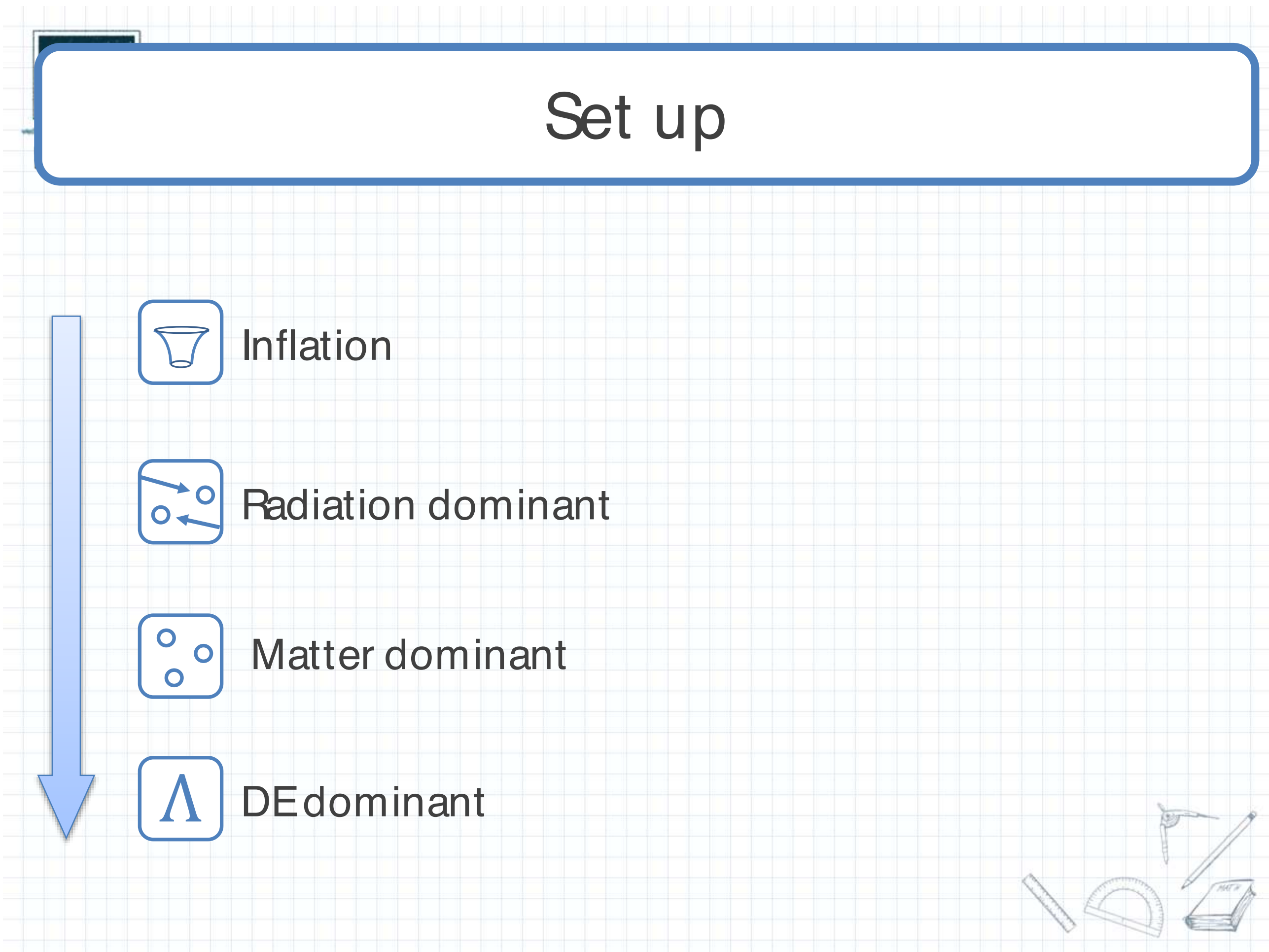
Set up
Inflation
Radiation dominant
Matter dominant
DE dominant

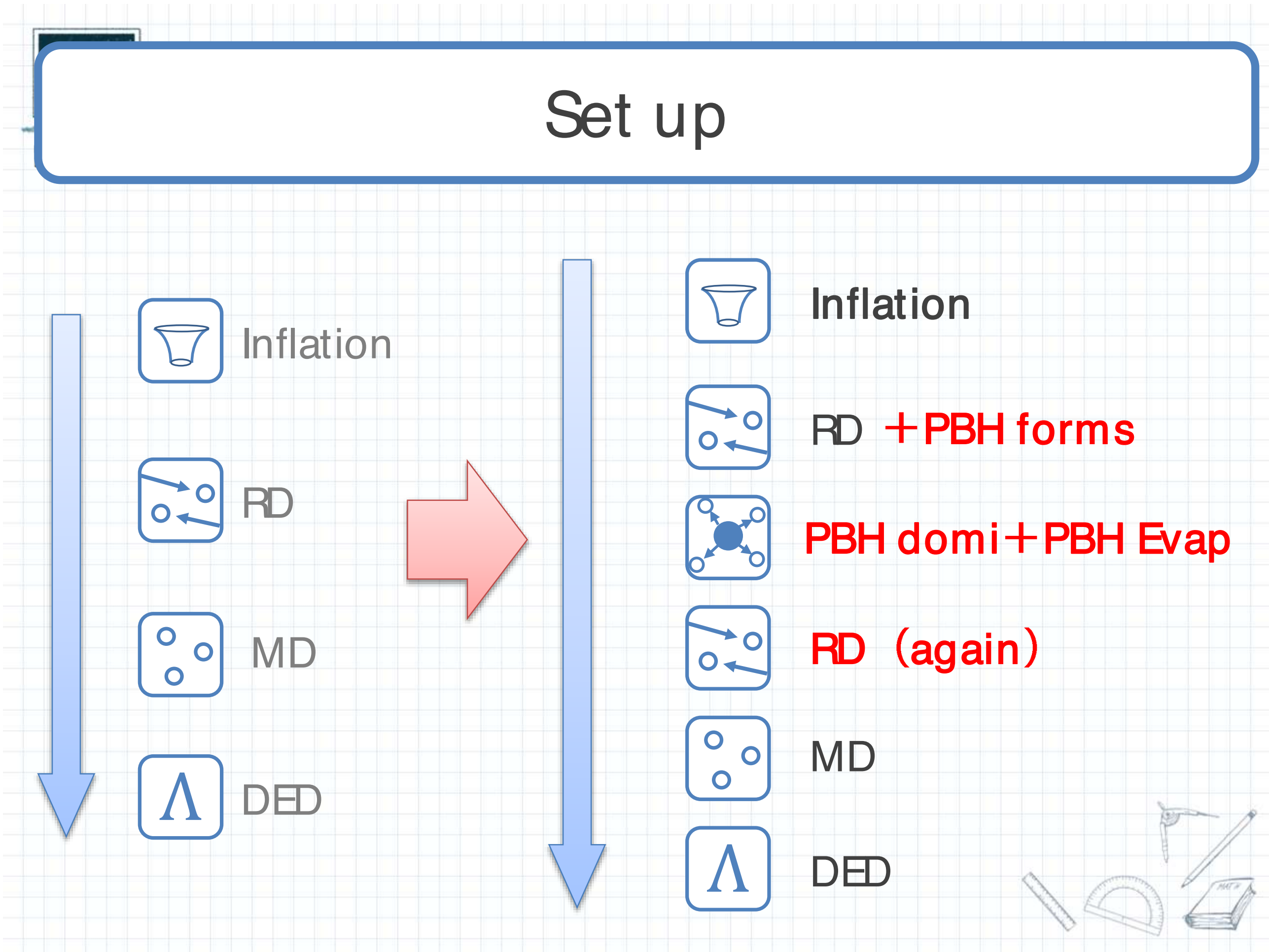
Set up
Inflation
RD
MD
DED
Inflation
RD +PBH forms
PBH domi+PBH Evap
RD (again)
MD
DED

Set up

PBHs dominate the universe before evaporation

Set up

Not so stringent condition

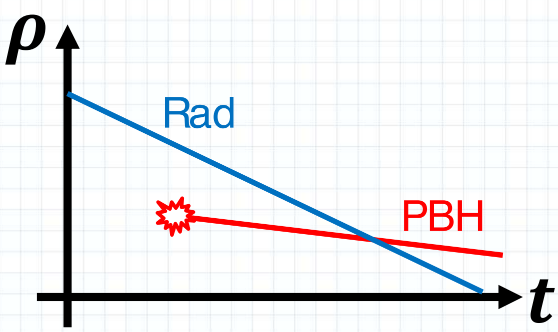

$$\rho_{\mathrm{rad}} \propto a^{-4}$$

$$\rho_{\mathrm{PBH}} \propto a^{-3}$$

Set up

Not so stringent condition

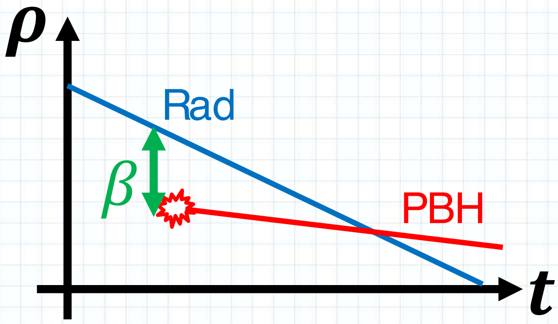

$$\rho_{\mathrm{rad}} \propto a^{-4}$$

$$\rho_{\mathrm{PBH}} \propto a^{-3}$$

$$\beta > 10^{-6}\left(\frac{1\mathrm{g}}{M_{\mathrm{PBH}}}\right)$$

Set up

Not so stringent condition

PBHs once dominate the universe

THE THEME
OF CHAPTER IS...

Generation of ζ_{CMB}

Single slow-roll inflation

$$\phi_{\text{inf}} \begin{cases} \bullet \quad N_{\text{inf}} > 60 \\ \bullet \quad \zeta_{CMB} \end{cases}$$

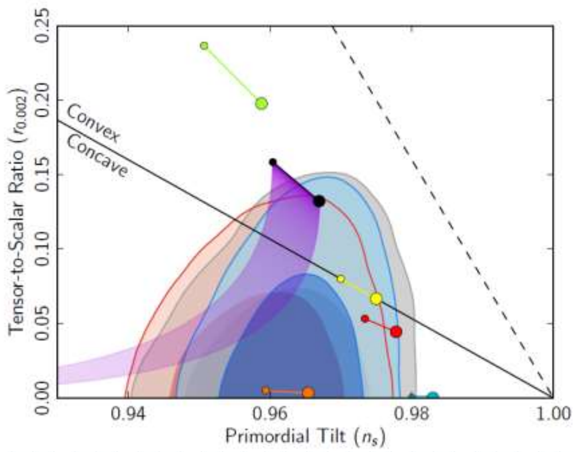

⇒ Not so easy

Curvaton like scenario

ϕ_{inf} $\left\{ \quad N_{\text{inf}} > 60 \right.$

- Curvaton
- Modulated Reheating
- Inhomogeneous end of inf.
- PBH New!!

$\Bigg\} \; \zeta_{CMB}$

1 Introduction

PRESENTATION

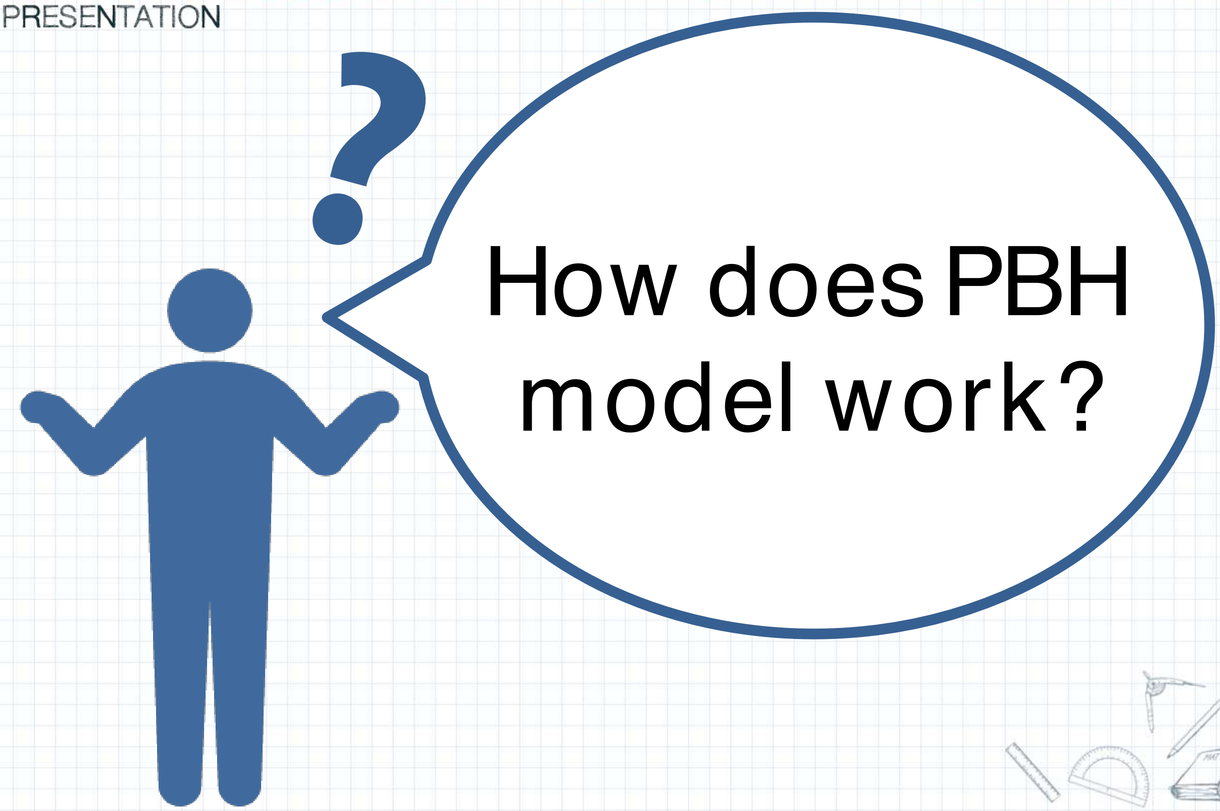

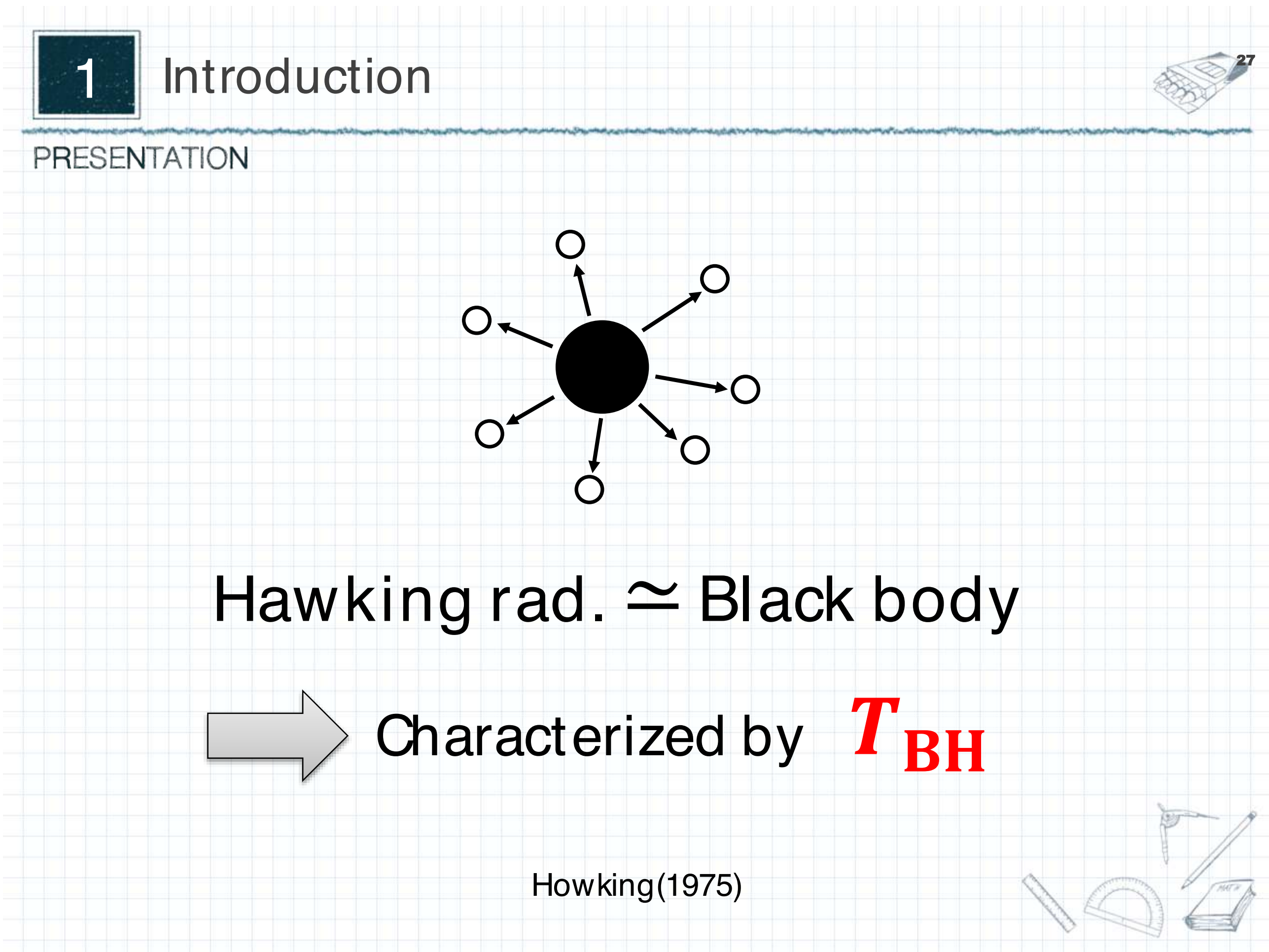
1 Introduction
PRESENTATION
Hawking rad. ≃ Black body
Characterized by T_{BH}
Howking(1975)

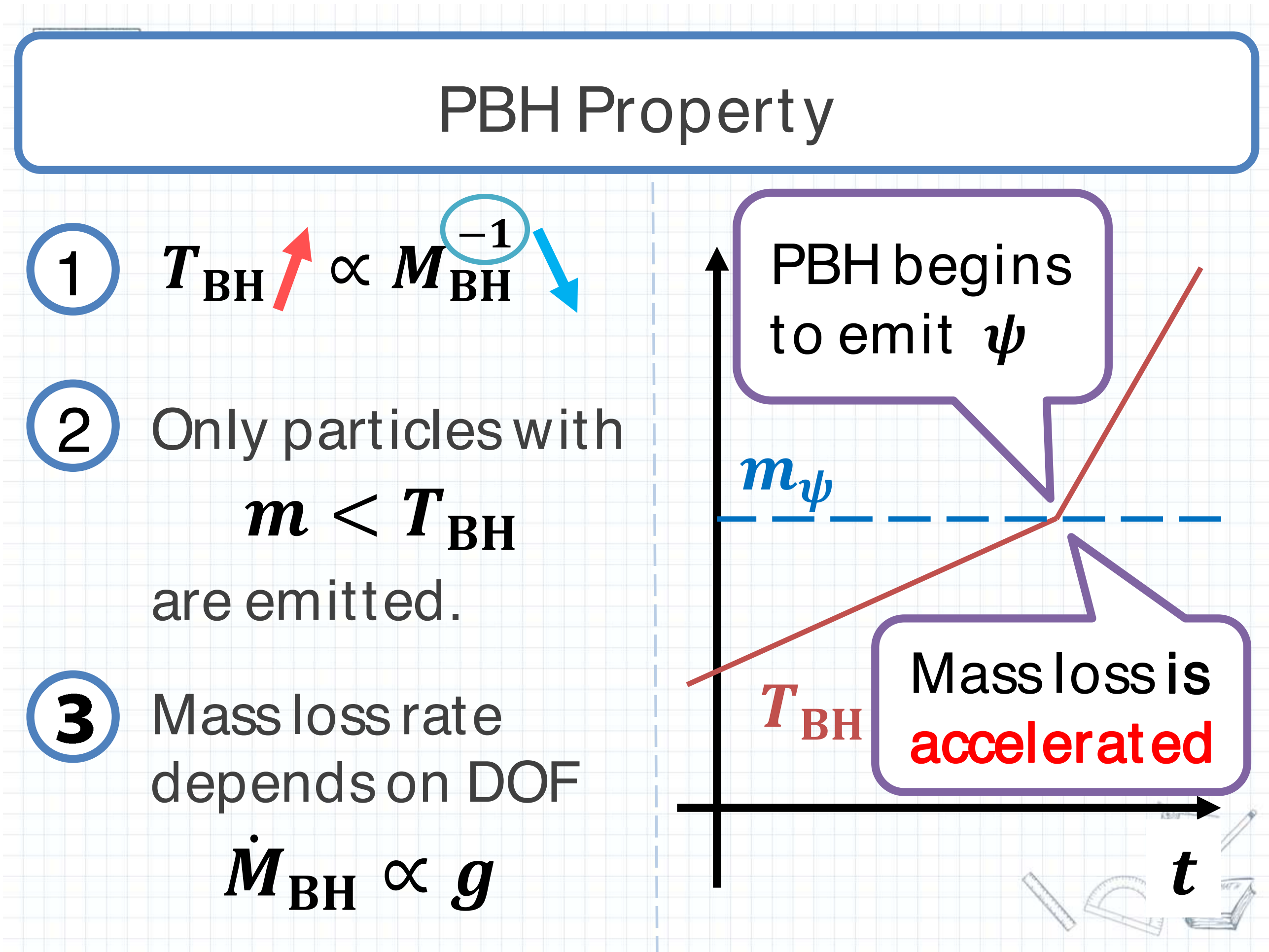
PBH Property
1 $T_{BH} \propto M_{BH}^{-1}$
2 Only particles with
$m < T_{BH}$
are emitted.
3 Mass loss rate
depends on DOF
$\dot{M}_{BH} \propto g$
PBH begins to emit ψ
m_ψ
T_{BH}
Mass loss is accelerated
t

Mechanism 1

- Introduce ϕ & ψ

$\delta\phi \Leftarrow$ inflation

- Higgs mechanism

$$m_\psi = y\phi$$

$$\Rightarrow \quad \delta m_\psi = y\delta\phi$$

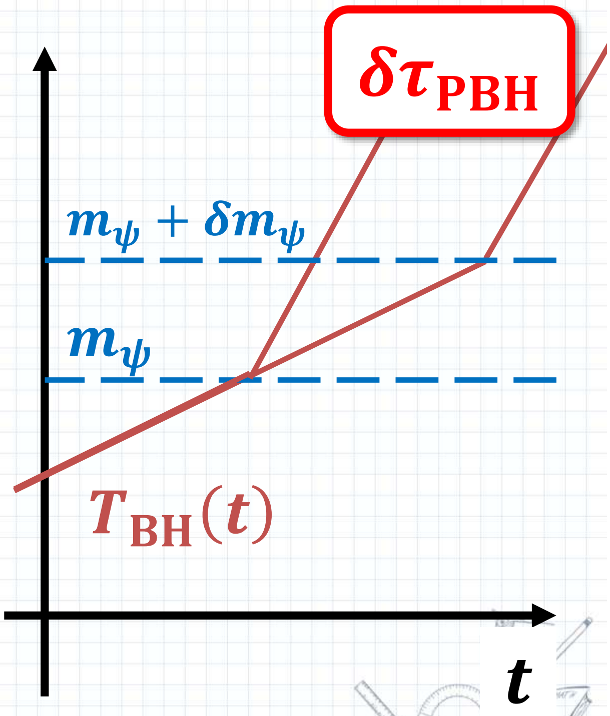

Mechanism 2

$\delta\phi$ — Inflation perturbes ϕ

⇓

δm_ψ — Higgs mech: $m_\psi = y\phi$

⇓

$\delta\tau_{\mathrm{PBH}}$ — m_ψ triggers the acceleration of mass loss

⇓

δN — Modulated 2nd Reheating

Result

$$\mathcal{P}_\zeta^{1/2} \approx 10^{-5}\left(\frac{y}{0.3}\right)\left(\frac{g_\psi}{1}\right)\left(\frac{H_{\rm inf}}{m_\psi}\right)^4$$

Result

$$\mathcal{P}_\zeta^{1/2} \approx 10^{-5}\left(\frac{y}{0.3}\right)\left(\frac{g_\psi}{1}\right)\left(\frac{H_{\rm inf}}{m_\psi}\right)^4$$

$\Rightarrow$ $m_\psi \simeq H_{\rm inf}$ OK!

Fine ~~tuning~~??

Result

$$\mathcal{P}_\zeta^{1/2} \approx 10^{-5}\left(\frac{y}{0.3}\right)\left(\frac{g_\psi}{1}\right)\left(\frac{H_{\rm inf}}{m_\psi}\right)^4$$

$$\Rightarrow \quad m_\psi \simeq H_{\rm inf} \quad \text{OK!}$$

If ϕ gives many ψs masses,
one ψ may have $m_\psi \simeq H_{\rm inf}$

Sales point

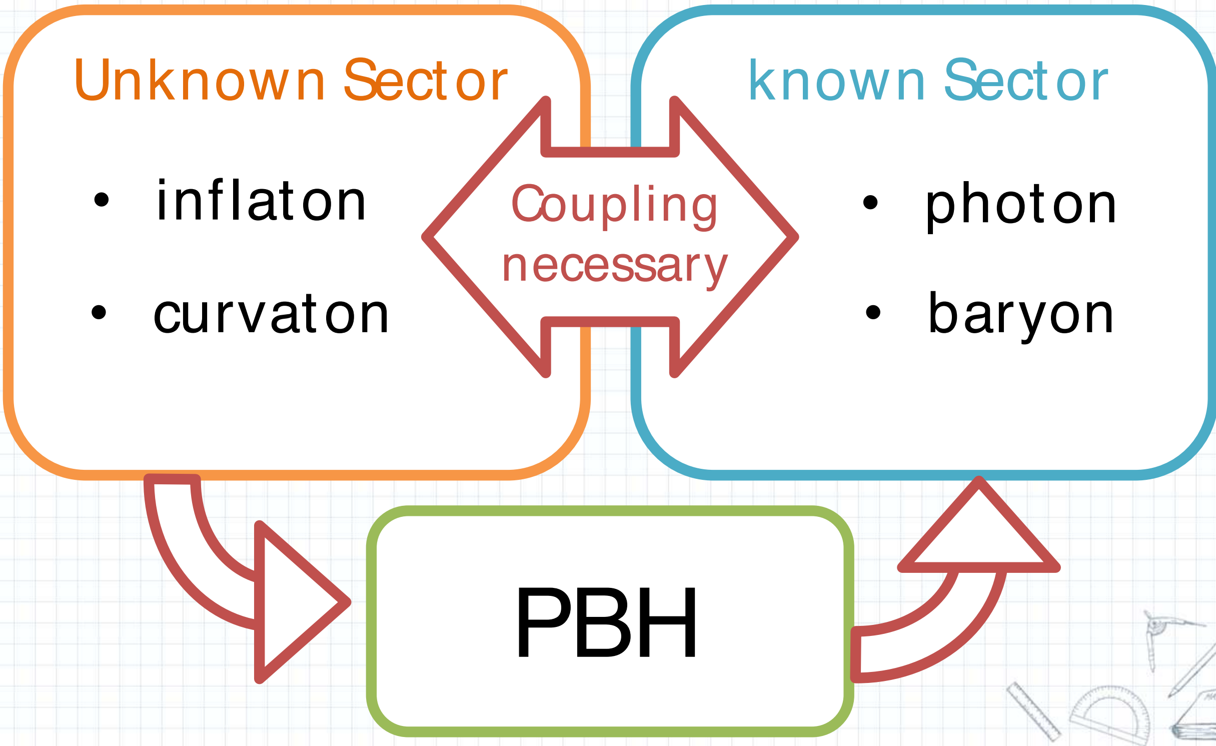

Quick Summary

PBH formation
Higgs mechanims

PBH ζ Generation

2 Fairytales

PRESENTATION

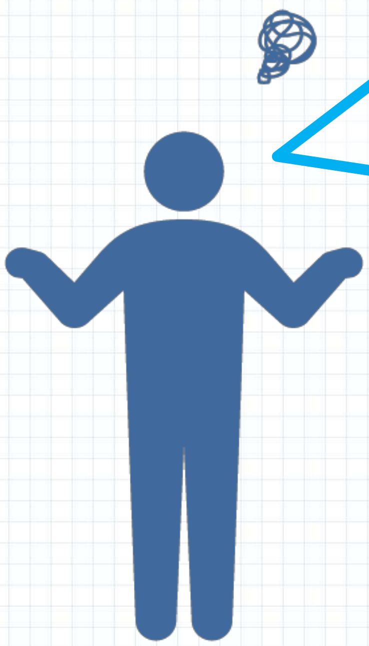

It sounds like a Fairytale.

（おとぎ話）

2 Fairytales

PRESENTATION

Consider

Observation

3

THE THEME
OF CHAPTER IS...

GW detection

How to observe PBH evaporation?

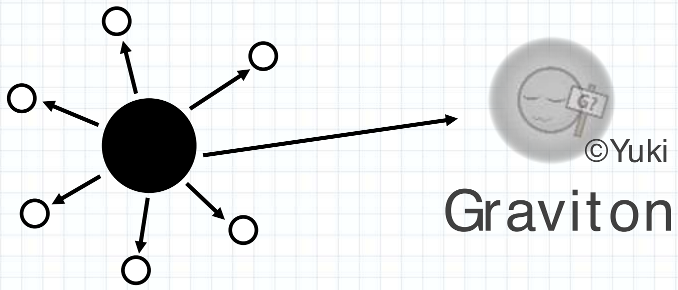

⇨ **Detect GW!!**

Frequency of GW

$$k_{\mathrm{PBH}} \sim T_{\mathrm{BH}} \times \text{redshift}$$

Frequency of GW

$$k_{\mathrm{PBH}} \sim T_{\mathrm{BH}} \frac{T_{\mathrm{now}}}{T_{\mathrm{evap}}}$$

Frequency of GW

$$k_{\mathrm{PBH}} \sim T_{\mathrm{BH}} \frac{T_{\mathrm{now}}}{T_{\mathrm{evap}}}$$

M_{PBH}

Frequency of GW

$$k_{\mathrm{PBH}} \sim T_{\mathrm{BH}} \frac{T_{\mathrm{now}}}{T_{\mathrm{evap}}}$$

k_{CMB}

M_{PBH}

Frequency of GW

$$k_{\mathrm{PBH}} \sim T_{\mathrm{BH}} \frac{T_{\mathrm{now}}}{T_{\mathrm{evap}}}$$

k_{CMB}

M_{PBH}

$$\sim 10^3 k_{\mathrm{CMB}} \left(\frac{M_{PBH}}{1\mathrm{g}}\right)^{\frac{1}{2}}$$

Detectability

[Anantua et al.(2009); Dolgov&Ejlli(2011)]

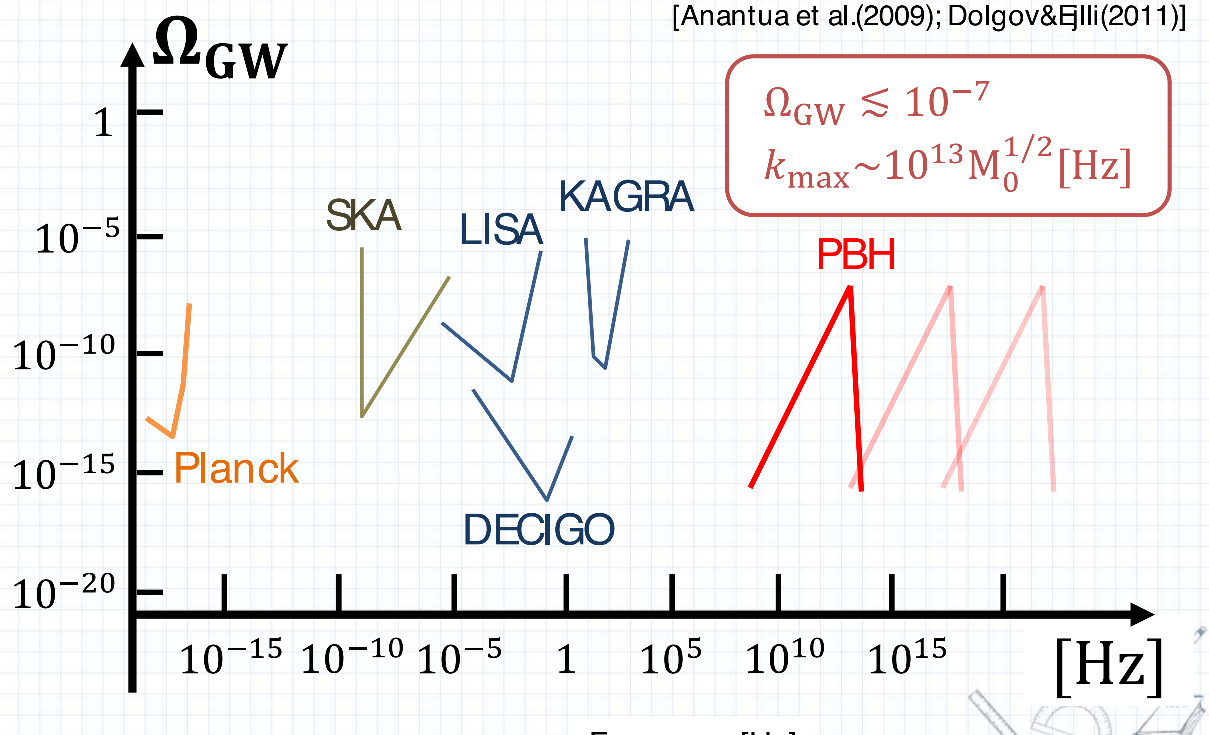

Detectability

[Anantua et al.(2009); Dolgov&Ejlli(2011)]

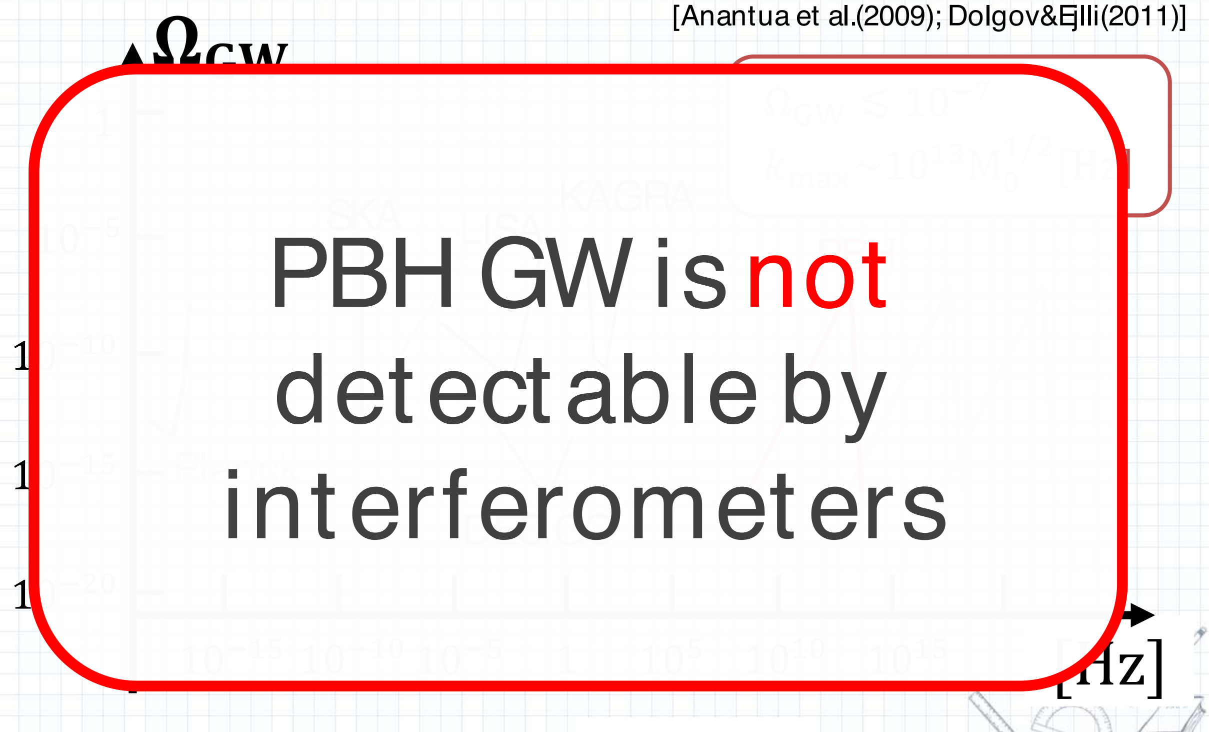

PBH GW is not detectable by interferometers

G-effect detector

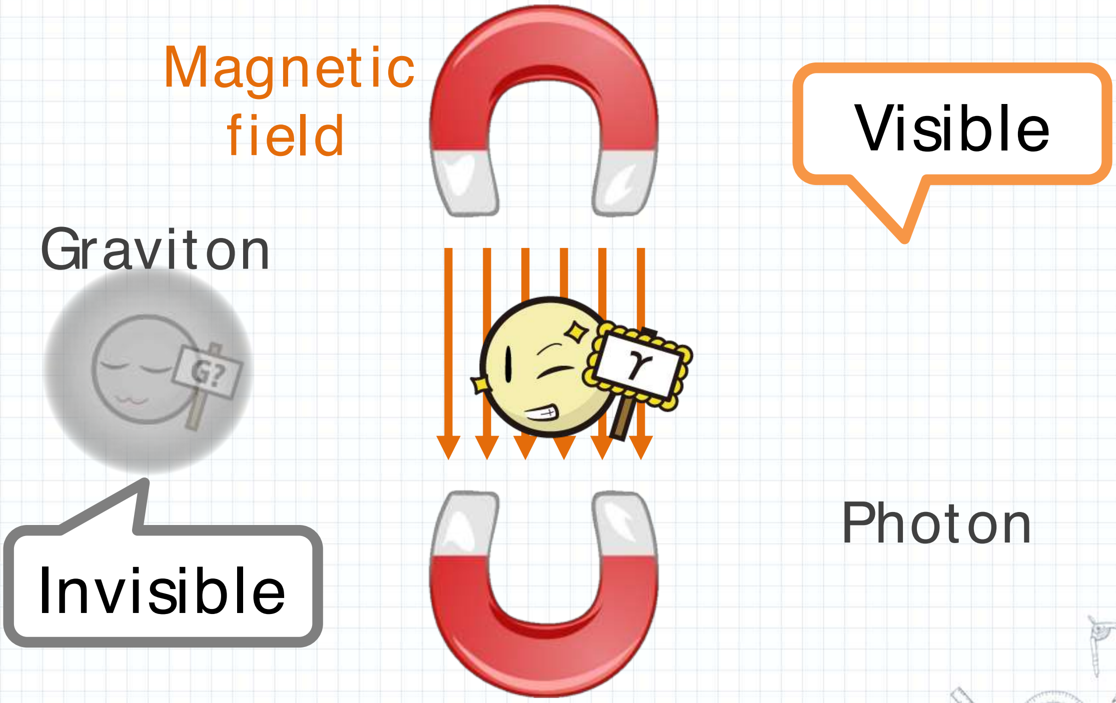

Gertenshtein-effect

[Gertenshtein(1966)]

With GW  and Static MF 
Maxwell eq. has a source term.

$$\nabla \times \boldsymbol{B} = \dot{\boldsymbol{E}} + ikB_s \boldsymbol{h} e^{i(kz-\omega t)}$$

induces 

Sensitivity of G-effect detector

M Cruise made a prototype

[AM Cruise(2006)]

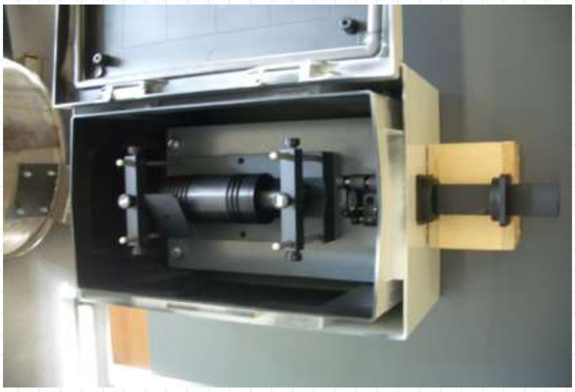

Development Path- no seeding

UNIVERSITY OF BIRMINGHAM

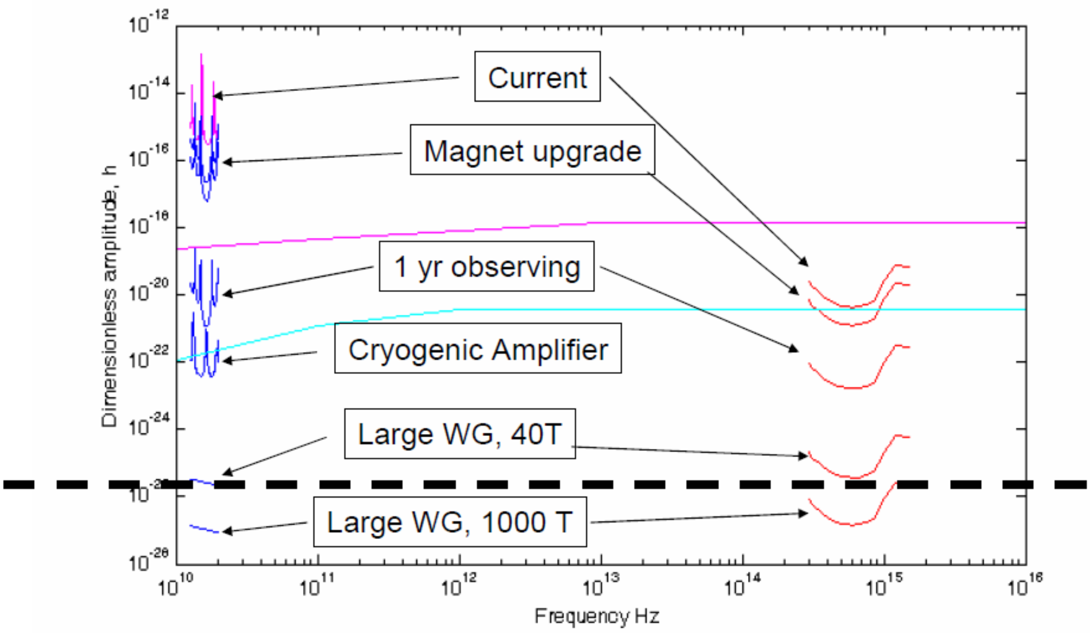

UNIVERSITY OF BIRMINGHAM

Development Path- no seeding

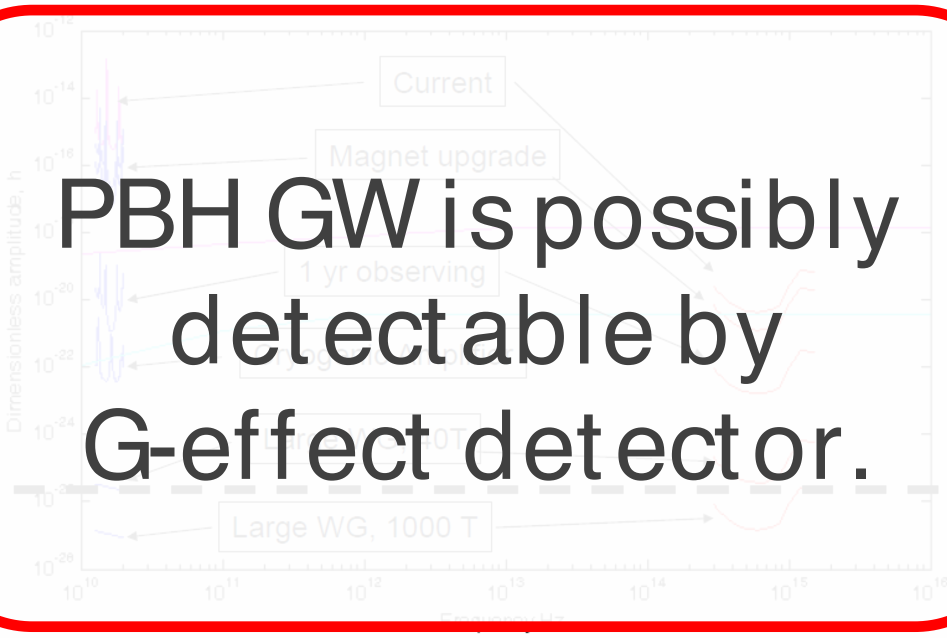

PBH GW is possibly detectable by G-effect detector.

Summary

1 Plan of Talk

53

PRESENTATION

PBH evaporation
is interesting
both theoretically
and observationally

5 Summary

54

PRESENTATION

1. PBH evaporation can play big roles in very early universe.

   ⇒ PBH can generate ζ_{CMB}

2. HFGW from PBH evaporation may be detectable in the future by

   ⇒ G-effect detector

THE THEME
OF CHAPTER IS...

Thank you!

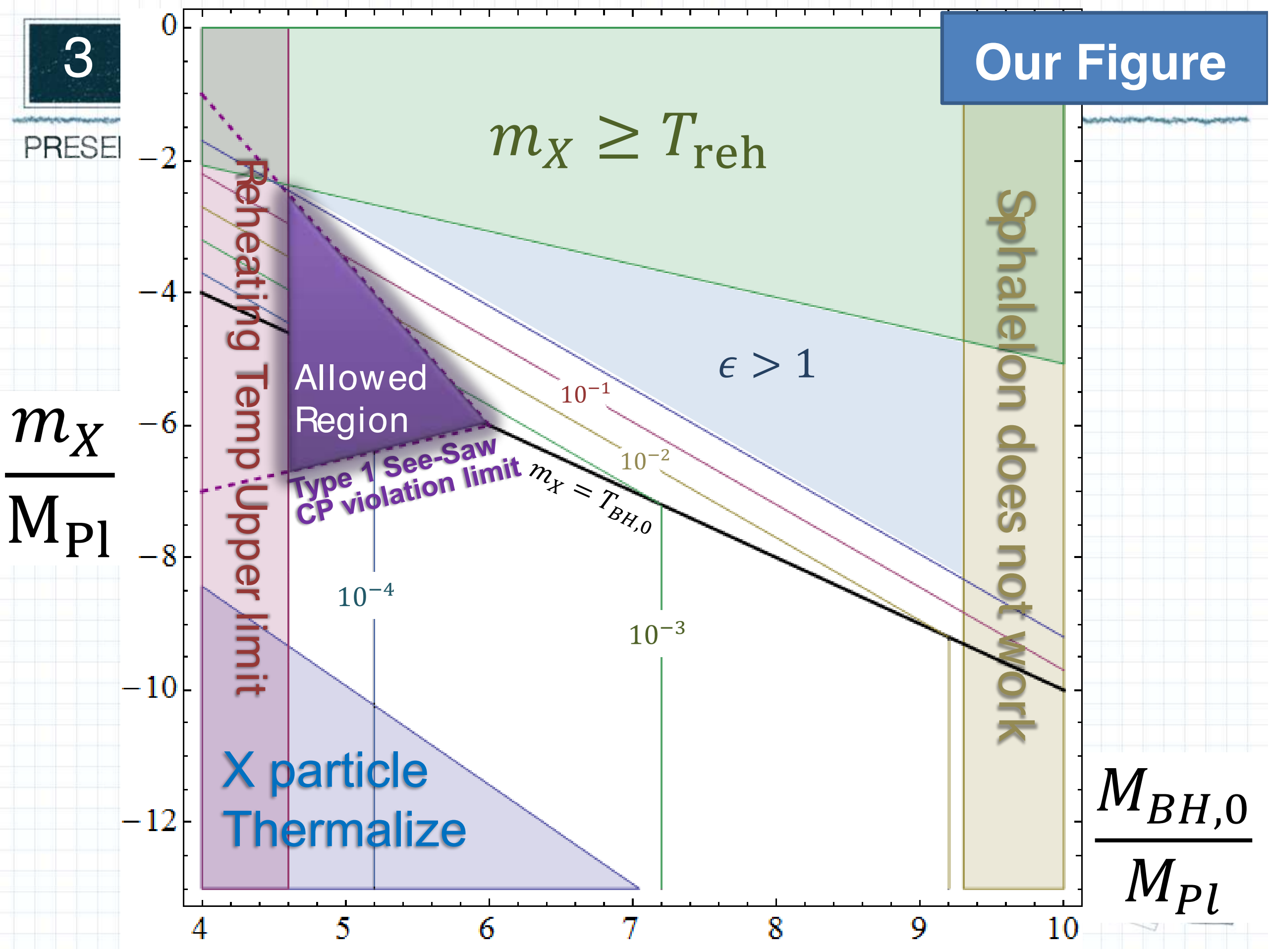

G-effect detector

New

Convert GW into EM wave by strong MF and detect EM wave.

→ Sensitive to high frequency GW!

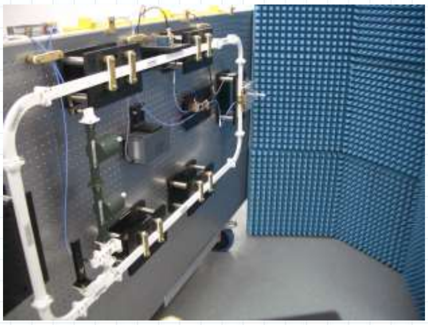

Prototype was already made in Birmingham univ.

Sensitivity is insufficient but several ideas for Improvement are proposed.

G-effect detector

[LP Grischuk(2003); Fangyu Li et al.(2008); Fangyu Li et al.(2009); J Lin et al.(2009); AM Cruise(2012)]

No sensitivity curve yet...

Amplitude of 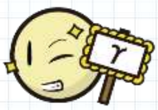

$\sim hk\, B_s L_B$

G-effect detector

[LP Grischuk(2003); Fangyu Li et al.(2008); Fangyu Li et al.(2009); J Lin et al.(2009); AM Cruise(2012)]

No sensitivity curve yet...

Amplitude of 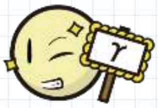 $\sim hk\, B_s L_B$

Strength & Length of Static MF

⇒ Strong & Long MF improves sensitivity

“Estimation of gravitational wave spectrum from cosmic domain walls”

by Ken'ichi Saikawa

[JGRG23(2013)110713]

Estimation of gravitational wave spectrum from cosmic domain walls

Ken'ichi Saikawa
Tokyo Institute of Technology

Collaborate with T. Hiramatsu (YITP) and M. Kawasaki (ICRR)

Based on:
T. Hiramatsu, M. Kawasaki, KS, hep-ph/1309.5001. (submitted to JCAP)

Abstract

- 3D Numerical simulation of domain walls
- Estimate spectrum of gravitational waves
- Update & correct the results of previous studies with larger simulation box

T. Hiramatsu, M. Kawasaki, KS, JCAP05(2010)032
M. Kawasaki, KS, JCAP09(2011)008

Domain wall

Example: Z2 → 1 $$V(\phi) = \frac{\lambda}{4}(\phi^2 - \eta^2)^2$$

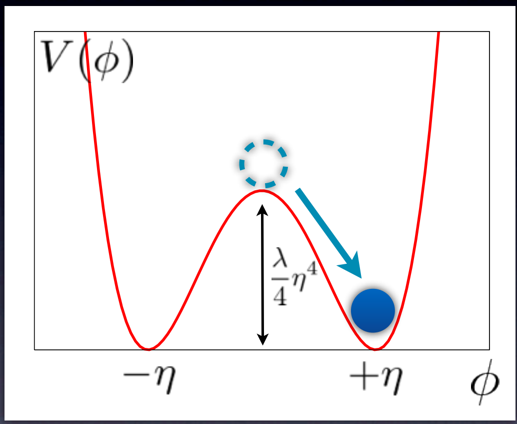

field space

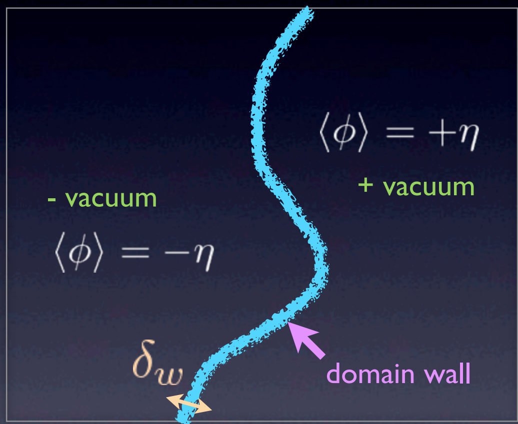

real space

Width of wall : $\delta_w \sim m_\phi^{-1} \sim (\sqrt{\lambda}\eta)^{-1}$

Surface energy density : $\sigma_{\rm wall} \sim \delta_w \times \frac{\lambda}{4}\eta^4 \sim \lambda^{1/2}\eta^3$

Domain wall problem

- Scaling solution Press, Ryden, Spergel, ApJ 347, 590 (1989)
  - One wall per one Hubble radius

    $$L \sim H^{-1} \sim t$$

    L : distance between two neighboring walls

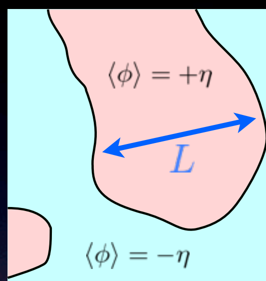

  - Energy density

    $$\rho_{\rm wall} \sim \sigma_{\rm wall} L^2/L^3 \sim \sigma_{\rm wall}/t$$

    decays slower than $\rho_{\rm matter} \propto a^{-3}$ and $\rho_{\rm radiation} \propto a^{-4}$

- Come to overclose the universe (DW problem)

  Zel'dovich, Kobzarev, Okun, JETP 40, 1 (1975)
  - One way to avoid the problem:
    consider the unstable domain walls

Collapse of domain walls

Approximate discrete symmetry (bias) Vilenkin, PRD23, 852 (1981)

$$\Delta V \sim \epsilon\eta^4 \qquad \epsilon \ll 1$$

Act as the volume pressure

$$p_V \sim \Delta V \sim \epsilon\eta^4$$

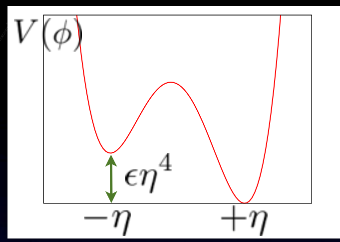

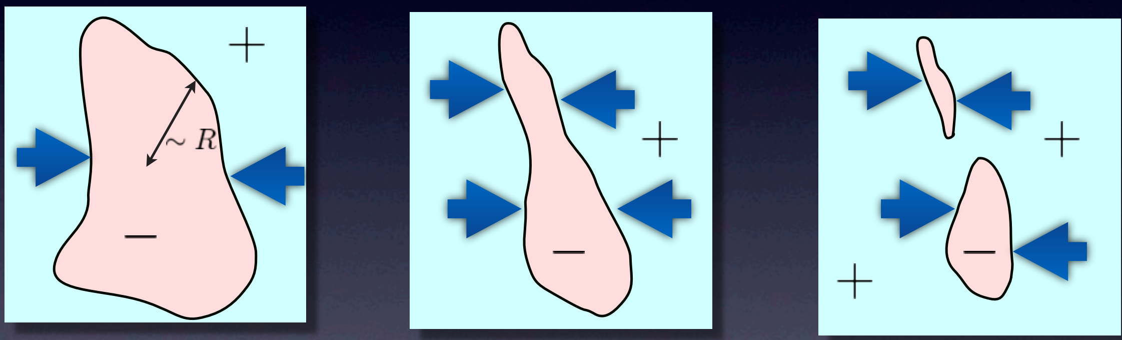

Annihilation occurs when

$$p_V \sim p_T$$

$p_T \sim \sigma_{\rm wall}/R \sim \lambda^{1/2}\eta^3/R$

: tension of walls

R : curvature radius

Decay time

$$t_{\rm dec} \sim R \sim \lambda^{1/2}/\epsilon\eta$$

Gravitational waves from domain walls

- Continuously produced during the scaling regime
  → It terminates at $t \sim t_{\rm dec}$
- Magnitude of gravitational waves
  - Quadrupole formula

$$P \sim G\dddot{Q}_{ij}\dddot{Q}_{ij} \sim M_{\rm wall}^2/t^2$$: Power [energy / time]

$$Q_{ij} \sim M_{\rm wall}t^2$$

$$M_{\rm wall} \sim \sigma_{\rm wall}\mathcal{A}t^2$$

During the scaling regime

$L \sim t$

$\rho_{\rm wall} \sim \sigma_{\rm wall}/t$

$\mathcal{A} \equiv \frac{\rho_{\rm wall}}{\sigma_{\rm wall}}t \simeq {\rm const.\ of\ } \mathcal{O}(1)$

  - Energy density

$$\rho_{\rm gw} \sim \frac{Pt}{t^3} \sim G\mathcal{A}^2\sigma_{\rm wall}^2$$

Previous studies

Hiramatsu, Kawasaki, KS, JCAP05(2010)032
Kawasaki, KS, JCAP09(2011)008

- Numerical simulations of classical scalar field on the lattice
  - Lattice points were small ($N^3 = 256^3$)
    = dynamical range was short
    - Affected by initial condition ?
    - Parameter dependence was not thoroughly investigated (width of the wall $\propto \lambda^{-1/2}$ was fixed)
    - Some errors in the numerical code
- This study :
  Correct and clarify these ambiguities by performing simulations with larger grids ($N^3 = 1024^3$)

Numerical simulation

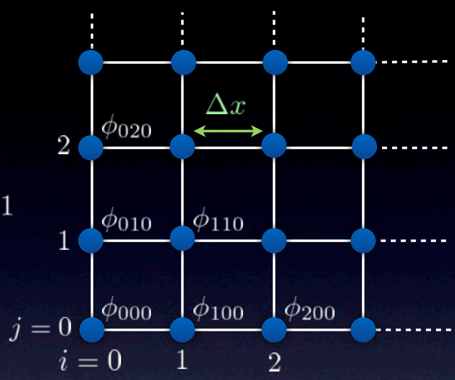

- Discretize the spatial coordinate

$$\vec{\mathbf{x}} \quad \rightarrow \quad (i, j, k)$$

$$i, j, k = 0, 1, \ldots, N-1$$

$$\phi(\vec{\mathbf{x}}) \quad \rightarrow \quad \phi_{i,j,k}$$

$$\nabla^2\phi(\vec{\mathbf{x}}) \rightarrow (\nabla^2\phi)_{i,j,k}$$

$$= \frac{1}{12(\Delta x)^2}[16(\phi_{i+1,j,k} + \phi_{i-1,j,k} + \phi_{i,j+1,k} + \phi_{i,j-1,k} + \phi_{i,j,k+1} + \phi_{i,j,k-1}) - (\phi_{i+2,j,k} + \phi_{i-2,j,k} + \phi_{i,j+2,k} + \phi_{i,j-2,k} + \phi_{i,j,k+2} + \phi_{i,j,k-2}) - 90\phi_{i,j,k}]$$

- Solve the classical EOM for real scalar ϕ on 3D lattice $N^3 = 1024^3$

$$\ddot{\phi} + 3H\dot{\phi} - \frac{\nabla^2}{a^2(t)}\phi = -\frac{\partial V}{\partial \phi}$$

- With small Gaussian fluctuations as initial conditions

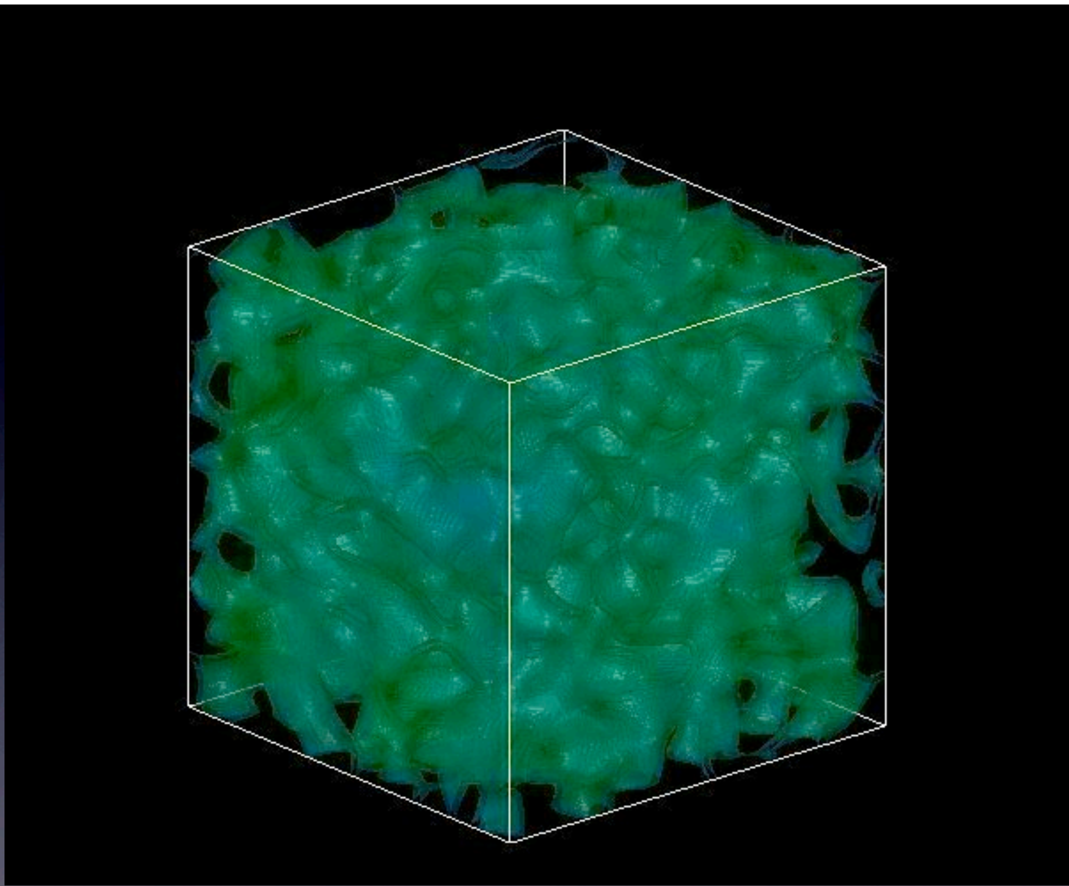

9/15

Spectrum of gravitational waves

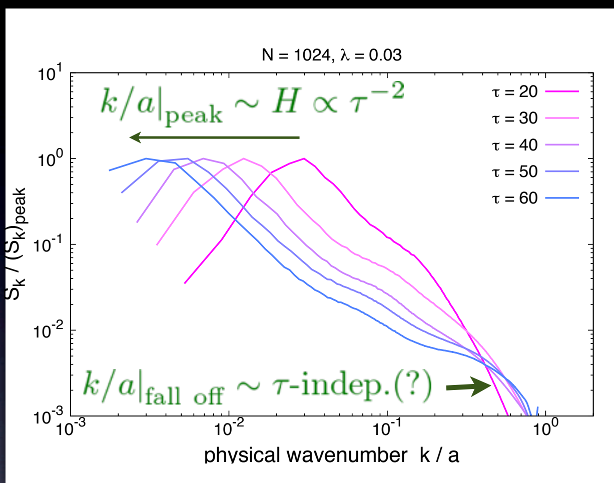

$$S_k(\tau) \equiv \frac{2\pi^2 V a^4(\tau)}{G} \frac{d\rho_{\rm gw}(\tau)}{d\ln k} = k \int d\Omega_k \sum_{ij} \left(\left| C_{ij}^{(1)} \right|^2 + \left| C_{ij}^{(2)} \right|^2 \right)$$

$$C_{ij}^{(1)} = -\int_{\tau_i}^{\tau} k d\tau' \sin(k\tau') a(\tau') T_{ij}^{TT}(\mathbf{k}, \tau')$$

$$T_{ij}^{\rm TT} \sim \nabla_i \phi \nabla_j \phi$$

$$C_{ij}^{(2)} = \int_{\tau_i}^{\tau} k d\tau' \cos(k\tau') a(\tau') T_{ij}^{TT}(\mathbf{k}, \tau')$$

10/15

Spectrum (λ dependence)

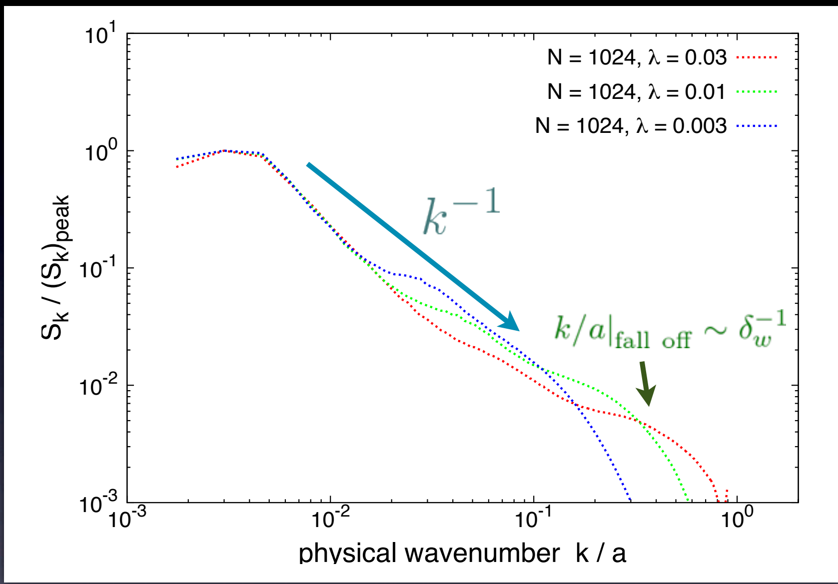

- Fall off at $k/a \sim \delta_w^{-1} \sim \sqrt{\lambda}\eta \propto \lambda^{1/2}$ (wall width)
- k^{-1} in the intermediate scales

Magnitude of gravitational waves

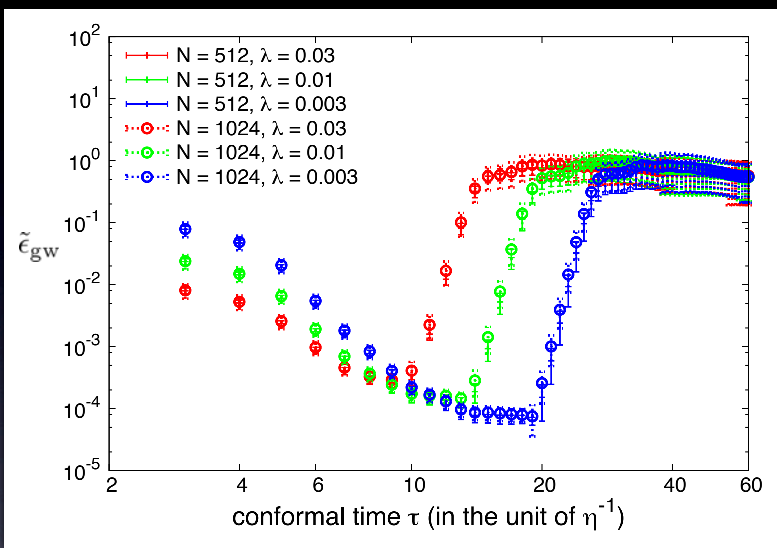

$$\tilde{\epsilon}_{\rm gw} \equiv \frac{1}{G\mathcal{A}^2\sigma_{\rm wall}^2}\left(\frac{d\rho_{\rm gw}}{d\ln k}\right)_{\rm peak}$$

c.f.

$$\rho_{\rm gw} \sim G\mathcal{A}^2\sigma_{\rm wall}^2 \sim {\rm const.}$$

during the scaling regime

$$\tilde{\epsilon}_{\rm gw} \simeq 0.7$$

Estimation of the present density

- Assume that the production of gravitational waves terminated at $t = t_{\rm dec}$
- Peak amplitude

$$\Omega_{\rm gw}(t_{\rm dec}) = \frac{1}{\rho(t_{\rm dec})}\left(\frac{d\rho_{\rm gw}}{d\ln k}\right)_{\rm peak} = \frac{8\pi\tilde{\epsilon}_{\rm gw}G^2\mathcal{A}^2\sigma_{\rm wall}^2}{3H^2(t_{\rm dec})} \qquad H(t_{\rm dec}) = \frac{1}{2t_{\rm dec}} \simeq \sqrt{\frac{2}{\lambda}}\epsilon\eta$$

$$\Rightarrow \boxed{\Omega_{\rm gw}h^2(t_0) \simeq 1.0\times 10^{-21}\times\lambda^2\epsilon^{-2}\left(\frac{g_*}{100}\right)^{-1/3}\left(\frac{\eta}{10^{15}{\rm GeV}}\right)^4}$$

g_* : relativistic degrees of freedom at $t_{\rm dec}$

- Peak frequency

$$\boxed{f_{\rm peak}(t_0) = \frac{a(t_{\rm dec})}{a(t_0)}H(t_{\rm dec}) \simeq 6.7\times 10^9\times\lambda^{-1/4}\epsilon^{1/2}\left(\frac{\eta}{10^{15}{\rm GeV}}\right)^{1/2}{\rm Hz}}$$

- Depend on three theoretical parameters $\lambda,\ \epsilon,\ \eta$

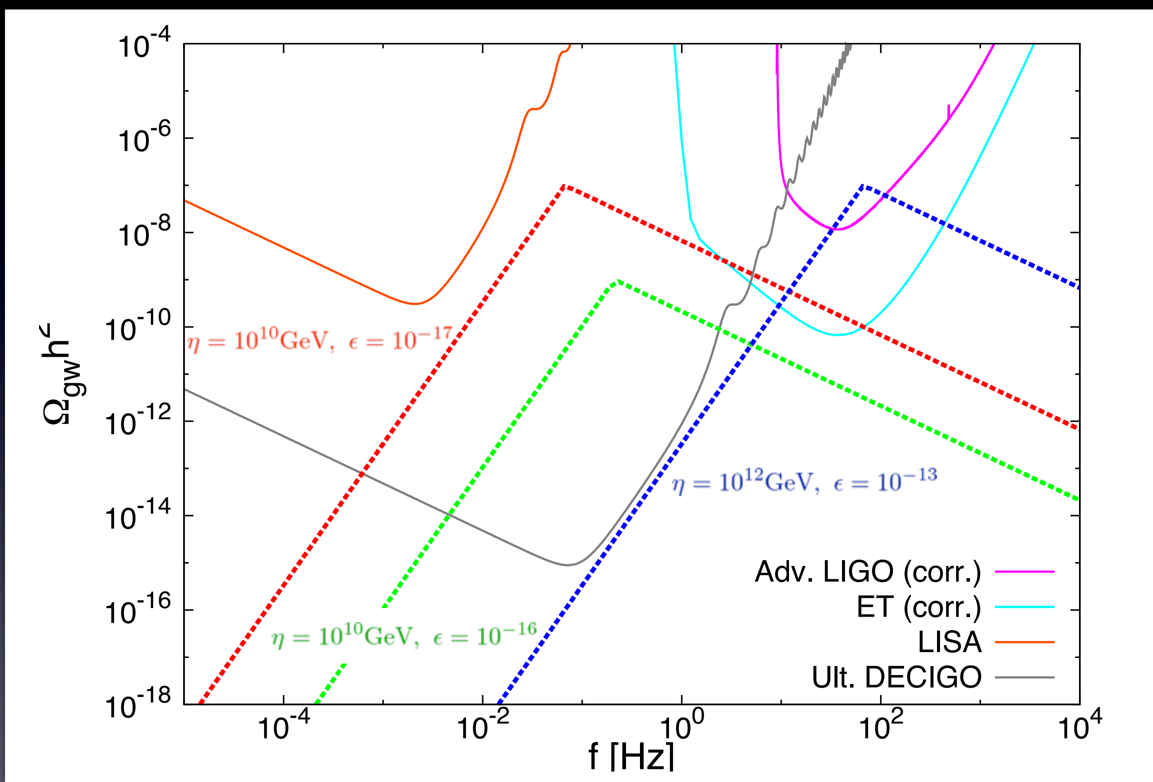

Summary

- Computed gravitational waves from domain walls based on the lattice simulations with improved dynamical ranges
- Peaks at $k/a \sim H(t_{\rm dec})$, and falls off at $k/a \sim \delta_w^{-1}$
- Behaves as $\propto k^{-1}$ between $H(t_{\rm dec})$ and δ_w^{-1}
- Signals can be proved in the future gravitational wave interferometers

“Axion Bosenova and Gravitational Waves”

by Hirotaka Yoshino

[JGRG23(2013)110714]

Axion Bosenova
and
Gravitational Waves

Hirotaka Yoshino
Hideo Kodama (KEK)

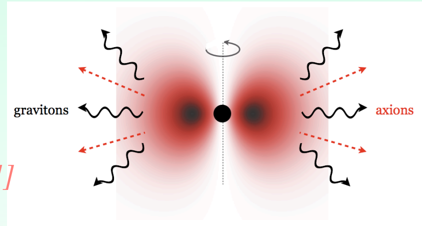

PTP128, 153 (2012) [arXiv:1203.5070[gr-qc]]
& Preliminary Results

JGRG23 @ Hirosaki University
(November 7th, 2013)

Contents

- Introduction
- Axion Bosenova *PTP128, 153 (2012) [arXiv:1203.5070[gr-qc]]*
- Gravitational Waves *in Preparation*
- Summary

Introduction

Very interesting era of GR

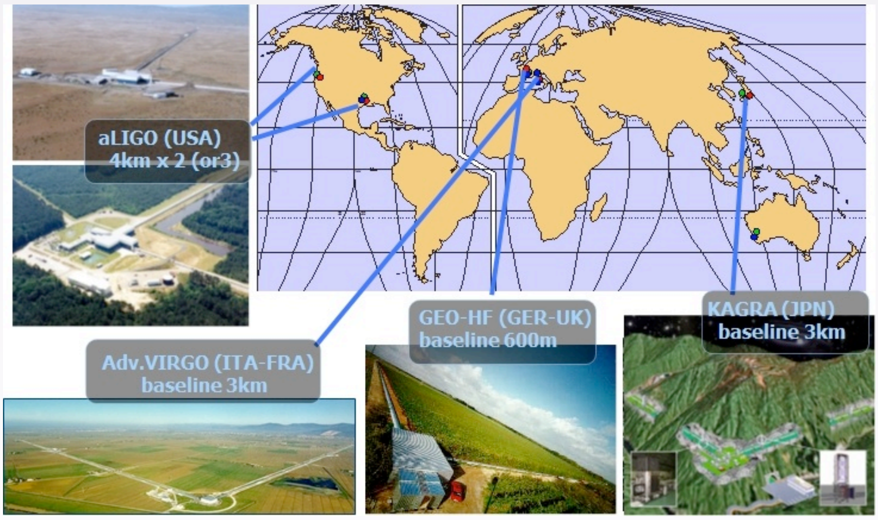

- One of the interesting possibilities is to find new physics beyond GR!

Can we find a signal of string theory?

Arvanitaki, Dimopoulos, Dubvosky, Kaloper, March-Russel, PRD81 (2010), 123530.

Maybe Yes, if there are String Axions with very tiny mass

- In string theory, many moduli appear when the extra dimensions get compactified.
- Some of them (10-100) are expected to behave like scalar fields with very tiny mass, which are called string axions.

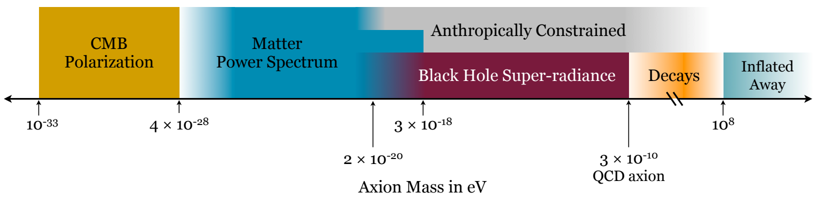

AXIVERSE SCENARIO

What happens if axion field exist around a rotating black hole?

- Axion field extract the rotation energy of the BH and forms an axion cloud.

$$\nabla^2\Phi - \mu^2\Phi = 0$$

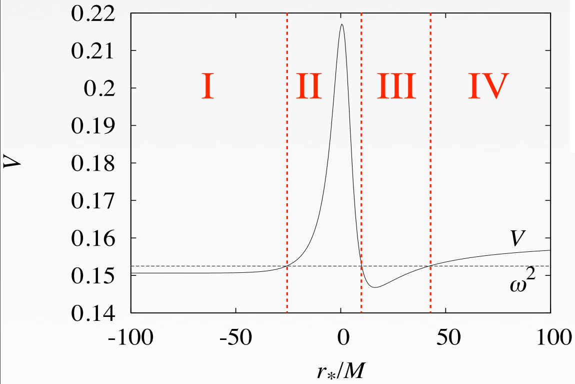

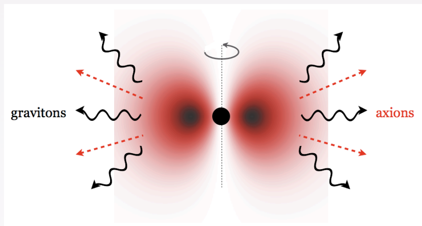

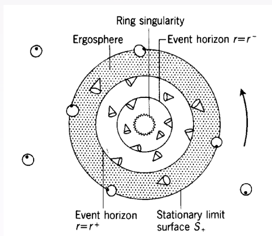

$\omega < \Omega_H m$ ⇨ negative energy falls into the BH ⇨ Superradiant instability

Growth rate

- Growth rate
  (continued fraction method)

  Dolan, PRD76 (2007), 084001.

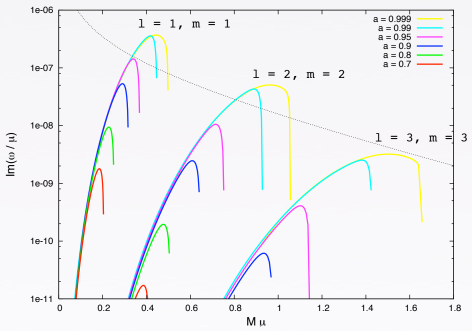

- Time evolution

  $l = m = 1 \qquad M\mu = 0.4$

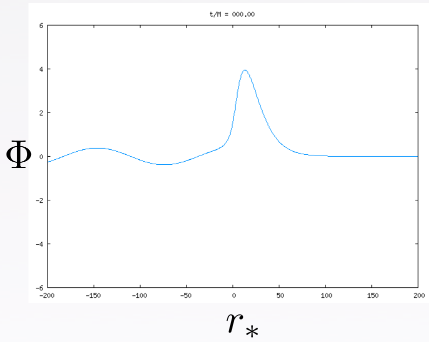

- Typical time scale:

$$M = M_\odot \qquad \begin{array}{ll} \omega_I M \sim 10^{-7} & \Rightarrow \quad \sim 1 \text{ min.} \\ \omega_I M \sim 10^{-12} & \Rightarrow \quad \sim 1 \text{ day} \end{array}$$

BH-axion system

(1) Nonlinear Self-Interaction (Bosenova)

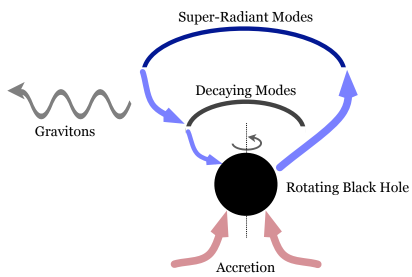

Arvanitaki and Dubovsky

(2) GW emission

BH-axion system

(1) Nonlinear Self-Interaction (Bosenova)

$$V = f_a^2 \mu^2 [1 - \cos(\Phi/f_a)]$$

$$\Rightarrow \boxed{\nabla^2 \varphi - \mu^2 \sin\varphi = 0} \qquad \varphi \equiv \frac{\Phi}{f_a}$$

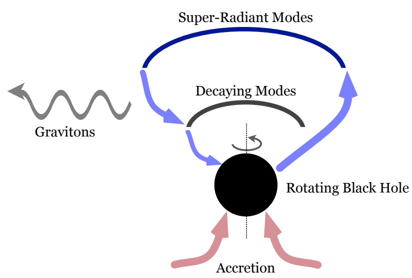

Arvanitaki and Dubovsky

(2) GW emission

BH-axion system

(1) Nonlinear Self-Interaction (Bosenova)

$$V = f_a^2 \mu^2 [1 - \cos(\Phi/f_a)]$$

$$\Rightarrow \boxed{\nabla^2 \varphi - \mu^2 \sin\varphi = 0} \qquad \varphi \equiv \frac{\Phi}{f_a}$$

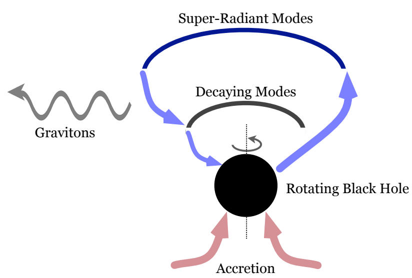

Arvanitaki and Dubovsky

- We want to clarify what happens when the nonlinear self-interaction becomes important at the last stage of the superradiant instability.
- We perform a 3D simulation of a Sine-Gordon field in a Kerr background.

(2) GW emission

Bosenova in condensed matter physics

http://spot.colorado.edu/~cwieman/Bosenova.html

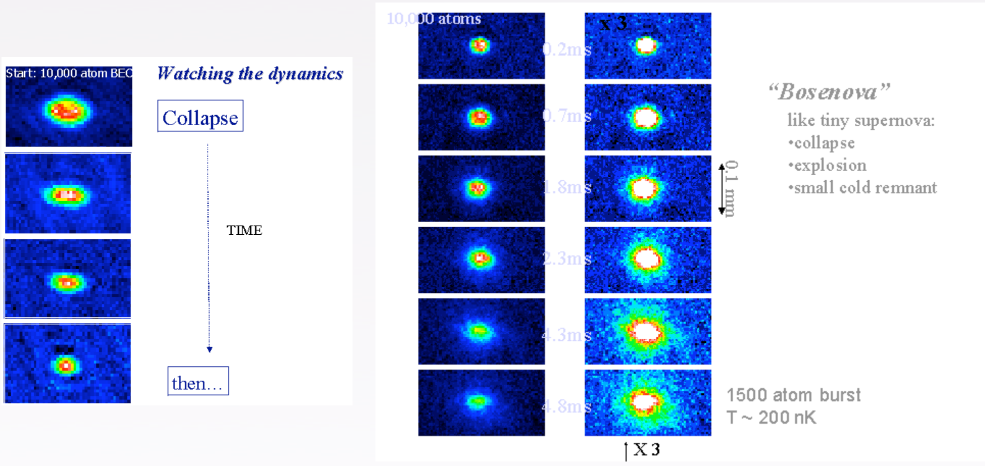

BEC state of Rb85 (interaction can be controlled)

Switch from repulsive interaction to attractive interaction

Wieman et al., Nature 412 (2001), 295

Axion Bosenova

Setup of a typical simulation (l = m = 2)

- Equation $\nabla^2 \varphi - \mu^2 \sin \varphi = 0$
- Setup $a/M = 0.99, \quad M\mu = 0.89$

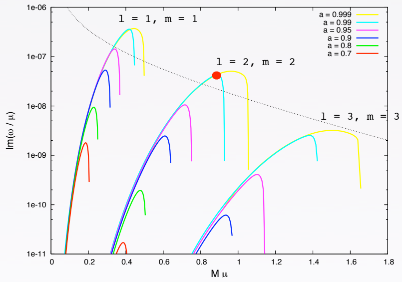

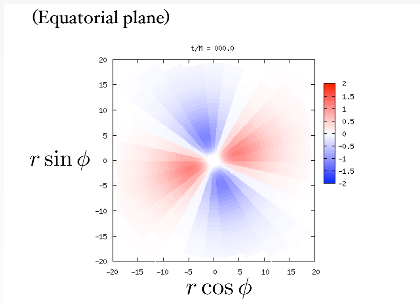

- Initial condition:

  The bound state of the Klein-Gordon field of the l = m = 2 mode.

- Initial amplitude = 1.2

Typical simulation (l=m=2)

- Axion field on the equatorial plane $(\theta = \pi/2)$

$(\phi = 0)$

Φ

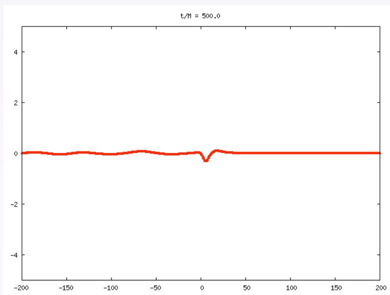

$-200 \leq r_*/M \leq 200$

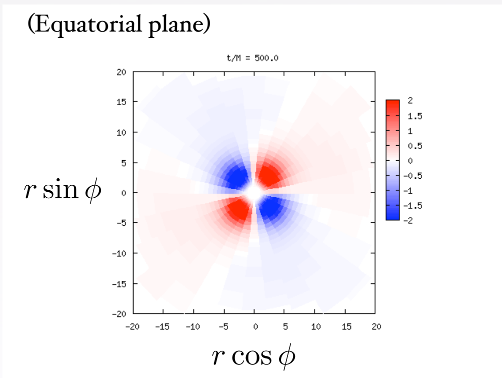

Summary of the typical simulation (l = m = 2)

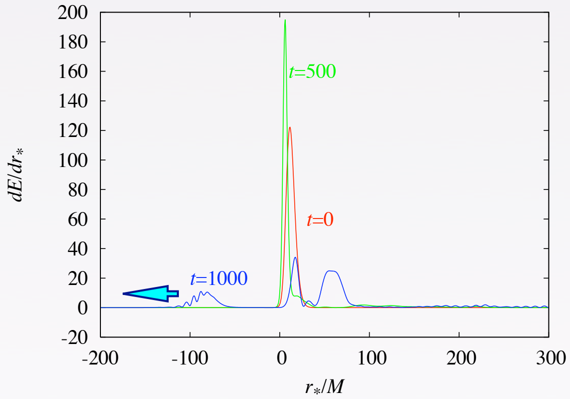

- When the peak value is sufficiently large, fairly large amount of axion cloud (20% of total energy) suddenly falls into the black hole in a relatively short time scale.
- This "bosenova implosion" occurs when $E \approx 1450 \times (f_a/M_p)^2 M$

Gravitational Waves

Motivation for studying GWs

- Does the GW emission stop the growth of axion cloud by the superradiant instability?

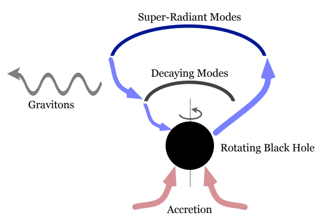

$$\frac{dE_{\mathrm{GW}}}{dt} \propto E_a^2$$

$$\frac{dE_a}{dt} \propto E_a$$

- If the bosenova happens, can we observe the signal by GW detectors?

  What kind of signal can be expected?

Steps of our research

- Does the axion cloud grow until bosenova?
  - Flat approximation
  - Perturbation of Kerr spacetime
- Perturbation of Kerr spacetime (during bosenova)

Steps of our research

- Does the axion cloud grow until bosenova?
  - Flat approximation
  - Perturbation of Kerr spacetime
- Perturbation of Kerr spacetime (during bosenova)

Steps of our research

- Does the axion cloud grow until bosenova?
  - Flat approximation
  - Perturbation of Kerr spacetime
- Perturbation of Kerr spacetime (during bosenova)

Flat approximation

- Axion Compton wavelength $\gg$ BH radius $\qquad M\mu \ll 1$

  (Axion cloud distributes in a distant region)

We calculate
- Axion Cloud by Newton Gravity
- GWs by Perturbation of a Flat Spacetime

- Ignore the nonlinear self-interaction

$$\Phi = \Re\left[-\frac{\sqrt{2E_a}}{\omega}(2k)^{3/2}\sqrt{\frac{(n-\ell-1)!}{2n(n+\ell)!}}e^{-i\omega t}e^{-kr}(2kr)^{\ell}L_{n-\ell-1}^{2\ell+1}(2kr)Y_{\ell m}(\theta,\phi)\right]$$

$$k := \sqrt{\mu^2-\omega^2} \approx \frac{M\mu^2}{n}$$

Axion cloud grows!

- Energy extraction rate $\qquad$ Detweiler (1970)

$$\frac{dE_a}{dt} = 2\boxed{\left(\frac{E_a}{M}\right)}\boxed{a_*(M\mu)^{4\ell+5}}\frac{2^{4\ell+2}\ell(n+\ell)!}{n^{2\ell+4}(n-\ell-1)!}\left[\frac{\ell!}{(2\ell+1)!(2\ell)!}\right]^2\prod_{j=1}^{\ell}\left[j^2+a_*^2(\ell^2-j^2)\right].$$

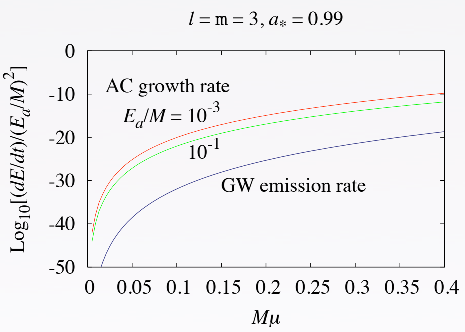

- Energy loss by GW emission

$$\frac{dE_{\mathrm{GW}}}{dt} = \boxed{\left(\frac{E_a}{M}\right)^2}\boxed{(M\mu)^{4\ell+10}}\frac{16^{\ell+1}\ell(2\ell-1)\Gamma(2\ell-1)^2\Gamma(\ell+n+1)^2}{n^{4\ell+8}(\ell+1)\Gamma(\ell+1)^4\Gamma(4\ell+3)\Gamma(n-\ell)^2}$$

Steps of our research

- Does the axion cloud grow until bosenova?
  - Flat approximation
  - Perturbation of Kerr spacetime
- Perturbation of Kerr spacetime (during bosenova)

GW energy flux in a Kerr background (1)

- The formula for evaluating the amplitude

$$\int_{\partial D} \left(\boxed{h^*_{ab}} \nabla_c \boxed{\psi^{ab}} - \psi^{ab} \nabla_c h^*_{ab}\right) n^c d\Sigma = -16\pi G \int_D h^*_{ab} T^{ab} \sqrt{-g} d^4 x$$

Physical perturbation

Homogeneous solution

- Rate of GW energy emission/absorption

$$\frac{dE^{(\mathrm{out})}_{\mathrm{GW}}}{dt} \sim \tilde{\omega}^2 \left| \langle h^{(\mathrm{out})}_{\alpha\beta}, T^{\alpha\beta} \rangle \right|$$

$$\frac{dE^{(\mathrm{in})}_{\mathrm{GW}}}{dt} \sim (\tilde{\omega} - m\Omega_H)\tilde{\omega} \left| \langle h^{(\mathrm{down})}_{\alpha\beta}, T^{\alpha\beta} \rangle \right|$$

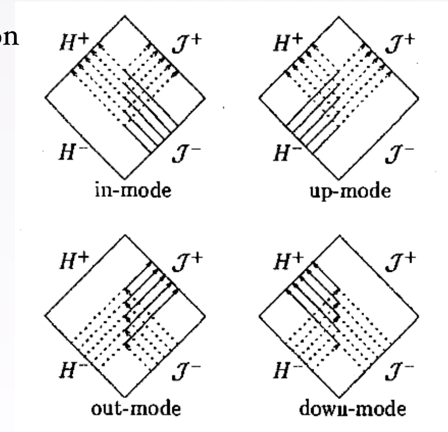

GW energy flux in a Kerr background (2)

- Homogeneous solution
  - Teukolsky equation

$$\left[\frac{(r^2+a^2)^2}{\Delta} - a^2\sin^2\theta\right]\frac{\partial^2\psi}{\partial t^2} + \frac{4Mar}{\Delta}\frac{\partial^2\psi}{\partial t\partial\phi} + \left[\frac{a^2}{\Delta} - \frac{1}{\sin^2\theta}\right]\frac{\partial^2\psi}{\partial\phi^2}$$
$$-\Delta^{-s}\frac{\partial}{\partial r}\left(\Delta^{s+1}\frac{d\psi}{dr}\right) - \frac{1}{\sin\theta}\frac{\partial}{\partial\theta}\left(\sin\theta\frac{\partial\psi}{\partial\theta}\right) - 2s\left[\frac{a(r-M)}{\Delta} + \frac{i\cos\theta}{\sin^2\theta}\right]\frac{\partial\psi}{\partial\phi}$$
$$-2s\left[\frac{M(r^2-a^2)}{\Delta} - r - ia\cos\theta\right]\frac{\partial\psi}{\partial t} + (s^2\cot^2\theta - s)\psi = 4\pi\Sigma T$$

  - Radial Teukolsky equation

$$\Delta^{-s}\frac{d}{dr}\left(\Delta^{s+1}\frac{dR}{dr}\right) + \left(\frac{K^2 - 2is(r-M)K}{\Delta} + 4is\omega r - \lambda\right)R = 0,$$

$$K = (r^2+a^2)\omega - am \quad \text{and} \quad \lambda = {}_sA_{lm} + a^2\omega^2 - 2am\omega$$

GW energy flux in a Kerr background (3)

- Several studies on reconstruction of the metric

Wald, JMP14 (1973), 1453.

Cohen and Kegeles, Phys. Lett. 54A (1975), 5.

Chrzanowski, PRD11 (1975), 2042.

Wald, PRL41 (1978), 203.

Dias, Reall and Santos, arXiv:0906.2380 [hep-th]

- Reconstructed metric (outgoing radiation gauge) Chrzanowski (1975)

$$h_{\mu\nu}(\tilde{l}\tilde{m}\tilde{\omega}P) = \rho^{*-4}\{-n_\mu n_\nu(\delta - 3\alpha^* - \beta + 5\pi^*)(\delta - 4\alpha^* + \pi^*) - m_\mu m_\nu(\Delta + 5\mu^* - 3\gamma^* + \gamma)(\Delta + \mu^* - 4\gamma^*)$$
$$+n_{(\mu}m_{\nu)}[(\delta + 5\pi^* + \beta - 3\alpha^* + \tau)(\Delta + \mu^* - 4\gamma^*) + (\Delta + 5\mu^* - \mu - 3\gamma^* - \gamma)(\delta - 4\alpha^* + \pi^*)]\}\,{}_{+2}R_{\tilde{l}\tilde{m}\tilde{\omega}}(r)\,{}_{-2}S_{\tilde{l}\tilde{m}\tilde{\omega}}(\theta,\phi)e^{-i\tilde{\omega}t}$$
$$+P\rho^{-4}\{-n_\mu n_\nu(\delta^* - 3\alpha - \beta^* + 5\pi)(\delta^* - 4\alpha + \pi) - m^*_\mu m^*_\nu(\Delta + 5\mu - 3\gamma + \gamma^*)(\Delta + \mu - 4\gamma)$$
$$+n_{(\mu}m^*_{\nu)}[(\delta + 5\pi + \beta^* - 3\alpha + \tau^*)(\Delta + \mu - 4\gamma) + (\Delta + 5\mu - \mu^* - 3\gamma + \gamma^*)(\delta^* - 4\alpha + \pi)]\}\,{}_{+2}R_{\tilde{l}\tilde{m}\tilde{\omega}}(r)\,{}_{+2}S_{\tilde{l}\tilde{m}\tilde{\omega}}(\theta,\phi)e^{-i\tilde{\omega}t}$$

Agreement with the flat approximation

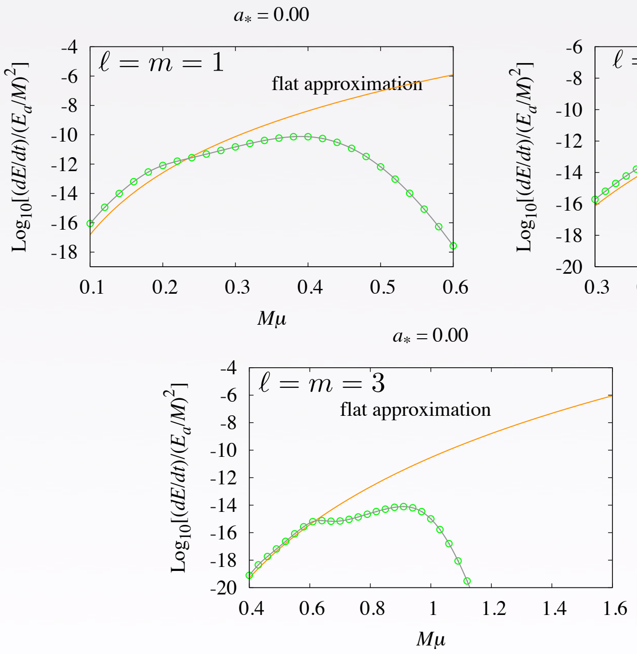

(Schwarzschild, a=0)

Axion cloud in l = m = 1 mode

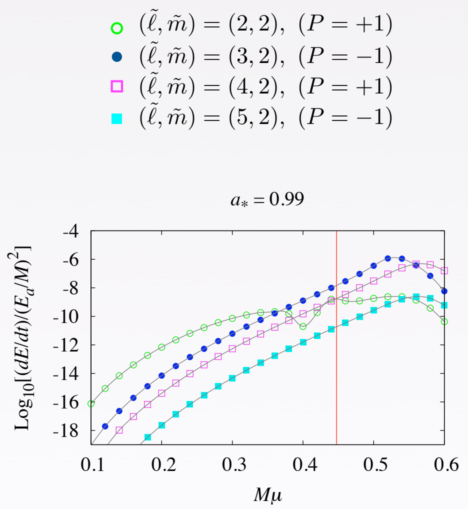

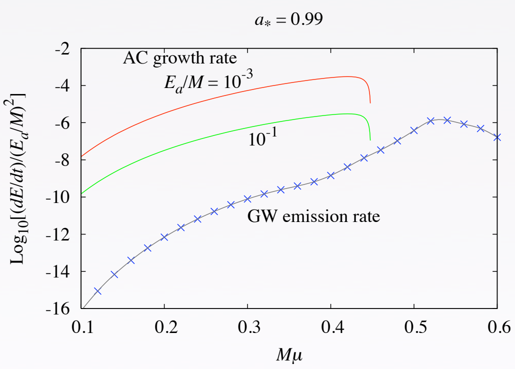

Axion cloud in l = m = 2 mode

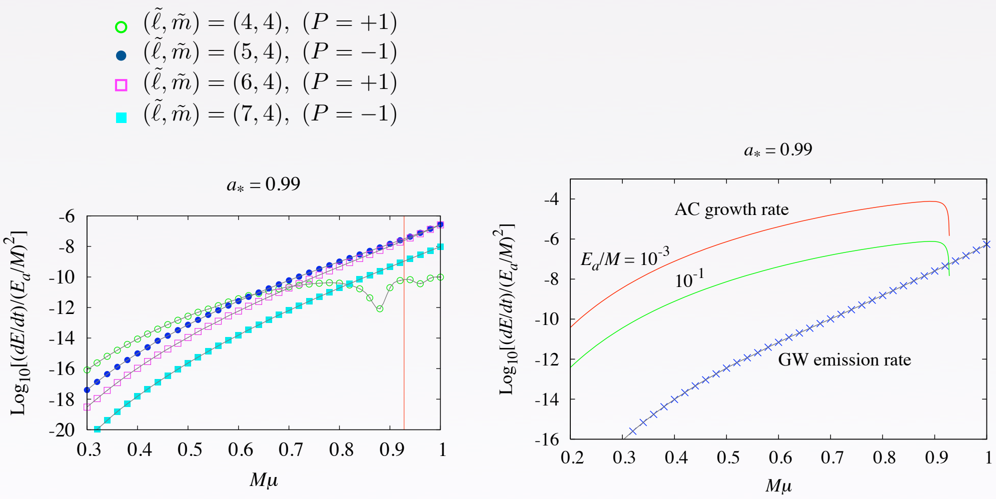

Axion cloud in l = m = 3 mode

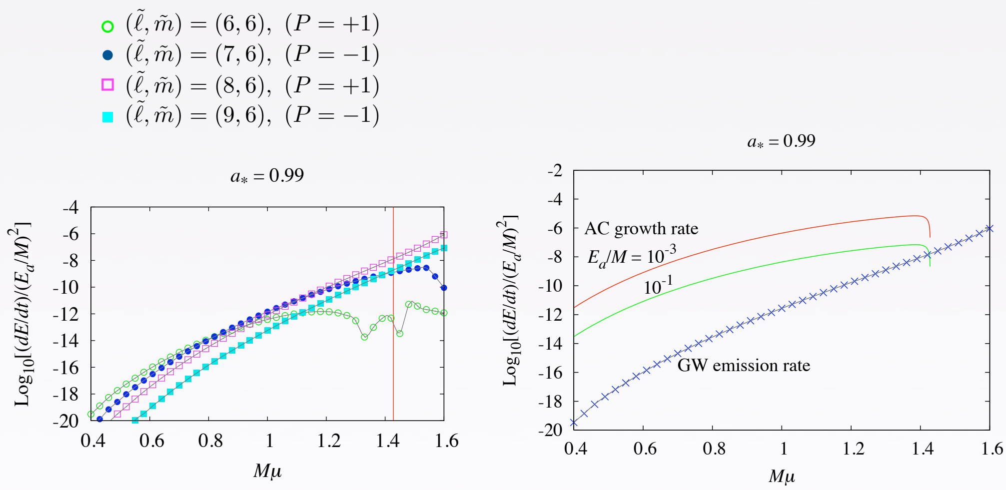

Summary

Summary

- Axion Bosenova
  - Effect of nonlinear self-interaction stops the superradiant instability and causes the bosenova,
  - Bosenova is characterized by sudden infall of positive energy
- Gravitational Waves
  - We studied GW emission from the BH-axion system in the superradiant regime (before the bosenova)

    ⇨ GW emission is weak and does not stop the growth by the superradiant instability
  - Axion cloud continues to grow by the superradiant instability until the occurrence of the bosenova.

“Dynamical process in Holographic QCD”

by Shunichiro Kinoshita

[JGRG23(2013)110715]

The 23rd workshop on General Relativity and Gravitation in Japan
Hirosaki University

Dynamical process in Holographic QCD

Shunichiro Kinoshita
(OCAMI, Osaka City U.)
K. Murata (Keio), N. Tanahashi (Cambridge),
T. Ishii (Crete)

in preparation

AdS/CFT correspondence

- AdS_5/CFT_4

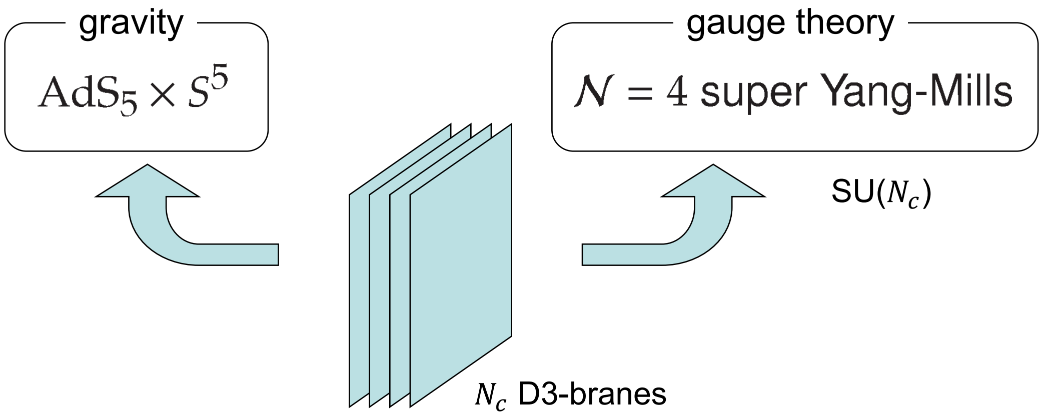

Strongly coupled gauge theory corresponds to classical gravity
A new type brane will be added for quark degrees of freedom

Holographic QCD

Karch, Katz (2002), Grana, Polchinski (2002), Bertolini *et al.* (2002)

- D3/D7 system
  - A probe D7-brane is embedded in $AdS_5 \times S^5$ geometry generated by N_c D3-brane

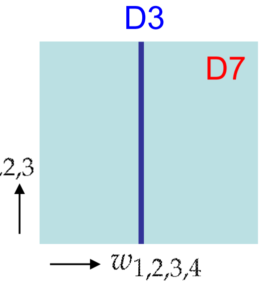

$$
\begin{aligned}
\mathrm{d}s^2 =& r^2[-\mathrm{d}t^2 + \mathrm{d}\vec{x}_3^2] + \frac{\mathrm{d}r^2}{r^2} + \mathrm{d}\Omega_5^2 \\
=& \boxed{r^2\underbrace{\boxed{[-\mathrm{d}t^2 + \mathrm{d}\vec{x}_3^2]}}_{\text{D3}} + \frac{1}{r^2}[\mathrm{d}\rho^2 + \rho^2 \mathrm{d}\Omega_3^2}_{\text{D7}} + \mathrm{d}w_5^2 + \mathrm{d}w_6^2]
\end{aligned}
$$

$$\rho^2 = w_1^2 + w_2^2 + w_3^2 + w_4^2, \quad r^2 = \rho^2 + w_5^2 + w_6^2$$

DBI action: $S_{\mathrm{D7}} = -\mu_7 \int \mathrm{d}^8 y \sqrt{-\det\left(g_{\mu\nu}(X)\frac{\partial X^\mu}{\partial y^a}\frac{\partial X^\nu}{\partial y^b}\right)}$ ⇨ Embedding function $w_6(\rho) = m = \mathrm{const.}$ $\boxed{\text{quark mass}}$

string between D3-branes and D7-brane ⇔ "quark"
fluctuations of D7-brane ⇔ "meson"

Finite temperature

Mateos, Myers, Thomson (2006, 2007)

- We consider asymptotically AdS BH as the bulk spacetime
  - Black hole in the bulk theory ⇔ finite temperature in the boundary theory

Hawking temperature: $T = \frac{r_\mathrm{h}}{\pi}$

AdS-Schwarzschild × S^5

$$\mathrm{d}s^2 = -r^2\left(1 - \frac{r_\mathrm{h}^4}{r^4}\right)\mathrm{d}t^2 + \frac{1}{r^2}\left(1 - \frac{r_\mathrm{h}^4}{r^4}\right)^{-1}\mathrm{d}r^2 + r^2 \mathrm{d}\vec{x}_3^2 + \mathrm{d}\Omega_5^2$$

  - Embedding function

$$w(\rho) \sim \underbrace{\boxed{m}}_{\text{quark mass}} + \frac{\boxed{c}}{\rho^2} + \cdots$$

quark condensate: $\langle \mathcal{O}_m \rangle \neq 0$

- Phase transition
  - The brane intersects with the black hole when the black hole is large (high temperature)
  - Fluctuations will dissipate (QNM) ⇔ meson melting

Phase diagram of static embeddings

- Whether the brane intersects with the horizon or not

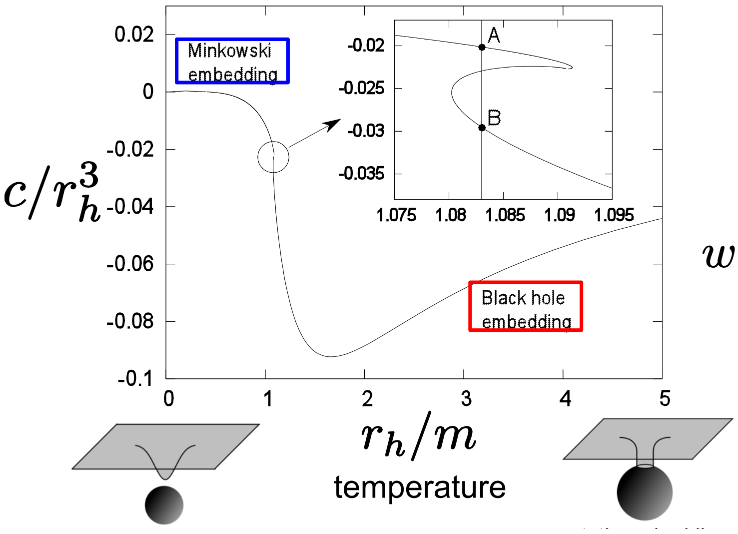

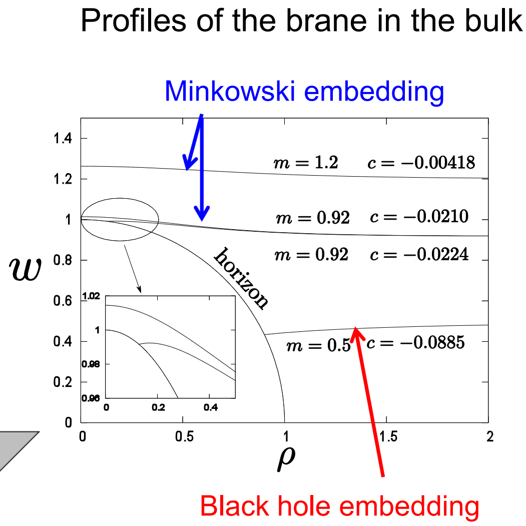

Minkowski embedding Black hole embedding

Time evolution?

- Black hole formation ⇔ thermalization of plasma
  - Dynamical background spacetime
- Change of brane embedding ⇔ phase transition
  - Time evolution of branes

- We would like to know dynamics of the D7-brane where BH is forming.
  - How will the brane fall into the horizon?
  - What does happen to dynamical embedding?

Our setup

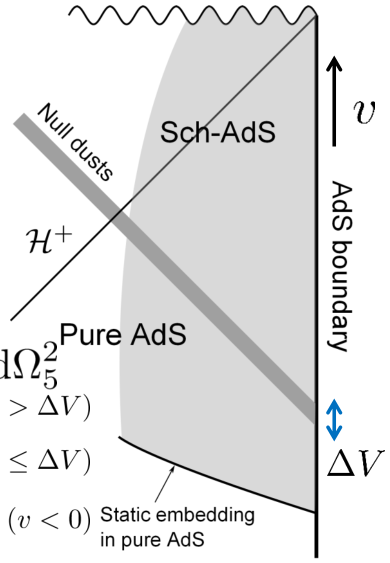

- Background: AdS-Vaidya
  - From pure AdS to BH

$$ds^2 = \frac{1}{z^2}[-F(v,z)dv^2 - 2dvdz + d\vec{x}_3^2] + d\Omega_5^2$$

$$F(v,z) = 1 - M(v)z^4 \quad M(v) = \begin{cases} M_f & (v > \Delta V) \\ M_f \sin^2 \dfrac{\pi v}{2\Delta V} & (0 \le v \le \Delta V) \\ 0 & (v < 0) \end{cases}$$

Final radius: $r_\mathrm{h} \quad (M_f \equiv r_\mathrm{h}^4)$ Duration of the energy injection: ΔV

- D7-brane

$$S_{\mathrm{D7}} = -\mu_7 \int d^8 y \sqrt{-\det\left(g_{\mu\nu}(X)\frac{\partial X^\mu}{\partial y^a}\frac{\partial X^\nu}{\partial y^b}\right)}$$

We will numerically solve dynamics of the D7-brane on this background

Equations of motion

- Evolution equations (2d wave eqs.)

$$D^2 V - \frac{3}{Z}D_a Z D^a V - 3\frac{\sin\Phi}{\cos\Phi}D_a\Phi D^a V - \left(\frac{\partial_z F}{2} - \frac{F}{Z}\right)D_a V D^a V + \frac{Z}{2}\lambda = 0,$$

$$D^2 Z - \frac{3}{Z}D_a Z D^a Z - 3\frac{\sin\Phi}{\cos\Phi}D_a\Phi D^a Z + \left(\frac{1}{2}\partial_v F + \frac{F\partial_z F}{2} - \frac{F^2}{Z}\right)D_a V D^a V$$
$$+ \left(\partial_z F - \frac{2F}{Z}\right)D_a V D^a Z - \frac{2}{Z}D_a Z D^a Z - \frac{ZF}{2}\lambda = 0,$$

$$D^2\Phi - \frac{3}{Z}D_a Z D^a \Phi - 3\frac{\sin\Phi}{\cos\Phi}D_a\Phi D^a\Phi - \frac{\sin\Phi}{2\cos\Phi}\lambda = 0,$$

- Constraint equaions

$$\gamma_{ab} = -\frac{6}{\lambda Z^2}[-F(V,Z)D_a V D_b V - 2D_{(a}V D_{b)}Z + Z^2 D_a\Phi D_b\Phi]$$

$$ds^2 = \frac{1}{z^2}[-F(v,z)dv^2 - 2dvdz + d\vec{x}_3^2] + d\phi^2 + \cos^2\phi\, d\Omega_3^2 + \sin^2\phi\, d\varphi^2$$

Embedding functions: $v = V(y_0,y_1), z = Z(y_0,y_1), \phi = \Phi(y_0,y_1)$

Double-null coordinates

- EOM

gauge: $\gamma_{uu} = \gamma_{vv} = 0$

constraints

$$C_1 \equiv -F(\partial_u V)^2 - 2\partial_u V \partial_u Z + Z^2(\partial_u \Phi)^2 = 0,$$
$$C_2 \equiv -F(\partial_v V)^2 - 2\partial_v V \partial_v Z + Z^2(\partial_v \Phi)^2 = 0.$$

evolution eqs. $\partial_u \partial_v \mathbf{X} + \mathbf{f}(\mathbf{X}, \partial_u \mathbf{X}, \partial_v \mathbf{X}) = 0 \qquad \mathbf{X} = (V, Z, \Phi)$

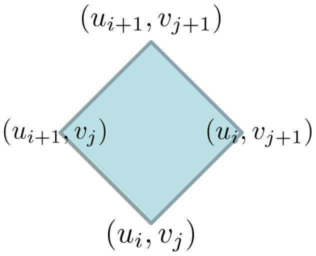

$$\left[\begin{aligned}
&2\partial_u\partial_v V - 3\frac{\sin\Phi}{\cos\Phi}(\partial_u\Phi\partial_v V + \partial_u V\partial_v\Phi) - \left(F_{,Z} - 5\frac{F}{Z}\right)\partial_u V\partial_v V - 3Z\partial_u\Phi\partial_v\Phi = 0,\\
&2\partial_u\partial_v Z - \frac{10}{Z}\partial_u Z\partial_v Z - 3\frac{\sin\Phi}{\cos\Phi}(\partial_u\Phi\partial_v Z + \partial_u Z\partial_v\Phi) + \left(F_{,V} + FF_{,Z} - 5\frac{F^2}{Z}\right)\partial_u V\partial_v V\\
&\qquad + \left(F_{,Z} - \frac{5F}{Z}\right)(\partial_u V\partial_v Z + \partial_u Z\partial_v V) + 3ZF\partial_u\Phi\partial_v\Phi = 0,\\
&2\partial_u\partial_v\Phi - \frac{3}{Z}(\partial_u Z\partial_v\Phi + \partial_u\Phi\partial_v Z) - 3\frac{\sin\Phi}{\cos\Phi}\partial_u\Phi\partial_v\Phi - \frac{\sin\Phi}{\cos\Phi}\frac{3}{Z^2}\\
&\qquad \times (F\partial_u V\partial_v V + \partial_u V\partial_v Z + \partial_u Z\partial_v V) = 0,
\end{aligned}\right.$$

$$\mathbf{X}_{i+1,j+1} = \mathbf{X}_{i+1,j} + \mathbf{X}_{i,j+1} - \mathbf{X}_{i,j} - \int_{u_i}^{u_{i+1}} \mathrm{d}u \int_{v_j}^{v_{j+1}} \mathrm{d}v \mathbf{f}$$

Sub-critical case (low temperature)

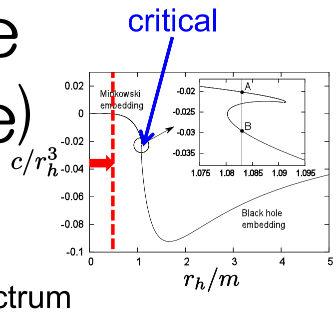

- Quark condensate

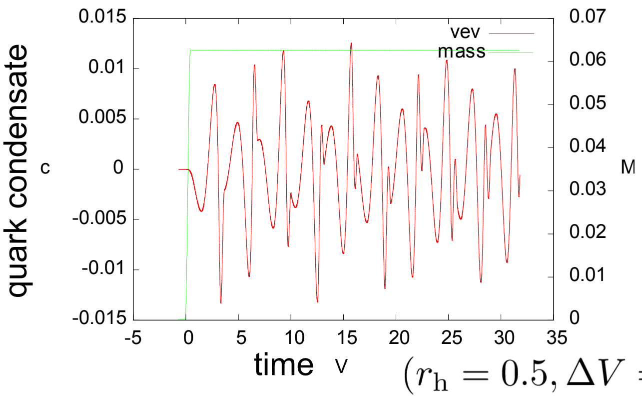

$(r_\mathrm{h} = 0.5, \Delta V = 0.5)$

Power spectrum

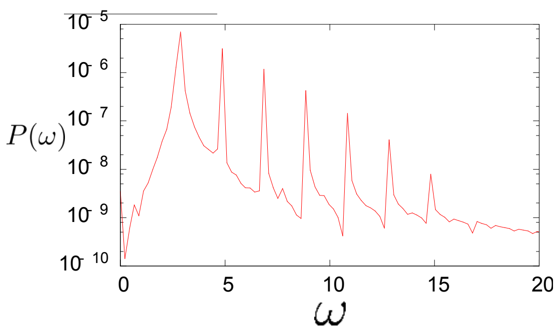

- After the energy injection, the D7-brane remains the Minkowski embedding with periodic oscillations.
- Excitations on the brane have discrete spectrum. ⇔ stable meson

- Relation with injection time-scale: ΔV

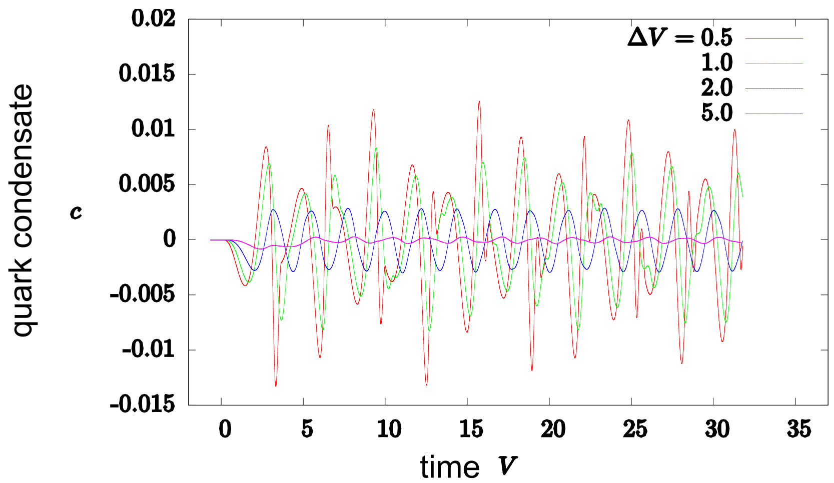

- As the time-scale of the injection is shorter, the excitations are harder.
- Non-adiabaticity is important for meson excitations.

Super-critical case (high temperature)

critical

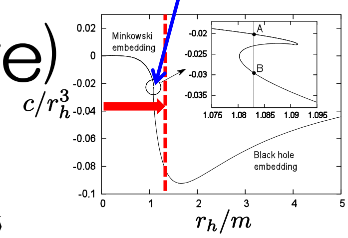

- Quark condensate

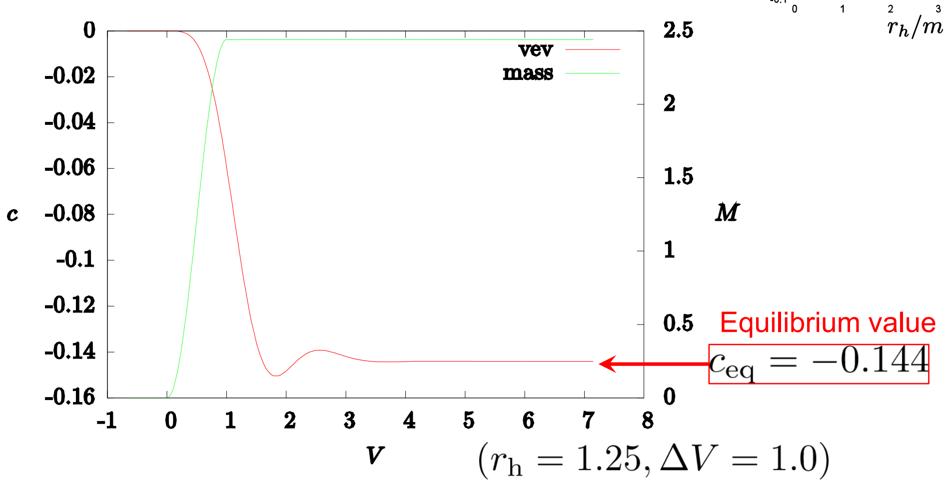

$(r_{\rm h} = 1.25, \Delta V = 1.0)$

- The quark condensate settles into an equilibrium value of the static BH embedding.
- The excitations dissipate. (quasi-normal mode) ⇔ meson melting

- Snapshots of time-evolution of the D7-brane

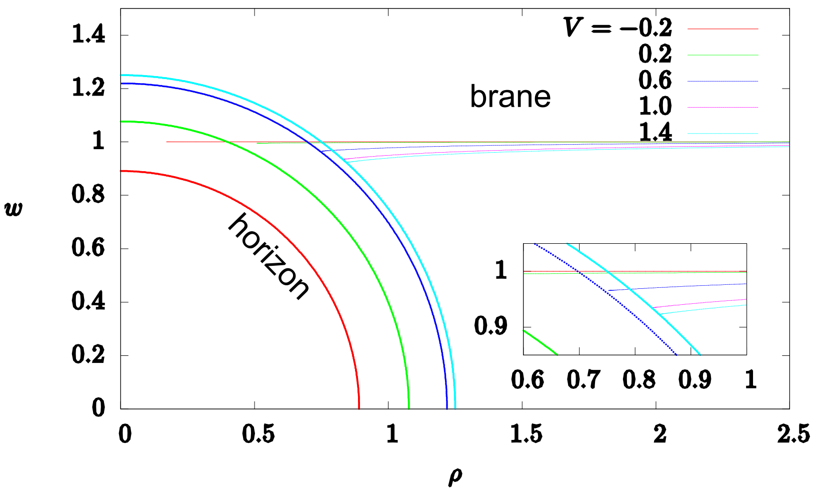

$$\left(\rho = \frac{\cos\phi}{z}, w = \frac{\sin\phi}{z}\right)$$

Eventually, the brane becomes the equilibrium solution of the BH embedding.

Overeager phase

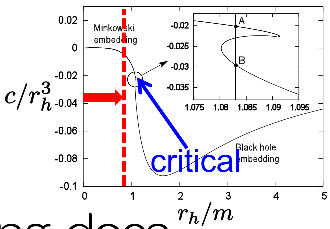

- Although any equilibrium BH embedding does not exit if static, the brane can intersect with the horizon dynamically. (because of inertia)

Quark condensate

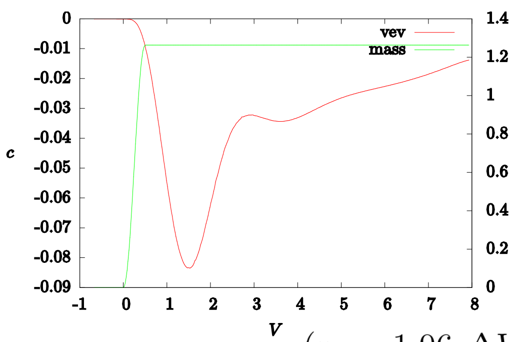

$(r_{\rm h} = 1.06, \Delta V = 0.5)$

Snapshot (late time)

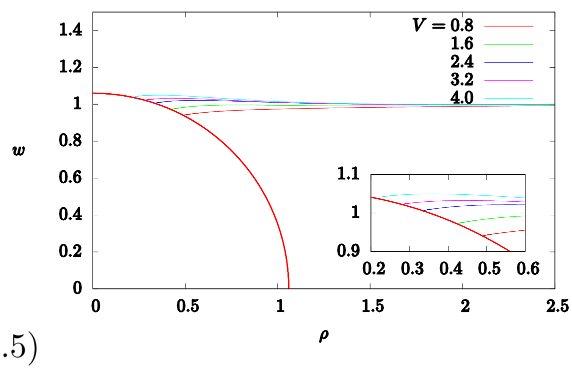

- While the black hole has settled into the final state, the brane remains dynamical intersecting with the horizon.

- If the energy injection is sufficiently slow, the brane can not intersect with the horizon.

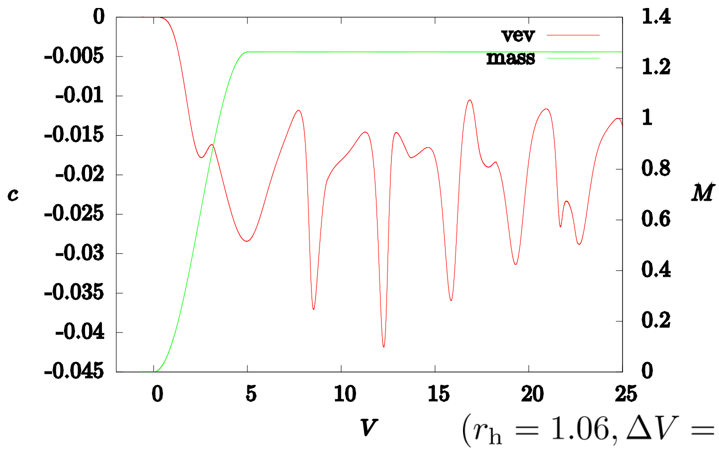

$(r_{\rm h} = 1.06, \Delta V = 5.0)$

- This is just sub-critical where the brane remains the Minkowski embedding.
- non-adiabaticity plays an important role in the overeager phase.

Summary

- We have numerically solved time evolutions of the D-brane in the AdS
  - The equations of motion become a set of 2d nonlinear wave equations and constraint equations
- Three cases depending on final temperatures and injection time-scales.
  - Overeager case other than sub-critical and super-critical cases
  - Non-adiabaticity of the energy injection is important.

- What is the final fate of the overeager cases?
  - It is expected that the brane will be singular within finite time from extrapolation of our numerical result.
  - Stringy effect? (Finite N?, reconnection?, and so on)
  - How can we interpret it in the boundary theory?

“No-boundary wave function toward good inflation models”

by Dong-han Yeom

[JGRG23(2013)110716]

No-boundary wave function toward good inflation models

京都大学基礎物理学研究所 Yukawa Institute for Theoretical Physics
염동한 ヨムドンハン Dong-han Yeom

Based on

- Hwang, Sahlmann and DY, arXiv:1107.4653
- Hwang, Lee, Sahlmann and DY, arXiv:1203.0112
- Hwang, Kim, Lee, Sahlmann and DY, arXiv:1207.0359
- Hwang, Lee, Stewart, DY and Zoe, arXiv:1208.6563
- Sasaki, DY and Zhang, arXiv:1307.5948
- Saito, Sasaki, DY and Zhang, in preparation
- Hwang, Park and DY, in preparation
- Hwang, Kim, Lee and DY, in preparation
- ⋯, in preparation

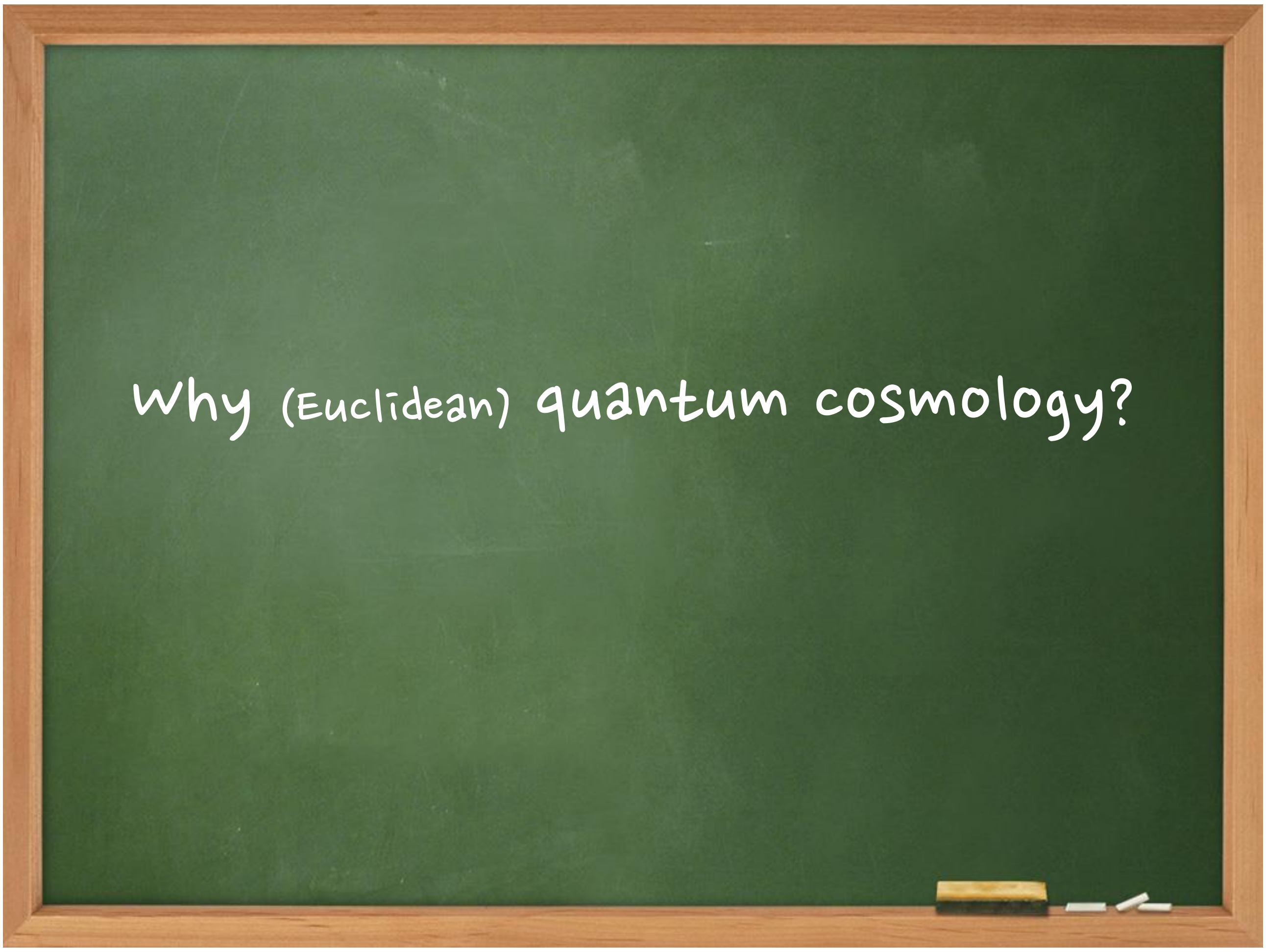
Why (Euclidean) quantum cosmology?

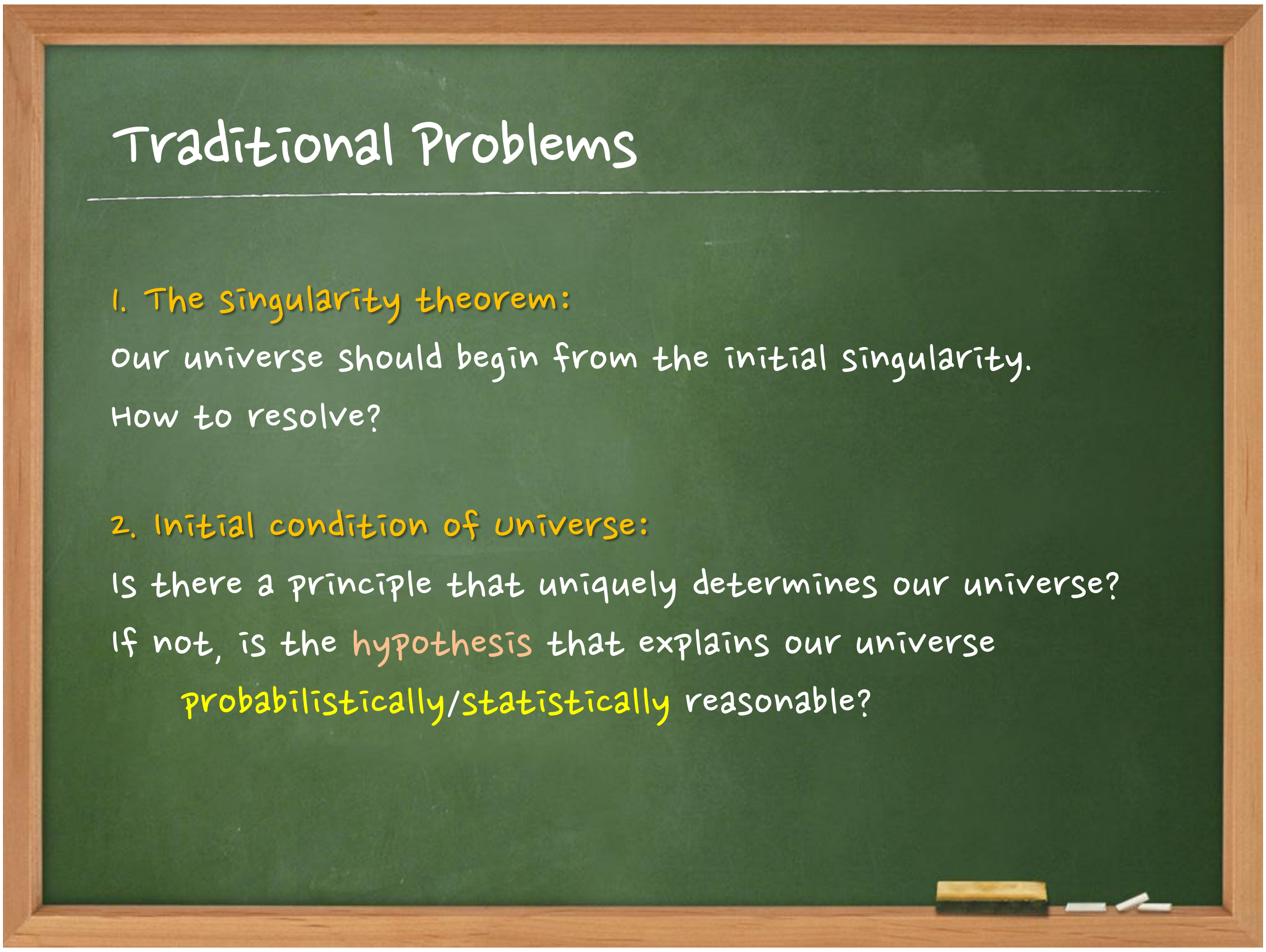
Traditional Problems
1. The singularity theorem:
Our universe should begin from the initial singularity.
How to resolve?
2. Initial condition of universe:
Is there a principle that uniquely determines our universe?
If not, is the hypothesis that explains our universe
probabilistically/statistically reasonable?

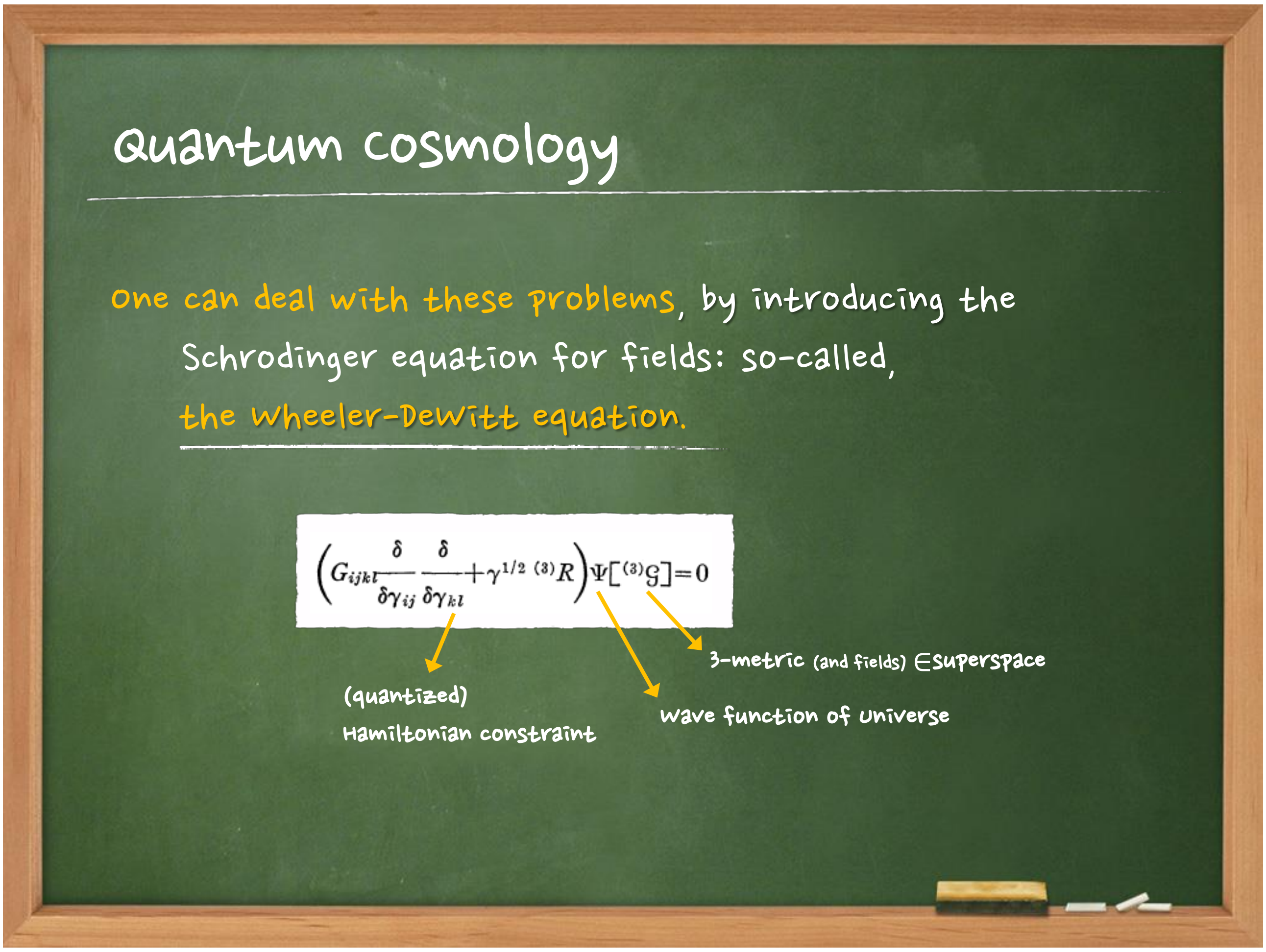
Quantum cosmology
One can deal with these problems, by introducing the Schrodinger equation for fields: so-called, the Wheeler-DeWitt equation.
$\left(G_{ijkl}\frac{\delta}{\delta\gamma_{ij}}\frac{\delta}{\delta\gamma_{kl}}+\gamma^{1/2}\,{}^{(3)}R\right)\Psi[{}^{(3)}\mathcal{G}]=0$
3-metric (and fields) ∈superspace
wave function of universe
(quantized)
Hamiltonian constraint

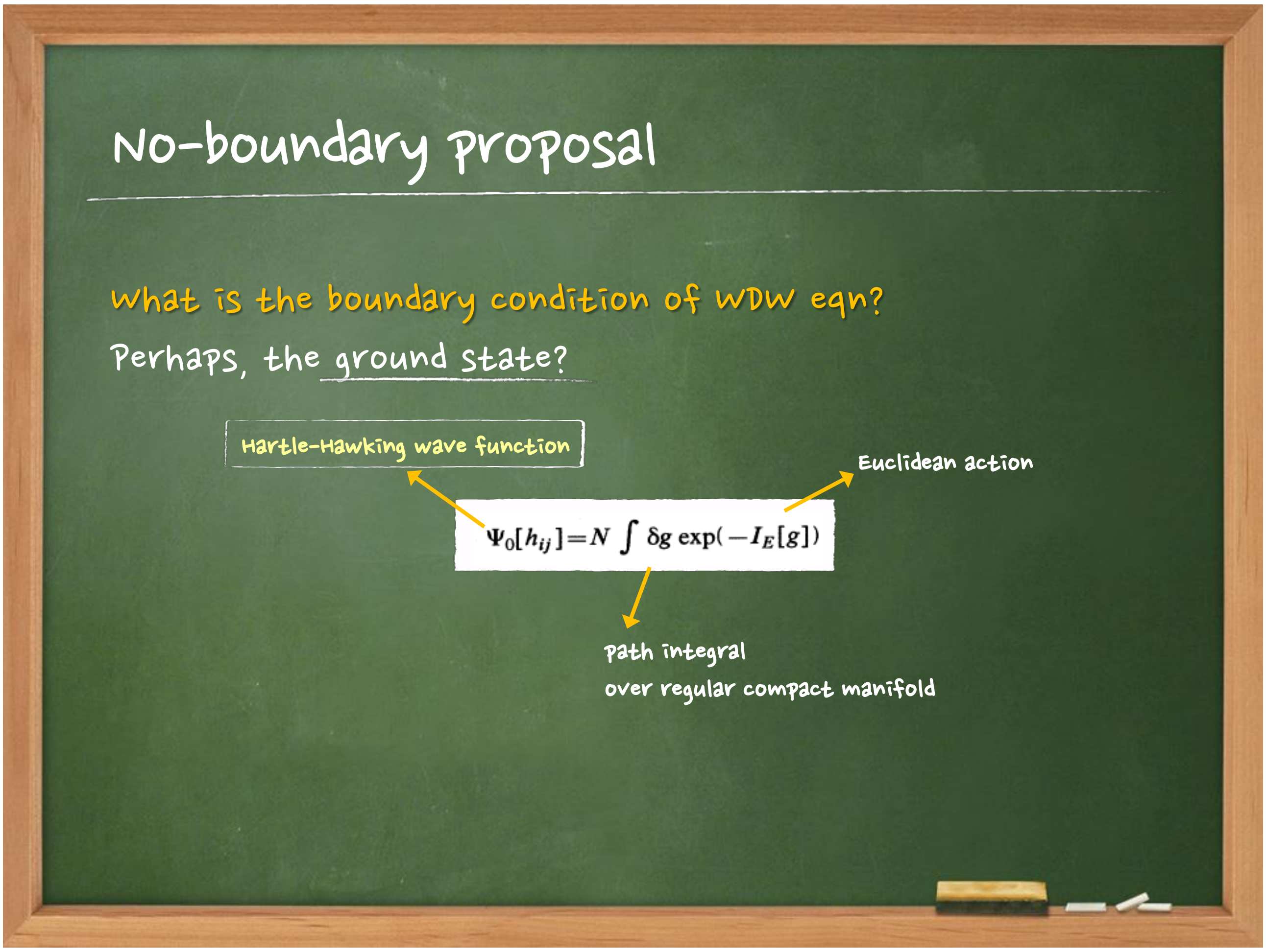
No-boundary proposal
What is the boundary condition of WDW eqn?
Perhaps, the ground state?
Hartle-Hawking wave function
Euclidean action
$\Psi_0[h_{ij}]=N\int\delta g\,\exp(-I_E[g])$
path integral
over regular compact manifold

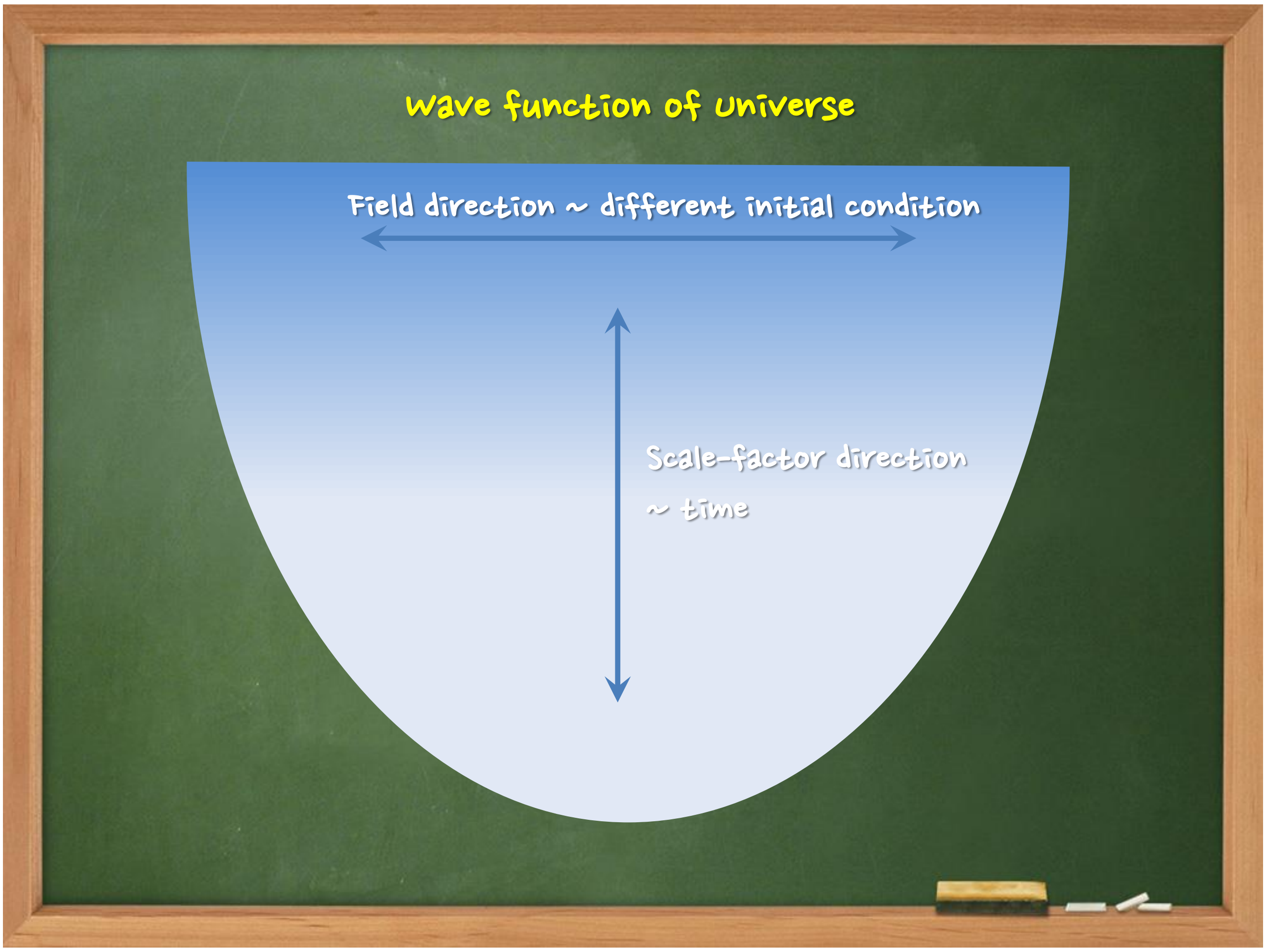
Wave function of universe
Field direction ~ different initial condition
Scale-factor direction
~ time

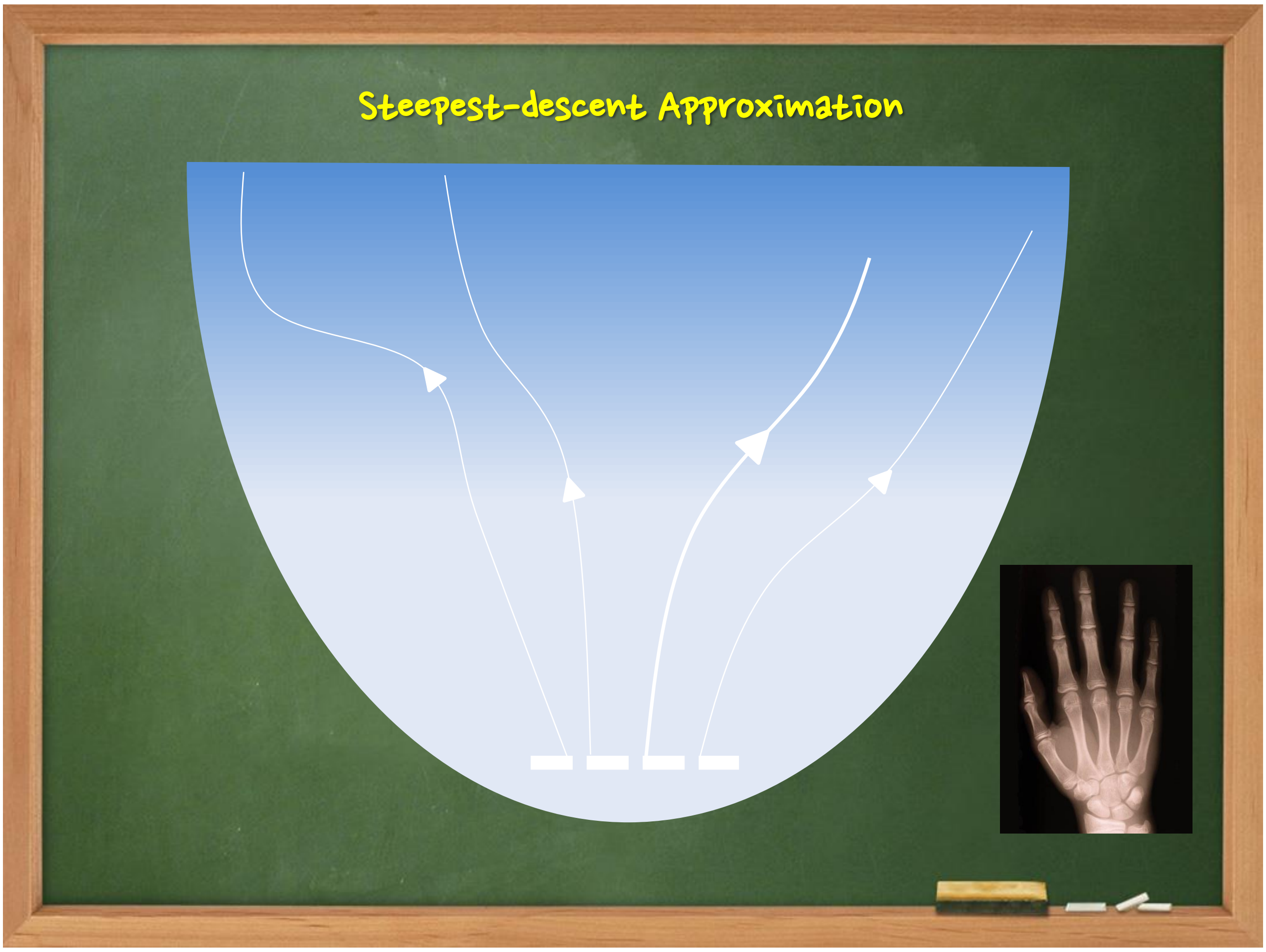
Steepest-descent Approximation

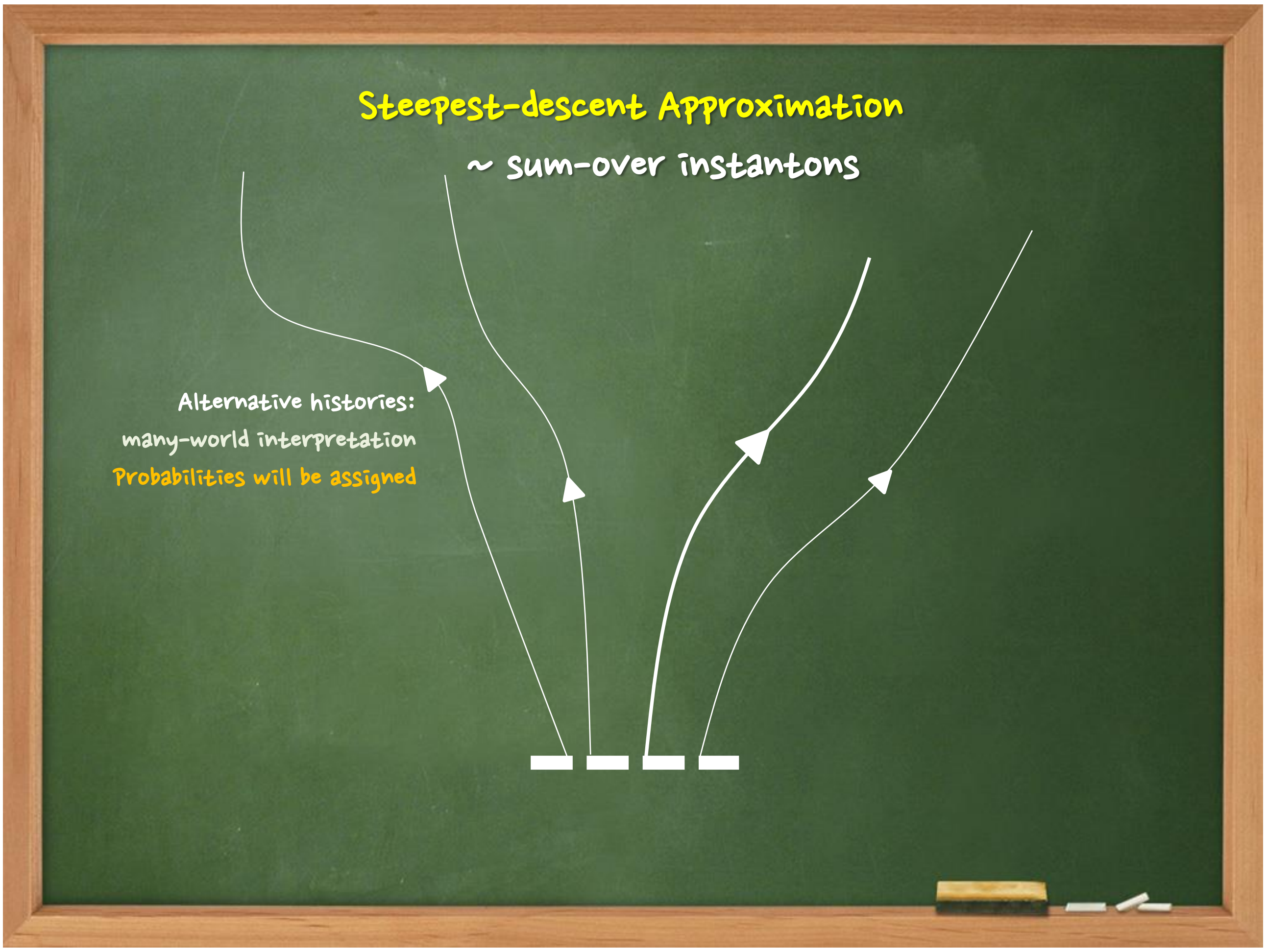
Steepest-descent Approximation
~ sum-over instantons
Alternative histories:
many-world interpretation
Probabilities will be assigned

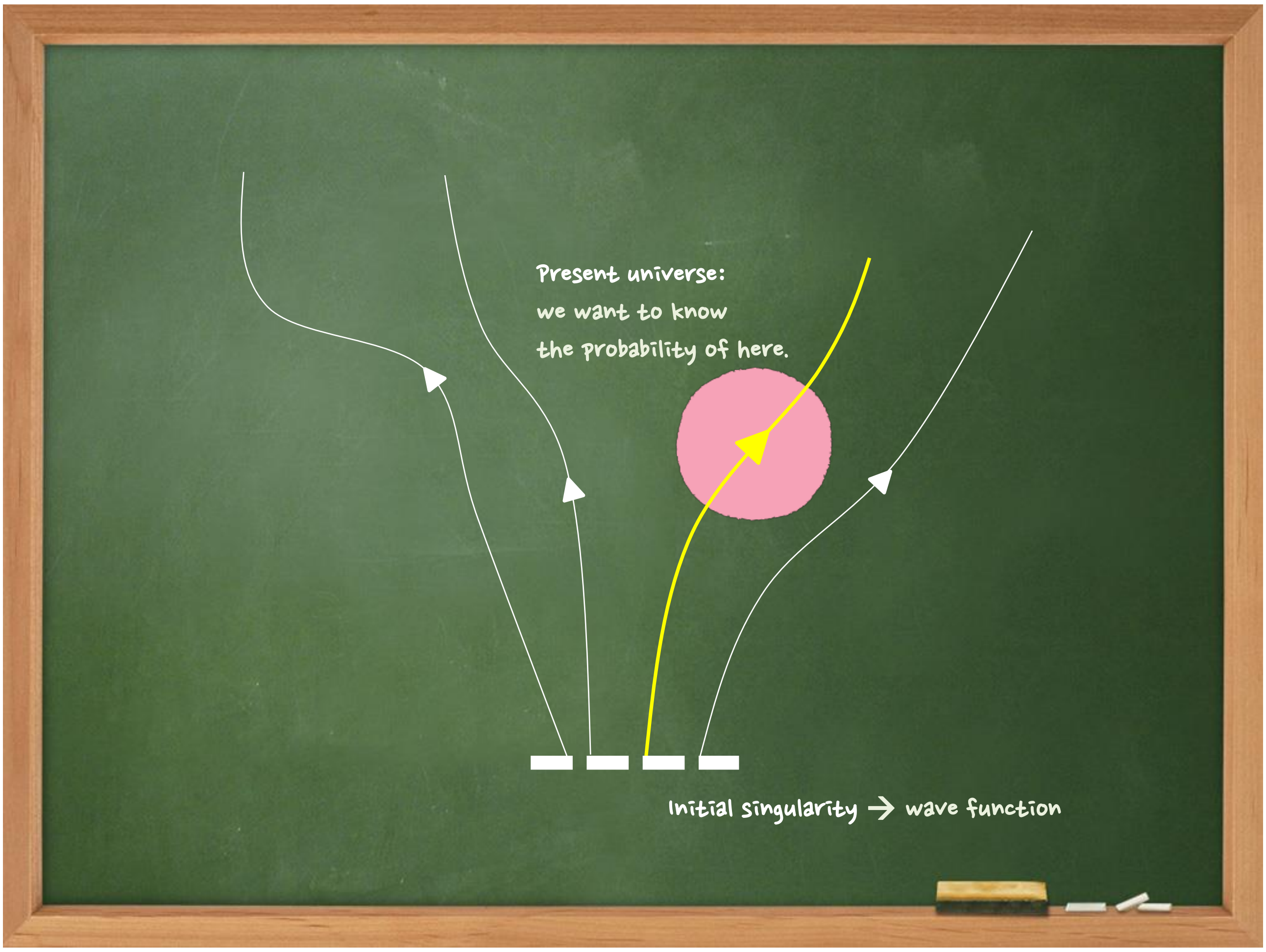
Present universe:
we want to know
the probability of here.
Initial singularity → wave function

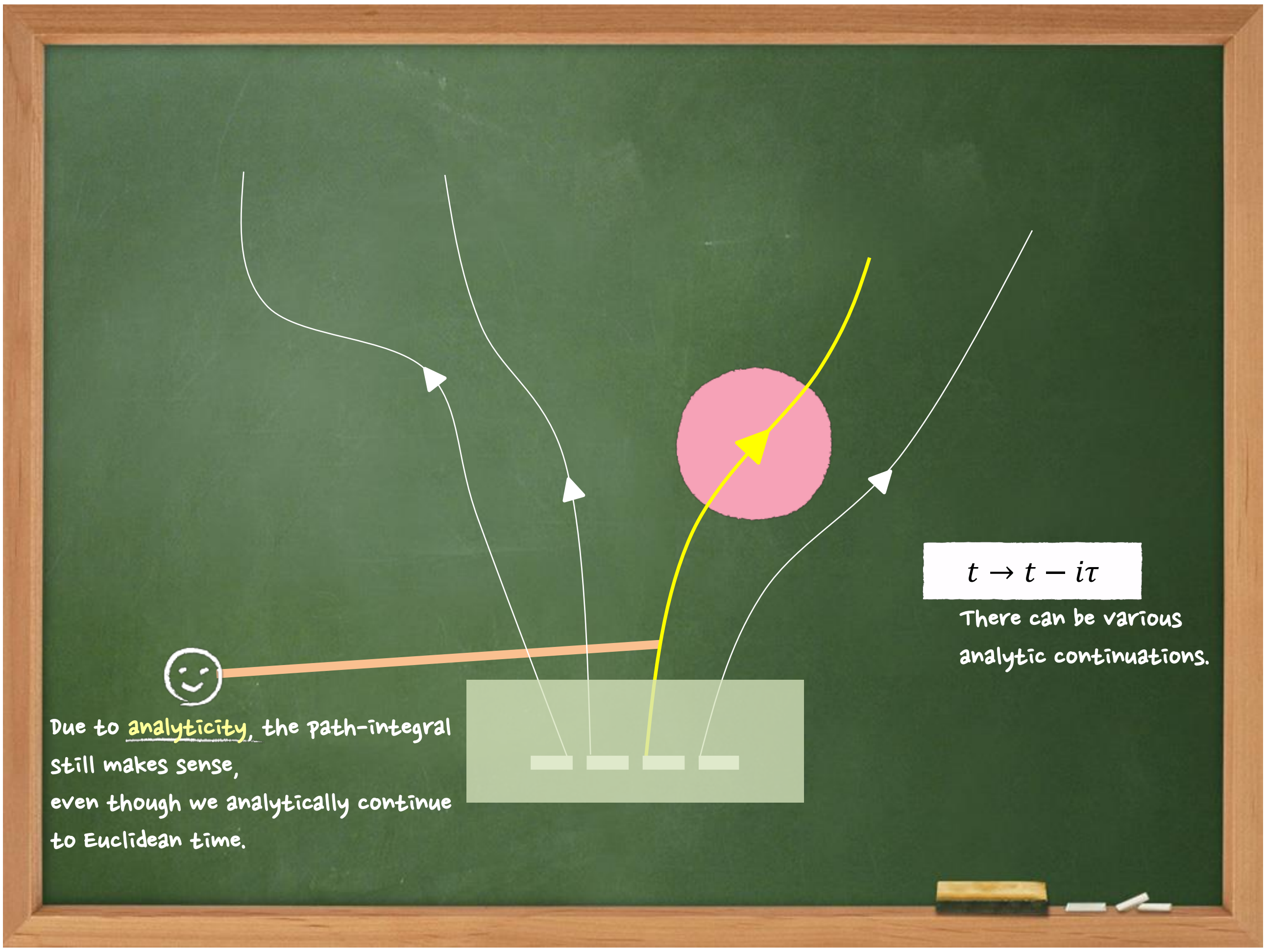
$t \to t - i\tau$
There can be various
analytic continuations.
Due to analyticity, the path-integral
still makes sense,
even though we analytically continue
to Euclidean time.

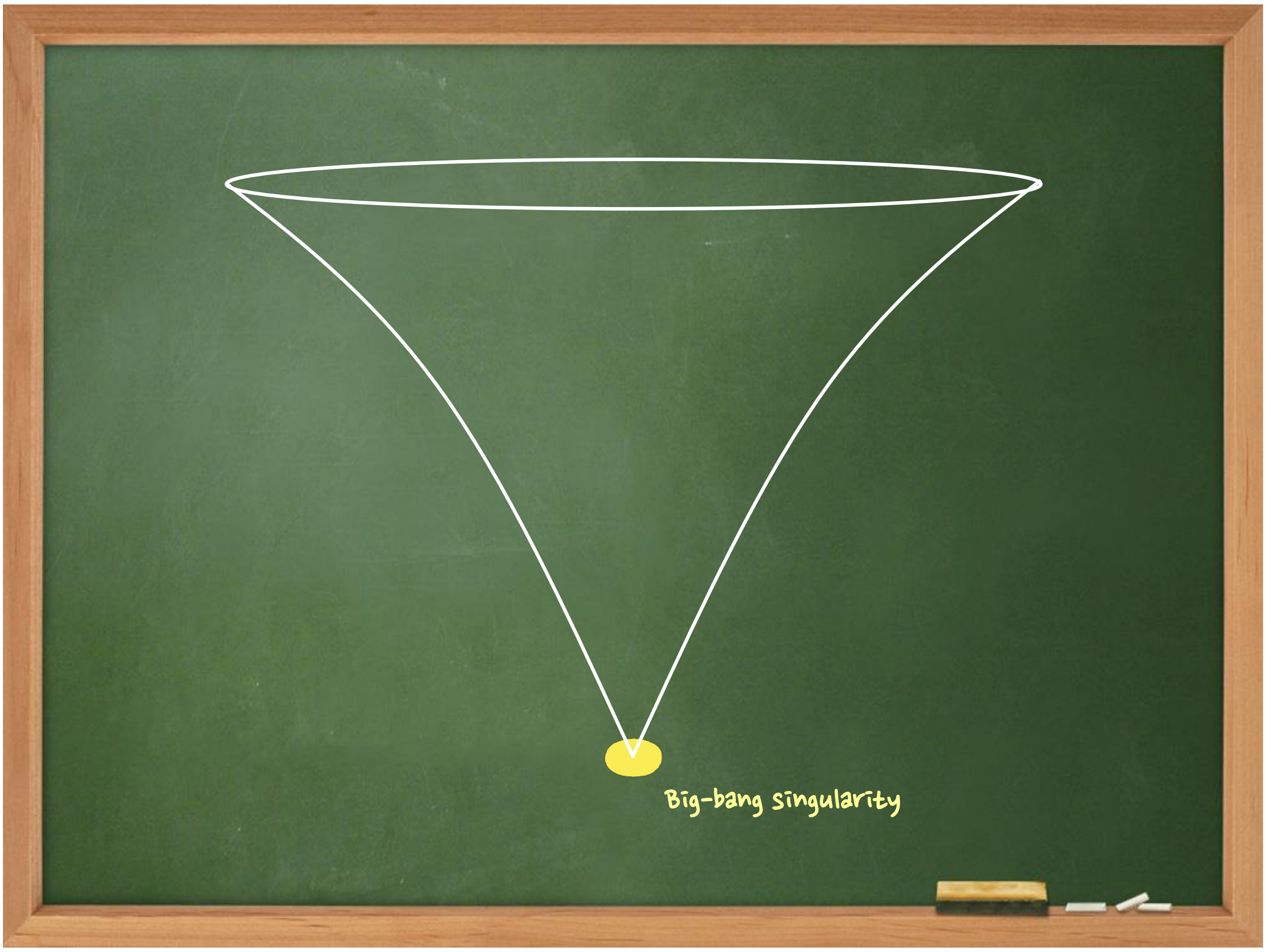
Big-bang singularity

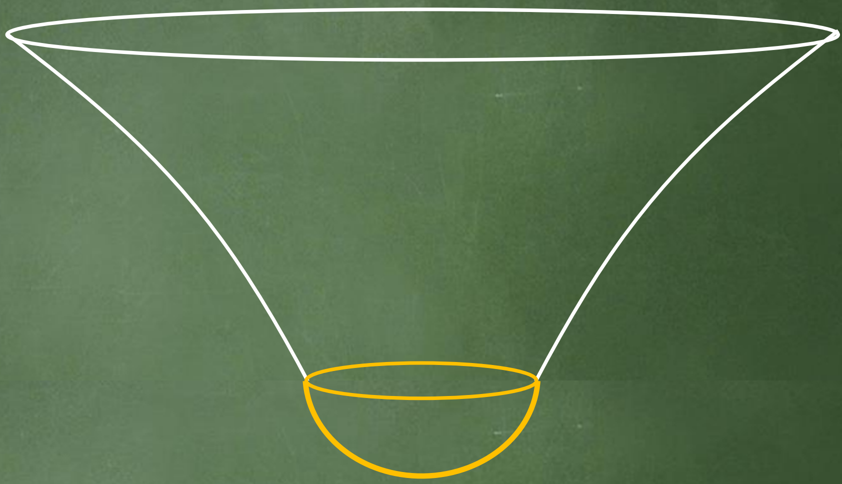

Find geometry over the complex time, until the geometry to be regular.

How to calculate path integral?

Approximation I: Mini-superspace

$$ds_{\mathrm{E}}^2 = N^2(\eta)d\eta^2 + \rho^2(\eta)(d\chi^2 + \sin^2\chi(d\theta^2 + \sin^2\theta d\varphi^2))$$

$$S_{\mathrm{E}} = -\int d^4x\sqrt{+g}\left(\frac{1}{16\pi}R - \frac{1}{2}(\nabla\phi)^2 - V(\phi)\right)$$

$$S_{\mathrm{E}} = 2\pi^2\int d\eta\left[-\frac{3}{8\pi}\left(\rho\dot{\rho}^2 + \rho\right) + \frac{1}{2}\rho^3\dot{\phi}^2 + \rho^3 V(\phi)\right]$$

How to calculate path integral?

Approximation 2: Steepest-descent (sum-over fuzzy instantons)

$$\Psi_{\mathrm{HH}}(q) \approx \sum_{\mathrm{ext}} P(q_{\mathrm{ext}}) e^{-S_{\mathrm{E}}[q_{\mathrm{ext}}]/\hbar}$$

$$S_{\mathrm{E}} = 2\pi^2 \int d\eta \left[-\frac{3}{8\pi}\left(\rho\dot{\rho}^2 + \rho\right) + \frac{1}{2}\rho^3\dot{\phi}^2 + \rho^3 V(\phi) \right]$$

$$\Downarrow$$

$$S_{\mathrm{E}} = 4\pi^2 \int d\eta \left(\rho^3 V - \frac{3}{8\pi}\rho \right)$$

How to calculate path integral?

Approximation 2: Steepest-descent (sum-over fuzzy instantons)

$$\Psi_{\mathrm{HH}}(q) \approx \sum_{\mathrm{ext}} P(q_{\mathrm{ext}}) e^{-S_{\mathrm{E}}[q_{\mathrm{ext}}]/\hbar}$$

$$S_{\mathrm{E}} = 2\pi^2 \int d\eta \left[-\frac{3}{8\pi}\left(\rho\dot{\rho}^2 + \rho\right) + \frac{1}{2}\rho^3\dot{\phi}^2 + \rho^3 V(\phi) \right]$$

$$\Downarrow$$

$$S_{\mathrm{E}} = 4\pi^2 \int d\eta \left(\rho^3 V - \frac{3}{8\pi}\rho \right)$$

9 parameters determine 1 history.
6 of them are determined by
regularity + compactness.

How to calculate path integral?

Requirement: classicality

$$|(\nabla I_R)^2| \ll |(\nabla S)^2|$$

By tuning 2 parameters, we satisfy classicality of matter and metric.

How to calculate path integral?

Requirement: classicality

$$|(\nabla I_R)^2| \ll |(\nabla S)^2|$$

By tuning 2 parameters, we satisfy classicality of matter and metric.

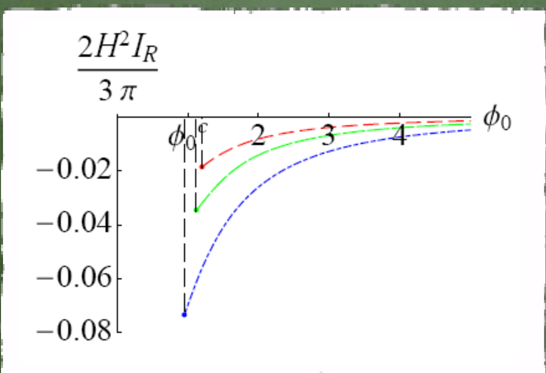

In the end, we obtain the probability distribution as a one (field) dimensional function.

(Hartle, Hawking and Hertog, 2007)

How to calculate path integral?

Requirement: classicality

$$|(\nabla I_R)^2| \ll |(\nabla S)^2|$$

cutoff due to classicality

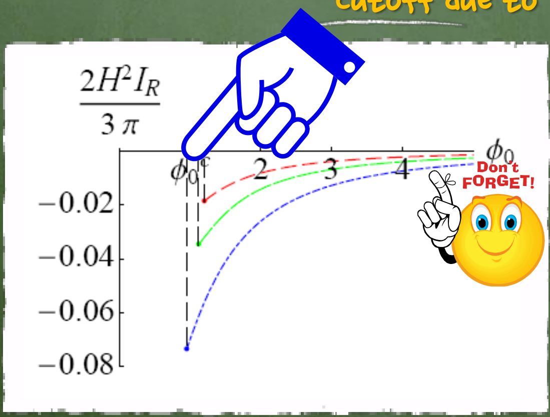

Large e-folding is exponentially suppressed!

(Hartle, Hawking and Hertog, 2007)

Does this prefer inflation?

Unfortunately, Euclidean probability does not prefer inflation.

Possible answers:

Does this prefer inflation?

Unfortunately, Euclidean probability does not prefer inflation.

Possible answers:

1. Inflation is wrong (Ekpyrotic, big bounce, string gas cosmology, etc.)
2. Ground state is wrong (Vilenkin's tunneling proposal)
3. Quantum cosmology is wrong (Susskind's multiverse + anthropic)
4. Small modification (Hartle-Hawking-Hertog's volume weighting)

Is there any better explanation, apart from these unsatisfactory opinions?

Toward good inflation models

Preference of large e-foldings

criterion of a good model

(Hwang, Park and DY, in preparation)

Typicality for a given hypothesis

$$\mathcal{T} \equiv \frac{P[\mathcal{N} \geq 50]}{P[\mathcal{N} < 50]}$$

For a given probability cutoff, there is corresponding typicality bound.

If the typicality is smaller than the bound, then we reject 棄却 the hypothesis.

Three ways to prefer inflation

(Hwang, Park and DY, in preparation)

1. The first inflation began at large energy scale.

$$-\frac{2}{V_0}\Delta + \Xi \gtrsim \log \mathcal{T}_{\rm cut}$$

2. Potential shape is finely tuned.

3. There are something new effects.

$$\Delta \equiv \left| \tilde{S}_{\rm E}[\phi_{\rm M}] - \tilde{S}_{\rm E}[\phi_{\rm top}] \right|$$

$$\Xi \equiv \log \frac{\phi_{50} - \phi_{\rm top}}{\phi_{\rm M} - \phi_{50}}$$

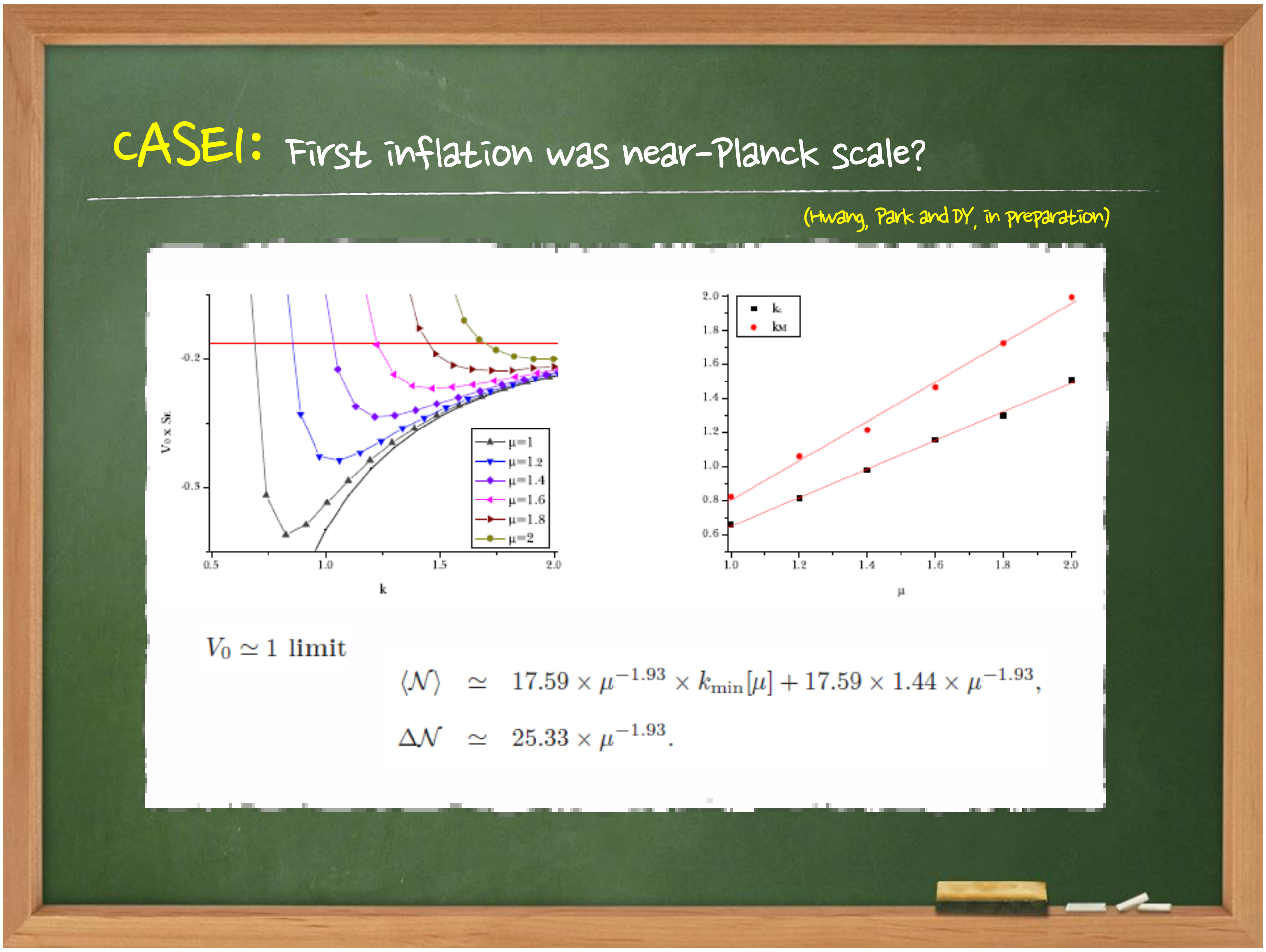
CASEI: First inflation was near-Planck scale?
(Hwang, Park and DY, in preparation)
$V_0 \times S_E$
k
μ=1
μ=1.2
μ=1.4
μ=1.6
μ=1.8
μ=2
kc
kM
μ
$V_0 \simeq 1$ limit
$\langle \mathcal{N} \rangle \simeq 17.59 \times \mu^{-1.93} \times k_{\min}[\mu] + 17.59 \times 1.44 \times \mu^{-1.93},$
$\Delta \mathcal{N} \simeq 25.33 \times \mu^{-1.93}.$

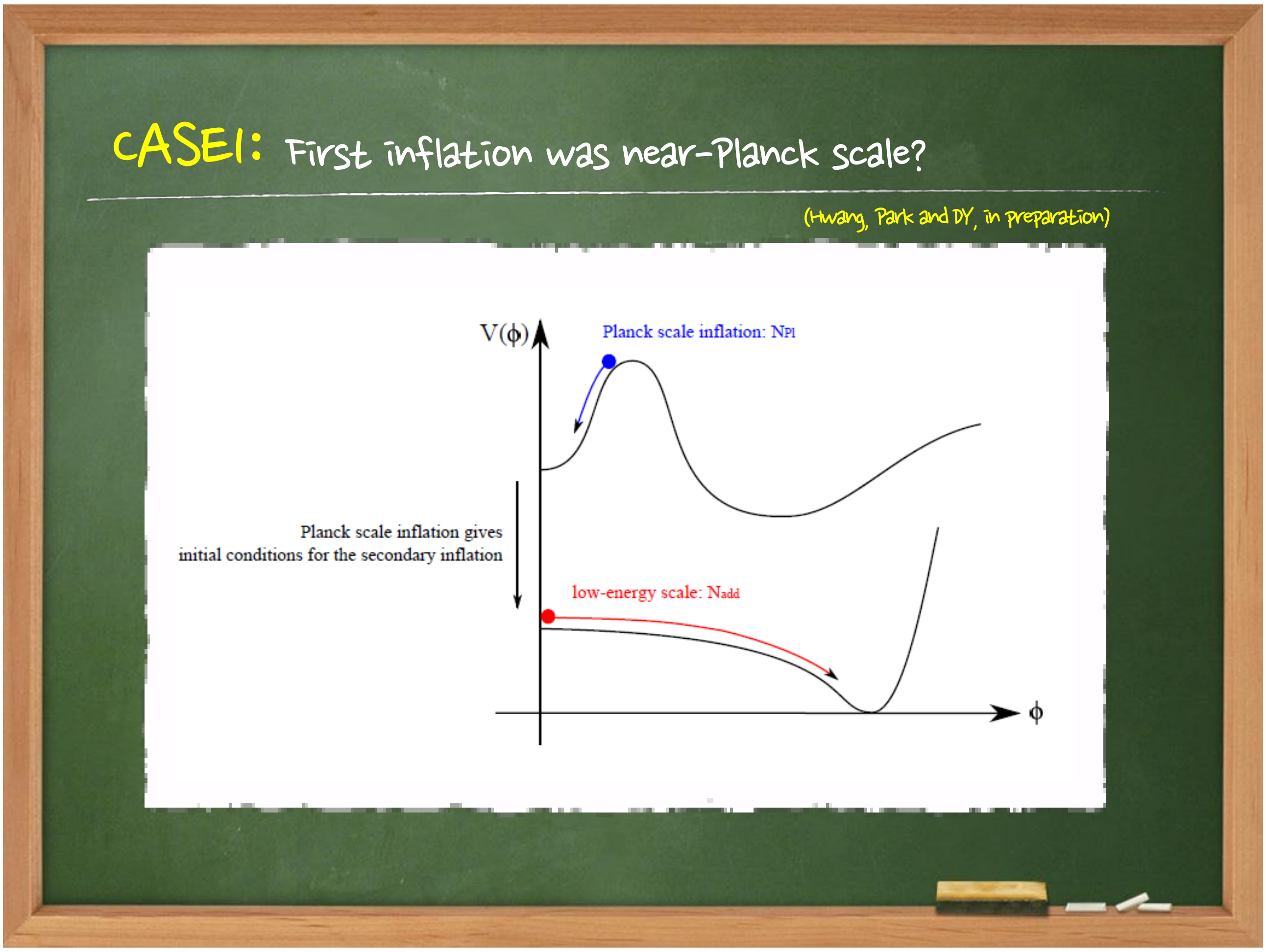
CASEI: First inflation was near-Planck scale?
(Hwang, Park and DY, in preparation)
V(ϕ)
Planck scale inflation: NPl
Planck scale inflation gives
initial conditions for the secondary inflation
low-energy scale: Nadd
ϕ

CASE2: Fine-tuning of the potential (Hwang, Park and DY, in preparation)

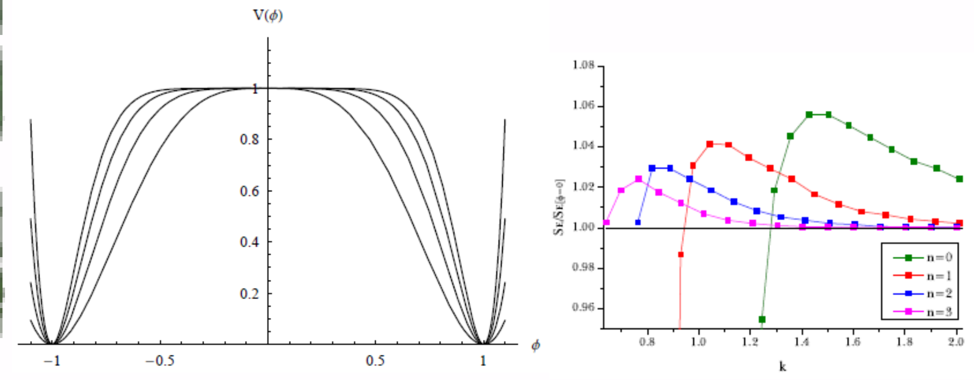

CASE2: Starobinski-like model (Kallosh and Linde, 2013)

$$\mathcal{L}_{\text{total}} = \sqrt{-g_J}\left[\frac{R(g_J)}{2}\left(1-\frac{\phi^2}{6}\right)-\frac{1}{2}\partial_\mu\phi\partial^\mu\phi-\frac{\lambda}{4}\left(\phi^2-6\right)^2\right]$$

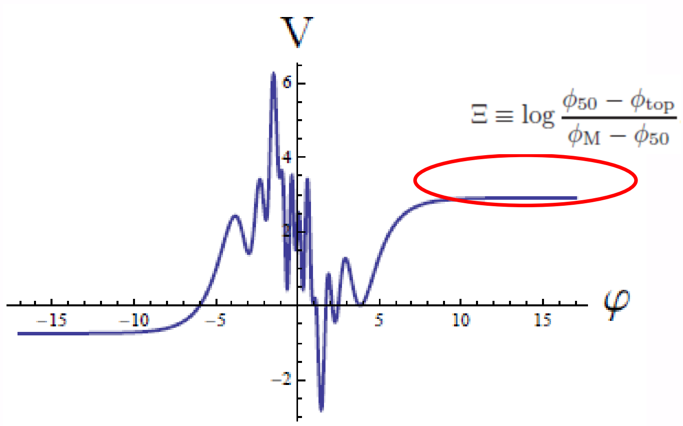

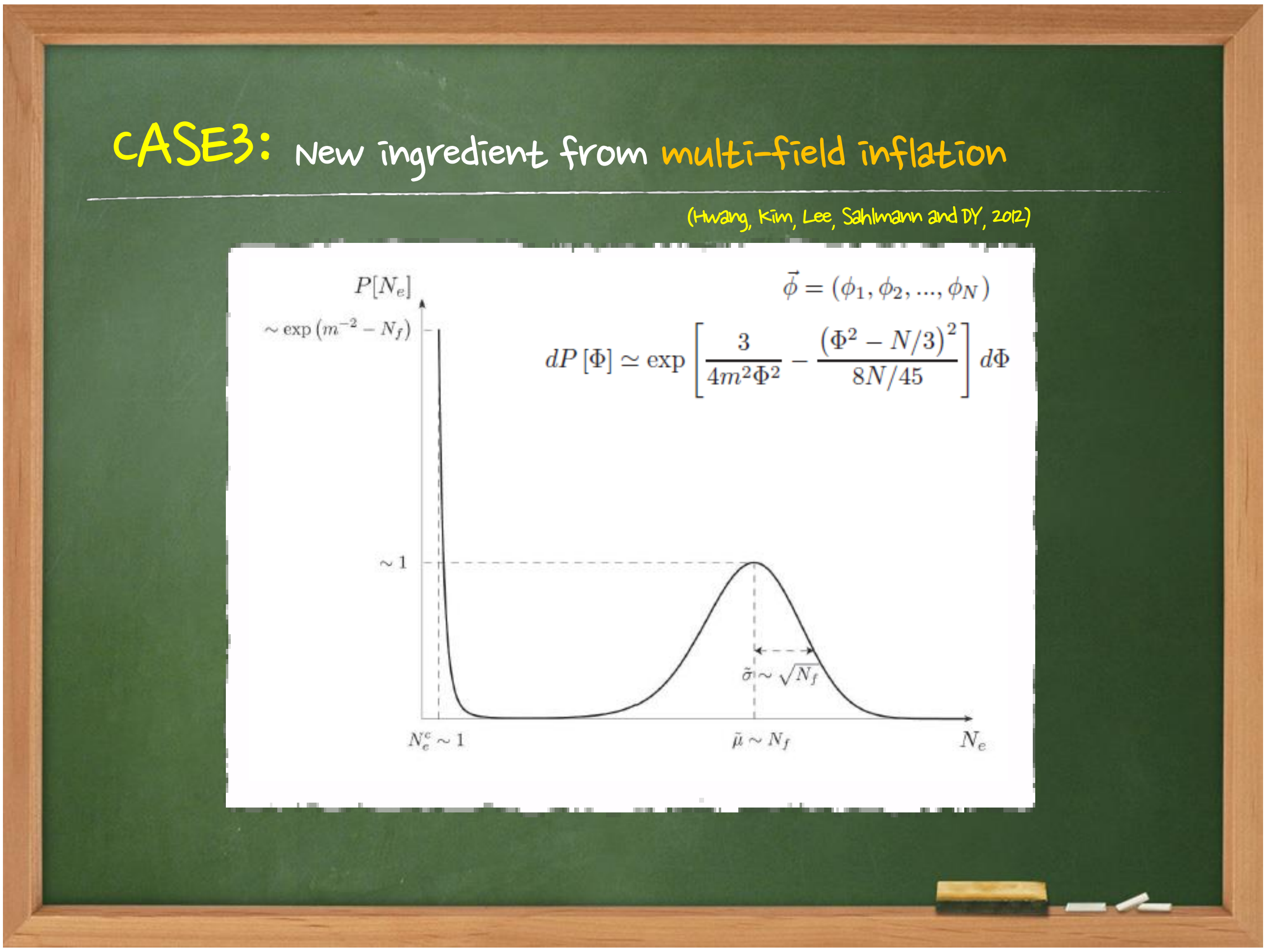
CASE3: New ingredient from multi-field inflation
(Hwang, Kim, Lee, Sahlmann and DY, 2012)
$P[N_e]$
$\sim \exp\left(m^{-2} - N_f\right)$
$\vec{\phi} = (\phi_1, \phi_2, ..., \phi_N)$
$dP[\Phi] \simeq \exp\left[\frac{3}{4m^2\Phi^2} - \frac{\left(\Phi^2 - N/3\right)^2}{8N/45}\right] d\Phi$
~ 1
$\tilde{\sigma} \sim \sqrt{N_f}$
$N_e^c \sim 1$
$\tilde{\mu} \sim N_f$
N_e

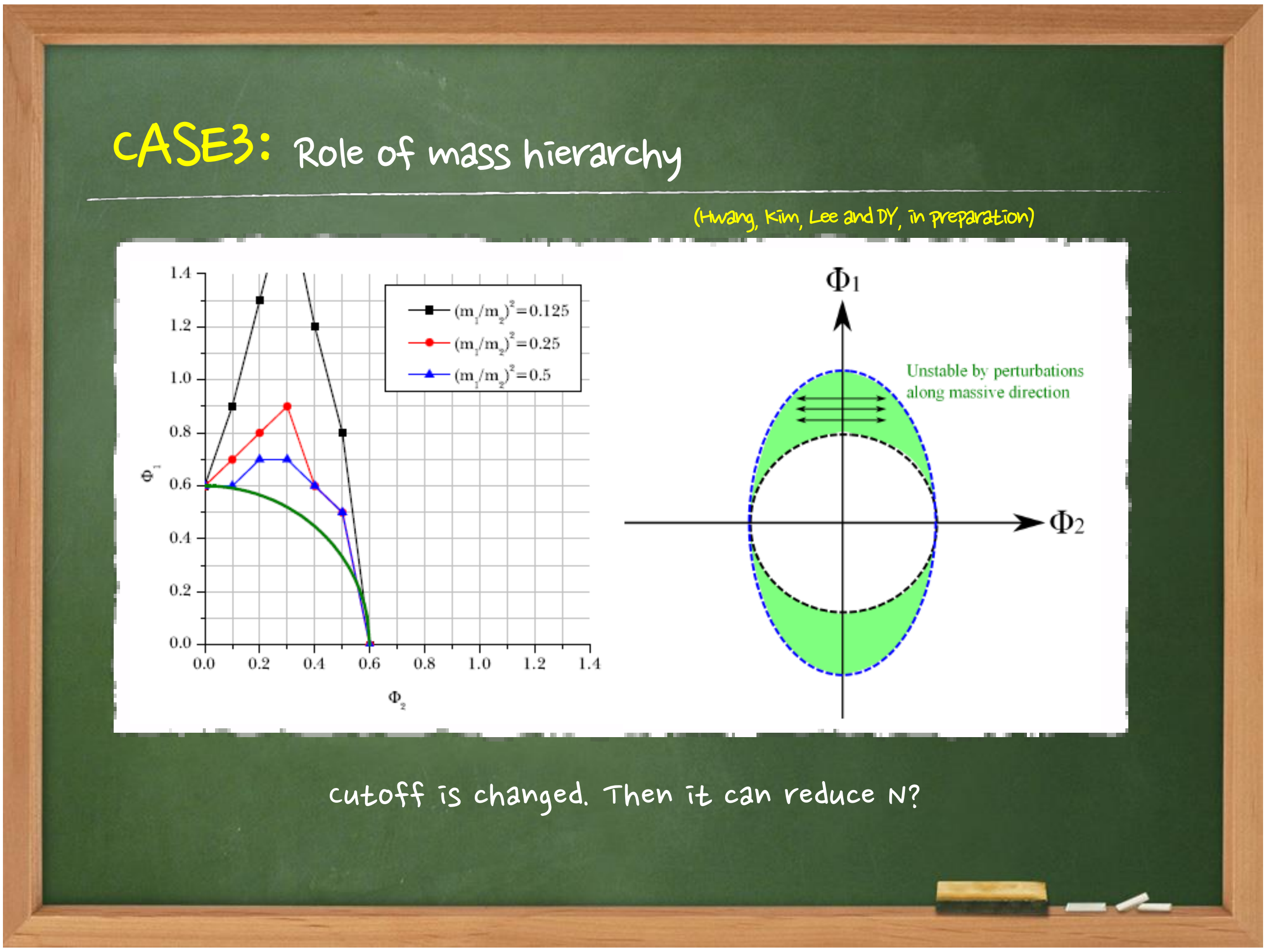
CASE3: Role of mass hierarchy
(Hwang, Kim, Lee and DY, in preparation)
$(m_1/m_2)^2=0.125$
$(m_1/m_2)^2=0.25$
$(m_1/m_2)^2=0.5$
Φ_1
Φ_2
Unstable by perturbations along massive direction
cutoff is changed. Then it can reduce N?

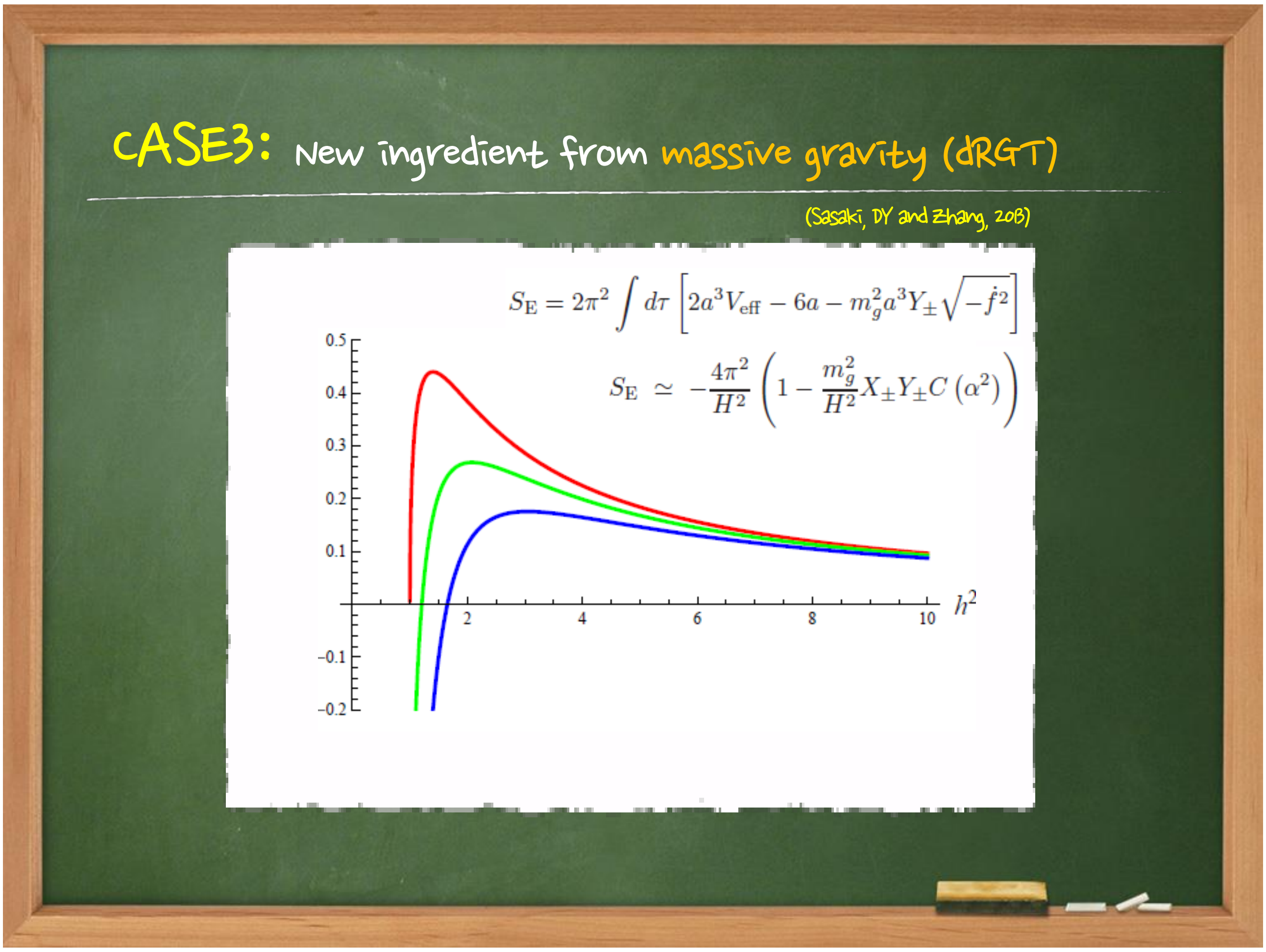
CASE3: New ingredient from massive gravity (dRGT)
(Sasaki, DY and Zhang, 2013)
$S_{\rm E} = 2\pi^2 \int d\tau \left[2a^3 V_{\rm eff} - 6a - m_g^2 a^3 Y_\pm \sqrt{-\dot{f}^2}\right]$
$S_{\rm E} \simeq -\frac{4\pi^2}{H^2}\left(1 - \frac{m_g^2}{H^2} X_\pm Y_\pm C\left(\alpha^2\right)\right)$
h^2

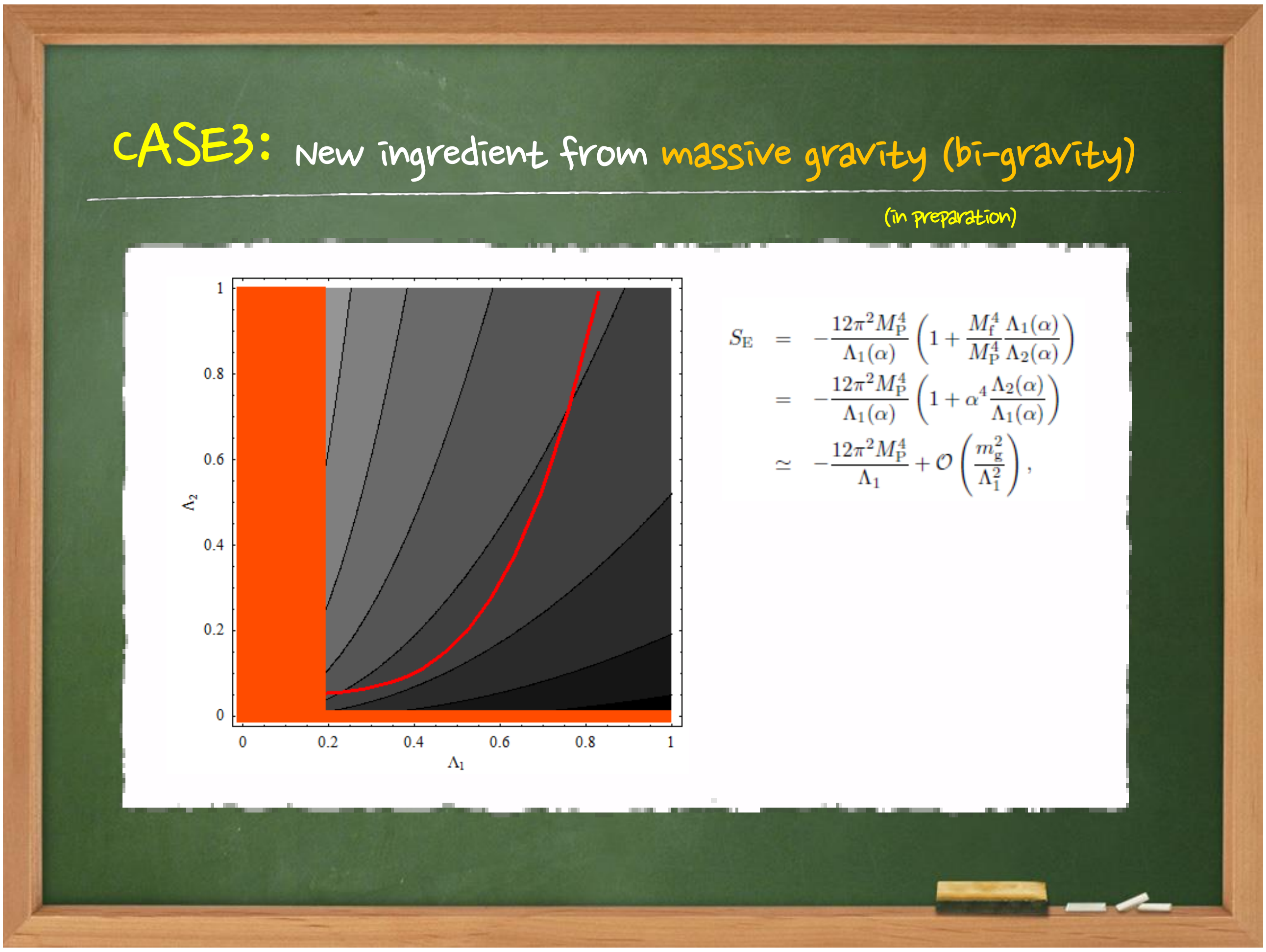
CASE3: New ingredient from massive gravity (bi-gravity)
(in preparation)
Λ_2
Λ_1
$S_{\rm E} = -\frac{12\pi^2 M_{\rm P}^4}{\Lambda_1(\alpha)}\left(1 + \frac{M_{\rm f}^4}{M_{\rm P}^4}\frac{\Lambda_1(\alpha)}{\Lambda_2(\alpha)}\right)$
$= -\frac{12\pi^2 M_{\rm P}^4}{\Lambda_1(\alpha)}\left(1 + \alpha^4 \frac{\Lambda_2(\alpha)}{\Lambda_1(\alpha)}\right)$
$\simeq -\frac{12\pi^2 M_{\rm P}^4}{\Lambda_1} + \mathcal{O}\left(\frac{m_g^2}{\Lambda_1^2}\right),$

Quantum cosmology can be a

new motivation for massive gravity!

dRGT, bi-gravity, SO(3), …?

can it remain imprints?

“On the graceful exit from Higgs G-inflation”

by Taro Kunimitsu

[JGRG23(2013)110717]

Graceful Exit from Higgs G-inflation

Taro Kunimitsu (RESCEU, Univ. of Tokyo)

arXiv:1309.7410 [hep-ph]

in collaboration with Kohei Kamada, Tsutomu Kobayashi, Masahide Yamaguchi, Jun'ichi Yokoyama

Higgs in cosmology

- Only scalar field in the Standard model

  →Might be the responsible for inflation

Higgs in cosmology

- Only scalar field in the Standard model

  →Might be the responsible for inflation

$$S = \int \sqrt{-g} \left[\frac{1}{2} M_P^2 R + X - \frac{1}{4} \lambda \varphi^4 \right]$$

$$X = -\frac{1}{2} g^{\mu\nu} \partial_\mu \varphi \partial_\nu \varphi \qquad \lambda \sim 0.1$$

Higgs Inflation

$$\mathcal{L}_{SM} \ -\frac{1}{2}\xi\varphi^2 R$$

with $\xi \sim 5 \times 10^4$

Bezrukov, Shaposhnikov (2008)

$$\rightarrow \ r = 0.003, \ n_s = 0.967$$

- Small tensor fluctuations
  →Cannot be observed in the near future

Higgs G-inflation

- Kamada et al. (2011)

$$S = \int d^4x\sqrt{-g}\left[\frac{M_P^2}{2}R + X - \frac{1}{4}\lambda\varphi^4 - \underline{G(\varphi, X)\Box\varphi}\right]$$

Higgs G-inflation

- Kamada et al. (2011)

$$S = \int d^4x\sqrt{-g}\left[\frac{M_P^2}{2}R + X - \frac{1}{4}\lambda\varphi^4 - \underline{G(\varphi, X)\Box\varphi}\right]$$

$$G(\varphi, X) = -\frac{\varphi X}{M^4}$$ in the original model

Higgs G-inflation

- Kamada et al. (2011)

slow-roll equation of motion

$$\left(1 - \underline{\frac{3H\varphi\dot{\varphi}}{M^4}}\right)3H\dot{\varphi} + \lambda\varphi^3 = 0$$

Extra friction term

$$r = 0.14, \quad n_s = 0.967$$

After inflation

Ohashi, Tsujikawa (2012)

- equation of motion

$$\left(\underline{1 - 6H\frac{\varphi\dot{\varphi}}{M^4} + 2\frac{\dot{\varphi}^2}{M^4} + \frac{3\varphi^2\dot{\varphi}^4}{2M_P^2 M^8}}\right)\ddot{\varphi} + 3H\dot{\varphi} + \lambda\varphi^3$$
$$- \left(9H^2 - \frac{3\dot{\varphi}^2}{2M_P^2} - \frac{3\dot{\varphi}^4}{2M_P^2 M^4} + \frac{3\lambda\varphi^4}{4M_P^2}\right)\frac{\varphi\dot{\varphi}^2}{2M^4} = 0$$

After inflation

Ohashi, Tsujikawa (2012)

- equation of motion

$$\left(\underline{1 - 6H\frac{\varphi\dot{\varphi}}{M^4} + 2\frac{\dot{\varphi}^2}{M^4} + \frac{3\varphi^2\dot{\varphi}^4}{2M_P^2 M^8}}\right)\ddot{\varphi} + 3H\dot{\varphi} + \lambda\varphi^3$$
$$- \left(9H^2 - \frac{3\dot{\varphi}^2}{2M_P^2} - \frac{3\dot{\varphi}^4}{2M_P^2 M^4} + \frac{3\lambda\varphi^4}{4M_P^2}\right)\frac{\varphi\dot{\varphi}^2}{2M^4} = 0$$

After inflation

Ohashi, Tsujikawa (2012)

- equation of motion

$$\left(1-6H\frac{\varphi\dot{\varphi}}{M^4}+2\frac{\dot{\varphi}^2}{M^4}+\frac{3\varphi^2\dot{\varphi}^4}{2M_P^2M^8}\right)\boxed{\rightarrow 0}+\lambda\varphi^3$$
$$-\left(9H^2-\frac{3\dot{\varphi}^2}{2M_P^2}-\frac{3\dot{\varphi}^4}{2M_P^2M^4}+\frac{3\lambda\varphi^4}{4M_P^2}\right)\frac{\varphi\dot{\varphi}^2}{2M^4}=0$$

After inflation

Ohashi, Tsujikawa (2012)

- sound speed

$$c_s^2=\frac{1-(4H\dot{\varphi}+2\ddot{\varphi})\frac{\varphi}{M^4}-\frac{\varphi^2\dot{\varphi}^4}{2M_{Pl}^2M^8}}{1-6H\frac{\dot{\varphi}\varphi}{M^4}+2\frac{\dot{\varphi}^2}{M^4}+\frac{3\varphi^2\dot{\varphi}^4}{2M_{Pl}^2M^8}}$$

After inflation

Ohashi, Tsujikawa (2012)

- sound speed

$$c_s^2 = \frac{1 - (4H\dot{\varphi} + 2\ddot{\varphi})\frac{\varphi}{M^4} - \frac{\varphi^2\dot{\varphi}^4}{2M_{Pl}^2 M^8}}{1 - 6H\frac{\dot{\varphi}\varphi}{M^4} + 2\frac{\dot{\varphi}^2}{M^4} + \frac{3\varphi^2\dot{\varphi}^4}{2M_{Pl}^2 M^8}} < 0$$

→instability at small scales

Solution

Solution

Add an X^2 term

$$S = \int d^4x\sqrt{-g}\left[\frac{M_P^2}{2}R + X + \frac{1}{2\widetilde{M}^4}X^2 - \frac{1}{4}\lambda\varphi^4 + \frac{\varphi X}{M^4}\Box\varphi\right]$$

Solution

Add an X^2 term

equation of motion

$$\left(1+\frac{3\dot{\varphi}^2}{2\widetilde{M}^4} - 6H\frac{\varphi\dot{\varphi}}{M^4} + 2\frac{\dot{\varphi}^2}{M^4} + \frac{3\varphi^2\dot{\varphi}^4}{2M_P^2M^8}\right)\ddot{\varphi} + 3\left(1+\frac{\dot{\varphi}^2}{2\widetilde{M}^4}\right)H\dot{\varphi} + \lambda\varphi^3$$
$$-\left(9H^2 - \frac{3\dot{\varphi}^4}{8M_P^2\widetilde{M}^4} - \frac{3\dot{\varphi}^2}{2M_P^2} - \frac{3\dot{\varphi}^4}{2M_P^2M^4} + \frac{3\lambda\varphi^4}{4M_P^2}\right)\frac{\varphi\dot{\varphi}^2}{2M^4} = 0$$

Solution

Add an X^2 term

equation of motion

$$\left(1+\frac{3\dot\varphi^2}{2\widetilde{M}^4}-6H\frac{\varphi\dot\varphi}{M^4}+2\frac{\dot\varphi^2}{M^4}+\frac{3\varphi^2\dot\varphi^4}{2M_P^2M^8}\right)\ddot\varphi+3\left(1+\frac{\dot\varphi^2}{2\widetilde{M}^4}\right)H\dot\varphi+\lambda\varphi^3 -\left(9H^2-\frac{3\dot\varphi^4}{8M_P^2\widetilde{M}^4}-\frac{3\dot\varphi^2}{2M_P^2}-\frac{3\dot\varphi^4}{2M_P^2M^4}+\frac{3\lambda\varphi^4}{4M_P^2}\right)\frac{\varphi\dot\varphi^2}{2M^4}=0$$

Solution

Add an X^2 term

sound speed

$$c_s^2=\frac{1+\frac{1}{2\widetilde{M}^4}\dot\varphi^2-(4H\dot\varphi+2\ddot\varphi)\frac{\varphi}{M^4}-\frac{\varphi^2\dot\varphi^4}{2M_{Pl}^2M^8}}{1+\frac{3}{2\widetilde{M}^4}\dot\varphi^2-6H\frac{\dot\varphi\varphi}{M^4}+2\frac{\dot\varphi^2}{M^4}+\frac{3\varphi^2\dot\varphi^4}{2M_{Pl}^2M^8}}$$

Solution

Add an X^2 term

sound speed

$$c_s^2 = \frac{1 + \frac{1}{2\widetilde{M}^4}\dot{\varphi}^2 - (4H\dot{\varphi} + 2\ddot{\varphi})\frac{\varphi}{M^4} - \frac{\varphi^2\dot{\varphi}^4}{2M_{Pl}^2 M^8}}{1 + \frac{3}{2\widetilde{M}^4}\dot{\varphi}^2 - 6H\frac{\dot{\varphi}\varphi}{M^4} + 2\frac{\dot{\varphi}^2}{M^4} + \frac{3\varphi^2\dot{\varphi}^4}{2M_{Pl}^2 M^8}}$$

Solution

Add an X^2 term

sound speed

$$c_s^2 = \frac{1 + \frac{1}{2\widetilde{M}^4}\dot{\varphi}^2 - (4H\dot{\varphi} + 2\ddot{\varphi})\frac{\varphi}{M^4} - \frac{\varphi^2\dot{\varphi}^4}{2M_{Pl}^2 M^8}}{1 + \frac{3}{2\widetilde{M}^4}\dot{\varphi}^2 - 6H\frac{\dot{\varphi}\varphi}{M^4} + 2\frac{\dot{\varphi}^2}{M^4} + \frac{3\varphi^2\dot{\varphi}^4}{2M_{Pl}^2 M^8}}$$

$\rightarrow$ Both problems avoided!

Solution

$$S = \int d^4x\sqrt{-g}\left[\frac{M_P^2}{2}R + X + \underline{\frac{1}{2\widetilde{M}^4}}X^2 - \frac{1}{4}\lambda\varphi^4 + \underline{\frac{\varphi X}{M^4}\Box\varphi}\right]$$

$$r = 0.116 - 0.155,$$
$$n_s = 0.958 - 0.964$$

$M \to \infty$ smallest M without instabilities

New Class of inflationary models

- Generalize kinetic and Galileon terms

$$X + \frac{1}{\widetilde{M}^{\ell-1}}X^\ell - \frac{1}{4}\lambda\varphi^4 + \frac{\varphi^{2n+1}X^m}{M^{2n+4m}}\Box\varphi$$

$$X + \frac{1}{\widetilde{M}^{\ell-1}} X^{\ell} - \frac{1}{4}\lambda\varphi^4 + \frac{\varphi^{2n+1} X^m}{M^{2n+4m}} \Box\varphi$$

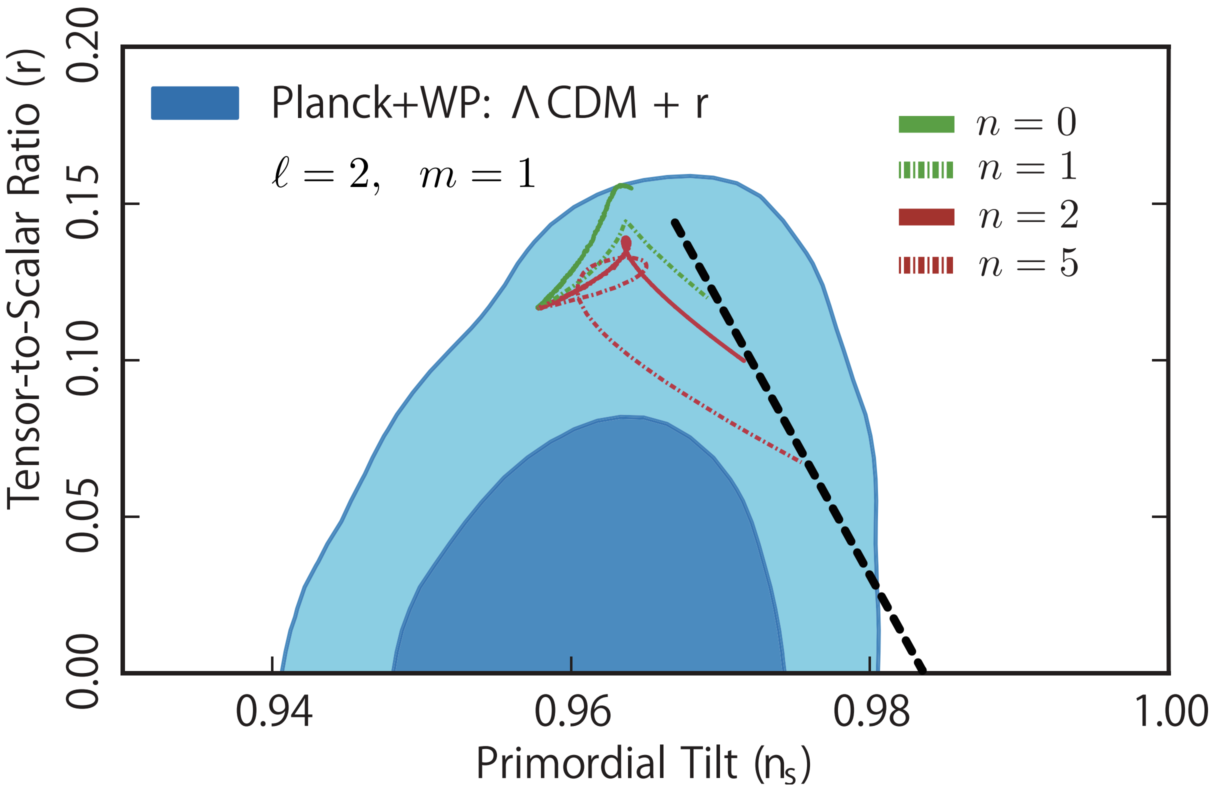

$$X + \frac{1}{\widetilde{M}^{\ell-1}} X^{\ell} - \frac{1}{4}\lambda\varphi^4 + \frac{\varphi^{2n+1} X^m}{M^{2n+4m}} \Box\varphi$$

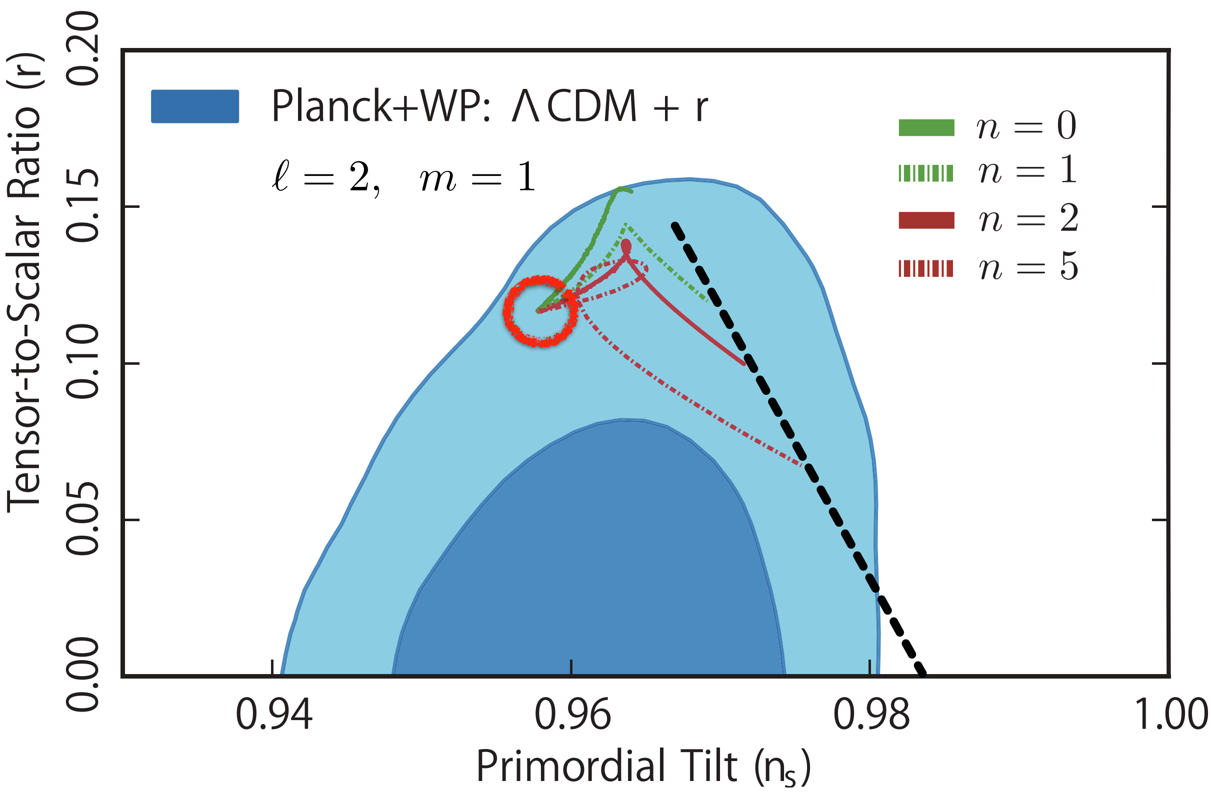

$$X + \frac{1}{\widetilde{M}^{\ell-1}} X^{\ell} - \frac{1}{4}\lambda\varphi^4 + \frac{\varphi^{2n+1} X^m}{M^{2n+4m}} \Box\varphi$$

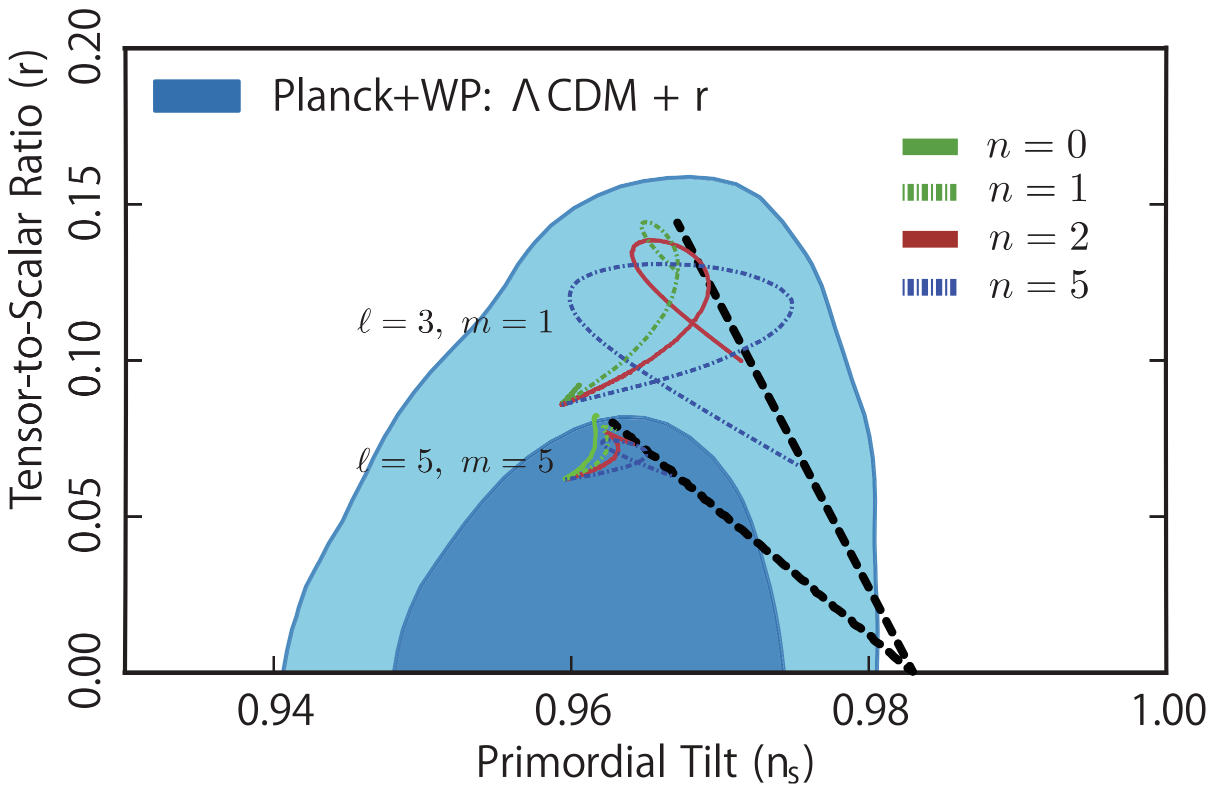

Summary

- Instabilities in Higgs G-inflation avoided by adding a higher order kinetic term
- New class of Higgs inflation models, consistent throughout inflation and reheating
- (Typically) a large tensor-to-scalar ratio →Would be detected by Planck

Backups

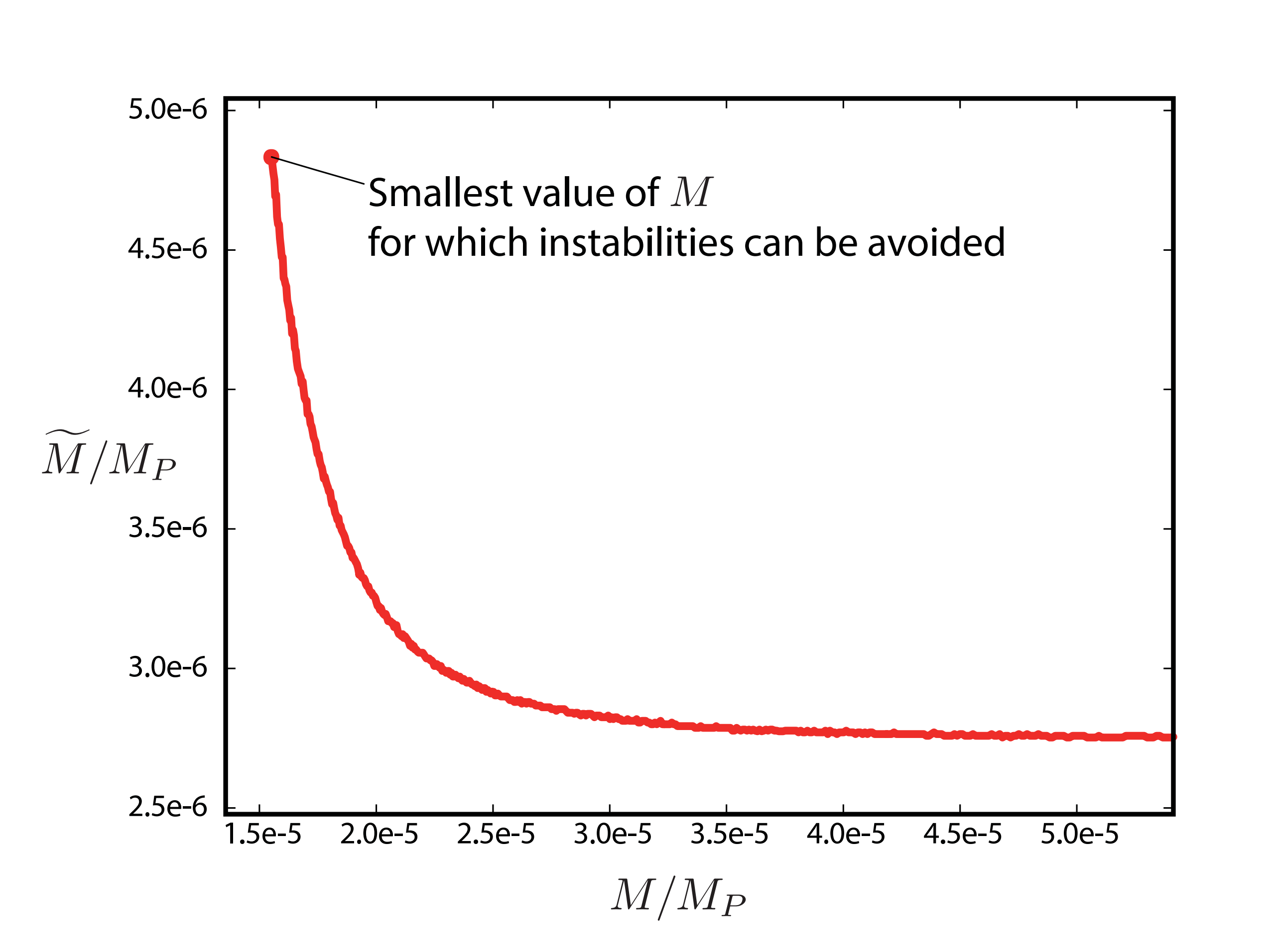

5.0e-6
4.5e-6
4.0e-6
3.5e-6
3.0e-6
2.5e-6
$\widetilde{M}/M_P$
Smallest value of M
for which instabilities can be avoided
1.5e-5
2.0e-5
2.5e-5
3.0e-5
3.5e-5
4.0e-5
4.5e-5
5.0e-5
M/M_P

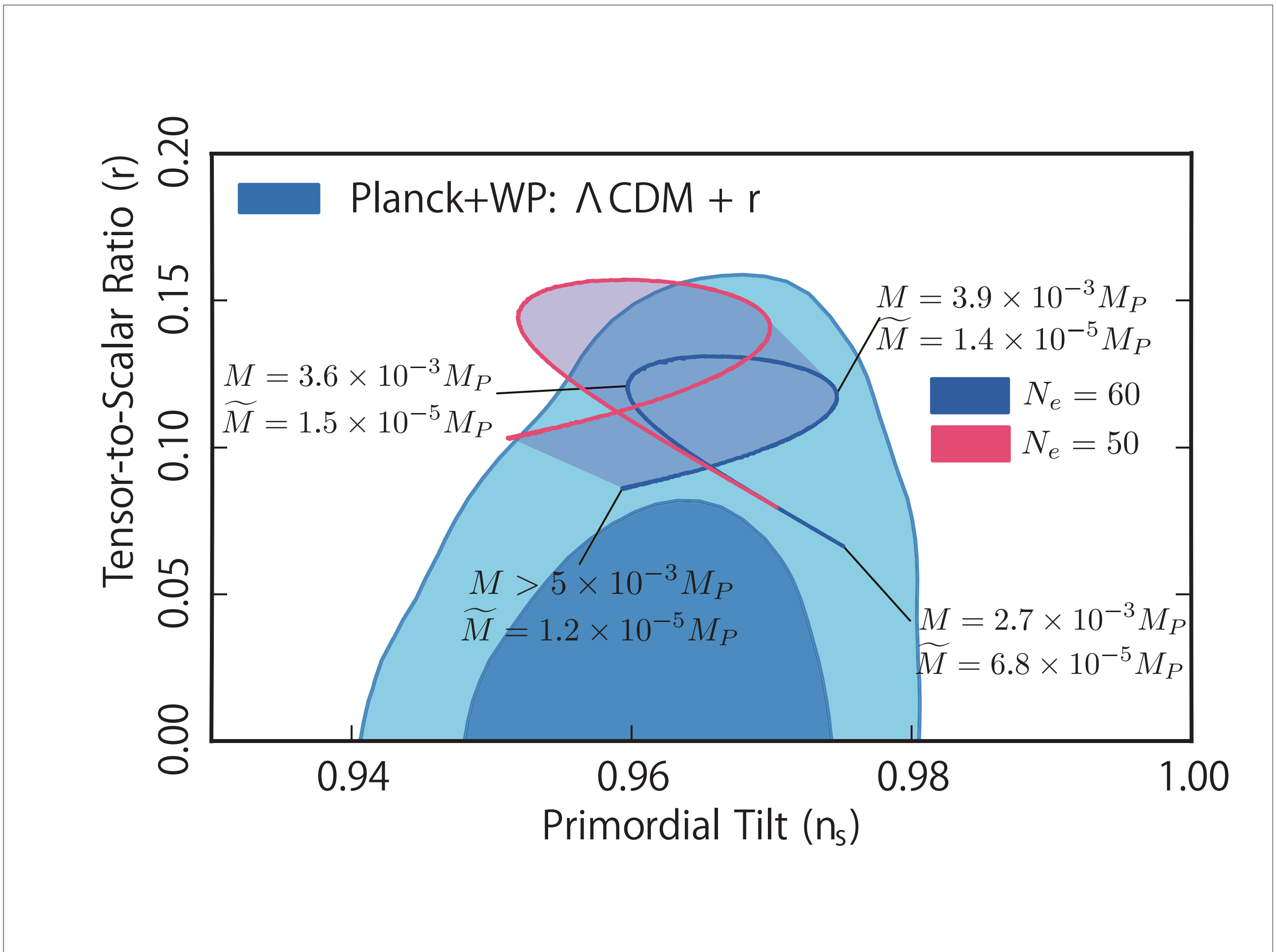

Planck+WP: ΛCDM + r
$M = 3.9 \times 10^{-3} M_P$
$\widetilde{M} = 1.4 \times 10^{-5} M_P$
$M = 3.6 \times 10^{-3} M_P$
$\widetilde{M} = 1.5 \times 10^{-5} M_P$
$N_e = 60$
$N_e = 50$
$M > 5 \times 10^{-3} M_P$
$\widetilde{M} = 1.2 \times 10^{-5} M_P$
$M = 2.7 \times 10^{-3} M_P$
$\widetilde{M} = 6.8 \times 10^{-5} M_P$
Tensor-to-Scalar Ratio (r)
0.00
0.05
0.10
0.15
0.20
0.94
0.96
0.98
1.00
Primordial Tilt (n_s)

$$
\begin{aligned}
S_2 &= M_P^2 \int d^4x\, a^3 \left[\mathcal{G}_S \dot{\zeta}^2 - \frac{\mathcal{F}_S}{a^2} (\vec{\nabla}\zeta)^2\right],\\
\mathcal{F}_S &= \frac{M_P^2 X}{\Theta^2}\left[K_X - 2G_\varphi + 4H\dot{\varphi}G_X + 2\ddot{\varphi}G_X + 2X\ddot{\varphi}G_{XX} + 2XG_{X\varphi} - \frac{2}{M_P^2}X^2G_X^2\right]\\
&= \frac{M_P^2 X}{\Theta^2}\left\{k_X + \frac{Hgh\dot{\varphi}}{X}\left[-4m - (m-1)\alpha + 2(m^2 + Xm_X)\eta\right] - \frac{2}{M_P^2}g^2h^2m^2\right\},\\
\mathcal{G}_S &= \frac{M_P^2 X}{\Theta^2}\left[K_X + 2XK_{XX} - 2G_\varphi + 6H\dot{\varphi}G_X + 6H\dot{\varphi}XG_{XX} - 2XG_{X\varphi} + \frac{6}{M_P^2}X^2G_X^2\right]\\
&= \frac{M_P^2 X}{\Theta^2}\left\{k_X + 2Xk_{XX} + \frac{Hgh\dot{\varphi}}{X}\left[-6\left(m^2 + Xm_X\right) + (m+1)\alpha\right] + \frac{6}{M_P^2}g^2h^2m^2\right\},\\
\Theta &= M_P^2 H\left(1 + m\frac{Hgh\dot{\varphi}}{M_P^2H^2}\right).
\end{aligned}
$$